TRIB2 in human AML: a biological and clinical investigation

Joana Monteiro de Campos
BSc, MRes

A thesis submitted in fulfilment of the requirements for the degree of Doctor of Philosophy

Institute of Cancer Sciences
College of Medical, Veterinary and Life Sciences
University of Glasgow

July 2016

Abstract

Acute myeloid leukemia (AML) involves the proliferation, abnormal survival and arrest of cells at a very early stage of myeloid cell differentiation. The biological and clinical heterogeneity of this disease complicates treatment and highlights the significance of understanding the underlying causes of AML, which may constitute potential therapeutic targets, as well as offer prognostic information. Tribbles homolog 2 (*Trib2*) is a potent murine oncogene capable of inducing transplantable AML with complete penetrance. The pathogenicity of Trib2 is attributed to its ability to induce proteasomal degradation of the full length isoform of the transcription factor CCAAT/enhancer-binding protein alpha (C/EBPα p42). The role of TRIB2 in human AML cells, however, has not been systematically investigated or targeted.

Across human cancers, *TRIB2* oncogenic activity was found to be associated with its elevated expression. In the context of AML, TRIB2 overexpression was suggested to be associated with the large and heterogeneous subset of cytogenetically normal AML patients. Based upon the observation that overexpression of TRIB2 has a role in cellular transformation, the effect of modulating its expression in human AML was examined in a human AML cell line that expresses high levels of TRIB2, U937 cells. Specific suppression of TRIB2 led to impaired cell growth, as a consequence of both an increase in apoptosis and a decrease in cell proliferation. Consistent with these *in vitro* results, TRIB2 silencing strongly reduced progression of the U937 *in vivo* xenografts, accompanied by detection of a lower spleen weight when compared with mice transplanted with TRIB2-expressing control cells. Gene expression analysis suggested that *TRIB2* modulates apoptosis and cell-cycle sensitivity by influencing the expression of a subset of genes known to have implications on these phenotypes. Furthermore, *TRIB2* was found to be expressed in a significant subset of AML patient samples analysed. To investigate whether increased expression of this gene could be afforded prognostic significance, primary AML cells with dichotomized levels of *TRIB2* transcripts were evaluated in terms of their xeno-engraftment potential, an assay reported to correlate with disease aggressiveness observed in humans. A small cohort of analysed samples with higher *TRIB2* expression did not associate with preferential leukaemic cell engraftment in highly immune-deficient mice, hence, not predicting for an adverse prognosis. However, further experiments including a larger cohort of well characterized AML patients would be needed to clarify TRIB2 significance in the diagnostic setting. Collectively, these data support a functional role for TRIB2 in the maintenance of the oncogenic properties of human AML cells and suggest TRIB2 can be considered a rational therapeutic target.

Proteasome inhibition has emerged as an attractive target for the development of novel anti-cancer therapies and results from translational research and clinical trials support the idea that proteasome inhibitors should be considered in the treatment of AML. The present study argued that proteasome inhibition would effectively inhibit the function of TRIB2 by abrogating C/EBPα p42 protein degradation and that it would be an effective pharmacological targeting strategy in TRIB2-positive AMLs. Here, a number of cell models expressing high levels of TRIB2 were successfully targeted by treatment with proteasome inhibitors, as demonstrated by multiple measurements that included increased cytotoxicity, inhibition of clonogenic growth and anti-AML activity *in vivo*.
Mechanistically, it was shown that block of the TRIB2 degradative function led to an increase of C/EBPα p42 and that response was specific to the TRIB2-C/EBPα axis.
Specificity was addressed by a panel of experiments showing that U937 cells (express detectable levels of endogenous TRIB2 and C/EBPα) treated with the proteasome inhibitor bortezomib (Brtz) displayed a higher cytotoxic response upon TRIB2 overexpression and that ectopic expression of C/EBPα rescued cell death. Additionally, in C/EBPα-negative leukaemia cells, K562 and Kasumi 1, Brtz-induced toxicity was not increased following TRIB2 overexpression supporting the specificity of the compound on the TRIB2-C/EBPα axis. Together these findings provide pre-clinical evidence that TRIB2- expressing AML cells can be pharmacologically targeted with proteasome inhibition due, in part, to blockage of the TRIB2 proteolytic function on C/EBPα p42.
A large body of evidence indicates that AML arises through the stepwise acquisition of genetic and epigenetic changes. Mass spectrometry data has identified an interaction between TRIB2 and the epigenetic regulator Protein Arginine Methyltransferase 5 (PRMT5). Following assessment of TRIB2's role in AML cell survival and effective targeting of the TRIB2-C/EBPα degradation pathway, a putative TRIB2/PRMT5 cooperation was investigated in order to gain a deeper understanding of the molecular network in which TRIB2 acts as a potent myeloid oncogene. First, a microarray data set was interrogated for *PRMT5* expression levels and the primary enzyme responsible for symmetric dimethylation was found to be transcribed at significantly higher levels in AML patients when compared to healthy controls. Next, depletion of *PRMT5* in the U937 cell line was shown to reduce the transformative phenotype in the high expressing TRIB2 AML cells, which suggests that PRMT5 and TRIB2 may cooperate to maintain the leukaemogenic potential. Importantly, PRMT5 was identified as a TRIB2-interacting protein by means of a protein tagging approach to purify TRIB2 complexes from 293T

cells. These findings trigger further research aimed at understanding the underlying mechanism and the functional significance of this interplay.

In summary, the present study provides experimental evidence that TRIB2 has an important oncogenic role in human AML maintenance and, importantly in such a molecularly heterogeneous disease, provides the rational basis to consider proteasome inhibition as an effective targeting strategy for AML patients with high TRIB2 expression. Finally, the identification of PRMT5 as a TRIB2-interacting protein opens a new level of regulation to consider in AML. This work may contribute to our further understanding and therapeutic strategies in acute leukaemias.

Table of Contents

List of Tables

List of Figures

List of Appendices

List of Publications

O'Connor C, Lohan F, **Campos J**, Ohlsson E, Salomè M , Forde C, Artschwager R, Liskamp R, Cahill M, Kiely P, Porse B, Keeshan K (2016). The presence of C/EBPα and its degradation are both required for TRIB2 mediated leukaemia. *Oncogene*.

Salomé M, **Campos J**, Keeshan K. (2015). TRIB2 and the ubiquitin-proteasome system in cancer. *Biochem Soc Trans*, 43 (5).

O'Connor C, **Campos J**, Osinski JM, Gronostajski RM, Michie AM, Keeshan K. (2015). Nfix expression critically modulates early B lymphopoiesis and myelopoiesis. *PLoS One*, 10 (3).

Rishi L, Hannon M, Salomé M, Hasemann M, Frank A, **Campos J**, Timoney J, O'Connor C, Cahill M, Porse B, Keeshan K. (2014). Regulation of Trib2 by an E2F1-C/EBPα feedback loop in AML cell proliferation. *Blood*, 123 (15).

Acknowledgement

First and foremost I would like to thank my principal supervisor, Dr. Karen Keeshan, for her help in directing this project and for providing guidance and assistance when obstacles were met. I am indebted to her for the scientific training I have received. A significant mention goes to Professor Tessa Holyoake and all members of the Paul O'Gorman Leukaemia Research Centre in Glasgow for creating an inspiring work environment that is conducive to professional growth. As a result of this, I truly enjoyed my three years of research. I am particularly grateful to my colleagues with whom I shared office 5. Thank you for providing constant support at different levels. Earning your friendship was an invaluable "side effect" of my PhD. This research would have not been possible without the funding from the Howat foundation, Children with Cancer UK and the Children´s Leukaemia Research Project. Para a Cila, o Juca e a Rita, o agradecimento mais especial.

Author’s Declaration

Except where explicit reference is made to the contribution of others, this work represents original work carried out by the author and has not been submitted in any form to any other University.

List of Abbreviations

2-HG	2-Hydroxyglutarate
α-KG	α-ketoglutarate
ABL	V-Abl Abelson Murine Leukaemia Viral Oncogene Homolog
AML	Acute Myeloid Leukaemia
ALL	Acute Lymphocytic Leukaemia
APL	Acute Promyelocytic Leukaemia
ATRA	All-*Trans* Retinoic Acid
ATP	Adenosine Triphosphate
BM	Bone Marrow
BMT	Bone Marrow Transplantation
bp	Base pairs
Brtz	Bortezomib
BSA	Bovine Serum Albumin
C/EBPα	CCAAT/enhancer-binding protein alpha
CFC	Colony-Forming Cell
Cfz	Carfilzomib
C-L	Caspase-Like
CLL	Chronic Lymphocytic Leukaemia
CLP	Common Lymphoid Progenitors
CML	Chronic Myeloid Leukaemia
CMP	Common Myeloid Progenitors
CN	Cytogenetically Normal
CNS	Central Nervous System
CNV	Copy Number Variation
Co-IP	Co-Immunoprecipitation
COP1	Constitutive Photomorphogenic 1
COSMIC	Catalogue of Somatic Mutations in Cancer
Ct	Cycle Threshold
CT-L	Chymotrypsin-Like
d	Day
DAPI	4´,6-diamidino-2-phenylindole
DMEM	Dulbecco´s Modified Eagle Medium
DMSO	Dimethyl Sulfoxide
DNA	Deoxyribonucleic Acid

DNMT3A	DNA (cytosine-5-)-methyltransferase 3 alpha
DUBs	Deubiquitinating enzymes
ER	Endoplasmic Reticulum
FAB	French–American–British
FACS	Fluorescence-Activated Cell Sorting
FBS	Foetal Bovine Serum
FDA	Food and Drug Adminintration
FLT3	FMS-like tyrosine kinase 3
FSA	Forward Scatter
GFP	Green Fluorescent Protein
GMPs	Granulocyte-Macrophage Progenitors
Gy	Gray (unit)
h	Hours
HoxA9	Homeobox 9
HSCs	Haemopoietic Stem Cells
IC50	Half Maximal Inhibitory Concentration
IDH1	Isocitrate dehydrogenase 1
IDH2	Isocitrate dehydrogenase 2
IMDM	Isocove´s Modified Dulbecco´s Medium
i.p.	intraperitoneal
IRES	Internal Ribosome Entry Site
ITD	Internal Tandem Duplication
K	Lysine
kb	Kilobases
kDa	Kilodalton
KD	Knockdown
LGA	Leukemia Gene Atlas
LMPP	Lymphoid-primed Multipotent Progenitors
LSK	Lineage- Sca1+ c-Kit+ stem cells
LT-HSCs	Long-Term reconstituting HSCs
MDa	Megadalton
MEP	Megakaryocyte-Erythroid Progenitors
MEP50	Methylosome Protein 50
min	minutes
MLL	Mixed lineage leukaemia

MNCs	Mononuclear Cells
MPP	Multipotent Progenitors
mRNA	messenger Ribonucleic Acid
M.W.	Molecular Weight
NF-kB	Nuclear Factor of kB
NK cells	Natural Killer cells
NPM1	Nucleophosmin
n.s	Not Significant
NSG	non-obese diabetic (NOD)/LtSz-severe combined immunodeficiency (SCID) IL-2Rγc^{null}
O/N	Overnight
PB	Peripheral Blood
PBS	Phosphate Buffered Saline
PDCD4	Programmed Cell Death 4
PI	Propidium Iodine
PN	Product Number
PRMTs	Protein Arginine Methyltransferases
PRMT5	Protein Arginine Methyltransferase 5
PTMs	Post-Translational Modifications
qPCR	Quantitative Polymerase Chain Reaction
R	Arginine
RARα	Retinoic Acid Receptor α
Rb	Retinoblastoma
RPMI 1640	Roswell Park Memorial Institute 1640
RT	Room Temperature
RT-PCR	Reverse Transcriptase Polymerase Chain Reaction
SD	Standard Deviation
SDS-PAGE	Sodium Dodecyl Sulphate Polyacrylamide Gel Electrophoresis
sec	seconds
SF	Peptido Sulfonyl Fluoride
shRNA	short-hairpin RNA
Smurf1	Smad ubiquitination regulatory factor 1
snRNP	small nuclear Ribonucleoprotein
SSC	Side Scatter
ST-HSCs	Short-Term reconstituting HSCs

T-ALL	T-cell ALL
t-AML	Therapy-related AML
TCF4	Transcription Factor 4
TET2	Ten-eleven-translocated gene 2
T-L	Trypsin-Like
TRIB2	Tribbles homolog 2
Ub	Ubiquitin
uORF	upstream Open Reading Frame
UPS	Ubiquitin Proteasome System
V	Volts
WBC	White Blood Cell
WHO	World Health Organisation
WT	Wild Type

Chapter 1
Introduction

1.1 Haemopoiesis

Haemopoiesis describes the commitment and differentiation processes by which all blood cellular components are produced. In mammals, the anatomical sites of haemopoiesis change during development and sequentially include the yolk sac, an area surrounding the dorsal aorta termed the aorta-gonad mesonephros region, placenta, foetal liver and bone marrow (BM) – the primary adult haemopoietic centre (Orkin and Zon, 2008).The blood-forming system is organized as a cellular hierarchy sustained at its apex by a rare population of haemopoietic stem cells (HSCs), which is defined by a dual capability of self-renewal and multilineage differentiation and has been isolated in both mice and human (Spangrude et al., 1988, Baum et al., 1992, Morrison and Weissman, 1994, Osawa et al., 1996). The existence of the HSCs was firstly postulated by Arthur Pappenhein in 1917, as reviewed by (Huntly and Gilliland, 2005). In the 1950s, research evolved from experiments showing that an intravenous transplant of normal adult mouse BM cells could rescue irradiated mice from lethality by replacing the destroyed blood-forming system with a new and sustained source of lymphoid and myeloid cells (Jacobson et al., 1951, Ford et al., 1956). In 1961, Till and McCulloch demonstrated the existence of clonogenic BM cells that could give rise to multilineage haemopoietic colonies in the spleen of lethally irradiated mice. Some of these colonies contained a subset of clonogenic cells that could reconstitute haemopoiesis of irradiated mice in secondary transplants and thus where proposed to be HSCs (Till and McCulloch, 1961). The hallmarks of HSCs underlie the enormous utility of bone marrow transplantation as a clinical procedure (Weissman, 2000).

During steady-state haemopoiesis, the BM HSCs are relatively quiescent (Bradford et al., 1997, Cheshier et al., 1999) but upon cell cycle entry give rise to a hierarchy of differentiating progenitor populations that undergo the immense proliferative expansion required to replenish the mature and predominantly short-lived blood cells. HSCs can be divided into long-term reconstituting HSCs (LT-HSCs) and short-term reconstituting HSCs (ST-HSCs) (Figure 1.1). LT-HSCs maintain self-renewal and multilineage differentiation potential throughout life. ST-HSCs derive from LT-HSCs and exhibit more-limited self-renewal potential, although preserving multipotency (Morrison and Weissman, 1994). ST-HSCs differentiate into multipotent progenitors (MPPs) (Morrison et al., 1997) (Figure 1.1), which do not or briefly self-renew and have the ability to differentiate into oligolineage-restricted progenitors that ultimately give rise to functionally mature cells of either lymphoid or myeloid lineage. The common lymphoid progenitors (CLPs) produce T lymphocytes, B lymphocytes and natural killer (NK) cells (Kondo et al., 1997) (Figure

1.1). On the other hand, common myeloid progenitors (CMPs) are responsible for generating granulocyte-macrophage progenitors (GMPs) - which undergo further restriction into granulocytes (basophil, neutrophil, eosinophil) and monocytes/macrophages- and megakaryocyte-erythroid progenitors (MEPs), which differentiate into megakaryocytes/platelets and erythrocytes (Akashi et al., 2000). Both lymphoid and myeloid differentiation can give rise to dendritic-cells (Manz et al., 2001) (Figure 1.1). Human and murine haemaopoiesis seem to be generally comparable, except for the unique combinations of cell surface markers that phenotypically identify HSCs and progenitor populations by fluorescence-activated cell sorting (FACS) (Doulatov et al., 2012).

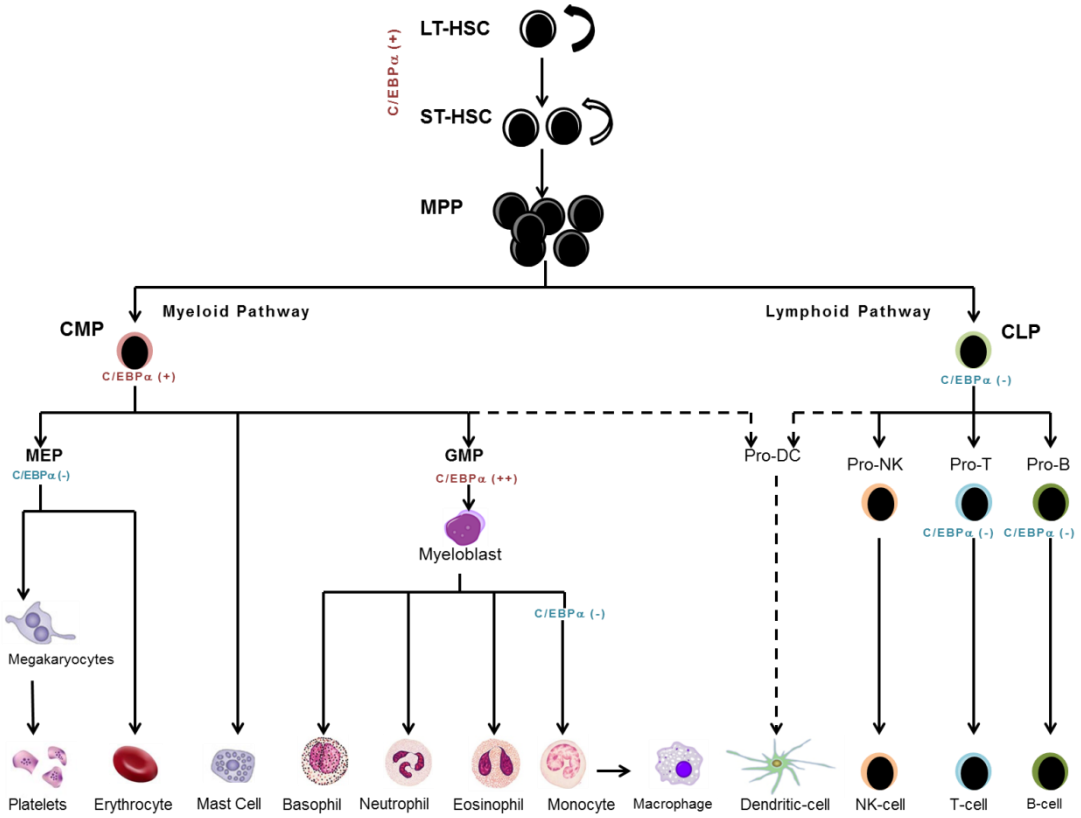

Figure 1.1 The haemopoietic classic hierarchy
HSCs, haemopoietic stem cells; LT-HSCs, long-term reconstituting HSCs; ST-HSCs, short-term reconstituting HSCs; MPPs, multipotent progenitors; CLPs, common lymphoid progenitors; NK, natural killer cells; CMPs, common myeloid progenitors; GMPs, granulocyte-macrophage progenitors; MEPs, megakaryocyte-erythroid progenitors; Pro-DC, pro-dendritic cell; C/EBPα, CCAAT/enhancer binding protein-α.

Throughout the maturational pathways that direct transition from haemopoietic stem and progenitor cells to terminally differentiated blood cells, a tightly regulated network of transcription factors is highly important in defining cellular fates. Examples of these include Notch-1, GATA-3 and Pax5, which mediate T- and B-cell development; GATA-1 and FOG-1, which are involved in the development of erythrocytes and megakaryocytes; and PU.1 and C/EBPα, which control the commitment of myeloid cells (Orkin, 2000, Xie and Orkin, 2007). The role of C/EBPα (further characterized in section 1.2.4) as a master regulator of granulopoiesis (Zhang et al., 1997) is highlighted in Figure 1.1, where it is shown to be expressed in HSCs and GMPs, downregulated as CMPs differentiate to MEPs and absent in precursors of lymphoid cells (Miyamoto et al., 2002). In addition to transcriptional regulation, signals from the BM niche (microenvironment), including the ones from cytokines and growth factors, are critical for the early cell fate decisions (Dorantes-Acosta and Pelayo, 2012). It was once considered that cellular differentiation was unidirectional, that is, once progenitors have committed to a particular linear pathway their fate is sealed due to precise combinations of lineage transcription factors and epigenetic modifications to the chromatin. However, the unidirectional and irreversible nature of the process has been questioned by a number of findings that, instead, support plasticity of early progenitor cells. Indeed, cells of one haemopoietic lineage can be redirected to another through forced expression of carefully chosen transcription factors or loss of these regulators, a process called cellular reprogramming (Orkin, 2000, Xie and Orkin, 2007). For example, introducing C/EBPα into B- or T-cells converts them into functional macrophages (Xie et al., 2004, Laiosa et al., 2006). Ectopic GATA-1 can also reprogram common B and T progenitor cells into megakaryocytic/erythroid cells (Iwasaki et al., 2003) while pro-B cells lacking Pax5 ($Pax5^{-/-}$) are not restricted in their lineage fate (Nutt et al., 1999).

The classical view of the blood hierarchy (Figure 1.1) has recently been challenged. In the murine system, the identification of lymphoid-primed multipotent progenitors (LMPP) argued that the megakaryocytic/erythroid lineage diverts earlier, without implicitly going through a shared CMP stage (Adolfsson et al., 2005, Mansson et al., 2007). Recently, Notta *et al.* added an additional layer of complexity by suggesting a developmental shift in the human progenitor cell architecture from the foetus, where many stem and progenitor cell types are multipotent, to the adult, where the stem cell compartment is multipotent but the progenitors are unipotent (Notta et al., 2015). While these and other studies challenge the classical view of haemopoiesis hierarchy, in the absence of a clear consensus on a revised model, the standard model is still used extensively as an operational paradigm.

Defects in the regulatory pathways that control haemopoiesis severely perturb normal development and lie at the root of haematological malignancies, such as leukaemia.

1.2 Acute Myeloid Leukaemia

Acute Myeloid Leukaemia (AML) is best understood by first describing the larger group of haemopoietic malignancies in which it is embedded, that is leukaemia.

1.2.1 History and classification of leukaemia

Reports from the early 19th century first establish the possibility that sustained leukocytosis could occur in the absence of infection. The first published description of a case of leukaemia in medical literature dates to 1827, when French physician Alfred Velpeau described a 63-year-old Parisian patient who was noted at post-mortem examination to have substantial enlargement of the liver and spleen, as well as blood resembling “gruel”. In 1845, a series of patients who died with enlarged spleens and changes in the "colours and consistencies of their blood" were reported by the Edinburgh-based pathologist J.H. Bennett, who used the term "leucocythemia" to describe this pathological condition. In 1847, the German pathologist Virchow was credited with coining the term “leukaemia” (Greek for "white blood") to describe the abnormal excess of white blood cells in patients with the previously reported clinical syndrome (Beutler, 2001, Piller, 2001, Freireich et al., 2014).

Leukaemia, nowadays a well-recognized distinct entity, is characterized by disruption of the processes directing self-renewal, differentiation and haemopoietic cell expansion, which leads to the accumulation of immature, non-functioning neoplastic cells. According to the American Cancer Society, an estimated 54,270 new cases of leukaemia were expected in 2015 (3% of total cancers) in the USA (American Cancer Society, 2015). Clinically and pathologically, the term leukaemia comprises a spectrum of haematological malignancies that are mainly subdivided in four categories: acute lymphocytic leukaemia (ALL), acute myeloid leukaemia (AML), chronic lymphocytic leukaemia (CLL) and chronic myeloid leukaemia (CML). According to progression of the untreated disease and maturity of the affected cells, leukaemia has traditionally been designated as acute or chronic. Acute forms of the disease progress rapidly and require prompt treatment. They target immature cells, causing symptoms to appear quickly. Chronic forms of leukaemia, on the other hand, target more mature cells and develop over long periods of time, with

symptoms arising often at later stages. The second factor in classifying leukaemia concerns the type of blood cells that are affected: lymphoblastic or myeloid, as outlined in Figure 1.1. Symptoms are generally the same regardless of which cell is affected; the difference is mainly important for therapeutic-management of the patients. Some forms of leukaemia are far more common than others and rates of incidence also vary by age. In the USA, the majority (91%) of leukaemia cases are diagnosed in adults 20 years of age and older. Among adults, the most common types are CLL (36%) and AML (32%). In contrast, ALL is most common before age 20, accounting for 76% of cases. Overall leukaemia incidence rates have been slowly increasing over the past few decades; from 2007 to 2011, rates increased by 1.6% per year in males and 0.6% per year in females (American Cancer Society, 2015).

1.2.2 Pathology, epidemiology and etiology of AML

In AML, differentiation block and increased proliferation affect the myeloid lineage and result in the accumulation of abnormal immature cells (blasts) within the BM and blood, which are incapable of differentiating towards granulocytes or monocytes (Lowenberg et al., 1999). Infiltration of blasts, that replace normal cells in these tissues, causes the first clinical signs and symptoms usually found at presentation of AML - fatigue, haemorrhage or infections and fever due to decreases in red blood cells (anaemia), platelets (thrombocytopenia) or neutrophils (neutropenia), respectively. Leukaemic infiltration of other tissues, including the liver (hepatomegaly), spleen (splenomegaly), skin (leukaemia cutis), lymph nodes (lymphadenopathy), bone (bone pain) and central nervous system can produce a variety of other symptoms (Lowenberg et al., 1999). At least 20% of cells in a BM aspirate or circulating blood need to be blasts of myeloid lineage for disease diagnosis. Blast lineage is assessed by multiparameter flow cytometry with CD33 and CD13 being surface markers typically expressed by human myeloid blasts (Estey, 2012).

While it can occur in children (usually during the first two years of life), the prevalence of AML increases with age and is generally a disease of elderly people with an average age at diagnosis of 70 years and more common in men than in women. The American Cancer Society estimated 20,830 new cases of AML (12,730 in men and 8,100 in women) to occur

in the USA in 2015, accounting for 32% of all leukaemia cases in adults 20 years of age and older (American Cancer Society, 2015)[1].

The vast majority of AML are sporadic and are the consequence of acquired somatic alterations in haemopoietic progenitor cells but association with risk factors has been reported. Congenital disorders such as Fanconi's anemia, Bloom's, Down's, Kostmann's and Diamond-Blackfan syndromes can increase the relative risk of developing AML. Risk is also increased in individuals with acquired haematologic disorders including the myeloproliferative and myelodysplastic syndromes and paroxysmal nocturnal haemoglobinuria. Therapy-related AML (t-AML) may develop as a consequence of exposure to chemotherapy, including alkylating agents, epipodophyllotoxins and ionizing radiation. Smoking is also reported as a risk factor to the development of AML associated with benzene exposure (Gilliland and Tallman, 2002, Estey and Dohner, 2006).

1.2.3 AML classification

AML comprises a group of disorders with great variability regarding clinical course and response to therapy. Diversity is also detected at the genetic and molecular basis of the pathology, which can be associated with chromosomal translocations, genetic mutations and transcription factors perturbations. Such heterogeneity has been used for disease stratification into specific subgroups to improve prognostication and support risk-adapted therapeutic management of AML patients. The first proposed standardized method of classification was that developed in 1976 by the French–American–British (FAB) Cooperative Group. The FAB system divides AML into seven distinct subtypes (M0 to M7) according to the myeloid lineage involved/degree of leukaemic-cell differentiation, and is based on conventional morphologic and histochemical analysis of peripheral blood (PB) and BM leukaemia blasts (Bennett et al., 1976, Bennett et al., 1985) (Table 1.1). While this method is still commonly used for morphologic diagnosis, progress made during recent years in deciphering the molecular basis of AML and in defining new diagnostic and prognostic markers, refined the classification approach. Hence, new standardized systems have been proposed, correlating cytogenetic and molecular genetic information with clinical data. Amongst them, the World Health Organization (WHO)

[1] Epidemiology of leukaemia and, in particular, AML here reported are based on the US population since the most recent and detailed data concerning this subject are provided by the American Cancer Society. However, information available from Cancer Research UK (www.cancerresearchuk.org) should be mentioned as well. According to this source, in 2013 AML accounted for 0.8% of all new cancer cases in the UK, and 32% of all leukaemia types combined. In the same year, there were 2,942 new cases of AML: 1,715 (58%) in males and 1,227 (42%) in females.

classification for haematological malignancies is widely used by clinicians and categorizes the increasing number of acute leukaemias as distinctive clinico-pathologic-genetic entities. The 2008 revised fourth edition included AML with mutated nucleophosmin (*NPM1)* and AML with mutated *CEBPA* as provisional entities, and strongly recommended a routine mutational screen of *NPM1*, *CEBPA* and FMS-like tyrosine kinase 3-ITD (*FLT3-ITD)* (Vardiman et al., 2009); genes afforded prognostic significance by other stratification models, such as the European Leukemia Net system (Dohner et al., 2010). The 2016 edition (Table 1.1) represents a revision of the prior classification. Refinements in gene names are included as well as new provisional entities of AML (Arber et al., 2016).

Table 1.1 AML classification systems

	French-American-British (FAB) classification
M0	Undifferentiated
M1	Myeloblastic without/with minimal maturation
M2	Myelobastic with maturation
M3	Promyelocitic-hypergranular; APL[a]
M3v	Promyelocitic-hypogranular variant; APL[a]
M4	Myelomonocytic
M4eo	Myelomonocytic with eosinophilia
M5a	Monocytic
M5b	Monocytic with differentiation
M6	Erythroleukaemia
M7	Megakaryoblastic
	2016 release of the World Health Organization (WHO) Classification
1	AML with recurrent cytogenetic abnormalities: -AML with t(8;21)(q22;q22.1); *RUNX1-RUNX1T1* -AML with inv(16)(p13.1;q22) or t(16;16)(p13.1;q22); *CBFβ-MYH11* -APL[a] with *PML-RARα* -AML with t(9;11)(p21.3;q23.3); *MLLT3-KMT2A* -AML with t(6;9)(p23;q34.1); *DEK-NUP214* -AML with inv(3)(q21.3;q26.2) or t(3;3)(q21.3;q26.2); *GATA2, MECOM* -AML (megakaryoblastic) with t(1;22)(p13.3;q13.3), *RBM15-MKL1* -provisional entities: AML with *BCR-ABL1* , AML with mutated *RUNX1* -AML with mutated *NPM1* -AML with biallelic mutations of *CEBPA*
2	AML with myelodysplasia-related changes
3	Therapy-related myeloid neoplasm (t-AML)
4	Myeloid sarcoma
5	Myeloid proliferations associated with Down syndrome
6	Blastic plasmacytoid dendritic cell neoplasm
7	AML not otherwised specified (AML-NOS)[b]

[a] APL, Acute Promyelocytic Leukaemia
[b] Further subdivided based on morphologic criteria similar to those of the FAB classification

In addition, large collaborative studies have proposed risk stratification into favourable, intermediate or adverse groups based upon cytogenetic profile found at presentation (Grimwade et al., 1998, Grimwade et al., 2001). Non-random, clonal chromosome aberrations are detected in the leukaemic blasts of approximately 55% of adults with AML (Dohner and Dohner, 2008) and have long been recognized as important independent predictors for achievement of complete remission, risk of relapse and overall survival in AML (Mrozek et al., 2001). Patients carrying t(8;21)(q22;q22) leading to a fusion of *RUNX1* gene to *RUNX1T1* gene, inv(16)(p13.1q22) or t(16;16)(p13.1q22) both leading to the fusion of the *CBF* and *MYH11* genes, or t(15;17) with the resulting *PML-RARα* rearrangement generally have a favourable prognosis. On the opposite side of the spectrum, patients with t(6;9), 11q23 (mixed lineage leukaemia (*MLL)* gene) abnormalities, monosomies of chromosomes 7 or 5 or showing complex karyotype (independent alterations of three or more chromosomes in the absence of t(8;21), inv(16) or t(16;16) and t(15;17)) have a distinctively poor prognosis (Löwenberg, 2001). The remaining large group of patients (~45%), with cytogenetically normal AML (CN-AML), are classified in the intermediate prognostic category (Walker and Marcucci, 2012). Specific mutations were also recently identified to predict AML outcome and improve risk stratification independent of historically recognized risk factors. That is the case of FLT3, NPM1, and C/EBPα recurrent molecular abnormalities, shown to improve risk stratification for patients with CN-AML (Walker and Marcucci, 2012), as further detailed below (section 1.2.4.2).

1.2.4 Molecular pathogenesis of AML

1.2.4.1 Two-hit model

The observation that a single mutation appears generally insufficient for overt leukaemia to develop in mouse models supported the two-hit model of leukaemogenesis (Kelly and Gilliland, 2002, Speck and Gilliland, 2002). This hypothesis considers AML development to be a multistep process, requiring the collaboration of two classes (I and II) of mutations for transformation of a myeloid precursor. Class I mutations confer a survival/proliferation advantage and those that impair haemopoietic differentiation are included in class II (Figure 1.2). Survival or proliferative mutations typically involve activation of tyrosine kinase signaling (FLT3, c-KIT, RAS) or tyrosine phosphatase (PTPN11) pathways, while defects in myeloid differentiation often result from chromosomal translocations (*e.g.*, generation of novel oncogenes such as *RUNX1-RUNX1T1* or *PML-RARα*) or mutations in

CEBPA or *NPM1* (Gilliland and Tallman, 2002, Renneville et al., 2008). However, not all the genetic aberrations that have been found in human AML fall within the two categories (Figure 1.2), implicating that the two-hit model may be an oversimplification. This is best exemplified by the growing evidence suggesting that changes in the epigenetic landscape have a role in leukaemia development and maintenance (Greenblatt and Nimer, 2014). Mutations affecting DNA (cytosine-5-) -methyltransferase 3 alpha (*DNMT3A),* additional sex combs like 1 (*ASXL1),* ten-eleven-translocated gene 2 (*TET2)* or isocitrate dehydrogenase 1 (*IDH1*) and isocitrate dehydrogenase 2 (*IDH2*) genes were shown to be implicated in AML and could, therefore, be ascribed to a third important mechanistic pathway involving epigenetic regulators (O´Brien et al., 2014) (Figure 1.2).

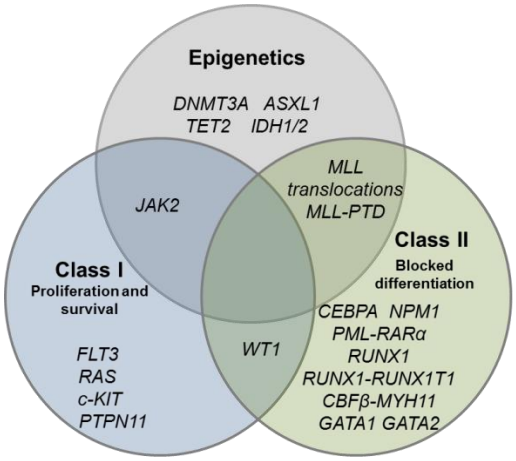

Modified from (O´Brien et al., 2014)

Figure 1.2 Molecular pathogenesis of AML
The Venn diagram depicts some of the key mutated genes found in AML. They are grouped according to the two-hit model classes (I and II) and are also included in new proposed classes.

1.2.4.2 Recurrent genetic mutations

1.2.4.2.1 Mutations in the epigenetic modifiers

The use of next-generation sequencing techniques to sequence whole-genomes and exomes has identified several new molecular alterations in AML patients. Most of these mutations affect epigenetic regulation, as they involve genes encoding, IDH1 and IDH2, TET2, as well as DNMT3A. Mutations affecting *IDH1* and its mitochondrial homolog, *IDH2*, occur in 15 to 20% of newly diagnosed AML patients, particularly in those with normal cytogenetics (Mardis et al., 2009, Abbas et al., 2010). The IDH metabolic enzymes convert isocitrate into α-ketoglutarate (α-KG), which is not only an intermediate in the Krebs cycle, but also affects normal function of several dioxygenases, including TET2. The *IDH* mutations are heterozygous and affect critical arginine (R) residues in the active site of the

enzyme: R132 in IDH1 and R140 and R172 in IDH2 (Chou et al., 2011). The subsequent amino acid substitution prevents the normal catalytic function of the enzyme and results in the conversion of α-KG to 2-Hydroxyglutarate (2-HG), which is a competitor inhibitor of dioxygenases (Dang et al., 2009). In AML it has been show that the accumulation of this putative oncogenic metabolite not only blocks the function of TET2 protein, leading to aberrant DNA methylation, but also impairs histone demethylation and interferes with normal differentiation of cells. *IDH1/2* mutations and *TET2* mutations, which lead to loss of function, are associated with similar epigenetic defects (Figueroa et al., 2010). Moreover, Chaturvedi and colleagues found that mutant *IDH1* in combination with homeobox 9 (*HoxA9)* greatly accelerates leukaemogenesis in a murine model (Chaturvedi et al., 2013). While the prognostic impact of *IDH*-mutations is still controversial (Thiede, 2012), the effect of mutations in the *DNMT3A* appears to be more consistent across studies. *DNMT3A* mutations are an unfavourable prognosis biomarker in AML (Renneville et al., 2012, Shivarov et al., 2013). The overall prevalence is ~18-23% and is particularly higher in CN-AML (29-36%) (Thiede, 2012). The majority of *DNMT3A* somatic mutations are missense alterations in the R882 residue located near the carboxyl terminus of the DNMT3A protein. DNMT3A belongs to a family of DNA-methyltransferases whose role is to catalyse the addition of methyl groups onto the 5′-position of cytosine residues of CpG dinucleotides. However, the function and biological consequences of *DNMT3A* mutations in AML have yet to be fully elucidated (Im et al., 2014). Ferreira and colleagues have recently reported that in the absence of MLL-fusion proteins, an alternative pathway for engaging a leukaemogenic MEIS1-dependent transcriptional program can be mediated by *DNMT3A* mutations (Ferreira et al., 2015).

1.2.4.2.2 *NPM1*

NPM1 is the most common single gene mutated in AML (30-35%) (Thiede, 2012). Alterations in *NPM1* gene encoding a nucleocytoplasmic shuttling protein with prominent nucleolar localization are almost exclusively detected in AML. They consist of a 4 base pair (bp)-frameshift mutation occurring in exon 12 that converts a nucleolar localization signal into a nuclear export signal, resulting in aberrant cytoplasmic localization in the AML blasts (Falini et al., 2005). 50% of the CN-AML patients are identified with a mutant *NPM1*, also frequently associated with alterations in *FLT3*, *DNMT3A* and *IDH1/2* genes. As a result, *NPM1*-mutated AML was defined as a distinct leukaemia entity by the WHO classification (Table 1.1), shown to be a predictor for a favourable outcome in the absence of *FLIT3-ITD* mutations (Dohner et al., 2005, Schnittger et al., 2005, Thiede et al., 2006).

1.2.4.2.3 FLIT3

Two major types of mutations affecting the *FLIT3* receptor kinase have been described in AML patients. Internal tandem duplication (ITD) mutations of the juxtamembrane region are present in 15-20% of AML (Nakao et al., 1996), particularly in certain cytogenetically defined groups, as CN-AML, t(15;17) and t(6;9). Also, patients carrying *NPM1* and *DNMT3A* mutations more often display *FLIT3-ITD* (Thiede, 2012). The other predominant type of mutations are missense single base pair exchanges in the second tyrosine kinase domain, typically involving codon D835. They are also more prevalent in patients with normal karyotype and are commonly detected in association with *NPM1* and inv(16) (Thiede, 2012). Both lead to constitutive activation of the FLT3 protein, expressed on early haemopoietic progenitor cells, and while *FLIT3-ITD* mutations are generally associated with poor outcome (Estey, 2010), debate exists on whether mutations in the tyrosine kinase domain are either irrelevant for prognosis (Thiede et al., 2002) or associated with inferior outcome (Whitman et al., 2008).

1.2.4.2.4 CEBPA

CEBPA (19q13.1) encodes the transcription factor C/EBPα and is the most commonly studied gene in AML, with a mutational frequency of ~9% across this disease. Mutations are particularly higher in the M2 subtype (up to 20%) and in the CN-AML patients (15%) (Nerlov, 2004, Thiede, 2012). C/EBPα is a member of the basic-region leucine zipper (BR-LZ) family of transcription factors and consists of highly homologous C-terminal DNA-binding (basic-region) and dimerization (leucine zipper) motifs and two less conserved N-terminal transactivation domains (TAD 1 and TAD 2), via which transcription is activated (Tenen et al., 1997) (Figure 1.3). C/EBPα was originally isolated as a rat liver transcription factor regulating hepatic and adipocyte genes (Cao et al., 1991, Watkins et al., 1996, Timchenko et al., 1996) and controls the proliferation and differentiation of various cell types (Hendricks-Taylor and Darlington, 1995). Within haemopoiesis, its expression is detected in early myeloid progenitors, specifically upregulated in myeloid cells undergoing granulocytic differentiation and rapidly downregulated during the alternative monocytic pathway (Scott et al., 1992, Radomska et al., 1998). Accordingly, C/EBPα knockout mice, which die at birth because of severe hypoglycemia, display a complete lack of mature granulocytes. Adult mice with induced loss of C/EBPα have normal numbers of CMPs but are devoid of GMPs and consecutive granulocytic stages but not monocytes, indicating that C/EBP is essential for the transition of CMPs to GMPs (depicted in Figure 1.1) (Wang et al., 1995, Zhang et al., 2004b). C/EBPα's critical role in lineage commitment during

haemopoietic differentiation is executed by coupling the direct transcriptional activation of myeloid-specific genes with the arrest of cell proliferation (Nerlov, 2004). *CEBPA* is an intronless gene whose mRNA can be differentially translated into two isoforms of 42 kDa (p42) and 30 kDa (p30) by usage of alternative start AUG codons within the same open reading frame. C/EBPα-p30 lacks the N-terminal transactivation domain TAD 1 that is only present on the full-length form (Lin et al., 1993). As a consequence, the p30 isoform lacks domains mediating the contact with the transcriptional apparatus, whereas other functions such as dimerization or regions involved in protein-protein interactions are preserved in both p30 and p42 proteins (Figure 1.3). Hence, only the p42 isoform of C/EBPα can promote proliferation arrest and is able to induce differentiation of granulocytes (Kirstetter et al., 2008).

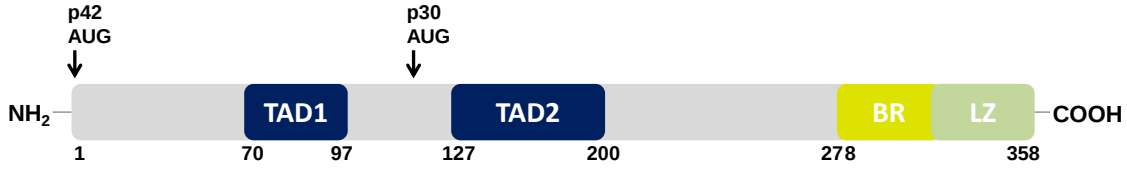

Figure 1.3 Diagram of C/EBPα
Two transactivation domains (TAD1, TAD2) are depicted as well as a basic region (BR) mediating DNA binding and a leucine zipper region (LZ). The protein translated from the AUG at amino acid 1 encodes the p42 isoform whereas the 30 kDa form is translated from the AUG at amino acid 120.

Regulation of the p42/p30 ratio controls cell proliferation and differentiation. Initially, the generation of truncated cellular C/EBP isoforms was proposed to occur via differential translation initiation from internal AUG codons through a mechanism called leaky scanning of ribosomes (Descombes and Schibler, 1991, Lin et al., 1993, Ossipow et al., 1993). However, it has been suggested that instead cells regulate the p42/p30 ratio by responding to extracellular conditions. Under nutrient- or growth factor-rich conditions, proliferation is promoted by increasing the activity of eukaryotic translation initiation factors eIF-2α/eIF-4E, possibly through an increase in c-MYC activity (Rosenwald et al., 1993). High eIF-2α/eIF-4E activity leads to an increased production of p30 at the expense of p42, as eIF-2α and eIF-4E promote the translation of a small upstream open reading frame (uORF) that results in a bypass of the p42 initiation codon. When levels of factors eIF2α and eIF4E are low, translation is primarily initiated from the p42 start codon (Calkhoven et al., 2000).

The spectrum of *CEBPA* mutations observed in AML patients includes two main categories affecting the N- or C-terminus. The N-terminal frame-shift mutations abolish p42 protein expression while retaining the truncated-C/EBPα isoform (p30), initiated further downstream from an internal translational start site. The C-terminal mutations generate in-frame insertions/deletions within the BR-LZ region that compromise DNA binding of both isoforms and may result in dominant-negative homodimers or heterodimers with other C/EBP family members (Nerlov, 2004). These two classes of mutations often co-occur in a biallelic manner and double mutations in *CEBPA*, but not single, have been identified as an independent favorable prognostic factor in cytogenetically normal AML patients by several studies (Wouters et al., 2009, Pabst et al., 2009, Dufour et al., 2010, Taskesen et al., 2011, Fasan et al., 2014).

Besides mutations in the N- and C-terminus, other molecular mechanisms are responsible for C/EBPα inactivation or modulation. These include inhibition of transcription due to the leukaemic fusion protein AML1-ETO (Pabst et al., 2001) or *CEBPA* promoter methylation (Wouters et al., 2007), and post-translational modifications, such as phosphorylation of serine 21 by ERK1/2 (Ross et al., 2004) and the p38 MAP kinase (Geest et al., 2009). Moreover, C/EBPα protein expression can also be modulated by proteasomal degradation mediated by Trib1 or Trib2, which are members of the Tribbles family of proteins.

1.3 Tribbles

1.3.1 Introduction to the Tribbles family

The *tribbles* gene was first identified in the year 2000 in *Drosophila* mutational screens for genes that control cell division and migration. *Drosophila tribbles* was found to mediate degradation of the CDC25 homolog String, resulting in a protracted G2/M transition during gastrulation and morphogenesis (Grosshans and Wieschaus, 2000, Mata et al., 2000, Seher and Leptin, 2000). In addition, *Drosophila tribbles* was shown to regulate oogenesis by inducing ubiquitination and proteasomal degradation of the protein encoded by the gene *slow border cells* (*slbo*), the *Drosophila* homolog of C/EBP transcription factors (Rorth et al., 2000). *Drosophila tribbles* was named after the fictional animals featuring Star Trek television series that first appeared in the episode titled ‘‘The Trouble with Tribbles”. Phenotype displayed by fly genes are in the origin of their names and Seher *et al*. (Seher

and Leptin, 2000) observed that the over-proliferating mesodermal cells seen in *tribbles* mutant embryos resembled these furry and fecund animals.

Tribbles encodes an evolutionarily conserved protein family. Currently, there are three known mammalian homologs of the *tribbles* gene: *TRIB1/C8FW/SKIP1*, *TRIB2/C5FW/SKIP2/SINK* and *TRIB3/NIPK/SKIP3*. The first member of the mammalian Tribbles family to be discovered was *TRIB2* as an mRNA upregulated in the dog thyroid upon stimulation by mitogens (Wilkin et al., 1996, Wilkin et al., 1997). The amino acid sequences of Tribbles are highly conserved among human and mouse (TRIB1, 97.5%; TRIB2, 99.2%; TRIB3, 81.2%) and also within the human family of sequences (TRIB1/TRIB2, 71.3%; TRIB1/ TRIB3, 53.3%; TRIB2/ TRIB3, 53.7%) (Yokoyama and Nakamura, 2011). The Tribbles family structurally shares three motifs that contribute to function:an N-terminal region, a central pseudokinase domain and a C-terminal region (Figure 1.4).

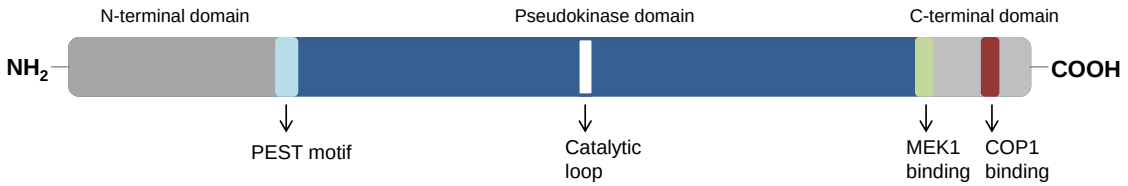

Figure 1.4 The structure of Tribbles proteins

The N-terminal regions are barely conserved between *Drosophila* and the three mammalian Tribbles. They are a relatively short sequence of the Tribbles protein (60 to 80 amino acid), characterized by a high serine and proline content (PEST). PEST regions are indicative of proteins with short half-lives. A putative nuclear localization signal, $[K/R]_2X_2[D/E]X[D/E]$, has been proposed byHegedus *et al.* and it is well conserved in the three mammalian Tribbles (Hegedus et al., 2007). Flanked by the N- and C-terminal sequences, the serine/threonine kinase-like domain is the defining feature of the Tribbles family and is highly conserved among orthologues throughout evolution (Hegedus et al., 2006). A canonical kinase domain consists of 12 subdomains, many of which include conserved sequence patterns of functional importance. The family of Tribbles proteins retains an invariant lysine residue necessary for adenosine triphosphate (ATP) orientation in subdomain II and also a catalytic aspartate residue in the DLKLRKF sequence in subdomain VIB of canonical kinases (Hegedus et al., 2007). Moreover, the predicted 3D structure of Tribbles proteins is consistent with that of a protein kinase (SWISS-MODEL)

(Hegedus et al., 2007). However, the consensus ATP-binding pocket is highly divergent between the conventional kinases and the kinase-like domain of Tribbles proteins (Seher and Leptin, 2000). The complete lack of $GXGX_2GXV$ motif in subdomain I, the loss of histidine and asparagine in $HRDLKX_2N$ in the catalytic cleft VIB and lack of the DFG (Asp-Phe-Gly) triplet in VII are important variations specific to Tribbles. They affect anchoring of ATP, phosphate transfer and Mg2+ chelation, which is necessary for catalysis and ATP orientation (Hegedus et al., 2007). Given these sequence characteristics that define Tribbles as pseudokinases (proteins which have a kinase-like domain lacking canonical motifs) it is believed that none of the Tribbles possess kinase activity and, indeed, specific Tribbles substrates are yet to be identified. However, such view has recently been challenged by Bailey and colleagues that reported a vestigial kinase activity in TRIB2 and TRIB3 pseudokinases (Bailey et al., 2015). With regards to the Tribbles C-terminal domain, two important motifs have been identified within this region: an E3 ubiquitin ligase COP1 (constitutive photomorphogenic 1) binding motif [D/E]QXVP[D/E] that triggers the ubiquitin-proteasome machinery for targeted protein degradation, and a MEK1 [MAPK (mitogen-activated protein kinase)/ERK (extracellular-signal-regulated kinase) kinase 1] binding site, ILLHPWF. Both the COP1- and MEK1-binding motifs are highly conserved in mammalian Tribbles homologues (Qi et al., 2006, Yokoyama and Nakamura, 2011). The presence of these two distinct protein-binding sites (Figure 1.4) highlights the functionally diverse roles of Tribbles as scaffold proteins, mediating degradation and changes to signalling pathways. In support of that, X-Ray structures were reported for COP1 WD40 domains with the binding motif of TRIB1 (Uljon et al., 2016). Also, Murphy *et al.* described the first crystal structure of a Tribbles pseudokinase, that of TRIB1. Further functional studies showed that TRIB1 recognizes a conserved stretch within a transactivation domain of C/EBP proteins and a model was suggested by which TRIB1 acts as a dynamic adapter for recruiting C/EBPs to COP1 (Murphy et al., 2015). Any of the interaction motifs described in Tribbles can be potentially suitable for small molecule ligand targeting. Foulkes and colleagues have begun to analyse small molecules that bind to TRIB2 using differential scanning fluorimetry (DSF) analyses (Foulkes et al., 2015).

1.3.2 Tribbles in AML

Both Trib2 and Trib1 overexpression can independently drive AML in mouse bone marrow transplantation (BMT) models (Keeshan et al., 2006, Dedhia et al., 2010). Trib2 and Trib1 transduced cells were found to exhibit growth advantage *in vitro,* as

overexpression of both genes conveyed serial plating potential to murine BM cells (Dedhia et al., 2010). In the BMT model, Trib2 was found to drive the induction of murine AML with a robust and short latency. Trib2 promotes monocyte and inhibits granulocytic differentiation in mice thereby perturbing myeloid development *in vivo.* However, the leukaemias that Trib2 gives rise to are clonal and this suggests that a secondary hit is occurring in order to give rise to overt AML (Keeshan et al., 2006). Both Trib2 and Trib1 can cooperate with other genes to induce murine AML. *Trib1*, by itself a transforming gene for myeloid cells, was first discovered as a cooperating gene in a murine model of HoxA9/Meis1 myeloid leukaemogenesis, in which it was shown to accelerated disease onset (Jin et al., 2007). Later, it was discovered that Trib2 also cooperates with HoxA9 in the induction of myeloid leukaemia, as mice reconstituted with HSCs co-transduced with Trib2 and HoxA9 have an accelerated onset of AML when compared to either gene alone (Keeshan et al., 2008). Trib2 has also been separately linked to Meis1 leukaemogenic activity. Trib2 was identified as a downstream target gene of Meis1 in Meis1/NUP98-HOXD13 leukaemia cells, being suggested that Trib2 replaces Meis1 function in leukemogenesis (Argiropoulos et al., 2008).

Unlike Trib2 and Trib1, ectopic expression of Trib3 cannot convey serial plating potential to transduced murine bone marrow nor can it induce murine AML (Dedhia et al., 2010). Trib2 and Trib1 differential capacity to induce leukaemia is linked to the ability of these proteins to degrade the full-length isoform of C/EBPα protein in hematopoietic cells, inducing a block of myeloid differentiation. Both Trib2 and Trib1 induce this degradation by complexing with the E3 ligase COP1 and this cooperation has been confirmed by *in vivo* experiments (Keeshan et al., 2010, Yoshida et al., 2013). Mutants of both proteins lacking a conserved COP1-binding site are unable to induce murine AML, indicating that this binding site is crucial for their leukaemic activity (Keeshan et al., 2010, Yokoyama et al., 2010).. Trib3, instead, links COP1 ligase to lipid metabolism. Trib3 stimulates lipolysis during fasting and loss of insulin signalling by triggering the degradation of the enzyme promoting fatty acid synthesis (acetyl-coenzyme A carboxylase) in adipose tissue (Qi et al., 2006).

1.3.3 TRIB2

TRIB2 was identified as a direct *NOTCH1*-regulated transcript in a distinct subset of immature AML with silenced *CEBPA* and a mixed myeloid/T-lymphoid phenotype (Keeshan et al., 2006, Wouters et al., 2007). As described above, Trib2 was found to cause fatal transplantable AML when introduced in murine hematopoietic stem cells *in vivo* (Keeshan et al., 2006), but its tumorigenic activity is not limited to leukaemia. In fact, there is accumulating evidence indicating broad involvement of TRIB2 in both solid and non-solid malignancies. In melanoma, TRIB2 mediates downregulation of the tumour suppressor FOXO3a by promoting its cytoplasmic sequestration and impairing its transcriptional control function (Zanella et al., 2010). In lung cancer, TRIB2 acts as a tumorigenic driver through a mechanism involving association with the E3 ligase TRIM21 and downregulation of the C/EBPα transcription factor (Zhang et al., 2012, Grandinetti et al., 2011). TRIB2 was also identified as a critical downstream effecter of Wnt signalling in liver cancer cells (Wang et al., 2013a). TRIB2 was found to downregulate the Wnt signalling key factors *β*-catenin and transcription factor 4 (TCF4) through its associated E3 ligases Smad ubiquitination regulatory factor 1 (Smurf1), *β*TrCP and COP1. The binding region of Smurf1 encompasses amino acids 1–5 in the N-terminal region of TRIB2 protein. The binding region of *β*TrCP encompasses TRIB2 amino acids 307–323, and the binding region of COP1 encompasses TRIB2 amino acids 324–343, both in the C-terminal domain. Deletion of the binding regions of these E3-ligases within the TRIB2 protein abolished its ability to decrease protein stability of *β*-catenin and TCF4 (Xu et al., 2014). In T-cell ALL (T-ALL), *TRIB2* was identified as a direct target for upregulation by the oncogenic transcription factor TAL1 and found to be required for the survival of T-ALL cells (Sanda et al., 2012).

It is noteworthy that TRIB2 expression was found to be elevated in the cancers in which it has an oncogenic role, highlighting the importance of understanding how its expression is governed. Indeed, several mechanisms underlying the regulatory network of TRIB2 have been identified in different cell contexts. These include the previously mentioned NOTCH1 (Wouters et al., 2007), MEIS1 (Argiropoulos et al., 2008) and TAL1 (Sanda et al., 2012), as well as GATA2, FOG1 (Mancini et al., 2012) and PITX1 (Nagel et al., 2011). A number of microRNAs also regulate the expression levels of TRIB2, including but not limited to miR-511, miR-1297 (Zhang et al., 2012), miR-99 (Zhang et al., 2013), miR-155 (Palma et al., 2014), and let-7 (Wang et al., 2013c). Moreover, the E3 ligase Smurf1 is also involved in the ubiquitination and proteasomal degradation of TRIB2 in liver cells, that

requires the phosphorylation of TRIB2 at Serine 83 by P70 S6 kinase (P70S6K) (Wang et al., 2013b). Stability and ubiquitination of TRIB2 in liver cells is additionally thought to be negatively regulated by the E3 ligase complex SKIP1-CUL1 (Cullin)-F-box (SCF) βTrCP (Qiao et al., 2013).

Collectively, the current knowledge on TRIB2 points towards a network of both regulatory molecules and binding partners in which *TRIB2* acts as a powerful oncogene. This is an on-going research, with new mechanisms yet to be identified. Significant for the current study, previous studies have connected TRIB2 with two protein arginine methyltransferases (PRMTs). Interaction with PRMT6 was reported by a yeast two-hybrid screening approach involving short-read second-generation sequencing (Weimann et al., 2013). TRIB2 was also recently associated with the post-translational modifier PRMT5 by a mass spectrometry assay (data from Prof Claire Eyers, University of Liverpool, further included in (Uljon et al., 2016)) and this will be detailed in Chapter 5. It is also significant that the tumorigenic role of TRIB2 is often associated with its ability to promote degradation of key substrates, whose stability and downstream targets are affected. This happens via association with E3 ubiquitin ligase enzymes and engagement of the ubiquitin proteasome system (UPS), hence considered an attractive therapeutic target and further discussed.

1.4 The proteasome as a therapeutic target

1.4.1 The UPS

Two main routes have been identified for intracellular eukaryotic protein degradation involving either lysosomes or proteasomes. Transmembrane proteins and proteins that enter the cell from the extracellular milieu after endocytosis are degraded in lysosomes, a proteolytic pathway that occurs mostly under stressed conditions. Proteasomes, via the UPS, are in turn, responsible for the highly selective turnover of intracellular proteins that occurs either under basal metabolic conditions or stress (Ciechanover, 1994). This mechanism of proteolysis was discovered at the beginning of the 1980s by Aaron Ciechanover, Avram Hershko and Irwin Rose, which resulted in the three scientists from the Fox Chase Cancer Center (Philadelphia, USA) being jointly awarded with the 2004 Nobel Prize in Chemistry for the discovery of “ubiquitin-mediated protein degradation”.

The UPS plays a central role in maintaining cellular protein homeostasis through the targeted degradation of approximately 80% of intracellular proteins. Selected targets are damaged, misfolded and short-lived regulatory proteins that control critical cellular functions, including cell cycle control, transcription, DNA damage repair, protein quality control and antigen presentation. Degradation via the UPS involves two distinct and consecutive steps: covalent attachment of multiple ubiquitin (Ub) molecules to a protein substrate and proteasomal degradation (Ciechanover, 1998).

1.4.1.1 Ubiquitination and ubiquitin as a versatile cellular signalling

Ub-labelling of proteins is known as ubiquitination and is mediated by a sequential series of enzymatic activities. An E1 Ub-activating enzyme, that can be either Ube1 or Ube1-L2, activates Ub in an ATP-dependent manner and connects it to one of several Ub-conjugating enzymes (E2). The activated Ub is then transferred to a target protein by a member of the E3 Ub-ligase family (Hershko and Ciechanover, 1998, Jariel-Encontre et al., 2008). Anchoring of the Ub moiety to the substrate occurs by covalent attachment to the amino ($-NH_2$) group of either the N-terminal residue (Breitschopf et al., 1998, Aviel et al., 2000, Reinstein et al., 2000) or internal lysine(s) (Glickman and Ciechanover, 2002). Replication of the three-step enzymatic cascade generates a poly-Ub chain that marks the protein for degradation in the proteasome (Figure 1.5A). Ubiquitination can be reversed through the action of deubiquitinating enzymes (DUBs). Balance between the opposing actions of ubiquitin ligases an DUBs plays a critical role in regulating protein turnover and function (Hochstrasser, 1995).

Ub chains of at least four molecules that form through their lysine residues at position 48 (K48) seem to invariably flag the protein for proteasome-mediated degradation (Thrower et al., 2000), even if some proteins enter this proteolytic route without the requirement of a Ub-tag, *e.g.*, ornithine decarboxylase (Murakami et al., 1992), p21/Cip1 (Sheaff et al., 2000), retinoblastoma (Rb) family of proteins (Kalejta and Shenk, 2003), hypoxia-inducible factor 1 (Kong et al., 2007), calmodulin and troponin C (Benaroudj et al., 2001). Given that Ub has seven acceptor lysines, the highly evolutionarily conserved 76-amino-acid molecule can also be conjugated via its K6, 11, 27, 29,33 and 63, forming chains with variable lengths and linkage types (Ikeda and Dikic, 2008). Ub can also modify substrate proteins in its monomeric form. Such different post-translational modifications serve, however, alternative purposes to proteolytic degradation. Mono-ubiquitination instead controls cellular processes such as regulation of transcription, DNA repair, cellular

localization, epigenetic events and protein trafficking in the endocytic pathway (Hicke, 2001, Raiborg et al., 2006). Also the formation of K63-linked poly-ubiquitin chains seem to serve purposes that partially overlap those of the mono-ubiquitination, including intracellular trafficking, transcription, DNA repair and replication (Pickart and Eddins, 2004, Haglund and Dikic, 2005).

1.4.1.2 Proteasomal degradation

Substrate proteins tagged with K48-linked Ub polymers are degraded to small peptides by the 26S proteasome. The 26S or constitutive proteasome is a multi-subunit complex localized in both the nucleus and the cytoplasm of eukaryotes. It combines two 19S regulatory caps, which contain ATPases and act as a recognition and entry site for proteins destined for proteolysis, with a central core termed the 20S proteasome (Figure 1.5B). In the 19S particle, free and recyclable Ub molecules are released and the target protein is unfolded, linearized and fed into the 20S proteasome (Groll et al., 2000, Navon and Goldberg, 2001), a cylindrical structure composed of four heptameric rings that create a chamber for proteolysis to occur. The two outer rings are composed of α-subunits, whereas seven distinct β-subunits form the two inner rings. At least 3 of the β-subunits harbor the proteolytically active sites of the proteasome (Groll et al., 1997) that are classified upon preference to cleave after a particular amino acid residue. The three catalytic activities, chymotrypsin-like (CT-L), trypsin-like (T-L) and caspase-like (C-L) are encoded by separate polypeptides, β5, β2 and β1, respectively (Figure 1.5B).

An alternative proteasome isoform known as the immunoproteasome can be formed predominantly in haemopoietic cells and in cells that have been exposed to gamma-interferon (IFN-γ) or particular proinflammatory cytokines (Akiyama et al., 1994, Stohwasser et al., 1997, Sijts and Kloetzel, 2011). The immunoproteasome expresses subunits LMP7, MECL1 and LMP2 in place of β5, β2 and β1, altering the proteasome to favour the generation of antigenic peptides to be presented by the major histocompatibility complex (MHC) class 1 molecules and, thus, potentiating the immune system response (Rock et al., 1994).

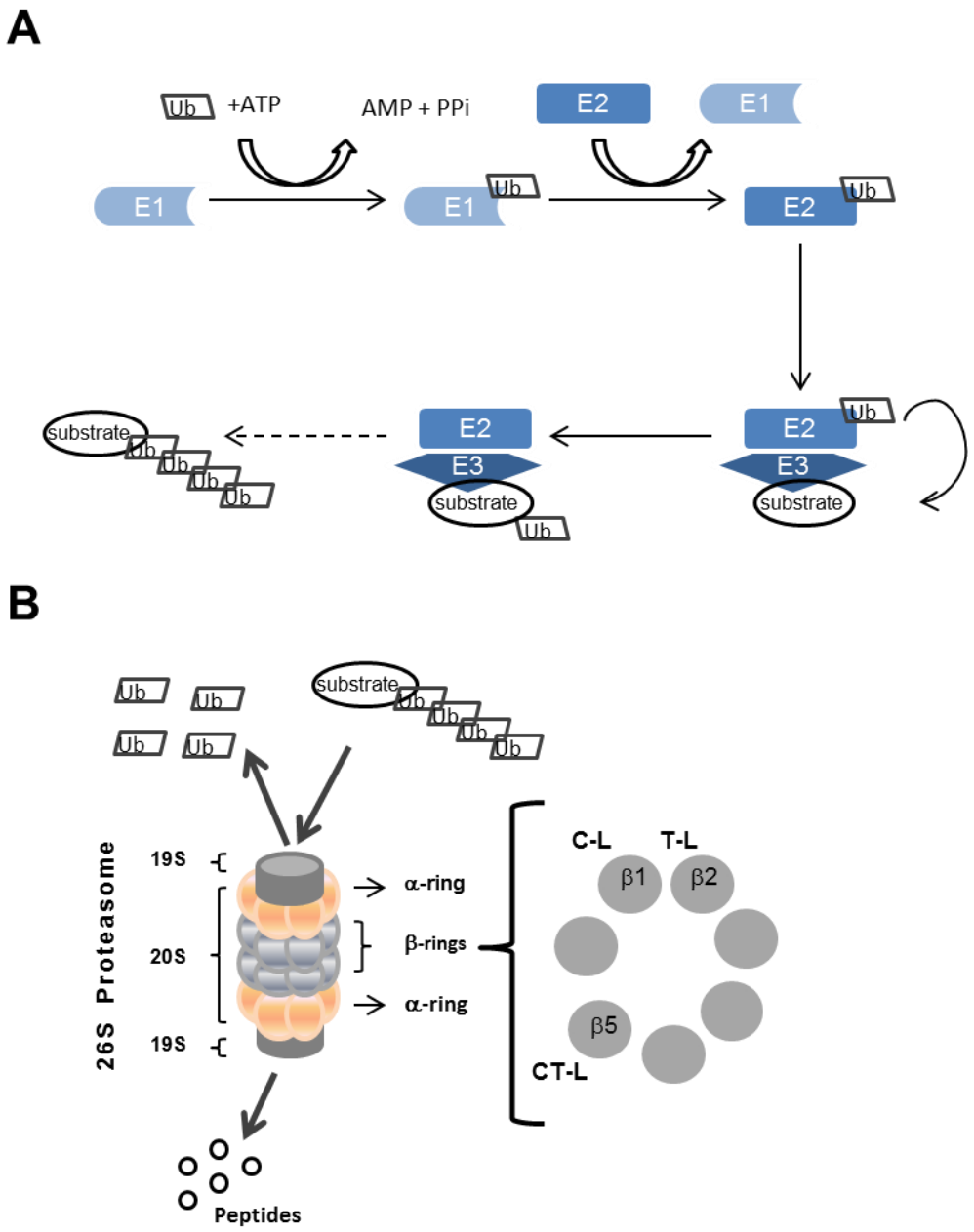

Figure 1.5 The ubiquitin proteasome system (UPS) for protein degradation
(A) The UPS is responsible for the degradation of poly-ubiquitinated proteins formed by a cascade of E1, E2 and E3 enzymes, which activate, conjugate and transfer multiple ubiquitin (Ub) moieties to protein substrates to be degraded, allowing tight regulation and high selectivity of degradation. (B) The functionally active 26S proteasome is a 2.4 MDa ATP-dependent proteolytic complex that consist of a 20S catalytic cylindrical complex capped at both ends by 19S regulatory subunits. Ub molecules are removed at the 19S cap through interaction with the outer α-rings and the protein is unfolded and fed into the inner catalytic chamber of the 20S proteasome, where the protein is cleaved into small peptides using 3 main catalytic activities, chymotripsin-like (CT-L), trypsin-like (T-L) and caspase-like (C-L).

Given the important role that the UPS plays in regulating protein stability and thus normal cellular function, it is not surprising that aberrant activity of this system has been implicated in a variety of pathologies, including Alzheimer´s Disease (Keller et al., 2000a), ischaemic stress (Keller et al., 2000b), diabetes (Broca et al., 2014) and cancer (Arlt et al., 2009, Yu et al., 2009), in which haematological malignancies are included (Crawford and Irvine, 2013). UPS abnormalities have been described as a result of deregulation in regulatory pathways that are mediated by proteasome substrates, rather than specific defects in proteasome structure or function (Adams, 2004).

1.4.2 Targeting the UPS

Targeting intracellular protein turnover by inhibiting the UPS has recently emerged as a rational strategy for cancer therapy. The catalytic molecular properties of the proteasome have been exploited chemically and pharmacological interference with UPS-mediated proteolysis has been validated by a class of compounds collectively referred to as proteasome inhibitors.

The possibility of targeting the proteasome for cancer therapeutics, although initially doubted due to the essential role the UPS plays in critical biological processes, was well supported by a wealth of experimental data. Pre-clinical results showed proteasome inhibitors to be well tolerated with activity against *in vivo* models bearing human malignancies (Orlowski et al., 1998). Moreover, it has been demonstrated that malignant cells harbor elevated proteasome activity compared with normal cells (Arlt et al., 2009, Ma et al., 2009) and have been shown to be relatively more sensitive to the effects of proteasome inhibitors than their non-malignant counterparts. This differential susceptibility was suggested to be associated with a higher dependency of highly proliferative malignant cells on the proteasome system to remove aberrant proteins. Another explanation is that inhibition of the proteasome activity interferes with cell-cycle or apoptosis molecules that have caused the development or maintenance of the cancerous phenotype (Adams et al., 1999)

Most proteasome inhibitors are based on peptides that serve as active-site analogs, which bind to the proteasome subunits. Eight classes of proteasome inhibitors have been recognized across natural compounds and synthetic molecules (peptide aldehydes, peptide vinyl sulfones, syrbactins, peptide boronates, peptide epoxyketones, peptide ketoaldehydes, β-lactones and oxatiazol-2-ones). Only representative members of some

classes have reached the stage of clinical trials investigations in cancer. Many have failed due to the lack of specificity and/or toxicity in preclinical studies. Potent inhibition of the CT-L activity of the proteasome is a shared property of the clinically relevant proteasome inhibitors (Bennett and Kirk, 2008) and is suggested to be a necessary feature of these drugs to produce an anti-tumor response (Parlati et al., 2009).

1.4.2.1 Bortezomib

The modified dipeptidyl boronic acid bortezomib (Brtz, former name PS-341, brand name Velcade) (Palombella et al., 1998, Adams et al., 1999) was the first proteasome inhibitor to be introduced into medical practice. Supported by preclinical and clinical studies, the US Food and Drug Administration (FDA) approved in 2003 and 2006 the use of Brtz for the treatment of multiple myeloma and mantle cell lymphoma, respectively (Kane et al., 2003, Kane et al., 2007). Moreover, the selective and reversible inhibitor of the CT-L (β5 and LMP7) subunit has shown *in vitro* and *in vivo* activity against a variety of other haematological malignancies and solid tumours, either as a single agent or as a part of combination therapy (Chen et al., 2011). Therapeutic proteasome inhibition has shown, however, better results in blood cancers than in solid tumours (Orlowski and Kuhn, 2008) and this could be due to the fact that leukaemic cells express high levels of proteasomes (Kumatori et al., 1990).

1.4.2.2 Other UPS inhibitors

The development of Brtz has transformed the treatment of multiple myeloma and mantle cell lymphoma. Following on its success, efforts are focused on the development of second-generation proteasome inhibitors and small molecule inhibitors of other UPS components. The core aim is to extend the spectrum of Brtz efficacy, hampered by the appearance of dose-limiting toxicity (particularly peripheral neuropathy), limited activity in solid tumours and drug-resistance. Recently, the FDA approved the epoxyketone peptide carfilzomib for the treatment of relapsed/refractory multiple myeloma, while oprozomib, ixazomib, marizomib and delanzomib have already reached clinical trials investigation (Crawford and Irvine, 2013). The activity of immunoproteasome-specific inhibitors is also currently being investigated and thought to be particularly efficacious for the treatment of haematologic maliganacies. The immunoproteasomes are predominantly expressed in cells of haemopoietic origin. Targeting them alone can, therefore, provide a certain amount of specificity and an opportunity to overcome toxicities associated with proteasome inhibition. Enzymes upstream of the proteasome are also being actively explored as

selective targets. In this category, compounds directed at E1, E2, E3 and DUB enzymes have been developed to block aberrant pathways in malignant cells (Crawford and Irvine, 2013). Other examples of therapeutic agents that interfere with UPS action include an inhibitor of the 19S ATPase reported to impair the degradation of folded proteins (Lim et al., 2007) and the Nutlins, which inhibit the interaction of the E3 ligase MDM2 with the tumour-suppressor protein p53 (Vassilev et al., 2004).

1.4.3 Mechanisms of anti-cancer activity of proteasome inhibitors

Although molecular mechanisms underlying proteasome inhibitors´ anti-cancer activity are not fully elucidated, it is clear that multiple pathways are involved, as detailed in several reviews (Almond and Cohen, 2002, Adams, 2004, Nencioni et al., 2007, Crawford and Irvine, 2013). One of the first mechanisms of action attributed to proteasome inhibitors was suppression of the nuclear factor kB (NF-kB) signaling pathway, which has a critical role in multiple myeloma pathogenesis, hence the first disease to be considered a target for proteasome inhibition therapy (Hideshima et al., 2001). While contradicted by recent studies (Dolcet et al., 2006, Hideshima et al., 2009), proteasome inhibition was shown to block activation of the inflammation-associated transcription factor NF-kB by preventing degradation of its inhibitory molecule IkB, which in response to stress (*e.g.* neoplasia and chemotherapy) becomes phosphorylated, ubiquitinated and deactivated by the 26S multi-subunit complex. Association of stabilized IkB with NF-kB confines them to inactivity in the cytoplasm, thereby downregulating levels of NF-kB transcriptional targets (such as IL-6) and promoting pro-survival pathways (Finco and Baldwin, 1995).

Although the UPS is the predominant non-lysosomal pathway of proteolysis in eukaryotic cells, proteasome inhibition also has other known effects. Many of these contribute to anti-tumour activity since proteasome substrates are often known mediators of proliferation and apoptotic signaling pathways that are deregulated in cancer. Proteasome inhibition has been proposed to induce apoptosis by stabilizing pro-apoptotic p53, Bax proteins and NOXA, while reducing levels of anti-apoptotic proteins such as Bcl-2 and inhibitor of apoptosis family of protein (Zhang et al., 2004a). Other mechanisms ascribed to proteasome inhibitors are disruption of the unfolded protein response (UPR) with pro-apoptotic endoplasmic reticulum (ER) stress induction (Lee et al., 2003) and increase of intracellular reactive oxygen species and oxidative stress (Perez-Galan et al., 2006). Moreover, studies on the proteasome inhibition effect in multiple myeloma cells showed that it triggers a dual apoptotic pathway of mitochondrial cytochrome c release and

caspase-9 activation, as well as activation of Jun kinase and a Fas/caspase-8-dependent apoptotic pathway (Mitsiades et al., 2002). Proteasome inhibitors were also shown to cause G2/M cell cycle arrest in cell lines of different origins, namely, ovarian (Bazzaro et al., 2006), prostate (Adams et al., 1999) and non-small lung cancer (Ling et al., 2002), multiple myeloma (Buzzeo et al., 2005) and AML (HEL cells) (Colado et al., 2008). The effect on cell cycle regulation is associated with stabilisation of the tumour suppressor molecule P27KIP1, which prevents activation of both cyclin D and cyclin E to negatively regulate progression through the G1/S phase of the cell cycle (Pagano et al., 1995). Furthermore, proteasome inhibition appears to regulate DNA repair (Motegi et al., 2009) and elicits anti-angiogenic effects on the tumour microenvironment, including reduced multiple myeloma cells migratory capacity in response to vascular endothelial growth factor (VEGF) (Podar et al., 2004, Roccaro et al., 2006). Other effects of proteasome inhibitors appear to promote cellular survival, such as activating multiple heat-shock protein (HSP) family members, inducing the stress response protein MKP-1 and promoting activity of the protein kinase B/Akt pathway. Fortunately, on balance, the net effect is typically a pro-apoptotic one, as evidenced by the findings of the first study of Brtz (Orlowski and Kuhn, 2008).

Given the central role of the proteasome in protein homeostasis and cellular physiology, discussion on the ultimate targets of proteasome inhibitors is ongoing and additional studies are needed to better understand the mechanisms of the apoptotic cascades mediated by this class of compounds. However, it seems clear that proteasome inhibition holds much promise as a new investigational avenue for treatment of haematological malignancies and cancer therapy in general.

1.5 Aims

The following thesis is an investigation on TRIB2 in the context of human AML, from both a biological and therapeutic angle. Experiments were designed to address the subsequent specific aims:

1.To evaluate *TRIB2* oncogenic properties in human AML cells;

2.To investigate if high TRIB2 AML cells are responsive to proteasome inhibition treatment;

3.To examine whether TRIB2 interacts with PMRT5.

Chapter 2:
Materials and Methods

2.1 Tissue Culture

Tissue culture was conducted using a laminar air flow hood. An aseptic technique was maintained with all materials sprayed in 70% alcohol prior to use.

2.1.1 Culture of cell lines

All cell lines were maintained at 37°C with 5% CO_2, counted and passaged every two days with warm fresh medium to maintain a density of ~$0.15x10^6$ cells/mL. Cell lines were passaged for a maximum of 2 months, after which new seed stocks were thawed and tested for mycoplasma contamination using the MycoAlert mycoplasma detection kit (Lonza, PN LT07-318) according to the manufacturer's instructions.

Adult AML cell lines OCI-AML5 and MUTZ-2, paediatric AML cells SB1690CB and SBRes, and the human bladder carcinoma cell line 5637 were kindly provided by Dr. Stefan Meyer (University of Manchester). SBRes cell line was derived from SB1690CB after selection for resistance to mitomycin-c. All cells were cultured in Roswell Park Memorial Institute (RPMI) 1640 (Life Technologies, PN 12633-012) medium supplemented as described in Table 2.1. The 5637 cell line-conditioned media was used as a source of several functional cytokines, including G-CSF and GM-CSF. Dr. Stefan Meyer also provided CV1665, CV1785, CV1810 and CV1939 cells. These cell lines are derived from patients carrying Fanconi anaemia-associated defects and were used as a model of non-AML cells. The U937, NB4 and Kasumi-1 AML cells were available *in-house* and grown in suspension culture (Table 2.1). K562 leukaemic cells were also grown in RPMI 1640 complete medium (Table 2.1). Human embryonic kidney cells 293T cells were used for lentiviral packaging and transient transfection, and mouse embryonic fibroblast 3T3 cells were grown for virus titration. Both of these adherent cell lines were maintained in Dulbecco's modified eagle medium (DMEM, Life Technologies, PN 11966-025) complete media (Table 2.1).

Table 2.1 Cell lines and growth media

Cell line	Culture Media
293T	DMEM, 10% FBS, 1% L-Glutamine 1% Pen/St
3T3	DMEM, 10% FBS, 1% L-Glutamine 1% Pen/St
CV1665	RPMI 1640, 15% FBS, 1% L-Glutamine 1% Pen/St
CV1785	RPMI 1640, 15% FBS, 1% L-Glutamine 1% Pen/St
CV1810	RPMI 1640, 15% FBS, 1% L-Glutamine 1% Pen/St
CV1939	RPMI 1640, 15% FBS, 1% L-Glutamine 1% Pen/St
K562	RPMI 1640, 10%FBS 1% L-Glutamine 1% Pen/St
Kasumi-1	RPMI 1640, 20% FBS, 1% L-Glutamine 1% Pen/St
MUTZ-2	RPMI 1640, 20% FBS, 15% conditioned medium from 5637 cells, *h* IL-3 (10 ng/mL)
NB4	RPMI 1640, 10% FBS, 1% L-Glutamine 1% Pen/St
OCI-AML5	RPMI 1640, 20% FBS, 15% conditioned medium from 5637 cells, *h* IL-3 (10 ng/mL)
SB1690CB	RPMI 1640, 20% FBS, 15% conditioned medium from 5637 cells, *h* IL-3 (10 ng/mL)
SBRes	RPMI 1640, 20% FBS, 15% conditioned medium from 5637 cells, *h* IL-3 (10 ng/mL)
U937	RPMI 1640 10% FBS, 1% L-Glutamine 1% Pen/St

FBS, foetal bovine serum (Life technologies); L-Glutammine (Life technologies); Pen/St, Penicillin/streptomycin solution, 10,000UmL^{-1}/10,000gmL^{-1} (Life technologies); *h*IL-3 (Peprotech).

2.1.2 Culture of murine primary cells

Primary murine cells collected from the BM were maintained in liquid culture in DMEM medium containing 15% FBS, 1% Pen/St, 1% L-Glutamine and supplemented with *m*IL-3 (10 ng/mL), *m*IL-6 (10 ng/mL) and *m*SCF (10 ng/mL) (PeproTech). Cytokines were freshly added, prior to cell culture.

2.1.3 Culture and recovery of human primary AML cells

PB samples from AML patients were collected following protocol approved by the Local Research and Ethics Committee and those involved gave their informed consent in accordance with the Declaration of Helsinki. Cells were either obtained from cryopreserved samples or cultured immediately after processing of the AML patients PB. For recovery of the cryopreserved samples, AML mononuclear cells (MNCs) were thawed in a 37ºC water bath and transferred into sterile 50 mL falcon tubes. To ensure slow rehydration of cells and prevent or minimize cell clumping, thawing media (Table 2.2) was supplemented with DNAse I 10000 units/L (Stemcell Technologies, PN 7900). 10 mL of the supplemented media (1 mL in 20 mL final volume of thawing media per sample) were added dropwise to each sample over 20 min with gentle swirling of the tubes, followed by centrifugation at 192 x g for 15 min at 4 ºC. Cells were resuspended in additional 10 mL of supplemented thawing media. After centrifugation at 192 x g for 10 min 4ºC, pellets were

resuspended in 1 mL of culture media supplemented with a freshly added growth factor cocktail for cell survival (Table 2.3). Cells were passed through sterile 70 µm cell strainers into new falcon tubes, seeded at a density of 1-2x10^6 cells/mL and incubated for a few hours or overnight (O/N) for recovery prior to downstream experiments. MNCs immediately obtained after possessing of patient samples were directly cultured in the culture media (Table 2.3). MNCs were isolated by using Histopaque (Sigma-Aldrich) and density-gradient centrifugation.

Table 2.2 Thawing media

FBS-ESC (Biosera, PN FB-10015/500-4253)	100 mL
Heparin (5000U/mL)	4 mL
L-Glutamine	5 mL
IMDM (Life Technologies, PN 12633-012)	up to 500 mL

Table 2.3 Culture media

StemSpan (Stemcell Technologies, PN 9650)	45 mL
Myelocult (Stemcell Technologies, PN H5100)	5 mL
*h*IL-3 (100 µg/mL stock, Pepro Tech)	5 µL
*h*IL-6 (100 µg/mL stock, Pepro Tech)	5 µL
*h*SCF (100 µg/mL stock, Pepro Tech)	5 µL
*h*FLIT3-L (100 µg/mL stock, Pepro Tech)	5 µL

2.1.4 Plasmid vectors

The expression plasmids PHMA-mTRIB2-Myc and pcDNA3.1-PRMT5-HA were used for Co-Immunoprecipitation. The latter was kindly provided by Dr. Stephen Nimer, University of Miami/Sylvester Comprehensive Cancer Center. pLKO.1-puro-CMV- TurboGFP or pLKO.1-puro-CMV-TurboGFP-shTrib2 (shCtrl/shTRIB2, Sigma-Aldrich) were used for lentiviral-mediated downregulation of TRIB2 (target sequence: GCGTTTCTTGTATCGGGAAAT). For TRIB2 overexpression, PhrCtrl was used as control and PhrTRIB2 was made by subcloning murine Trib2 into the phr-SIN-BX-IRES-EmGFP (Phr) lentiviral backbone. This is a a bicistronic (IRES - internal ribosome entry site) transfer vector expressing emerald green fluorescent protein (EmGFP) as a marker and generating self-inactivating (SIN) lentiviral particles for improved safety. shCtrl/shPRMT5#1/ShPRMT5#2 were used for PRMT5 knockdown and are expressed in pLKO.1-puro vector (kindly given by Dr. Xu Huang, University of Glasgow). The retroviral constructs produced for TRIB2 downregulation were the LMP control or LMP-shTrib2 (target sequence: TCCTAATCTCTTCAATCAATAAA). For overexpression of

full-length (42 kDa) C/EBPα, a bicistronic retrovirus (MigR1) was used, containing the IRES-GFP elements and carrying C/EBPα cDNA lacking the uORF.

2.1.5 Virus production

2.1.5.1 Lentivirus

For lentiviral vectors production, $4.5x10^6$ 293T cells were plated in 10 cm dishes 24 h before transfection ($CaCl_2$ method). 3-4 h prior to transfection, 10 mL of fresh medium (Table 2.1) were added to the cells. The lentiviral transfer vector DNA (15 µg), together with psPAX2 packaging (10 µg) and VSVG envelope plasmid DNA (6 µg) were combined. Plasmids were previously verified by restriction enzyme digestion (psPAX2 digested with EcoRI renders 1.7 and 4.3 kb fragments, and VSVG digested with BamHI results in two bands of 1.7 and 4.7 kb). The precipitate was formed by adding 31 µg of DNA to a final volume of 500 µL dH_2O and 61 µL 2.5M $CaCl_2$. The mixture was added dropwise to 500 µL 2X HEPES-buffered saline (280 mM NaCl, 50 mM HEPES, 1.5 mM Na_2HPO_4, pH 7.05) while vortexing the 15 mL falcon tube to vigorously bubble air through the DNA mix. The solution was incubated at room temperature (RT) for 5 min. Following this, the solution was added dropwise to the cells. Dishes were rocked gently in a circular motion to distribute the precipitates, and then returned to the incubator. 12 to 16 h later, the medium was replaced with fresh growth medium supplemented with 2% FBS and incubated at 5% CO_2 for 24 h prior to the initial collection of viral supernatant. A second collection was made after a further 24 h. The conditioned medium from the two harvests was centrifuged at 432 x g for 5 min at 4ºC to discard cell debris. Aliquots of viral supernatants were snap frozen on dry ice and stored at -80ºC.

2.1.5.2 Retrovirus

For retrovirus production, the same protocol described for lentivirus production was adopted, with the following changes: pCGP (digestion with HindIII renders 4.5 and 6.2 kb fragments) was used as packaging construct instead of psPAX2. Also, to prepare the DNA cocktail, $CaCl_2$ was used at 2M and 50 µL 10X NTE buffer (2 M NaCl, 1 M Tris-HCl pH 7.4, 0.25 M EDTA pH 8.0, dH_20 up to 100 mL) were also included in the mixture. The DNA mixture was added to only 3 mL of fresh media and replaced after 6 h transfection with 4.5 mL of pre-warmed media. Supernatants containing packaged virus particles were collected after 24, 48 and 72 h.

2.1.6 Virus titration

For constructs co-expressing GFP, titres were determined by transducing 3T3 cells. Cells were seeded the day before transduction at 2×10^5 in 6 cm dishes. After 24 h, 1 mL of fresh growth media (Table 2.1) was added to each plate, supplemented with 8 µg/mL polybrene (Sigma-Aldrich, PN 107689, stock at 4 mg/mL). Titres were determined with 1:10 and 1:100 dilutions of virus stocks added to the 3T3 cells plates. The following day, 2 mL of fresh growth medium were added to the plates. After further 24 h of incubation, cells were harvested and GFP expression was determined by flow cytometry using FITC channel on BD FACSCanto™ II. Acquired data were analysed using FlowJo software (Treestar, v10).

2.1.7 Transduction of suspension cells

Cells were seeded at $0.2x10^6$/mL on the day before transduction so as to be in the logarithmic growth phase at the beginning of the experiment. Cells were transduced either with lentiviral or retroviral constructs. Briefly, cells were harvested and resuspended in complete culture medium supplemented with extra 10% FBS and polybrene (Sigma-Aldrich, PN 107689, stock at 4 mg/mL) at 8 µg/mL. Cryopreserved aliquots with 1 mL of virus supernatant were thawed in a water bath and added into target cells. Cells were centrifuged for 60 min at 1250 x g and returned to the incubator. After 3-6 h, fresh media was added to the cells (up to a final volume of 10 mL) for O/N incubation. Selection of efficiently transduced cells was achieved by either sorting GFP+ cells or treatment with 2 µg/mL puromycin (Sigma-Aldrich, PN P7255, 10 mg/mL stock) for 48 h to eliminate non-infected cells. Non-transduced cells were included as a control for puromycin selection.

2.1.8 Drugs

Brtz (M.W. 384.24) was purchased from LC laboratories (PN B-1408) and prepared as a 25 mg/mL (65 mM) stock. Peptido sulfonyl fluoride (SF; M.W. 656.85) was provided by Professor Robert M. Liskamp and Raik Artschwager (School of Chemistry, University of Glasgow). Drug was prepared as a 21.9 mg/mL (33 mM) stock. Carfilzomib (Cfz; M.W. 719.91) was purchased from LC laboratories (PN C-3022). A 50 mg/mL (69 mM) stock was made. All drugs were prepared in dimethyl sulphoxide (DMSO) and stored as single use aliquots at -20ºC.

2.1.8.1 *In vitro* drug treatment

Cells were plated at $0.2x10^6$/mL and were treated with 10 nM Brtz, 500 nM SF, 10 nM Cfz or DMSO only. After 6, 8, 16 or 24 h cytotoxicity was assessed as described in section 2.8. Treatment time points are indicated in the related Figure legends.

2.1.8.2 Methylcellulose colony-forming assay of Brtz treated and untreated secondary Trib2 murine cells

Primary Trib2 murine AML cells propagated in secondary transplanted recipients were collected and treated with Brtz at 10 nM or DMSO. After 24 h, cells were counted by the trypan blue exclusion. 1.4×10^4 cells were then plated in duplicate in methylcellulose media (MethoCult™ GF M3434, Stem Cell Technologies). Colonies were scored at 7 days under an inverted microscope and analysed by FACS for detection of myeloid cell surface markers with CD11b-APC and Gr-1-PE or Gr-1-PECy7 antibodies (Table 2.13).

2.1.8.3 *In vivo* drug treatment

The 25 mg/mL stock of Brtz was diluted on day of treatment with sterile phosphate buffered saline (PBS). Treated mice were injected with Brtz at a dose of 0.5 mg/kg body weight.

2.2 PCR-based assays

2.2.1 Primer pair design

Primers for SYBR Green detection and fluidigm assay were designed using Primer-BLAST software available at NCBI website (http://www.ncbi.nlm.nih.gov/tools/primer-blast) and following specific considerations. Forward and reverse primers have approximately 20 bp with similar melting temperature (T_m ; ~60ºC) and a GC content in the range of 40-60%. All selected primers amplify *amplicons* within the target genes of about 100 to 180 bp and were checked for absence of self-complementary capability or complementary to the other primer in the reaction mixture. This encourages formation of hairpin structures and primer-dimers that would compete with the template for the use of primer and reagents and could lower the amplification yield of the desired target region. In addition, primers are either spanning an intron or overlapping an exon-exon junction to allow a product obtained from the cDNA to be distinguished from unspliced genomic DNA contamination. Primers that were found to anneal to sequences other than the

intended target were re-designed using the NCBI´s primer designing tool. The primer sequences are shown in Table 2.4. Primers were synthesised commercially by Integrated DNA Technologies and reconstituted with the appropriate volume of nuclease-free H_20 (Qiagen, PN 129114) to attain a stock concentration of 100 μM. Dilutions were made to achieve the appropriate working concentration of 10 μM and aliquots were prepared to ensure sterility and stored at -20ºC. For detection of some genes, validated sequences were provided by Dr. Helen Wheadon (University of Glasgow), as depicted in Table 2.4.

Table 2.4 Primer sequences

Gene Symbol	Specie	Oligonucleotide sequence (5'-3')
ABL [a,b]	human	*forward* TGGAGATAACACTCTAAGCATAACTAAAGGT *reverse* GATGTAGTTGCTTGGGACCCA
ATM	human	*forward* TGTGTAACTACTGCTCCAGACC *reverse* GCAGGTGGAGGGATTTGGTA
ATR	human	*forward* GCGCCACTGAATGAAACTGG *reverse* ACGGCAGTCCTGTCACTCTA
BAX	human	*forward* GCTGACATGTTTTCTGACGG *reverse* ATGATGGTTCTGATCAGTTCC
BCL2 [c]	human	*forward* GAGAAATCAAACAGAGGCCG *reverse* CTGAGTACCTGAACCGGCA
BID [c]	human	*forward* GGAACCGTTGTTGACCTCAC *reverse* GAGGAGCACAGTGCGGAT
BIM	human	*forward* CTCGGACTGAGAAACGCAAG *reverse* ACCTTGTGGCTCTGTCTGTA
B2M [b,c]	human	*forward* TTGTCTTTCAGCAAGGACTGG *reverse* ATGCGGCATCTTCTAACCTCC
BRCA2	human	*forward* GTTCCCTCTGCGTGTTCTCA *reverse* CCATCCACCATCAGCCAACT
CASP3	human	*forward* TGTGAGGCGGTTGTAGAAGTT *reverse* CGCTTCCATGTATGATCTTTGGTT
CASP8	human	*forward* GAGAGAAGCAGCAGCCTTGA *reverse* AGTTTGGGCACTTTCTCCCG
CDC 25 A	human	*forward* ACCTCAGAAGCTGTTGGGATG *reverse* CAGCCACGAGATACAGGTCT
ENOX2 [b,c]	human	*forward* GAGCTGGAGGGAACCTGATTT *reverse* CACTGGCACTACCAAACTGCA
MCL1 [c]	human	*forward* CATTCCTGATGCCACCTTCT *reverse* TCGTAAGGACAAAACGGGAC
P27KIP1	human	*forward* CCAAATGCCGGTTCTGTGGA *reverse* TCCATTCCATGAAGTCAGCGATA
PRMT5	human	*forward* CCTGTGGAGGTGAACACAGT *reverse* AGAGGATGGGAAACCATGAG
PTEN	human	*forward* CCGTTACCTGTGTGTGGTGA *reverse* AGGTTTCCTCTGGTCCTGGTA
RNF20 [b,c]	human	*forward* GGTGTCTCTTCAACGGAGGAA *reverse* TAGTGAGGCATCATCAGTGGC
TRIB2	human	*forward* AGCCAGACTGTTCTACCAGA *reverse* GGCGTCTTCCAGGCTTTCCA
XIAP	human	*forward* CGCTCATCGAGGGACGCC *reverse* TCCTTATTGATGTCTGCAGGTACAC
Hprt [b]	mouse	*forward* GAGAGCGTTGGGCTTACCTC *reverse* ATCGCTAATCACGACGCTGG
Trib2	mouse	*forward* AGCCCGACTGTTCTACCAGA *reverse* AGCGTCTTCCAAACTCTCCA

[a] Sequences retrieved from (Beillard et al., 2003); [b] Reference gene; [c] Sequences provided by Dr. Helen Wheadon

2.2.2 Total RNA extraction

An appropriate number of cells (0.2-1x10^6) were spun and washed in PBS by centrifugation at 432 x g for 5 min at 4°C before use. The RNeasy Mini Kit (Qiagen, PN 74106) was used as per manufacturer's instructions. The resulting RNA was quantified and examined for purity using a NanoDrop spectrophotometer ND-1000 (Labtech International Ltd). RNA was kept on ice at all times and stored diluted in nuclease-free H_20 at -80ºC.

2.2.3 Reverse Transcription PCR

cDNA was prepared from 1 µg RNA using the High-Capacity cDNA Reverse Transcription Kit (Applied Biosystems, PN 4368814) according to the manufacturer's instructions. 1 µg of RNA was converted to cDNA in a 20 µL reaction. When low RNA yields were obtained, the maximum volume of RNA was added to a 20 µL reaction. Briefly, RNA samples were prepared to a concentration of 1 µg per 13.2 µL in nuclease-free H_20 and mixed with 6.8 µL of pre-prepared 2X reverse transcription master mix in a PCR tube placed on ice. Components of the master mixture were added to give a final concentration/reaction of 1X RT-buffer, 4 mM dNTP mix, 1X RT random primers, 2.5 U/µL MultiScribe reverse transcriptase and 1 U/µL RNAase inhibitor. The 20 µL reaction mixture was run in a Mastercycler™ PCR machine. Thermal cycling conditions were used as per the manufacturer's instructions: 25ºC for 10 min, 37ºC for 120 min and 85ºC for 5 sec to denature the reverse transcriptase. The reaction was then cooled to 4°C. Synthesised cDNA prepared from 1 µg of RNA was further diluted to a final volume of 40 µL in nuclease-free H_20 and stored at -20°C.

2.2.4 Standard Polymerase Chain Reaction (PCR)

cDNA samples of human cell lines were amplified by PCR reaction for *TRIB2* detection. Primer sequences are listed in Table 2.4 and were also used for quantitative PCR analysis. PCR mix was prepared using FastStart High Fidelity PCR System (Roche, PN 03553426001) according to the manufacturer's instruction. Components of the mixture were added to each 0.2 mL PCR tube to give a final concentration per reaction of 1X reaction buffer, 200 µM of each dNTP, 0.4 µM of each forward and reverse primer, 2.5 U FastStart High Fidelity Enzyme Blend, 1.8 mM $MgCl_2$, 2 µL of cDNA and ddH_20 up to a final volume of 50 µL. The PCR tubes were heated to 95°C for 2 min and then 35 cycles of 95°C for 30 sec, 57°C for 45 sec and 72°C for 45 sec were set in a PCR Thermo Cycler. After all cycles finished, the tubes were heated to 72°C for 5 min for final extension and

then held at 4°C. PCR products were separated by 1.8% agarose gel electrophoresis in 1X TBE (5X TBE solution (Table 2.5) diluted in dH_20) and visualized by addition of SybrSafe™ (Invitrogen, PN S33102). A molecular ladder of 100 bp was run with samples to know the exact size of the PCR products. DNA was visualised under UV illumination, using the molecular imager® ChemiDoc Chemidoc™ XRS visualisation system.

Table 2.5 5X TBE

Components and final concentration	Amount to add per 1 L
445 mM Tris Base	54 g
445 mM Boric Acid	27.5 g
10mM EDTA (0.5 M, pH 8.0)	20 mL
dH_20	up to 1 L

2.2.5 Quantitative PCR (qPCR)

qPCR was performed using Fast SYBR® Green Master Mix (Applied Biosystems, PN 4385616). In a MicroAmp Optical 384-well reaction plate (Applied Biosystems, PN 4309849), a total volume of 10 µL/reaction was prepared containing 1X Fast SYBR® Green Master Mix (SYBR® Green I dye, AmpliTaq® Fast DNA Polymerase (Ultra Pure), Uracil-DNA glycosylase, dNTPs, ROX™ dye Passive Reference, in addition to optimised buffer components), 0.25 µM of each primer (forward and reverse at 10 µM) and 1 µL cDNA, diluted in nuclease-free H_2O. For each sample, each gene was assayed in technical triplicates with reference gene(s) used as internal control(s) to normalize input cDNA. Genes are indicated in the related Figure legends and primer sequences are listed in Table 2.4. A negative control containing nuclease-free H_2O in place of cDNA was included to reject the possibility of contamination. Plate wells were sealed and the plate was briefly centrifuged to eliminate any air bubbles and loaded onto a 7900HT Fast Real-Time PCR System (Applied Biosystems). The standard thermal cycling conditions were used as per the manufacturer's instructions: 95°C for 20 sec followed by 40 cycles of 95°C for 1 sec and 60°C for 20 sec and a final step of 50°C for 2 min. Data were acquired and analysed using SDS and RQ manager software (Applied Biosystems). Obtained baseline and threshold settings were reviewed and manually adjusted when needed. After normalization to the endogenous control gene(s), levels of gene mRNA expression in each sample were determined by the 2-ΔΔCT method of relative quantification and reported as fold change (Schmittgen and Livak, 2008). In the particular case of *ABL* (V-Abl Abelson Murine Leukaemia Viral Oncogene Homolog) and *TRIB2* mRNA amplification, a melt-curve profile was generated after qPCR reaction, confirming absence of non-specific

amplification and primer-dimer formation (Figure 2.1). Whenever indicated *ABL* was used as a reference gene based on a multicenter study aimed at selecting controls that are applicable for qPCR-based analysis of leukaemia patients. Beillard and colleagues selected *ABL*, *B2M* and *GUS* genes for extensive analysis. These genes were selected from 14 potential candidates based on the absence of pseudogenes and the level and stability of expression. Only *ABL* gene transcript levels did not differ significantly between normal and leukaemic samples at diagnosis and was therefore proposed to be used as reference gene for qPCR-based diagnosis in leukaemic patients, including quantification of fusion gene transcripts or aberrantly expressed genes (Beillard et al., 2003).

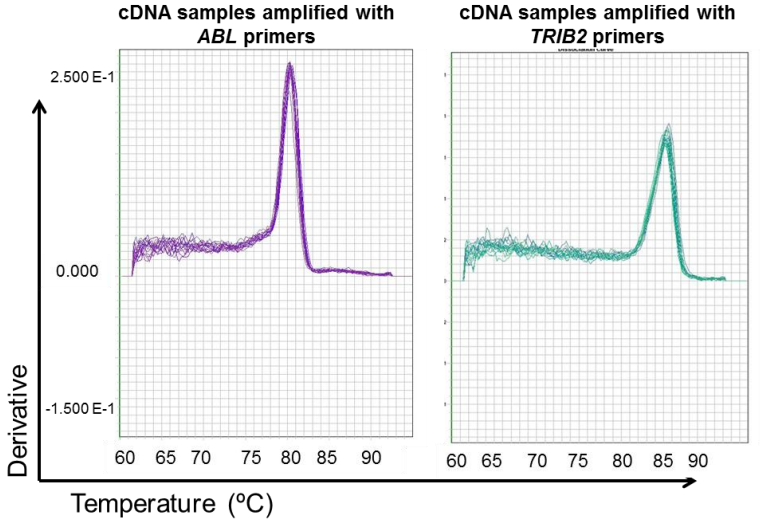

Figure 2.1 Melt-curve analysis confirmed specificity of *ABL* and *TRIB2* primers
Dissociation curve was obtained using the 7900HT Fast Real-Time PCR System. Because of their small size, primer-dimers usually melt at lower temperatures than the desired product. Additionally, non-specific amplification may result in PCR products that melt at temperatures above or below that of the desired product. A single peak matching either *ABL* (left) or *TRIB2* (right) amplification was detected, confirming specificity of the primers.

2.2.6 High-throughput qPCR – Fluidigm

High-throughput qPCR was performed on the 48.48 Dynamic Array™ IFC system (Fluidigm, PN BMK-M10-48.48EG) to analyse expression of target genes indicated in the related Figure legend. Primer sequences are listed in Table 2.4. Transcriptional analysis was conducted on cDNA samples that were purified from shCtrl- and shTRIB2-U937 sorted cells after 48 and 72 h transduction (2 independent replicates). For specific target pre-amplification, a primer mix was prepared by combining 1 µL of each of the 100 µM

primers to be included on the chip and diluting with TE buffer (Promega, PN V6231) to make a final volume of 200 µL. A total volume of 5 µL/reaction was prepared containing 3.75 µL of the pre-amplification mixture (1.25 µL primer mix and 2.5 µL Qiagen Multiplex PCR Kit (Qiagen, PN 206143)) and 1.25 µL of cDNA. The mixture was run in a Mastercycler™ PCR machine with the following conditions: 10 min at 95ºC followed by 14 cycles of 95 ºC for 15 s and 60 ºC for 4 min. The pre-amplified cDNAs were treated with Exonuclease I (New England Biolabs, PN M0293S), 5-fold diluted in 18 µL of TE buffer and stored at -20ºC. For the fluidigm assay, the 48.48 dynamic array was primed in order to close the interface valves and prevent premature mixing of samples and assays. The assay mix solutions were prepared by combining 3 µL of 2X Assay loading reagent (Fluidigm, PN 85000736), 0.3 µL TE buffer and 2.7 µL of each primer pair (from 100 µM stocks of combined forward and reverse primers). The sample solutions were prepared by mixing in each tube 3 µL 2X Taqman gene expression master mix (Applied Biosystems, PN 4369016), 0.3 µL 20X DNA binding dye sample loading reagent (Fluidigm, PN 100-0388), 0.3 µL 20X Evagreen DNA binding dye (Biotium, PN 31000) and 2.4 µL of the pre-amplified and Exo I-treated sample. 5µl of each "assay" and "sample" tube were loaded into their respective inlets on the left and right frames of the chip, respectively. All "sample" reactions were carried out in triplicate. Note that a non-template control was loaded in sample inlets number 22, 23 and 24. Next, the dynamic array was placed on the IFC controller and software interface was used to pressure load the assay components into reaction chambers. Assay components were automatically combined on-chip. Subsequently, the dynamic array was transferred to a BioMark Real-Time PCR System for thermal cycling and fluorescence detection. Amplifications were carried out at 95 ºC for 60 sec followed by 30 cycles of 96 ºC for 5 sec and 60 ºC for 20 sec on the BioMark System. qRT-PCR analysis software was used to visualise and interact with amplification curves performed analysis, colour-coded heat maps and Ct data for the run. Data was analysed as for qPCR, using *ABL*, *B2M*, *ENOX2* and *RNF20* as housekeeping genes.

2.3 Western blotting

Briefly, proteins were isolated, fractionated on a gel based on molecular weight and transferred to a membrane. Subsequent blotting, against antibodies specific to the proteins of interest, allowed expression analysis.

2.3.1 Protein lysate preparation

For preparation of cytoplasmic and nuclear extracts, equal cell numbers were washed two times in PBS. Cell pellets were resuspended in 150 µL of ice cold cytosolic extraction buffer (10 mM HEPES pH 7.9, 10 mM KCl, 0.1 mM EDTA pH 8.0, 0.1 mM EGTA pH 7.0) supplemented with freshly added protease inhibitors (1 mM PMSF, 2 µg/mL Aprotinin, 2 µg/mL Leupeptin, 1 µg/mL Pepstatin A, 1 mM Na3V04 and 1 mM NaF). Cells were incubated for 45 min on ice with intermittent vortexing for three times. This lysis buffer is hypotonic in nature, which allows cells to swell on ice. After 45 min, 4.7 µL of 10% NP-40 were added to each cell suspension and vortexed vigorously for 10 sec for cell lysis. After centrifugation at 10 000 x g, 4ºC for 1 min, supernatants (cytoplasmic extracts) were transferred to pre-chilled eppendorf tubes and stored at -80ºC. Nuclear pellet were resuspended in 25 µL of ice-cold nuclear extraction buffer (20 mM HEPES pH 7.9, 400 mM NaCl, 1 mM EDTA pH 8.0, 1 mM EGTA pH 7.0) containing protease inhibitors (as described above for cytosolic extraction buffer). Pellets were incubated on ice for 30 min with three intermittent vortexings. After centrifugation for 5 min at 10 000 x g at 4ºC, supernatants (nuclear extracts) were transferred to pre-chilled eppendorf tubes and stored at -80ºC until protein quantification.

For detection of proteins susceptible to degradation, *i.e.* C/EBPα, equal cell numbers (0.6-2.5x10^5) from each assay were washed with PBS (432 g for 5 min) and the supernatants were carefully removed. The cell pellets were immediately resuspended in 20 µL of 2X SDS sample/Laemmli lysis buffer (Table 2.6) with freshly added β-mercaptoethanol (30 µL β-mercaptoethanol to 470 µL 2X SDS), mixed by vortexing and heated at 95ºC for 3 min. Cell lysates were spun down and stored at -80°C. Prior to use, protein samples were heated at 95ºC for 3 min before the loading step for best resolution.

Table 2.6 2XSDS sample buffer

Components and final concentration	Amount to add per 50 mL
0.1 M Tris-HCL (1 M, pH6.8)	5 mL
40% (v/v) 10% SDS	20 mL
20% (v/v) Bromophenol Blue	10 mL
20% (v/v) Glycerol	10 mL
dH_20	5 mL

2.3.2 Protein quantification

Cytoplasmic and nuclear extracts were quantified using Bradford Reagent (Sigma Aldrich, PN B6916) as per the manufacturer's instructions. Briefly, a stock solution of bovine albumin serum (BSA) at 1 µg/µL was used to prepare six protein standards at varying concentrations in Bradford reagent fivefold diluted in dH_2O. For each standard, 200 µL were pipetted in triplicate to a 96-well plate. Test sample lysates were diluted also in Bradford reagent (1:1000) and pipetted in triplicate. Absorbance was read at 595 nM on a Spectramax M5 plate reader (MDS Analytical Technologies) and analysed with SoftMax Pro 5.2 software (MDS Analytical Technologies). Based on the obtained concentrations, equal amounts of protein were then added in each assay.

2.3.3 Gel electrophoresis

The denaturing separation method SDS-polyacrylamide gel electrophoresis (SDS-PAGE) was used to analyse protein samples. Protein samples quantified by Bradford assay were diluted in the negatively charged detergent 6X SDS sample buffer (Table 2.7) according to desired concentrations and boiled at 95ºC for 5 min. Samples were loaded onto an 8 or 10% acrylamide gel (Table 2.8) alongside 5 µL of pre-stained protein ladder (Biorad, PN 161-0374) to assess the molecular weight of proteins migrating through the gel. Samples were run in running buffer (Table 2.9) for about 2 h at 100 volts (V). Electric current allowed protein separation since the negatively charged proteins migrate towards a positive electrode at varying speeds according to their molecular weight.

Table 2.7 6X SDS sample buffer

Components and final concentration	Amount to add per 50 mL
72 mM Tris-HCL (0.5 M, pH6.8)	7.2 mL
12% (w/v) SDS	6 g
0.06% (w/v) Bromophenol Blue	0.03 g
47% (v/v) Glycerol	23.5 mL
120 mM DTT	0.93 g
dH_20	up to 50 mL

Table 2.8 Resolving and stacking gel

	Resolving gel		Stacking gel
	8%; 15 mL	**10%**; 15 mL	4 mL
ddH_20	6.9 mL	5.9 mL	2.7 mL
30% Acrylamide	4 mL	5 mL	0.67 mL
1.5M Tris (pH8.8)	3.8 mL	3.8 mL	-
1.5M Tris (pH6.8)	-	-	0.5 mL
10% SDS	0.15 mL	0.15 mL	0.04 mL
10% APS	0.15 mL	0.15 mL	0.04 mL
TEMED	9 µL	6 µL	4 µL

Table 2.9 Running buffer

Components and final concentration	Amount to add per 1 L
10% (v/v) 10X Western[a]	100 mL
1% (v/v) 10% SDS	10 mL
ddH_20	890 mL

[a] 250 mM Tris Base (30.03 g); 1.9 M Glycine (144 g) in 1L of ddH_20

2.3.4 Membrane transfer

After protein separation, proteins were transferred from the acrylamide gels onto nitrocellulose membranes with a 0.45 µm pore size, (GE Healthcare Life Science, PN 10600007). Briefly, the nitrocellulose membranes were equilibrated in transfer buffer (Table 2.10) prior to assembly of gel/membrane sandwiches using 1.0 mm gel blotting paper (Whatman) and sponges in a wet electroblotting system (Biorad). The transfer was performed at 100 V for 1 h.

Table 2.10 Transfer buffer

Components and final concentration	Amount to add per 1 L
10% (v/v) 10X Western[a]	100 mL
20% (v/v) Methanol	200 mL
ddH_20	700 mL

[a] 250 mM Tris Base (30.03 g); 1.9 M Glycine (144 g) in 1L of ddH_20

2.3.5 Immunolabelling

To very efficiency of the proteins' transfer onto the membrane and as a control for even protein loading, membranes were stained with 0.1% Ponceau S solution (Sigma, PN 7170). Ponceau S de-staining of the membrane occurred with dH_2O washes. To prevent antibodies from binding to the membrane non-specifically, the blots were blocked in 1X TBS-T (10X TBS (Table 2.11) diluted in ddH_20 and supplemented with 0.05% Tween 20) containing

5% BSA (Sigma-Aldrich, PN A3608) or 5% non-fat dried milk for 1 h at RT. Membranes were then transferred to a fresh blocking solution with the addition of the appropriate primary antibody (Table 2.12) with a gentle rotation at 4ºC O/N. Thereafter, the blots were washed 3 times with 1X TBS-T with gentle shaking and incubated with horseradish-peroxidase (HRP)-labelled secondary antibodies for 1 h at RT with gentle rotation. After 3 washes with 1X TBS-T, the blots were developed with the ECL solutions (West PICO (PN 10177533) / West FEMTO (PN 10391544) chemiluminescent substrate), as per manufacturer's instructions (Thermo Scientific Pierce). Protein signals were captured on X-ray films (Thermo Scientific Pierce, PN 10137683) and developed in a dark room using the Medical film processor SRX-101A (Konika Minolta). After visualisation of bands showing proteins of interest, the blots were blocked and probed with the appropriate primary antibody for housekeeping protein to ensure equal protein loading between samples. The blots were then probed with the appropriate secondary antibody, washed and visualised as detailed above. When proteins of similar sizes were viewed on the same gel, nitrocellulose membranes were stripped. For that, the Restore western blot stripping reagent (Thermo Scientific Pierce, PN 10057103) was used, following manufacturer´s instructions. To quantify protein expression, densitometric analysis of bands was carried out with ImageJ Software whenever indicated.

Table 2.11 10X TBS

Components and final concentration	Amount to add per 1 L
152mM Tris HCl	24 g
46mM Tris Base	5.6 g
1.5mM NaCl	88 g
ddH20	up to 1 L[a]

[a] pH adjusted to 7.6

Table 2.12 Western blotting antibodies

Name of Antibody	Reactive Species	Dilution	Manufacurer	PN
α-Tubulin	Mouse	1: 5000	Sigma-Aldrich	T5168
β-Actin	Mouse	1: 5000	Sigma-Aldrich	A5316
C/EBPα	Rabbit	1: 1000	Cell Signaling	2295
cMyc	Mouse	1: 1000	Santa Cruz	SC-40
HA	Mouse	1: 1000	Sigma-Aldrich	H9658
HDACI	Rabbit	1: 1000	Santa Cruz	sc-7872
PRMT5/Skb1Hs Methyltransferase	Rabbit	1: 1000	Cell Signaling	2252
TRB-2	Mouse	1: 250	Santa Cruz	sc-100878
anti-rabbit-HRP	Donkey	1: 2000	GE Healthcare	RPN4301
anti-mouse-HRP	Sheep	1: 2000	GE Healthcare	RPN4201

2.4 Crosslinking Co-Immunoprecipitation analysis from transfected cells

$4x10^6$ 293T human embryonic kidney cells were seeded in 10 cm dishes and after 24 h cells were either left untransfected or transiently co-transfected with plasmids expressing HA-tagged PRMT5 and Myc-tagged TRIB2. The corresponding empty vectors (pcDNA3 and PHMA) were used to equalize amounts of transfected DNA where appropriate and X-tremeGENE HP DNA Transfection reagent (Roche, PN 06 366 244 001) was used following manufacturer´s protocol. Briefly, 12 µg of plasmid DNAs (6+6 µg per 1 000 µL complex) were diluted in serum-free DMEM medium and 25 µL of transfection reaction were added to each mixture followed by 15 min of incubation at RT to allow complex formation. Transfection complexes were added to the cells in a dropwise manner and dishes were gently swirled to ensure even distribution. At 24 h post-transfection, cells were washed, scrapped off the plates in 1 mL of ice-cold PBS and harvested by centrifugation (11 000 x g for 45 sec at 4°C). Cell pellets were resuspended in 300 µL of HEPES lysis buffer (50 mM HEPES pH7.4, 150 mM NaCl, 1 mM EDTA, 0.5% NP-40 and 5% glycerol) supplemented with protease inhibitors (1 mM PMSF, 2 µg/mL Aprotinin, 2 µg/mL Leupeptin, 1 µg/mL Pepstatin A, 1 mM Na3V04 and 1 mM NaF) and incubated for 30 min on ice. To strengthen protein-protein interactions, lysates were crosslinked with

1.5 mM DSP (dithiobis (succinimidyl propionate)) prepared according to manufacturer's instructions (Thermo Scientific, PN 22585). After 1 h on ice, reaction was then quenched with 50 mM Tris pH 7.4 for 30 min on ice. Samples were spun at maximum speed for 45 sec at 4^{o}C and cleared supernatants transferred into new tubes for protein quantification by Bradford assay (see section 2.3.2). Aliquots containing 50 µg of protein were removed from each sample (inputs), heated at 95°C for 5 min with 6X SDS sample buffer (Table 2.7) and kept at -20°C until loading. Co-immunoprecipitation (Co-IP) was carried out with the remaining cell extracts. To eliminate non-specific protein binding, equal amounts of each protein lysate (4 mg) were incubated with 20 µL of immobilised protein A/G Ultralink (DAPI) (Fisher Scientific, PN 53132) beads at 4°C for 30 min in an eppendorf rotator. Pre-cleared supernatants were collected upon centrifugation (2 min, full speed at 4°C) and incubated with 20 µL of fresh beads and either α-cMyc (1.5 µg/mg of protein) or α-HA (3 µL/sample, concentration not stated on the datasheet) antibodies (Table 2.12). To capture the immunoprecipitated protein complexes, samples were kept at 4°C under O/N rotation. The pelleted beads were washed three times with 1 mL of ice-cold HEPES lysis buffer by centrifugation at maximum speed for 30 sec at 4°C. To elute the immune complexes from the beads, 25 µL of 2X SDS sample buffer (Table 2.6) were added to each sample followed by incubation at 95°C for 5 min. Eluates and inputs were analysed in an 8% gel by SDS-PAGE and immunoblotting (as described in section 2.3).

2.5 Animal work

2.5.1 Ethical issues

All animal work was performed in accordance with regulations set by the Animals Scientific Procedures Act 1986 and UK Home Office regulations. Animals were housed at the Beatson Institute for Cancer Research at the University of Glasgow. All experiments were carried out under the author´s personal licence (PIL number I4AE3E6BE) and Dr Karen Keeshan's project licence (PPL number 60/4512). Throughout all animal experiments, mice were regularly monitored for symptoms of disease (ruffled coat, hunched back, decreased activity and weight loss) using the project license scoring sheet.

2.5.2 *In vivo* models

2.5.2.1 Tertiary murine Trib2 transplants

Secondary AML cells from the BM of two independent MigR1-Trib2 transplanted C57BL/6 mice –Trib2 AML#A (79% GFP+ cells) and Trib2 AML#B (74% GFP+ cells)- were transplanted, respectively, into 4 and 3 sublethally irradiated B6.SJL mice (4.5 Gy, 4h prior to transplantation), by tail-vein injection of 0.8x 10^6 nucleated BM cells per recipient (*i.e.* tertiary transplanted AML cells). Mice were maintained on 2.5% Baytril (Bayer, enrofloxacin)-supplemented drinking water until 2 weeks after irradiation. The antibiotic regimen consisting of Baytril´s active metabolite (ciprofloxacin) has been shown to efficiently decontaminate aerobic Gram-negative and Gram-positive pathogens without major effects on haemopoiesis (Velders et al., 2004). Mice were monitored for % of GFP positive cells by tail-vein bleed at d28, 40, 53 and 65. Critical organs from tertiary recipients were collected and processed as described in 2.5.2.4 at d56 and 74 after transplantation, following detection of GFP + cells ≥10% in the PB. This value was used as a proxy for marked BM infiltration of leukaemic cells, as assessed by a secondary transplant not shown for the sake of redundancy.

2.5.2.2 Xenotransplantation of U937 AML cells

U937 cells were transduced with shCtrl or shTRIB2 lentivirus and selected 24 h after with 2 µg/mL puromycin (Sigma-Aldrich, PN P7255, 10 mg/mL stock) for 2 days. Transduced cells were harvested and washed, viable cells were counted using trypan blue exclusion and % of GFP positive cells was analyzed by FACS analysis on the day of transplant. Non-irradiated 12 to 18 week-old male non-obese diabetic (NOD)/LtSz-severe combined immune-deficiency (SCID) IL-2Rγc^{null} (NSG) mice were used in the *in vivo* study. A standardized number of 1.2x10^6 cells with equally high expression of GFP (~67%) was injected via tail vein in the xenograft study of shCtrl (n=5) and shTRIB2 (n=8) transplant. PB was collected by tail vein bleeding of mice at day 5 and 11. Mice were killed at day 16 after transplantation and critical organs were collected and processed as described in section 2.5.2.4. To assess human cell engraftment, cells were labelled with anti-human CD45 antibody conjugated with PE-Cy7 (Table 2.12, Figure 2.2A) and antibody expression was quantified alongside with % of GFP positive cells by flow cytometry. As a

negative control for FACS analysis of GFP expression, cells collected from 3 male NSG mice transplanted with 1.2x10^6 untransduced U937 cells were also included (Figure 2.2B).

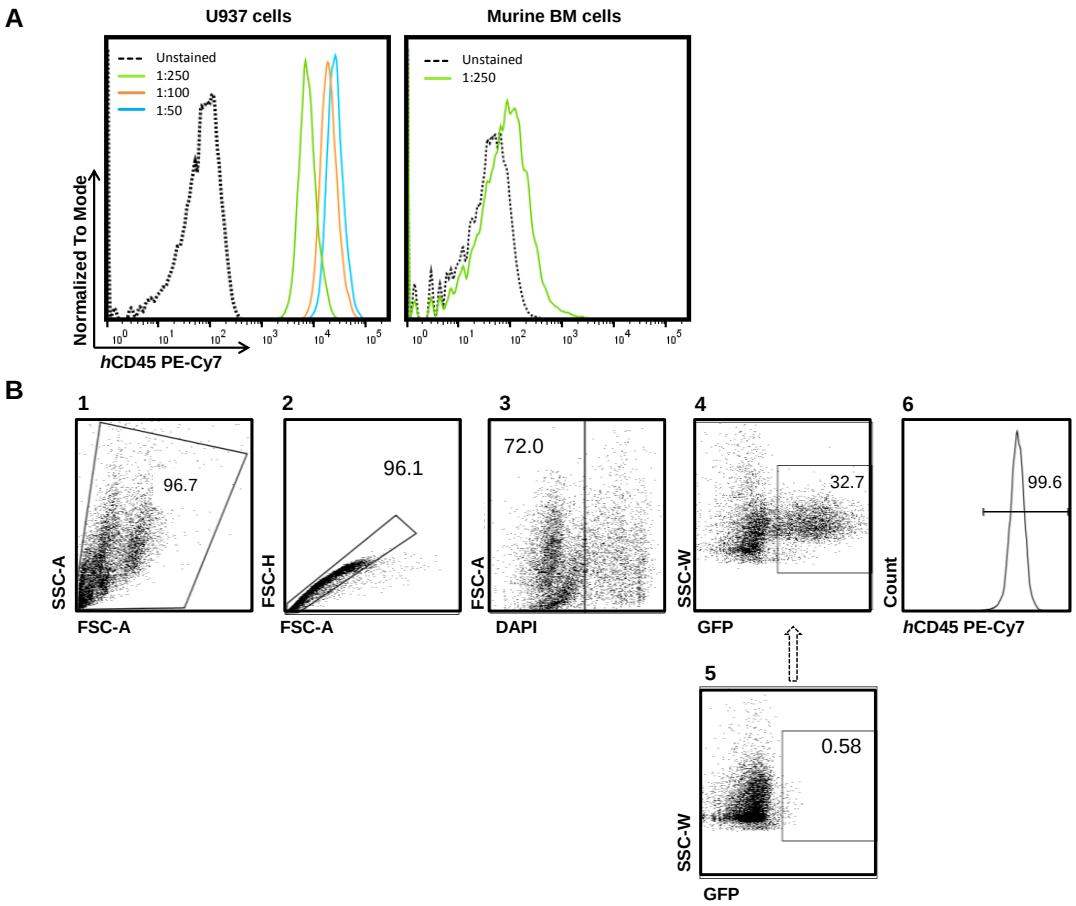

Figure 2.2 FACS gating strategy used to identify xeno-engrafted GFP+ U937 cells
(A) Titration of *h*CD45 PE-Cy7 in both U937 and BM murine cells by using a series of dilutions. The 1:250 dilution was selected for further use in the *in vivo* experiment as it resulted in detection of a clear signal for the positive population (left) with no unspecific binding (right). (B) Compensation and voltages were set up using single colour controls. Viable cells were identified using forward scatter (FSC) and side scatter (SSC) (1). Within the viable cells, single (2) and DAPI negative (3) cells were selected. Within the DAPI negative cells, % of GFP + cells (4) was determined using, as a negative control, cells collected from 3 male NSG mice transplanted with 1.2x10^6 untransduced U937 cells (5). Accuracy of the gate used for detection of human GFP + cells was also evaluated by detecting that this population was >90%+ for *h*CD45 PE-Cy7 (6). Numbers indicate percentages of cells within the indicated gates.

To assess Brtz *in vivo* efficacy, a similar experimental model to the one described above was established with the following changes: U937 cells were transduced only for GFP expression (shCtrl lentivirus) and five days after transplantation, mice were randomized

into two groups of 3 animals each to be treated with Brtz (0.5 mg/kg, intraperitoneal (i.p.) administration) or sterile PBS only on days 5, 7 and 11. PB was collected by tail vein bleeding of mice at day 5 and 11 before drug treatment. General physical status and weights were recorded daily during treatment to assess any signs of impairment of the animals caused by Brtz and to ensure that mice received a consistent dose of 0.5 mg/kg every treatment. Mice were killed at day 16 post-transplantation.

2.5.2.3 Xenotransplantation of primary human AML cells

Adult female NSG mice (6 to 11 week-old) were sublethally irradiated with 2.25 or 2.5 Gy of total body irradiation 24 h prior to injection of unsorted MNCs from PB of 6 AML patients. Recovery of the cryopreserved leukaemic cells was performed as described in section 2.1.3 and cells were incubated for few hours in appropriate culture media (Table 2.3). Thereafter, cells were cleared of aggregates and debris using a 0.2 μm cell filter and washed in PBS/2%FBS. Cells were then resuspended in PBS/2%FBS at a final concentration of 1.1-1.6x10^6 cells per 200 μL per mouse. Each sample was tail-vein injected into 3 NSG recipients. Mice were maintained on Baytril-supplemented drinking water for the duration of the experiment and were routinely monitored for symptoms of disease. Human AML burden was evaluated by flow cytometry of tail-vein blood with anti-human CD45 and CD33 (Table 2.13) at week 3, 5, 7 and 8 after transplant. Mice were analysed at week 12 post-transplantation for long-term engraftment evaluation. An engraftment criterion of >0.1% of *h*CD45+ *h*CD33+ in the murine BM cells was used as the biologically significant cut-off.

2.5.2.4 Dissection and processing of blood and critical organs from transplanted mice

Animals were sacrificed using appropriate schedule 1 methods and examined for evidence of leukaemia. PB was obtained after killing through cardiac puncture and collected into tubes containing EDTA to ensure anti-coagulation. Femur, tibia, hip bones, spleen and thymi were dissected and stored in PBS/2% FBS on ice. Brain-sculls were collected when indicated and fixed in 10% formalin. Approximately 20 μL of PB were subjected to analysis in the Hemavet 950FS system to obtain haematology profiles for each sample. Bones from femur, tibia and hips were crushed in PBS/2% FBS using a mortar and pestle and made into a single cells suspension through filtering through a sterile 0.2 μm filter. Single cell suspensions from spleen and thymi were made in PBS/2% FBS using a sterile

plunger and filtered. In all tissues red blood cells (RBC) were lysed in RBC lysis buffer (155 mM NH_4Cl, 10 mM $KHCO_3$, 0.1 mM EDTA).

2.6 Preparation of metaphase murine Trib2 AML cells for karyotyping

Total BM derived AML cells collected from two Trib2-leukaemic tertiary recipient mice were prepared for metaphase stage arrest. 1 mL of cell suspension (~$2x10^6$ cells) from each mouse was treated with 10 µL of demecolcine (Sigma-Aldrish, PN 477-30-5) to increase the yield of mitotic cells in metaphase. Cell suspensions were retrieved to the incubator for 45 min. Cells were then transferred to 15 mL falcon tubes and spun down at 200 g for 10 min. Tubes were flicked to loosen the pellet and 10 mL of pre-warmed 0.075M KCl hypotonic solution were added. Cells were vortexed at medium speed and incubated at 37ºC for 15 min. Cells were then centrifuged at 200 x g for 10 min and supernatant discarded. Pellets were disrupted by flicking the tube in remaining drops of the liquid and 5 mL of freshly prepared methanol:acetic acid (3:1) fixative solution were added dropwise while vortexing. Extra 5 mL of fixative solution were added. Cells were centrifuged at 200 x g for 10 min and supernatant discarded (leaving about 0.5mL). This step was repeated one extra time. Cells were resuspended in a small volume of fixative solution (~0.3 mL) and transferred to a 1.5 mL tube. To confirm the presence of metaphase cells, 5 µL of cell suspension were dropped on a slide. After waiting a few seconds for the slide to dry, DAPI (4´, 6´-diamidino-2-phenylindole) was added for fluorescence microscopy analysis. The slide was examined under oil immersion at 100X magnification using a UV light source. Extra fixative solution (~1 mL) was added to the preparation, the tubes were sealed with parafilm and stored at –20ºC until being sent for cytogenetic analysis at Cytocell Ltd (Cambridge).

2.7 Flow cytometry

2.7.1 Assessment of surface antigen expression

Cells were harvested and washed in PBS. Cell pellets were then resuspended in 50 µL of PBS containing the appropriate fluorochrome- conjugated antibody (Table 2.13 and indicated in the related Figure legend). Cells were incubated for 30 min at 4ºC protected from light. Cells were washed again in PBS and resuspended in 200 µL of PBS prior to FACS analysis. FACS analysis was performed using a BD FACSCanto™ II flow cytometer and acquired data was analysed using FlowJo software (Treestar, v10).

Table 2.13 FACS antibodies

Name of Antibody	Reactive Species	Clone	Format	Manufacturer	Dilution
CD33	human	WM53	APC	Biolegend	1: 250
CD45	human	HI30	PE Cy7	Biolegend	1: 250
CD11b	mouse	M1/70	APC	eBioscience	1: 250
CD11b	mouse	M1/70	PE	eBioscience	1: 250
Gr-1	mouse	RB6-8C5	APC	eBioscience	1: 250
Gr-1	mouse	RB6-8C5	PE	eBioscience	1: 250
Gr-1	mouse	RB6-8C5	PE Cy7	eBioscience	1: 250
B220	mouse	RA3-6B2	Biotin	eBioscience	0.5 µL per $1x10^7$cells
CD3	mouse	17A2	Biotin	eBioscience	0.5 µL per $1x10^7$cells
CD8a	mouse	53-6.7	Biotin	eBioscience	0.5 µL per $1x10^7$cells
CD11b	mouse	M1/70	Biotin	eBioscience	0.5 µL per $1x10^7$cells
CD4	mouse	GK1.5	Biotin	eBioscience	0.5 µL per $1x10^7$cells
Gr-1	mouse	RB6-8C5	Biotin	eBioscience	0.5 µL per $1x10^7$cells
Ter119	mouse	Ter-119	Biotin	eBioscience	0.5 µL per $1x10^7$cells
c-Kit	mouse	2B8	APC Cy7	Biolegend	1: 100
Sca-1	mouse	D7	PE Cy7	eBioscience	1: 100
Streptavidin	-	-	V450	BD	1: 100

2.7.2 Cell growth analysis

To monitor growth of transduced U937 cells, the cells were seeded at $0.15x10^6$/mL after 24 h transduction (GFP+ cells) or 48 h puromycin selection, as indicated in the related Figure legend. Viable cells were counted by trypan blue exclusion at the indicated time points. After 48 h counting, cells were split again at $0.15x10^6$/mL. For GFP+ cells, GFP % was assessed by FACS analysis at each time point and final results are normalized to the corresponding GFP expression.

2.7.3 Annexin V / DAPI staining

To analyse cells undergoing apoptosis, cells were harvested, washed once in PBS and resuspended in 100 µL of 1X Hanks' Balanced Salt solution (HBSS, Sigma-Aldrich) containing 1 µL of Annexin V-PE (BD Biosciences, PN 556422) per test. HBSS was used to ensure the physiological concentration of calcium required for Annexin V to bind to phosphatidylserine, which is translocated to the extracellular membrane of apoptotic cells. Cells were incubated for 15 min at RT protected from light. To stop the reaction, 400 µL of

1X HBSS were added to each sample and cells were analysed on a BD FACSCanto™ II flow cytometer within no more than 30 min post-staining. For combined analysis of apoptosis and necrosis, 1 µL of the nucleic acid stain DAPI (Sigma-Aldrich, PN 9542, stock at 1 mg/mL) was included in the 100 µL HBSS/Annexin V mixture. For single staining with DAPI, the nucleic acid stain was diluted in PBS and added to each sample (1 µg/mL) just prior to FACS analysis. Control tubes containing unstained cells, Annexin V or DAPI single-stained cells were recorded to set FSC/SSC voltages and compensation. For data analysis, the FlowJo software (Treestar, v10) was used.

2.7.4 Cell cycle analysis using Propidium Iodine (PI) staining

Cells were harvested upon centrifugation at 432 x g for 5 min at RT and washed in PBS. Pelleted cells were fixed by adding 1 mL of ice-cold 70% (v/v) ethanol while vortexing, and stored at -20°C O/N. Before FACS analysis, cells were spun for ethanol removal followed by one washing with PBS and resuspended in DNA staining solution (PI/RNase Staining Buffer, BD Pharmingen, PN 550825) for 15 min at RT in the dark. Fluorescence labelling of the cellular DNA content was used as a measure of cell cycle progression and was acquired by BD FACSCanto™ II flow cytometer. When stated, cell cycle profile was also used to estimate apoptosis (% of cells in Sub-G1 phase). Analysis was performed using FlowJo software (Treestar, v10).

2.7.5 GFP+ cells sorting

For selection of GFP+ cells, cells were harvested, resuspended in approximately 300 µL of PBS/2% FBS and passed through a sterile 70 µm cell strainer prior to sorting. Sorting was performed by Jennifer Cassels using FACSDiva (BD Biosciences, v6.1.2) flow cytometer, as depicted in Figure 2.3.

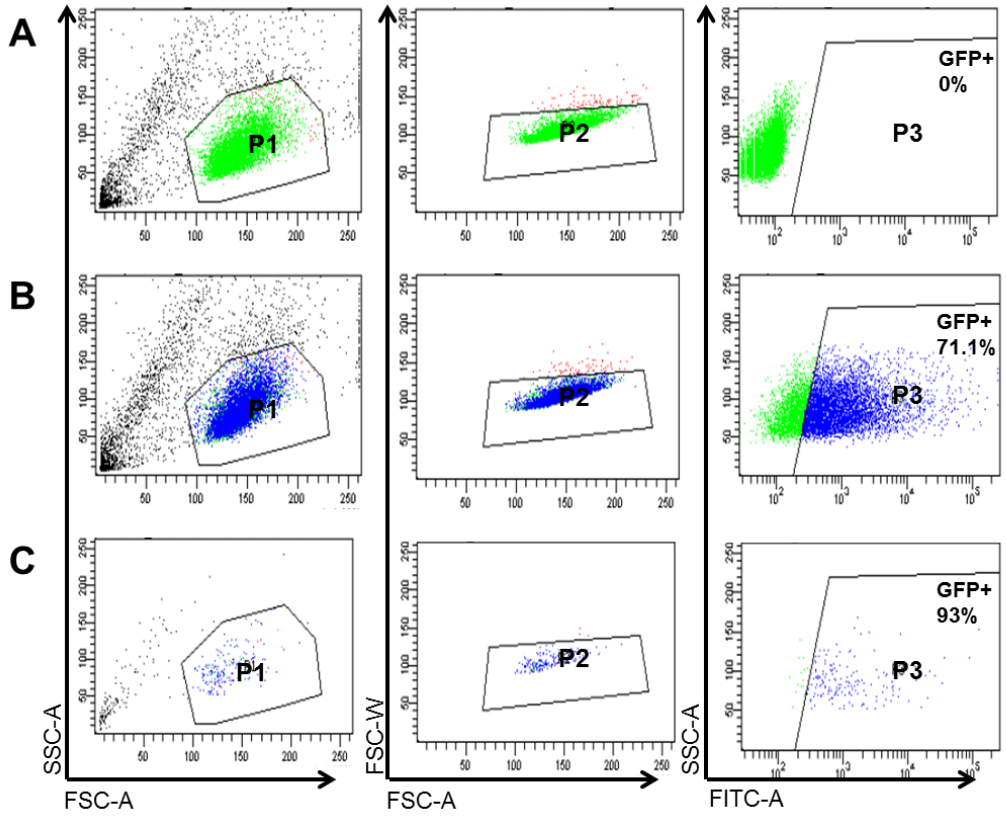

Figure 2.3 Representative plots demonstrating GFP+ cells sorting
(A) Untransduced, GFP- cells, (B) GFP+ cells prior to sort and (C) post-sort are shown. For all, viable (P1) and single (P2) cells were gated using FSC and SSC. % of GFP expression was assessed through P3 gate.

2.7.6 Lineage-Sca1+c-Kit+ (LSK) sorting with lineage depletion

BM cells from B6.SJL mice were flushed out of femurs and tibiae in PBS containing 2% FBS. Prior to sorting of LSK cells in the BM, lineage positive cells were separated as follows. RBC-depleted total BM cells were incubated with a panel of biotin-conjugated mouse antibodies (CD3, CD4, CD8a, B220, CD11b, Gr-1 and Ter119; Table 2.13) at 4ºC for 30 min. After washing with PBS containing 2% FBS, cells were incubated with Anti-Biotin MicroBeads (Milteny Biotec, PN 130-090-485) at 4ºC for 30 min and Lin- cells were purified by magnetic separation. Columns were flushed for collection of Lineage+ cells. The Lin- cells were further stained with antibodies against c-Kit, Sca-1 and SA-V450 (Table 2.13) and sorted by Jennifer Cassels, using FACSDiva (BD Biosciences, v6.1.2) flow cytometer.

2.8 Statistics

Statistical analyses and graphing were performed either with the Microsoft Office Excel software or the GraphPad Prism Software (v5.03) using the unpaired, two-tailed Student's *t*-test. When the Leukemia Gene Atlas (LGA) platform was used as a data analysis tool, the Welch's *t*-test was selected. *** for $P \leq 0.001$, ** for $P \leq 0.01$ and * for $P \leq 0.05$ were considered statistically significant and were indicated in the related Figure legends and graphs. Where n.s. is indicated, the *P* value is not significant. The results are shown as mean ± standard deviation (SD).

Chapter 3
Characterization of TRIB2 tumorigenic role in human AML

When indicated, results presented in this chapter have been published in (Rishi et al., 2014, Salome et al., 2015) and the PDFs of the publications are provided in Appendix E and F.

3.1 Introduction

TRIB2 is a pseudokinase that functions as a molecular adaptor mediating degradation and changes in signaling cascades as reviewed elsewhere (Lohan and Keeshan, 2013). There is accumulating evidence supporting its tumorigenic activity in a variety of malignancies, *i.e.* melanoma (Zanella et al., 2010), lung (Zhang et al., 2012, Grandinetti et al., 2011) and liver cancer (Wang et al., 2013a), as well as T-ALL (Sanda et al., 2012) (see Chapter 1, section 1.3.3). Significant for the current study, Keeshan *et al.* observed that murine BM cells retrovirally expressing this gene exhibit a growth advantage *ex vivo* and readily establish factor-dependent cell lines. *In vivo*, Trib2-reconstituted mice rapidly develop AML with a mean latency of 179 days and complete penetrance through a mechanism involving proteasomal-dependent degradation of C/EBPα p42, which is central to the induction of granulocytic development (Keeshan et al., 2006). Moreover, mice reconstituted with HSCs co-transduced with *Trib2* and *HoxA9* have an accelerated onset of AML when compared to either gene alone, indicating that these genes may co-operate to induce leukaemia (Keeshan et al., 2008). The AML oncogene *Meis1* may also promote Trib2 expression, which potentially complements the ability of NUP98-HOXD13 to induce AML, as shown in another murine BMT model (Argiropoulos et al., 2008). The *Trib2* role as a myeloid oncogene is thus supported by strong experimental data provided by murine models. In human leukaemic cells, its oncogenic potential has been highlighted by gene expression profiling studies. Valk *et al.* analysed 285 patients with de novo AML that was characterized by cytogenetic and molecular analyses. They used gene-expression profiling to comprehensively classify the disorder and identified sixteen distinct groups of patients on the basis of unsupervised cluster analysis (*i.e.*, without taking into account external information) and strong similarities in molecular signatures (Valk et al., 2004). The same microarray profiling was subsequently examined to investigate *TRIB2* mRNA expression in human AML patient samples. Based on signals from two different probe sets targeting this gene, Keeshan *et al.* found that *TRIB2* transcript levels were enhanced in cluster #4 when compared to other subsets. While cluster #4 is one of the two distinct expression subsets harboring most patients with *CEBPA* mutations, *TRIB2* was primarily elevated in tumors that did not carry mutations in the myeloid transcription factor *CEBPA*. This was suggestive of disruption of normal C/EBPα function by other mechanisms, explaining why these AMLs shared a *CEBPA* mutant gene expression signature, while lacking such mutations (Keeshan et al., 2006). Cluster #4 leukaemias lacking *CEBPA* mutations were further defined as a specific subgroup of AML. They were associated with *CEBPA* silencing, which was linked to frequent promoter CpG hypermethylation (4/6 patient

samples analysed). Comparison of silenced leukaemias to *CEBPA* mutant cases in cluster #4 also revealed that genes significantly overexpressed in the first group were related to T-cells and T-lymphoid development (*e.g.*, *CD7*). Moreover, *CEBPA* silenced leukaemias share an immature myeloid/lymphoid phenotype, as determined by simultaneously expression of surface markers CD34, CD13, CD7 and terminal deoxynucleotidyltransferase (TdT). These *TRIB2*-expressing AMLs lacking *CEBPA* mutations were further associated with aberrant activation of *NOTCH1* by mutations. Indeed, *TRIB2* was identified as a direct transcriptional target of *NOTCH1* (Wouters et al., 2007).

Altogether, leukaemic murine models and gene expression analyses of human AML cohorts link TRIB2 to tumors with altered C/EBPα function and suggest that elevated TRIB2 may have a pathogenic role in a subset of human AML. Therefore, this chapter aims to further understand the precise role of TRIB2 in the human leukaemic setting by means of functional analysis that are still lacking.

3.2 Aims and Objectives

The present study hypothesises that TRIB2 will be required for the oncogenic properties of human AML cells. To address this, the specific aims of this chapter were:

i. To investigate how *TRIB2* is altered at the genomic level across a panel of human tumours;

ii To establish a murine Trib2-AML model as a source of leukaemic cells for further characterization of TRIB2-driven AML

ii. To perform a phenotypic characterization of the role of TRIB2 in human AML cells, both *in vitro* and *in vivo*; assessing its putative contribution to AML cells survival

iii To investigate the clinical relevance of *TRIB2* by means of a transcriptional analysis in AML patient samples;

iv To investigate whether increased expression of *TRIB2* in AML patient samples correlates with the ability of these cells to engraft in the BM of NSG mice.

3.3 Results

3.3.1 *TRIB2* oncogenic activity is related to its elevated gene expression

The *TRIB2* gene was examined in the catalogue of somatic mutations in cancer (COSMIC, v72) database (http://cancer.sanger.ac.uk, (Forbes et al., 2015)), the most comprehensive source of curated analysed somatic mutations in human cancer to date. This analysis was intended to obtain an overview of whether *TRIB2* is altered at the genomic level across a panel of tumour samples identified by the tissue of origin. From a total number of 23,983 unique tumour samples, 86 showed missense (51%), synonymous (46%), nonsense (2%) and inframe deletion (1%) mutations in *TRIB2* (Figure 3.1A, lower panel). Interestingly, although the overall point mutation rate is low, tumours with documented roles for the *TRIB2* oncogene, such as malignant melanoma and lung cancer, do have detectable *TRIB2* point mutations. In tissues matching AML, which has a very strong association with *TRIB2* oncogenic activity, no mutations were retrieved from COSMIC curated data provided by scientific literature and resequencing results from the Cancer Genome Project at the Welcome Trust Sanger Institute (1/1942 haematopoietic and lymphoid tissue samples identified with a *TRIB2* mutation corresponded to a multiple myeloma patient sample) (Figure 3.1A, upper panel). Indeed, no mutations have been found in ~75 AML samples analysed by exome sequencing with good coverage across all exons (Ross Levine, personal communication to Dr. Karen Keeshan). Interrogation of other genomic alterations affecting *TRIB2* in the COSMIC database identified subsets of tumour tissues with overexpressed *TRIB2* (Figure 3.1B). Overall, the frequency rate for these alterations is higher and includes lung, skin, liver and haematopoietic and lymphoid tissues samples. Of note, 4/9 samples overexpressing *TRIB2* in the haematopoietic and lymphoid tissues matched AML samples. Given that there is strong evidence for a *TRIB2* oncogenic function in these tumours, these analyses suggest that an elevated *TRIB2* expression has potential implications on other tumour tissues yet to be explored, *e.g.* in the endometrium (endometrioid carcinoma), central nervous system (astrocytoma grade V), prostate and in large intestine samples (both with matches for adenocarcinoma). Other *TRIB2* gene alterations include copy number variation (CNV), which albeit rare, are found across different tumour tissues and are mainly associated with an increased copy number (all except for breast, thyroid and kidney, which showed CNV loss) (Figure 3.1C). Hypermethylation, associated with chromatin silencing, was found exclusively in prostate and large intestine tumour tissues (Figure 3.1D). Together, these analyses suggest that in

most cancers *TRIB2* oncogenic activity is related to its elevated gene expression rather than to different genomic alterations or mutations (data published in (Salome et al., 2015)).

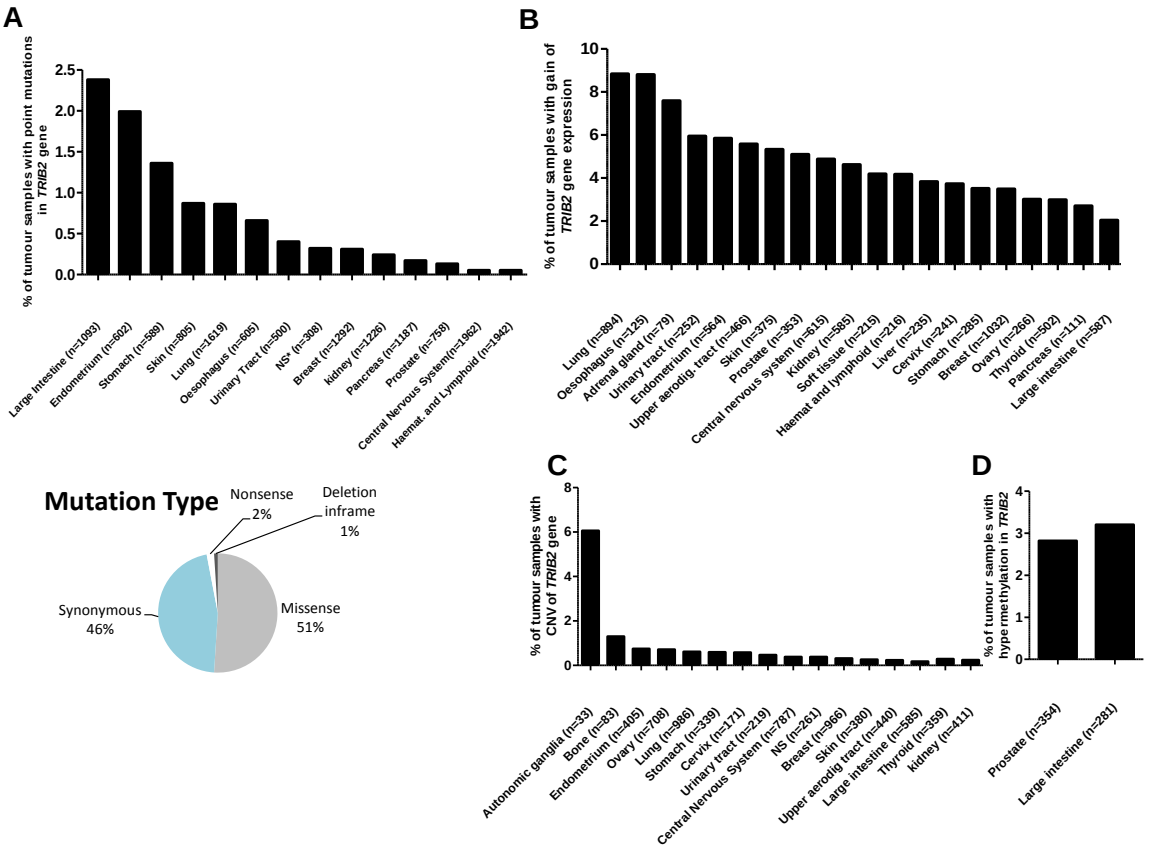

Figure 3.1 Genomic alterations in *TRIB2* gene
(A) Histogram presentation of point mutations in *TRIB2* gene in tumour samples using the COSMIC database (upper panel). Pie chart referring to the frequency of missense (51%), synonymous (46%), nonsense (2%) and deletion inframe (1%) point mutations in the identified tumour samples (lower panel). (B) Histogram presentation of gain of *TRIB2* gene expression in the tumour samples indicated. Among them 4/9 haematopoietic and lymphoid tissues samples match AML as part of the acute myeloid leukaemia study (COSU377) from The Cancer Genome Atlas [TCGA] in which over expression is defined after a z-score > 2. (C) Histogram displaying tumour tissues where CNV of the *TRIB2* gene was identified, with the respective frequency in tumour samples. (D) Histogram presenting tumour tissues where hypermethylation of the *TRIB2* gene locus was identified and respective frequency. Data were retrieved by v72 of COSMIC database (http://www.sanger.ac.uk) and only tissues displaying *TRIB2* alterations are shown. CNV, copy number variation; NS*, not specified with histology matching malignant melanoma; NS, not specified. The most commonly mutated gene in human cancer, *TP53* (Kandoth et al., 2013), was also examined as a positive control. The analysis using COSMIC database

confirmed that the majority of *TP53* mutations are missense substitutions and that approximately 50% of samples matching ovary tumour tissue have mutations in this tumour suppressor, as reported in the literature (Petitjean et al., 2007, Olivier et al., 2010).

3.3.2 Primary murine Trib2-BM derived AML cells propagate AML in serially transplanted mice

The above analysis suggests that genomic alterations or mutations in *TRIB2* are not commonly associated with cancer. Keeshan and colleagues reported that *Trib2* itself was a bona fide AML oncogene, capable of driving a potent murine AML that was transplantable to secondary recipients (Keeshan et al., 2006). It was therefore considered a logical approach to take advantage of this model to investigate further the transplantability and genomic characteristics of Trib2-driven AML, as it could be also used for expansion and propagation of Trib2-AML cells. For that, 0.8 x 10^6 BM derived AML cells from secondary transplanted mice retrovirally expressing Trib2 (MigR1-Trib2) were transplanted into sublethally irradiated (4.5 Gy) tertiary B6.SJL recipients. Trib2 was co-expressed with GFP in a bicistronic construct, thereby enabling disease monitoring by flow cytometric analysis of the GFP reporter in the PB. Mice developed GFP+ cells consistent with peripheral leukaemia (Figure 3.2A) and were killed at d56 (Trib2 AML#A1, A2, A3 and B1) and d74 (Trib2 AML#A4, B2 and B3) post-transplant when terminal symptoms consisting of %GFP+ ≥10 were detected by tail bleeding. All tertiary recipients (n=7) developed AML with similar levels of engraftment when compared to primary transplants described in (Keeshan et al., 2006), but with faster disease progression (medium survival of 65 vs 179 days after transplant). At necropsy, all mice displayed splenomegaly (n=7; range=0.15-0.36 g; Figure 3.2C) and opaque bones (data not shown). By flow cytometric analysis of % of GFP positive cells, tertiary leukeamias were associated with extensive BM involvement (>80% in all cases), followed by PB, spleen and thymus (Figure 3.2D and 3.2E, upper panel). Different from the primary transplant, leukocytosis reflecting excess of leukaemic cells, was absent throughout the experiment, probably due to increased latency of the disease. WBC count of 1.8 to 10.7 x10^6/100 mm^3 was within the normal range but values can also be found low, normal or high in human AML (Estey and Dohner, 2006). Notably, the infiltrating AML cells were detected in the choroid plexus and meninges of 6/7 brains examined by Dr. Christina Halsey and Dr. Anthony Cousins (University of Glasgow), as part of a collaboration with Dr. Karen Keeshan´s group. The immunophenotype of leukaemic cells in tertiary recipients paralleled observations previously reported for the primary disease (Keeshan et al., 2006), with most cells

retaining intermediate expression of Gr-1 and CD11b in the GFP+ population (Figure 3.2E, lower panel) – a characteristic of immature myeloid precursors and murine myeloid leukaemias (de Guzman et al., 2002, Cozzio et al., 2003). In addition to % of GFP positive cells, the leukaemic BM cells expressed the expected oncogene, as confirmed by mRNA detection of higher *Trib2* transcript levels (Figure 3.2B). Together, these data extend the previous study reporting *Trib2* as a potent murine myeloid oncogene (Keeshan et al., 2006) by indicating central nervous system (CNS) involvement and tertiary AML engraftments and propagation. Importantly, this model was shown to be useful as a valuable resource of leukaemic cells, as described in the section below.

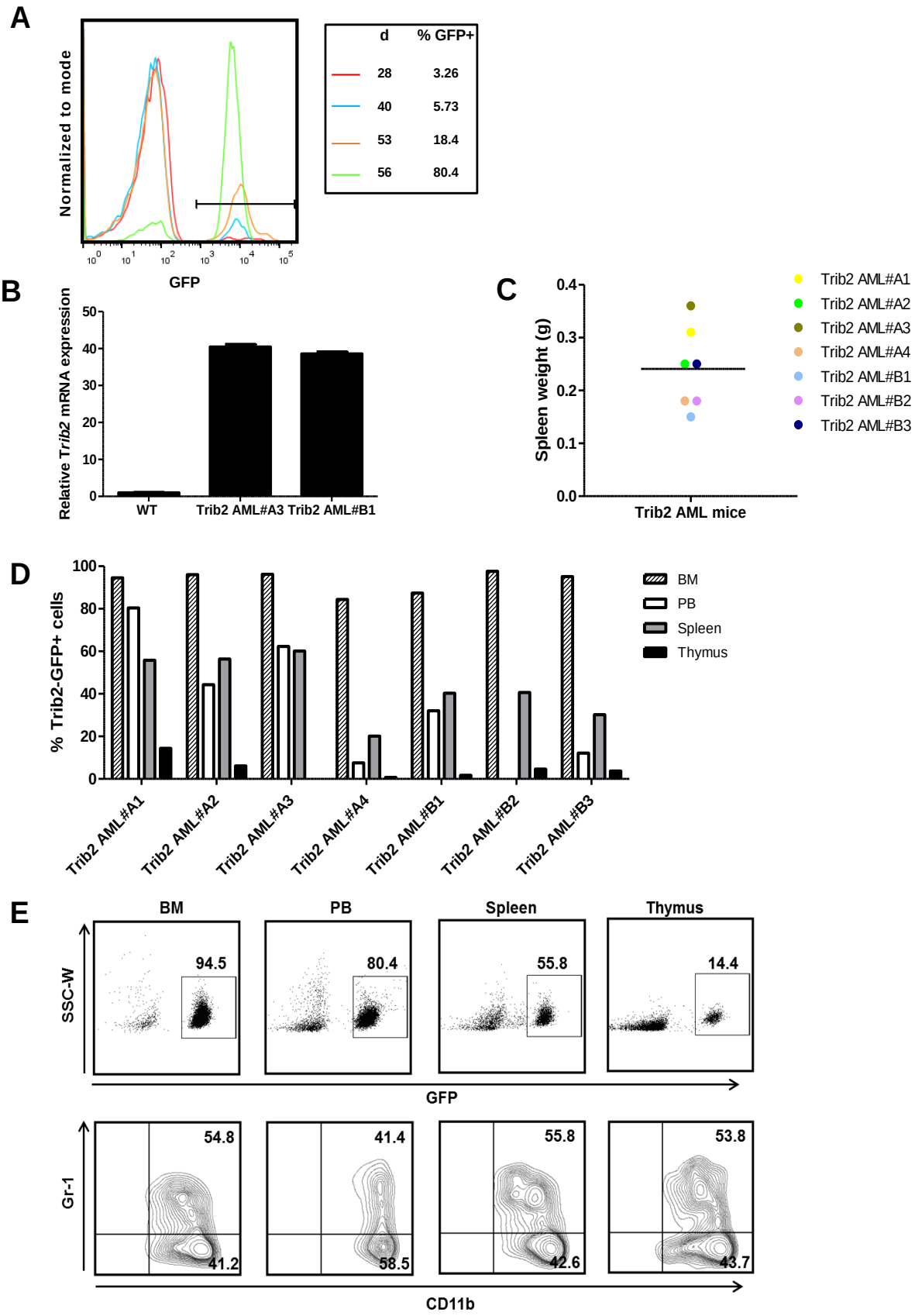

Figure 3.2 Robust tertiary engraftment of Trib2-induced AML
(legend on next page)

Figure 3.2 Robust tertiary engraftment of Trib2-induced AML (Figure on previous page). (A) Sublethally irradiated mice (4.5 Gy, n=7) received $0.8x10^6$ Trib2-BM cells from two secondary leukaemic recipients (named A and B). Mice were monitored for signs of illness for 74 days (d) and euthanized when % of GFP+ cells in the PB was above 10. Mice were killed at d56 (Trib2 AML#A1, A2, A3 and B1) and d74 (Trib1 AML#A4, B2 and B3). Representative histogram depicts increase of % of GFP positive cells in the PB detected at various time points (d28, 40 and 53) and at necropsy (d56). (B) Overexpression of mouse *Trib2* transcripts were verified by qPCR in two independent tertiary AMLs (Trib2 AML#A3 and #B1). Values represent gene expression relative to wild type (WT) BM and normalized to the reference gene *Hprt*. (C) Spleen weights were measured. Each symbol represents an individual mouse and horizontal bar represents mean value (0.24 g). For comparison purposes, spleens from control MigR1 mice were reported to have an average weight of 0.09 g (n=10; range=0.06-0.1 g) (Keeshan et al., 2006). (D) Cells from BM, PB, spleen and thymus were assessed by flow cytometry for quantification of GFP expression used as marker for leukaemic cells. Data are shown by bar graph and (E) representative FACS plots. Lower panel depicts Gr-1-PE and CD11b-APC profile of the GFP+ populations. For technical reasons % of GFP positive cells analysis was not recorded for thymus and PB of mouse Trib2 AML#A3 and #B2, respectively.

3.3.3 Murine Trib2-induced AML exhibits normal cytogenetics

AML is defined by molecular heterogeneity coupled with the current understanding that a single mutation appears generally insufficient for overt leukaemia to develop. This is supported by the two-hit model of leukaemogenesis, now considered an over-simplification of the reality, and is true for the Trib2-driven murine model as it is believed that at least a second hit must occur to explain the observed 6 month latency for the primary AML disease to develop *in vivo* (Keeshan et al., 2006). The second hits that may occur could include chromosomal alterations due to genomic instability in Trib2-expressing AML cells. Chromosomal alterations are of particular significance in AML, in terms of frequency and clinical implications. Thus, a karyotype analysis was performed with a view to gaining a better characterization of *Trib2* genomic instability in AML. To investigate the cytogenetic background of Trib2-leukaemia, total BM-derived AML cells collected from two tertiary recipient mice (Trib2 AML#A2 and Trib2 AML#B2; GFP+>90%, Figure 3.2D) were prepared for metaphase stage arrest. After microscopic visualization of metaphase chromosomes (Figure 3.3A), fixed cell suspensions were sent to Cytocell Ltd (Cambridge) to investigate numerical and structural changes in the tumour

cells genome. Analysis was performed using a method that combines an 8 square multi-probe slide and whole chromosome painting probes (labelled in FITC, Texas Red or Aqua spectra). The arrangement of chromosome combinations (3 chromosomes per square) is specifically designed to facilitate identification of the most common non-random chromosome rearrangements found in leukaemia (http://cytocell.com). Chromosome 12 – where mouse *Trib2* gene is localized- was analysed together with chromosomes 11 and 19, as depicted in Figure 3.3B. Trib2-AML murine cells were associated with a stable genome, with no evidence of copy number variants (normal diploid chromosome number 2n = 40) nor translocations (Gothami Fonseka, personal communication).

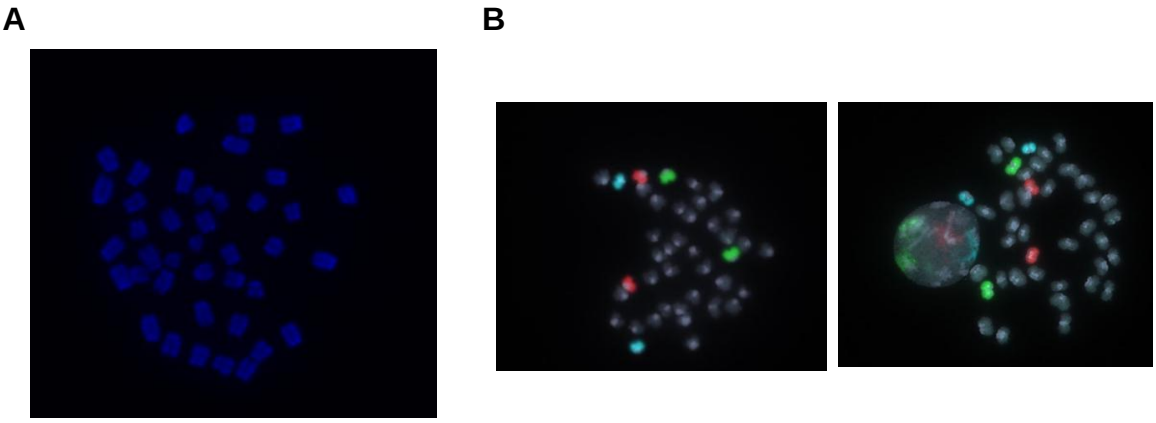

Figure 3.3 Murine Trib2-AML is genomically stable with no evidence of translocation or copy number variants
(A) Murine Trib2 leukaemic cells treated with a mitotic inhibitor were stained with DAPI (blue) for fluorescence microscopy analysis (100X magnification) and condensed and highly coiled chromosomes were detected, confirming arrest in metaphase stage. (B) Representative picture of three colour chromosome painting (60X magnification) showing chromosome 11 (red), 12 (green) and 19 (blue). No numerical or structural changes were detected by cytogenetic analysis (picture provided by Gothami Fonseka, Cytocell Ltd).

3.3.4 *TRIB2* mRNA was detected in a subset of human AML cell lines

The data above show that Trib2-induced AML in the murine setting does not, at least in the analysed leukaemic clones, correlate with chromosomal alterations as putative secondary mutagenic hits. As a starting point for assessing TRIB2 function in the human setting, expression of this gene at the mRNA level was tested and evaluated in a cohort of human cell lines. Human *TRIB2* gene is localized on chromosome 2 band p24.3 and according to Ensembl database (http://ensembl.org) has four splice variants. While one is described as a non-coding transcript, the other three are associated with known proteins. Of this last

group, only one (ENST00000155926, NM_021643) is highly annotated, with a Consensus Coding Sequence (CCDS1683) and a UniProt (Q92519) identifiers. Primers were, therefore, designed for specific detection of this transcript (sequences listed on Table 2.4; Figure 3.4A) and tested in a group of AML (SBRes, MUTZ, OCI-AML5, SB1690CB and U937) and non-AML cell lines (CV1810, CV1785, CV1665 and CV1939). cDNA analysis by PCR reaction identified the presence of *TRIB2* on an agarose gel by band analysis matching the expected size (142 bp, Figure 3.4B). For quantitative examination, expression was measured by qPCR reaction of cell lines from the AML subgroup. Consistent with the band intensity detected on agarose gel, *TRIB2* transcript levels were found to be the highest in U937 cells when compared to other five AML cell lines (Figure 3.4C), with an average Ct value of 23. These results validate the use of the described primers for subsequent *TRIB2* mRNA detection, suggesting the high expressing-U937 cells as the best suited model for further experiments.

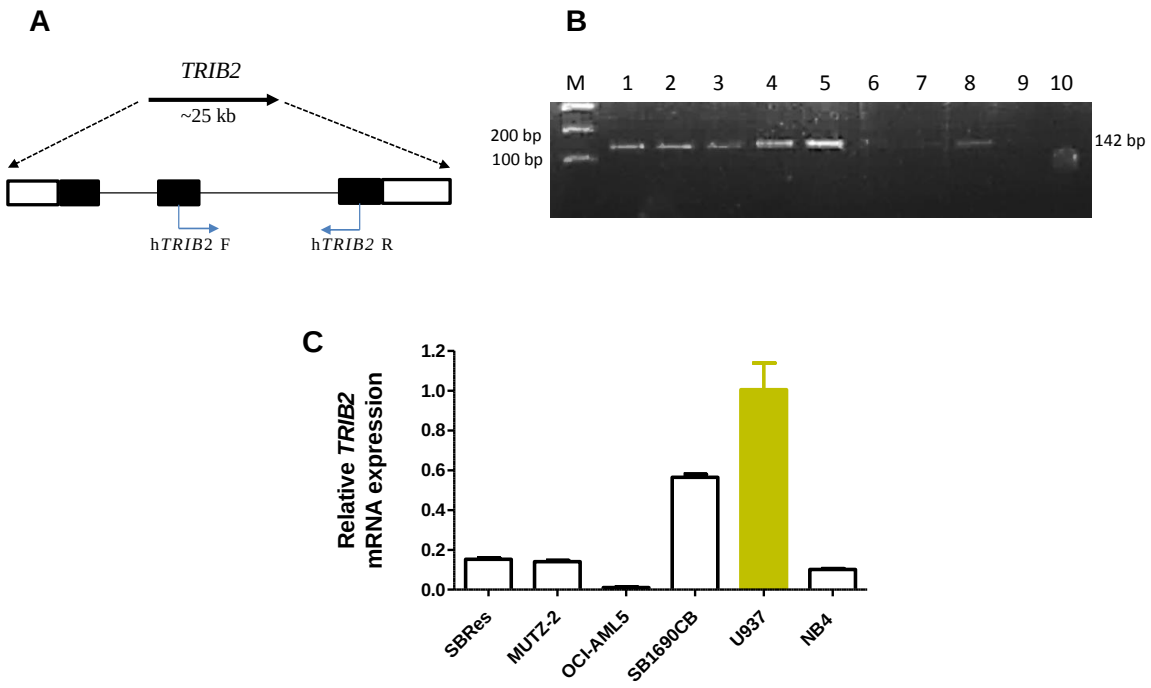

Figure 3.4 *TRIB2* expression was detected at mRNA level and shown to be highest in U937 cells when compared to other AML cell lines

(A) Human *TRIB2* is located on chromosome 2p24.3, covers 25 863 bases of genomic sequence and consists of 3 exons depicted by filled boxes. Unfilled boxes represent UnTranslated Regions (UTRs) and lines connecting the boxes are introns. Arrows in blue indicate primers designed for specific detection of the *TRIB2* protein-coding transcript. (B) cDNA samples of human cell lines were amplified by PCR reaction for *TRIB2* detection and expected amplicons (142 bp) were visualized in 1.8% agarose gel. Analysed cell lines were the following: SBRes (1), MUTZ (2), OCI-AML5 (3), SB1690CB (4), U937 (5),

CV1810 (6), CV1785 (7), CV1665 (8), CV1939 (9) and water negative control (10). M, 100bp DNA ladder; bp, base pairs. (C) Quantitative PCR (qPCR) analysis identified *TRIB2* mRNA expression to be highest in U937 cells when compared to other AML cell lines. Values represent gene expression relative to U937 cells and normalized to the reference gene *ABL*.

3.3.5 TRIB2 expression is important in the maintenance of the oncogenic properties of AML cells

Based upon observations that overexpression of TRIB2 has a role in cellular transformation, the effect of modulating its expression in human AML was examined in the U937 cell line, which was adopted as a model for high TRIB2 expressing human AML cells. While established from what was described as a diffuse histiocytic lymphoma of a 37-year-old patient (Sundström and Nilsson, 1976), U937 cells have been used to study myeloid differentiation (Ralph et al., 1983) as well as considered a valuable tool for AML research (Keeshan et al., 2006, Fang et al., 2011, Banerji et al., 2012). Importantly, *TRIB2* expression was not only detected in these cells but also shown to be the highest when compared to other AML cell lines (as detailed above). Therefore, to further examine whether TRIB2 is required for leukaemic cellular phenotype, gene knockdown was optimized in U937 cells using lentivirally expressed anti-TRIB2 small hairpin RNA (shTRIB2) or a control (shCtrl). Effective depletion of TRIB2 expression was verified by both mRNA (~80%) (Figure 3.5A) and protein (Figure 3.5B) analysis. Interestingly, western blotting also confirmed TRIB2 protein to be preferentially localized in the nucleus. While this conclusion has to be treated with caution as it only matches observations from one experiment, this is in keeping with the proposed putative nuclear localization sequence $[K/R]_2X_2[D/E]X[D/E]$ for TRIB family (Hegedus et al., 2006). Sub-cellular localization of mouse Trib2 was previously confirmed experimentally by the use of a GFP fusion protein and shown to be cytoplasmic (Kiss-Toth et al., 2006). However, overexpessed fusion proteins can affect intracellular localization and a better assessment is acquired by looking at the endogenous gene product. For subsequent TRIB2 detection, mRNA analysis was the preferentially used method, as it was thoroughly validated (Figure 3.4) and showed increased consistency over western blotting, likely hampered by TRIB2-specific antibody constraints. Gene knockdown inhibited the growth of U937 AML cells measured by cell counting with trypan blue exclusion (Figure 3.5C), induced apoptosis assessed by Annexin V staining (Figure 3.5D) and analysis of sub-G1 stage (Figure 3.5E), and promoted G1 cell cycle arrest with concomitant decrease in S phase (Figure 3.5E). The effect of TRIB2

downregulation on apoptosis and cell cycle was evaluated up to 5 days post-transduction and found to be more significant after 96 and 72 h transduction, respectively (Figure 3.5D and 3.5E), suggesting that U937 cells depleted from TRIB2 arrest in G1 phase before undergoing cell death. These results were further confirmed by means of an additional shRNA construct (LMP-shTRIB2). Modest knockdown (Appendix A-A) decreased the rate of cell growth, as assessed by cell counting by trypan blue exclusion assay, in comparison with cells expressing a retroviral control vector (LMP-Ctrl) (Appendix A-B). Altogether, these data indicate that TRIB2 expression is required for *in vitro* survival and proliferation of human AML cells (data included in (Rishi et al., 2014)).

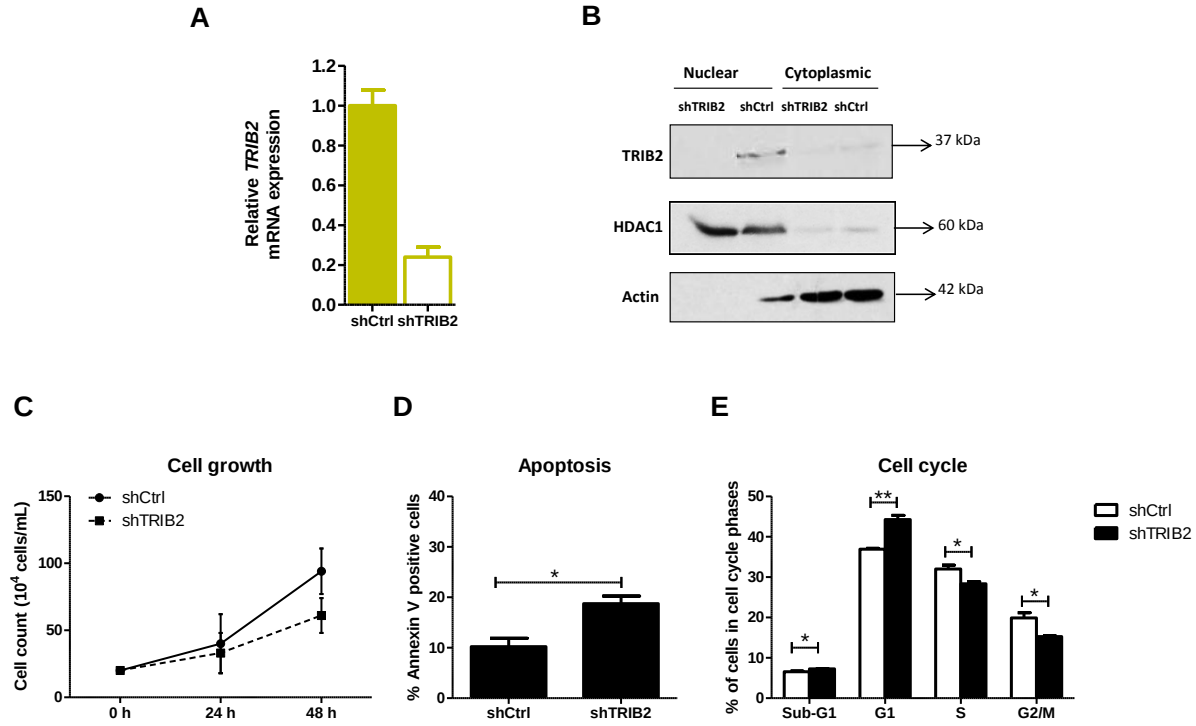

Figure 3.5 TRIB2 expression is required for growth and survival of U937 AML cells
(A) Downregulation of TRIB2 in U937 cells transduced with either shCtrl or shTRIB2 lentivirus was confirmed at mRNA and (B) protein level. In qPCR analysis values are normalized to the reference gene *ABL* and equal loading in western blot for nuclear and cytoplasmic extracts was confirmed by the specific detection of HDAC1 and actin expression, respectively. (C) Effect of TRIB2 silencing in shCtrl- or shTRIB2-U937 cells was assessed by analysis of cell growth by trypan blue exclusion, (D) cell death by Annexin V staining and (E) cell cycle was assayed by PI staining. Data presented are mean ± SD of duplicate cultures and are representative of 2 independent experiments. *$P \leq 0.05$, **$P \leq 0.01$ by Student´s *t*-test.

3.3.6 Maintenance of TRIB2 expression is required for induction of AML *in vivo*

To assess the requirement for TRIB2 during leukaemia progression *in vivo*, an AML xenograft model was used (Figure 3.6C). U937 cells were depleted of TRIB2 using the previously described lentiviral technology. Transduced cells were enriched by puromycin selection and high expression of GFP was confirmed before transplant into NSG xenografts (Figure 3.6A). Following efficient *TRIB2* knockdown (Figure 3.6B), shCtrl- or shTRIB2-U937 cells were xenografted in NSG mice. These are highly immune-deficient mice due to a targeted deletion in the IL-2 receptor γ-common chain that leads to severe impairment of B- and T- cell development and function, and completely prevents NK-cells development (Shultz et al., 2005). The timeframe (16 days) was chosen based on a previous study by Banerji V *et al*. reporting engraftment and survival of NSG mice transplanted with shCtrl-U937 cells to occur within a period of 20 days (Banerji et al., 2012). Spleen weights at the time of sacrifice (d16) were significantly decreased in the cohort of mice transplanted with shTRIB2-AML cells in comparison to control mice ($P \leq 0.05$; Figure 3.6D). Indeed, low levels of TRIB2 knockdown cells were detectable in the BM of xenotransplanted mice, while, in stark contrast, mice transplanted with control cells revealed a robust engraftment, as assayed by the percentage of engrafting GFP+ cells positive for human antibody CD45 expression (Figure 3.6E) and shown by representative FACS plots and bar graphs (Figure 3.6D, $P \leq 0.001$). Thus, in agreement with the *in vitro* studies, there is a significant growth advantage during leukaemia induction for cells that continue to express TRIB2 (data included in (O'Connor et al., 2016)) .

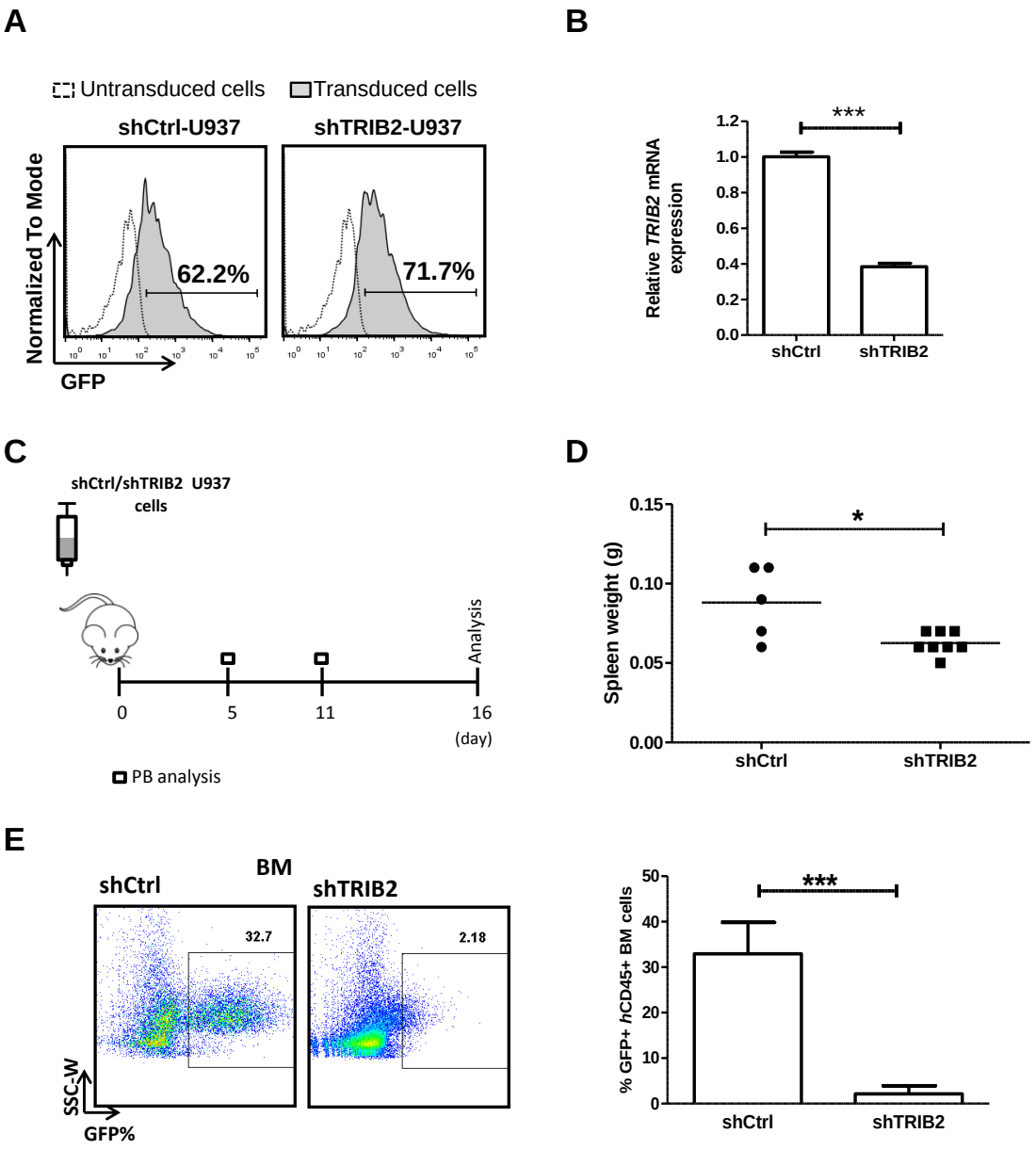

Figure 3.6 *In vivo* TRIB2 expression accelerates progression of AML
(A) U937 cells were transduced with shCtrl or shTRIB2 lentivirus and selected after 24 h with 2 µg/mL puromycin. After 2 days, equally high expression of GFP was detected by FACS analysis in both transduced cells. (B) *TRIB2* gene knockdown was confirmed at the mRNA level in shTRIB2-U937 cells. Values represent gene expression relative to shCtrl and normalized to the reference gene *ABL* (***$P \leq 0.001$ by Student´s *t*-test). (C) Schematic representation of the AML xenograft study. NSG mice were transplanted with 1.2×10^6 U937 cells transduced with shCtrl (n=5) or shTRIB2 (n=8) lentivirus. (D) Spleen weights were measured on day 16 after transplant. Each symbol represents an individual mouse and horizontal bars represent mean values (*$P \leq 0.05$ by Student´s *t*-test). (E) GFP and *h*CD45-PE Cy7 expression in BM were quantified by flow cytometry as a measure of disease burden in shCtrl- and shTRIB2-U937 mice and data are shown by representative FACS

pseudocolor plots (left panel) and bar graph (right panel) with means ± SD (***$P \leq 0.001$ by Student´s *t*-test).

3.3.7 *TRIB2* knockdown in U937 human AML cells changes expression of a subset of genes

To further explore the molecular mechanisms underlying TRIB2-induced phenotype in U937 AML cell line, expression of selected apoptosis- and cell cycle-relevant genes was investigated in these cells after downregulation of TRIB2. U937 cells transduced with either shCtrl- or shTRIB2-lentivirus were sorted and mRNA from two independent replicates was collected at 48 and 72 h post-transduction. High-throughput qPCR was carried out using the 48.48 Dynamic Array™ IFC system (Fluidigm). *TRIB2* knockdown was confirmed in both analyses (Figure 3.7A and B). When comparing expression of genes in response to *TRIB2* silencing, samples collected after 48 h transduction (Figure 3.7A) showed an increase in expression of the cell cycle regulator genes (*ATM*, *ATR*, *BRCA2*, *PTEN*, *P27KIP1* and *CDC25A*) and also of the pro-apoptotic *BIM* (*BCL2-Like11*), *CASP3*, *CASP8* and *BAX* genes. Even if a concomitant downregulation of the anti-apoptotic genes (except for *XIAP*) was not detected, the ratio of pro-apoptotic to anti-apoptotic genes was increased suggesting that *TRIB2* knockdown results in a pro-apoptotic phenotype. The enhanced mRNA expression of the pro-apoptotic genes when *TRIB2* was silenced correlates with results obtained for the cell death analysis that identified an increase in apoptosis after TRIB2 knockdown. Expression of the *P27KIP1* cyclin-dependent kinase inhibitor and the pro-apoptotic *BIM* remained transcriptionally up-regulated at 72 h post transduction. *P27KIP1* encodes a protein that binds to and prevents the activation of cyclin E-CDK2 or cyclin D-CDK4 complexes, and thus controls the cell cycle progression at G1 phase (Toyoshima and Hunter, 1994). *BIM* is a BH3-only protein from the BCL-2 family that is capable of inducing apoptosis (O'Connor et al., 1998). These findings are in line with the cell cycle arrest and apoptotic phenotypes observed after 72 and 96 h transduction, respectively (Figure 3.5 D and E). Importantly, the transcriptional changes were detected at time points (48 and 72 h) that either match or precede the abovementioned phenotypes, hence, supporting a cause-and-effect relationship. Results therefore suggest that TRIB2 modulates apoptosis and cell-cycle sensitivity by influencing the expression of a subset of genes known to have implications on these phenotypes. Together the *in vitro* and *in vivo* experiments support the role of TRIB2 in AML cell survival.

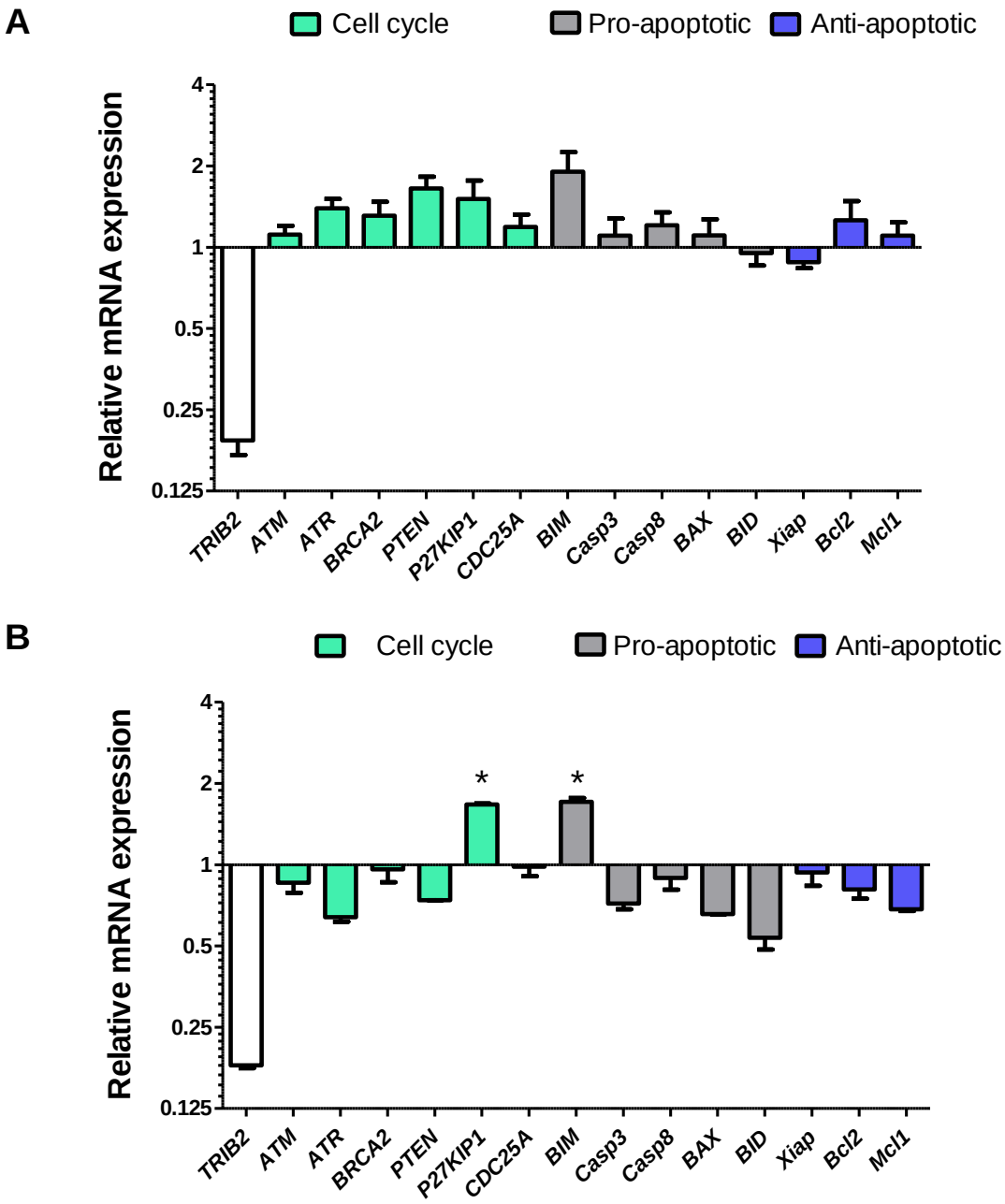

Figure 3.7 Differential expression of a subset of genes in U937 cells after modulation of *TRIB2* expression

(A) Gene expression analysis to compare *TRIB2* knockdown and U937 cells transduced with shCtrl was performed with samples collected after 48 and (B) 72 h transduction. Genes were normalized against the average of reference genes *ABL*, *B2M*, *ENOX2* and *RNF20*. Values are relative to shCtrl-U937 and are expressed as $\log_2$. *$P \leq 0.05$ by Student´s *t*-test.

3.3.8 *TRIB2* is expressed in a significant number of AML patient samples

The implication of TRIB2 expression in AML cell survival prompted the mRNA analysis of *TRIB2* across a cohort of twenty-eight AML patient samples. Transcript levels were compared to U937 cells and two non-AML cell lines (CV1665 and CV1939) with low levels of *TRIB2* were included. The clinical characteristics of patients included in this study that could be obtained are shown in Table 3.1. High percentage of blasts cells (indicated by CD33 antigen, >58%) and enrichment for a more primitive population (% of CD34+) were reported for few samples. qPCR analysis detected variable *TRIB2* expression across the cohort but a significant number of primary AML cells were identified with transcript levels comparable to that of the U937 cell line, used as a control reference for high expression (Figure 3.8). To avoid seeking an optimal cut point, AML patient samples were dichotomized at the mean fold change value (0.4) into 2 expressing level groups: a low *TRIB2* group with *TRIB2* values less than 0.4 (n=14/28; median fold change, 0.15; range, 0.02-0.34) and a medium to high *TRIB2* group consisting of patients with *TRIB2* values of more than 0.4 (n=14/28; median fold change, 0.76; range, 0.36-1.5).

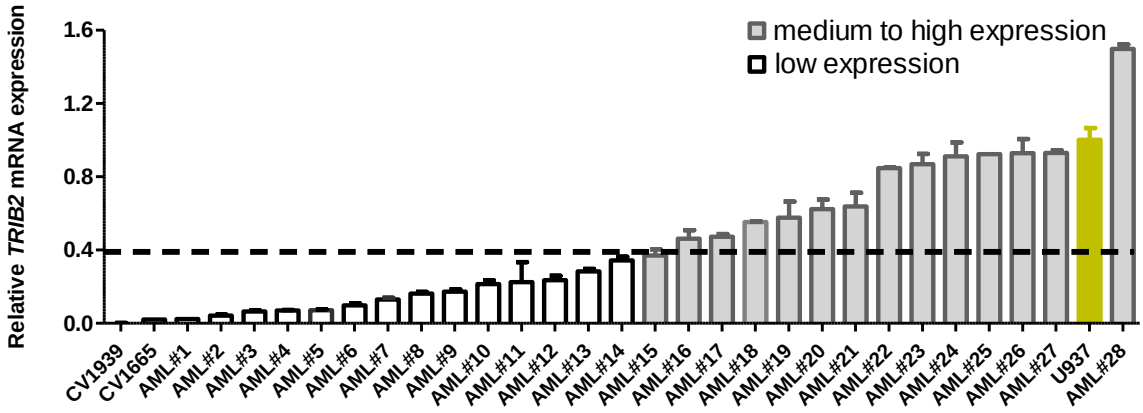

Figure 3.8 *TRIB2* is detected at significant levels in a cohort of AML patients
For *TRIB2* mRNA analysis U937 AML cell line was used for comparison purposes as a control for high *TRIB2* expression and two non-AML cell lines (CV1665 and CV1939) with low levels of *TRIB2* were included. A significant number of AMLs with medium to high levels of *TRIB2* mRNA (grey bars; 14/28) was detected when using the average of fold changes (0.4) as a cut-off value. Values represent gene expression relative to U937 cells (green bar) and normalized to the reference gene *ABL*.

There were no significant differences between low and medium to high *TRIB2*-expressing patients with respect to age (median age 65 vs 62, respectively), with the exception of AML#8 (36-years-old). Moreover, *TRIB2* expression levels were randomly distributed across gender and the FAB classes. Based on the available information regarding cytogenetic/molecular abnormalities and their prognostic relevance described in the literature, samples were further classified according to the risk-scoring system (Chapter 1, section 1.2.3), as depicted in Table 3.1. All 3/10 reported aberrations that predict for poor prognosis (complex karyotype, t (6;11) and monosomy 7) were found in patients with low *TRIB2* mRNA levels (AML#1, 2 and 13, respectively). Complex karyotype (three or more different cytogenetic aberrations) and monosomy of chromosome 7 are consistently associated with unfavourable outcome (Löwenberg, 2001) whereas t (6;11) translocation is rare in AML but also reported to indicate a poor prognosis (Martineau et al., 1998, Blum et al., 2004). Abnormalities associated with favorable outcome, t(8;21) and FLT3-WT, were detected in both low (AML#8) and high (AML#23 and 28) *TRIB2* expressing subgroups. Cytogenetically normal (CN) samples, included in the intermediate risk AML, were also detected in both cohorts defined based on *TRIB2* status. Taken together, these data identified *TRIB2* expression in human AML samples at levels, to some extent (14/28), comparable to the high expressing U937 AML cell line. Association with the available, while incomplete, karyotype/molecular information suggests that AML patients with higher *TRIB2* expression are more likely to be associated with the favourable or the intermediate prognostic subgroups.

Table 3.1 Characteristics of the AML patient samples screened for mRNA *TRIB2* expression

Patient ID	Gender	Age (Years)	Clinical Status	% CD33	% CD34	FAB classification	cytogenetic and molecular information	Risk-stratification	*TRIB2* mRNA
AML#1	F	57	-	58.1%	-	M0 or M1	Complex (47XX, +4[2]/48, idem, +10[3]/48, idem, der(2)?t(2,17(q37;q21),+10[8]/46,XX[2])	Poor	low
AML#2	-	-	-	-	-	-	t (6;11)	Poor	low
AML#3	M	79	-	-	52.6%	-	-	-	low
AML#4	F	70	Relapse	-	-	M6	-	-	low
AML#5	-	-	-	-	-	-	-	-	low
AML#6	M	57	-	-	-	CMML/M5	-	-	low
AML#7	M	73	-	-	-	-	-	-	low
AML#8	F	36	-	-	70.6%	M2	t (8;21); negative for FLT3 mutation	Favorable	low
AML#9	-	-	-	-	-	-	-	-	low
AML#10	M	-	Relapse	91.6%	-	M5	-	-	low
AML#11	F	82	-	-	-	-	-	-	low
AML#12	-	-	-	-	-	-	CN	Intermediate	low
AML#13	-	-	-	-	-	M2	monosomy 7	Poor	low
AML#14	-	-	-	-	-	MDS/M4	CN	Intermediate	low
AML#15	F	64	-	90.6%	14%	M6	CN	Intermediate	medium to high
AML#16	-	-	-	-	-	-	-	-	medium to high
AML#17	M	-	-	ψ	ψ	NOS	-	-	medium to high
AML#18	-	-	-	-	-	-	-	-	medium to high
AML#19	-	-	-	-	-	-	-	-	medium to high
AML#20	M	78	Diagnosis	ψ	ψ	M4	-	-	medium to high
AML#21	-	-	-	-	-	-	-	-	medium to high
AML#22	F	48	-	-	-	M3	-	-	medium to high
AML#23	-	-	-	-	-	M2	t (8;21)	Favorable	medium to high
AML#24	M	-	-	-	-	-	-	-	medium to high
AML#25	F	68	No treatmen	-	-	MDS/AML	-	-	medium to high
AML#26	-	-	-	-	-	-	-	-	medium to high
AML#27	-	-	-	-	-	-	chromosome 9 aberration	ψψ	medium to high
AML#28	F	51	-	-	-	-	negative for FLT3 mutation	Favorable	medium to high

FAB, French-American-British; CMML, Chronic Myelomonocytic Leukaemia; MDS, Myelodysplastic Syndrome; NOS, not otherwise specified; CN, cytogenetically normal; ψ, samples are positive for these cell surface markers but % values are unknown; ψψ, AML#27 was excluded from risk-stratification as different types of chromosome 9 aberrations described in the literature (trisomy 9 and del(9)) predict for distinctive AML outcomes (intermediate and favorable) (Flandrin, 2002, Sole et al., 2005, Zhang et al., 2005).

3.3.9 Higher expression of *TRIB2* in primary human AML samples is not predictive of preferential engraftment

TRIB2 was shown here to be important in the maintenance of the oncogenic properties of human AML cells (Figure 3.5). In light of these findings, together with the mRNA analysis indicating detectable high levels of *TRIB2* in a cohort of primary human AML cells, it was reasoned that *TRIB2* expression could correlate with engraftment capability of AML patient samples. Such an experimental approach would allow a deeper characterization of TRIB2 role in human AML biology while, simultaneously, assessing its predictive value in relation to clinical outcome of patients, as engraftment levels tend to be higher with AML samples harboring poor prognostic abnormalities than with those carrying changes associated with a favorable outcome (Ailles et al., 1999). To address this, samples from 6 AML patients classified according to FAB subtype and cytogenetic characteristics when available (Table 3.1) were selected for a xeno-engraftment study based on previous

dichotomization into low (AML#1, 4 and 10) and medium to high (AML#15, 17 and 20) *TRIB2* expression (Figure 3.8A). Choice of patient cells was narrowed by samples/number of cells that were available from the bio-bank. For the *in vivo* experiment, the immuno-permissive NSG mice were used as recipients. These mice not only have a longer life span (>90 weeks) than the NOD/SCID mice due to the unlikelihood of developing thymonas (Shultz et al., 2005), but also, and most importantly, represent an improved model over earlier immuno-deficient mouse strains. Improvements include both the robustness of engraftment and the expansion of unsorted human AML MNCs in primary, secondary and tertiary recipients in a manner that seems to model human leukaemic disease progression (Sanchez et al., 2009). Published experiments were used as guidelines to design the animal study (Figure 3.9A), to define irradiation dosage, sex and age of the animals, number of injected cells and time course adopted (Sanchez et al., 2009, Notta et al., 2010, Salvestrini et al., 2012, von Bonin et al., 2013, Barth et al., 2014, Pabst et al., 2014). Groups of 3 female NSG recipients/sample were injected with 1.1 to 1.6x10^6 unsorted leukaemic PB MNCs 24 h after sublethal irradiation (2.25/2.5 Gy). Engraftment was defined by the prevalence of *h*CD33 and *h*CD45 double positive cells, which are consistent with human AML. Mice were monitored by flow cytometric analysis of PB samples taken at week 3, 5, 7 and 8 after transplantation (data not shown, as values were overall below 0.1). When long-term engraftment of human leukaemic cells was evaluated following necropsy at 12 weeks post-injection, all mice showed >0.1% *h*CD45+*h*CD33+ AML cells replacement of the BM by FACS analysis (used cut-off value (Sanchez et al., 2009, Notta et al., 2010, Sarry et al., 2011)) (Figure 3.9C and D). BM was the primary site of leukaemic cells infiltration with 4/17 specimens displaying high levels of engraftment (over 10%), as depicted by Figure 9.D. In contrast to previous studies reporting that engraftment levels could shift from a heavily infiltrated BM to the spleen, which could be a result of progression to marrow fibrosis (Kuter et al., 2007, Sanchez et al., 2009), analysed spleens in this study showed limited leukaemic cell expansion (largely < 1%, data not shown). An overall correlation between spleen enlargement and efficiency of engraftment was detected in NSG mice, exemplified by mice transplanted with AML#10 presenting both high BM engraftment (Figure 3.9D) and spleen weight (Figure 3.9B left and right panels) and corroborating that NSG mice engrafted with human AML samples display features of the human disease. Importantly, this study showed a robust engraftment of unsorted leukaemic cells. Engraftment did not correlate with specific FAB subtypes, as samples were randomly distributed across classes, and from the cohort selected for NSG transplantation only two were annotated with cytogenetic/molecular information. Nevertheless, it is striking that the

highest levels of *h*CD45+*h*CD33+ AML cells were detected in mice tail injected with the complex karyotype AML#1 (Table 3.1), despite differences in the magnitude of engraftment (9%,37%,42%). With regard to the differential *TRIB2* expression, no statistically significant difference (*P*=0.08) was observed between the two cohorts in their ability to engraft the NSG BM with AML cells (Figure 3.9D). It is likely that a bias can be introduced by comparing a heterogeneous AML cohort with limited information regarding clinical and cytogenetic/molecular features. However, results suggest that a higher expression of this oncogene does not correlate with increased engraftment capability in NSG mice, and thus not predicting an association with adverse prognosis.

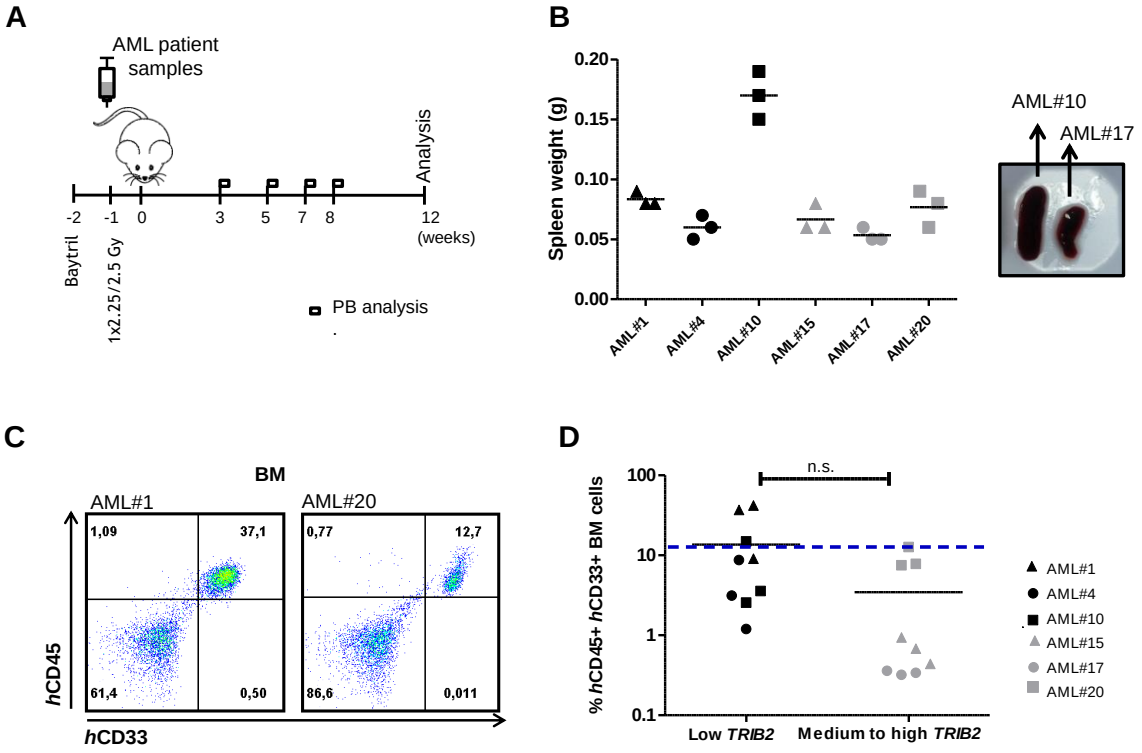

Figure 3.9 Engraftment ability of primary human AML with variable levels of *TRIB2* expression in NSG mice

(A) Schematic representation of the xenotransplantation. 1.1-1.6x10^6 human AML cells selected for low (AML#1, 4 and 10) and medium to high (AML#15, 17 and 20) *TRIB2* expression were injected through tail vein 24 h after sublethal irradiation of 6-11 week-old female NSG mice. Each sample was injected into 3 mice. (B) Spleen weights were measured following necropsy at 12 weeks after transplantation, as shown by graph (left panel) and representative images (right panel). Pictures are from spleens collected from mice transplanted with AML#10 (0.19 g) and AML#17 (0.06 g). (C) Engraftment was assessed by flow cytometry detection of *h*CD45 PE Cy7 +*h*CD33 APC+ double positive BM cells consistent with human AML, as depicted by representative FACS pseudocolor plots. (D) No statistically significant differences were detected in marrow engraftment

(> 0.1%) based on low vs medium to high *TRIB2* expression. Blue line in bar graph indicates a high level of engraftment of 10% of murine BM replaced with human AML (4/18 mice) detected in both cohorts. For (B) and (D), each symbol denotes a single mouse and horizontal bars represent mean values for a given cohort. Mice transplanted with AML samples expressing low *TRIB2* are highlighted in black whereas grey colour indicates mice injected with primary leukaemic cells with medium to high *TRIB2* expression; n.s., not significant by Student´s *t*- test.

3.4 Discussion

TRIB2 has been reported as a cancer driver in a variety of malignancies. Here, it is shown that in the majority of cancers retrieved from COSMIC database, in which AML is included, *TRIB2* oncogenic activity is related to its elevated gene expression rather than associated with different genomic alterations or mutations. This conclusion amplifies previous observations reporting a tumorigenic role for *TRIB2* in melanoma and lung cells found to overexpress this gene (Zanella et al., 2010, Grandinetti et al., 2011). Moreover, Trib2 ability to induce murine leukaemia also resulted from its overexpression. In addition, increased expression is unlikely to be a result of elevated gene copy number, as CNV was rarely found across the different tumours tissues analysed here, underscoring an important role for regulators of TRIB2 expression in cancer. Indeed, in a recent paper published during the course of the present study, a feedback loop mechanism for the positive upregulation of TRIB2 expression in AML was detailed. TRIB2 expression was shown to be regulated in AML cells by E2F1, that cooperates with the C/EBPα p30 oncogenic isoform to activate the *TRIB2* promoter, while in normal GMPs the wild type C/EBPα p42 is bound to the *TRIB2* promoter (Rishi et al., 2014).

The finding that mouse BM cells overexpressing *Trib2* gene could be propagated *in vivo* for three passages, retaining robust levels of engraftment accompanied by shorter latency, demonstrates their self-renewal properties and long-term leukaemogenic potential. In previous work (Keeshan 2006), serial transplantations to tertiary recipients were not performed. Data presented here show that Trib2 effectively and serially engrafts to tertiary recipients, maintains the primary AML phenotype and is not associated with secondary genomic instability characteristics, such as chromosomal alterations. Moreover, central nervous system (CNS) involvement detected in the tertiary recipients underpins aggressiveness of Trib2-induced leukaemia, as it can be a serious complication during the clinical course of patients with AML (Dohner et al., 2010), and hints at a possible use of

this model to investigate mechanisms and treatment of CNS leukaemia. When murine Trib2-BM cells were kayotyped for a more comprehensive analysis of this leukaemia, they were found in the absence of cytogenetically detectable rearrangements. It is noteworthy that other single genes reported to be overexpressed in AML (*BAALC* (Tanner et al., 2001, Baldus et al., 2003), *ERG* (Marcucci et al., 2005) and *MN1* (Heuser et al., 2005)) have been associated with adverse human leukaemia prognosis also in the large subset of CN-AML. This may be indicative that TRIB2 overexpression is rooted in the cytogenetically normal group, which could be of particular relevance to help defining a heterogeneous subtype for which the WHO classification fails to predict outcome. Indeed, recent studies have evaluated the usefulness of global gene-expression profiling to identify prognostic subgroups within the CN-AML patients (Baldus et al., 2007). TRIB2 overexpression does not seem, however, to be restricted to this cytogenetic subset of AML since it was shown to occur in AML patients with abnormal karyotypes (AML#23 and 27, Figure 3.8).

In contrast to the existing knowledge on Trib2 function in driving murine AML *in vivo*, the study of TRIB2 role in human AML settings is limited to expression analysis to date. With that in mind, TRIB2 function in the context of myeloid malignancies was characterized and strengthened in a human leukaemia setting. Functional assays clearly showed importance of TRIB2 expression for survival of U937 AML cells in liquid culture, which displayed an altered cellular phenotype after gene knockdown. TRIB2-specific suppression by means of two shRNA constructs led to impaired growth, as a consequence of both an increase in apoptosis and a decrease in cell proliferation. Cell culture-based systems are, however, limited on their ability to recapitulate primary disease as they cannot replicate cell extrinsic interactions with the immune cells or BM niche. Murine xenograft models, albeit limited in their ability to address leukaemia-immune cell interactions, are suitable to explore human cell specific biology in an *in vivo* environment (Cook and Pardee, 2013). Moreover, the use of well-established, easily grown human cell lines in NSG xeno-engraftment studies has the unique advantage of providing a model that recapitulates human disease in a timeframe of days or weeks, even if the extent to which they retain features of the original disease *in vivo* is a matter of debate (Kamb, 2005). Therefore, lentiviral knockdown of TRIB2 in U937 AML cells was performed and xenotransplantation into NSG mice used as a surrogate assay to study the modulating effect of TRIB2 on AML aggressiveness *in vivo*. Consistent with the results obtained *in vitro*, progression of the AML xenografts was significantly impaired ($P \leq 0.001$) following TRIB2 knockdown, accompanied by detection of a lower spleen weight in this cohort. A significant growth advantage during *in vivo* leukaemogenesis for cells that continue to express TRIB2 was, thus, suggested by the short

latency U937-NSG model, supporting the view that this gene is functionally important in the maintenance of the malignant phenotype of human AML cells. Based on the phenotypic changes observed upon TRIB2 knockdown, it was thus hypothesised that gene depletion could elicit downstream transcriptional modifications in genes related with the detected apoptotic response and cell cycle arrest. Indeed the overall expression pattern observed in cells collected at an earlier time point (48 h after transduction) suggested an increase in pro-apoptotic genes discreetly supported by a decrease in anti-apoptotic genes. This gene analysis has led to the identification of a smaller subset of genes that could explain, to some extent, the observed TRIB2-dependent phenotype. Based on the observation that the cell-cycle regulator *P27KIP1* and *BIM*, were consistently upregulated upon *TRIB2* knockdown, it was questioned whether FOXO3a, an upstream mediator of both these genes could be implicated by mediating TRIB2 regulation of both genes. The pro-apoptotic *BIM* is a transcriptional target of FOXO, which is in turn downregulated by TRIB2 in melanoma cells after cytoplasmic sequestration. No change in total FOXO3a subcellular localization was detected by western blotting after TRIB2 knockdown (data not shown). Although not extensively explored here, effects on FOXO3a function rather than expression are possible given the known relationship between TRIB2 and FOXO3a in melanoma cells (Zanella et al., 2010).

TRIB2 expression analysis in a cohort of AML patient samples revealed a significant number with elevated transcript levels comparable to that of the U937 cells, the human AML cell line found to express the highest *TRIB2* expression within a group of AML cell lines. This result disagrees with a previous study reporting TRIB2 expression to be overall low across AML karyotypes or FAB subtypes assessed from publically available microarray datasets (Liang et al., 2013). It is conceivable that differences are likely attributed to the criteria used to define expression levels. Previous studies reporting *TRIB2* overexpression in malignant melanoma and lung cancer (Zanella et al., 2010, Grandinetti et al., 2011) suggest that mRNA analysis of this oncogene would be better assessed by comparing tumor tissue of a given patient with its matched normal counterpart. In light of the observed *TRIB2* mRNA levels, it would be extremely interesting to evaluate C/EBPα protein status in these samples, given that elevated *TRIB2* expression has been linked with a subset of human AML characterized by deregulation of this transcription factor (Keeshan et al., 2006) and that C/EBPα is a downstream factor of TRIB2 proteolytic activity. TRIB2 was recently identified as a meaningful biomarker in malignant melanoma, as its expression strongly correlates with disease stage and clinical prognosis, predicting, as well, clinical response to chemotherapy (Hill et al., 2015). High risk B-cell chronic lymphocytic

leukaemia (B-CLL) patients were also associated with differentially expressed *TRIB2* (Johansson et al., 2010). Hence, it would be of interest to know the relapse rate, overall survival, disease-free survival and complete remission rate of the analysed leukaemic patients to assess if dichotomization based on TRIB2 expression is meaningful as a diagnostic marker in the context of AML.

The presence of *FLT3* mutations in AML patient samples correlates with an enhanced ability to engraft in NOD/SCID (Rombouts et al., 2000) and NSG (Sanchez et al., 2009) mice when compared with *FLT3* wild-type-containing human AML. Also, AML harboring *DNMT3A* mutations, which predict for adverse outcome, were shown to engraft with exceptional efficiency (Barth et al., 2014), supporting the view that a correlation exists between xeno-engraftment potential and disease aggressiveness in humans. With that in mind, the NSG model was used to investigate the *in vivo* leukaemia-initiating capacity of human primary AML cells with dichotomized levels of *TRIB2* transcripts while assessing whether increased expression of this gene could be afforded a prognostic significance. The severe impairment of NSG innate immunity and the associated prolonged life span have made them the gold standard for long-term studies of primary human AML engraftment. Indeed, a global analysis suggests that a robust engraftment can be attained with this model, as BM was shown to be replaced by >0.1% *h*CD45+*h*CD33+ AML cells. When ability to repopulate NSG mice was analysed in terms of *TRIB2* expression, higher transcript levels in AML patients did not correlate with preferential leukaemic cell engraftment. However, caution should be used when concluding differences based on TRIB2 expression since a number of other factors could be implicated in differential levels of engraftment, namely, elements of BM homing, survival in a foreign niche, expansion in the absence of specific human growth factors and supporting stromal cells, as well as intrinsic differences among AML samples (as exemplified by poor-risk associated AML#1). Further experiments including a larger cohort of well characterized AML patients would be needed to clarify TRIB2 significance in a diagnostic setting.

Taken together, these findings establish a functional role for deregulated TRIB2 expression in the pathogenesis of human AML and provided a contextual framework to further investigate this oncogene as a therapeutic target, as next described.

Chapter 4
Proteasome inhibition selectively targets AML with high TRIB2 expression

When indicated, results presented in this chapter have been published in (O'Connor et al., 2016) and the PDF of the publication is provided in Appendix G.

4.1 Introduction

AML is primarily a disease of elderly people for whom prognosis remains consistently dismal in spite of the past few decades' improvement in the overall outlook for younger patients. In addition, the mainstays of AML therapy have remained unchanged for the last 30 years (Tallman et al., 2005, Burnett, 2013, Ferrara and Schiffer, 2013). The combination of cytarabine (*e.g.*, cytosine arabinose, Ara-C) with an anthracycline (*e.g.*, daunorubicin, idarubicin) is the backbone of induction therapy, which has become the standard of care for patients not participating in a clinical trial. These patients receive cytarabine as a continuous intravenous infusion for 7 consecutive days, while anthracycline is given for 3 consecutive days as an intravenous push. The tolerance of elderly patients to this therapy is limited by host-related factors, as well as by the frequent development of myelodysplasia, unfavourable karyotypes and overexpression of the multidrug-resistance gene *MDR-1* at diagnosis (Smith et al., 2004). The main exception to the traditional cytotoxic chemotherapy known as "7+3" is the use of all-*trans* retinoic acid (ATRA), a derivative of vitamin A (or retinol) that has held great promise for differentiation-based therapy. ATRA, in combination with low-dose chemotherapy, is effective on the rare M3 acute promyelocytic leukaemia (APL) subtype (5-10% of AML) (Tallmann, 2004). Typically, this subtype carries the leukaemia-generating PML-RARα fusion protein, which results from t(15;17) translocation (Melnick and Licht, 1999). Pharmacological concentrations of the retinoic acid receptor (RAR)-specific ligand ATRA cause a conformational change of PML-RARα, which acts as a dominant negative inhibitor of the WT RARα. Co-repressors are then released, normal RARα- responsive gene regulation is restored and terminal APL cell differentiation into mature granulocytes is induced (Jing and Waxman, 2007). Unfortunately, ATRA is not clinically useful for other AML subtypes. Most non-APL leukaemia cells respond to ATRA but only at high concentrations, which leads to important cytotoxic effects (Gupta et al., 2012). Therefore, research strategies that seek to further extend treatment efficacy to non-APL cells are key.

The use of small-molecule drugs designed to inhibit the proteasome degradation pathway has sparked intensive research for the treatment of a variety of cancers, including AML. In fact, clinical trials for AML patients have been conducted and are currently on going to evaluate Brtz and identify drug combinations showing therapeutic efficacy. Despite the lack of single agent activity (Cortes et al., 2004, Horton et al., 2007), Brtz has shown promising results when used in combination regimens for AML. Two phase I studies for poor-risk groups demonstrated the feasibility and preliminary clinical activity of Brtz in

combination with idarubicin (Howard et al., 2013) or with the DNA hypomethylating agent decitabine, despite neurotoxicity concerns (Blum et al., 2012). Attar *et al*. randomized 95 patients (age 60 to 75 years) with untreated AML to evaluate the safety and efficacy of Brtz in combination with daunorubicin and cytarabine and assessed whether Brtz could improve the standard induction chemotherapy by increasing the remission rate. Despite the neurotoxicity observed in some patients, this phase II/I clinical study reported an encouraging remission frequency (Attar et al., 2013). Additionally, the effect of Brtz in combination with standard chemotherapy is presently being evaluated on a phase III trial in younger patients (0 to 30 years of age) with de novo AML (Children's Oncology Group (COG) study AAML1031).

It is known that the myeloid pathogenicity of TRIB2 relies on its ability to bind the full-length isoform of C/EBPα (C/EBPα p42) and mediate its proteasomal degradation through binding with COP1 E3 ligase while sparing p30 (Keeshan et al., 2006, Keeshan et al., 2010). Even in a broader tumour context, TRIB2 is found to have an oncogenic role via the UPS. In lung cancer, where its expression is elevated and has a role in cellular transformation, TRIB2 downregulates C/EBPα via targeting of the transcription factor for proteasomal degradation. By means of an immunoprecipitation-mass spectrometry approach, it was further found that interaction between TRIB2 at the C terminus and the E3 ligase TRIM21 is important to this process (Grandinetti et al., 2011). In liver cancer cells, TRIB2 binds other E3 ligases including βTrCP, COP1 and Smurf1 (Xu et al., 2014) (see Chapter 1, section 1.3.3). The strong link between TRIB2 and the UPS in cancer creates a framework for considering proteasome inhibition treatment.

4.2 Aims and Objectives

The present study hypothesises that proteasome inhibition would effectively inhibit TRIB2 function by abrogating C/EBPα p42 protein degradation and that it could be an effective pharmacological strategy in TRIB2-expressing AML cells. Therefore, the specific aims of this chapter were:

i. To investigate the chemotherapeutic response of both murine and human TRIB2-expressing AML cells to proteasome inhibition;

   a. *In vitro*
   b. *In vivo*

ii. To investigate specificity of proteasome inhibition on the TRIB2-C/EBPα axis.

4.3 Results

4.3.1 Murine Trib2 AML cells are sensitive to Brtz treatment *in vitro*

The antitumor effect of proteasome inhibition in TRIB2 positive leukaemic cells was first investigated using the boronic acid derivative Brtz and the murine Trib2-GFP+-AML model. This model was considered a logical approach for a first therapeutic evaluation, as it was thoroughly characterized and could be used as a source of leukaemic cells. Therefore, BM cells harvested from secondary Trib2-AML mice were treated *in vitro* either with Brtz or with DMSO as a vehicle-only control to measure the apoptotic effect. The concentration used for the *in vitro* Brtz treatment was 10 nM, based on the average 50% inhibitory concentration (IC50) in U937 cells reported in section 4.3.3. After a 24 h treatment, cells were analysed by FACS for GFP expression, which was used as a marker for both cell viability and detection of leukaemic cells. A significant reduction in Trib2-expressing cells was detected following Brtz treatment, as evidenced by a decrease in % of GFP positive cells depicted in the corresponding FACS plots (Figure 4.1A) and bar graph (Figure 4.1B). Subsequently, cells matching one biological replicate were plated for colony-forming cell (CFC) assay 24 h after Brtz treatment to determine the growth and clonal potential of any remaining cells. After 7 days, there was a significant reduction in the number of colonies formed from treated cells when compared to untreated (Figure 4.1C). Additionally, cell colonies were stained for the myeloid differentiation cell surface markers CD11b and Gr-1 and analysed by FACS to evaluate changes in expression of these myeloid markers. An increase in the percentage of double-positive cells for both antibodies was detected in treated cells (Figure 4.1D), suggesting that Brtz elicits differentiation of non-apoptotic AML cells.

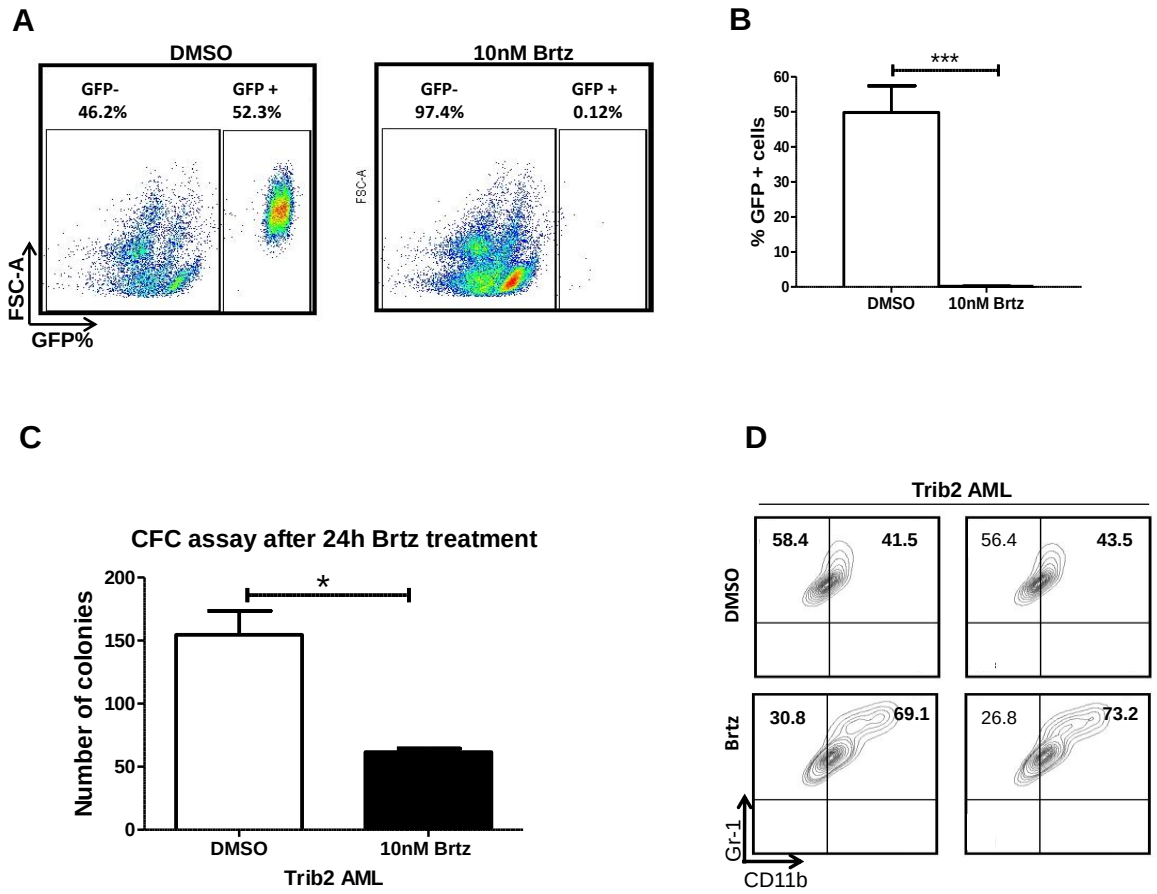

Figure 4.1Trib2 murine BM cells are sensitive to *in vitro* Brtz treatment
(A) BM cells collected from secondary recipient mice with Trib2-induced leukaemia were treated *in vitro* with either Brtz (10 nM) or DMSO. After 24 h, GFP expression was quantified. Data are shown by representative FACS pseudocolor plots and (B) representative bar graph of 3 independent experiments with mean ± SD of 3 biological replicates (3 samples x 3 mice, considered as 3 independent experiment performed in triplicate). (C) Brtz or DMSO treated cells from one biological replicate were plated for CFC assay. Colonies were scored at day 7 and were normalized to % of GFP positive cells (error bar represents the mean ± SD of 2 technical replicates). (D) On day 11 of CFC assay the myeloid phenotype was assessed by FACS analysis of CD11b-PE and Gr-1-APC of the GFP+ population, as shown by representative contour plots. ***$P \leq 0.001$, *$P \leq 0.05$ by Student´s *t*-test.

4.3.2 Brtz preferentially targets murine Trib2 AML cells rather than normal haemopoietic cells

To investigate whether targeting the UPS, a universal and broadly active cellular component, provides the selectivity and specificity required for cancer therapeutics, the proteasome inhibitor activity was assessed in normal bulk BM cells from wild type mice. Furthermore, it was evaluated whether a consistent result would be detected in normal BM stem cell populations. The stem cell populations were purified as outlined in section 2.7.6 of the methods section. Thus, both total normal BM cells and the most primitive (LSK) and more differentiated (lineage+) populations were treated with Brtz (10 nM) and DMSO for 24 h *in vitro* as described in section 2.1.8 of Chapter 2. Cell survival was analysed by staining with Annexin V and DAPI, and no significant differences were detected when comparing treated *versus* untreated cells in all populations (Figure 4.2A) at a concentration shown to have pro-apoptotic effect on Trib2 leukaemic murine BM cells. Consistent with these results, the myeloid phenotype (CD11b/Gr-1) of LSK and lineage positive cells did not show any change after the 24 h treatment, which rules out Brtz-induced differentiation at this time point (Figure 4.2B). Taken together with the data from section 4.3.1, the results suggest that Brtz is selectively pro-apoptotic towards leukaemic cells, while sparing normal BM cells.

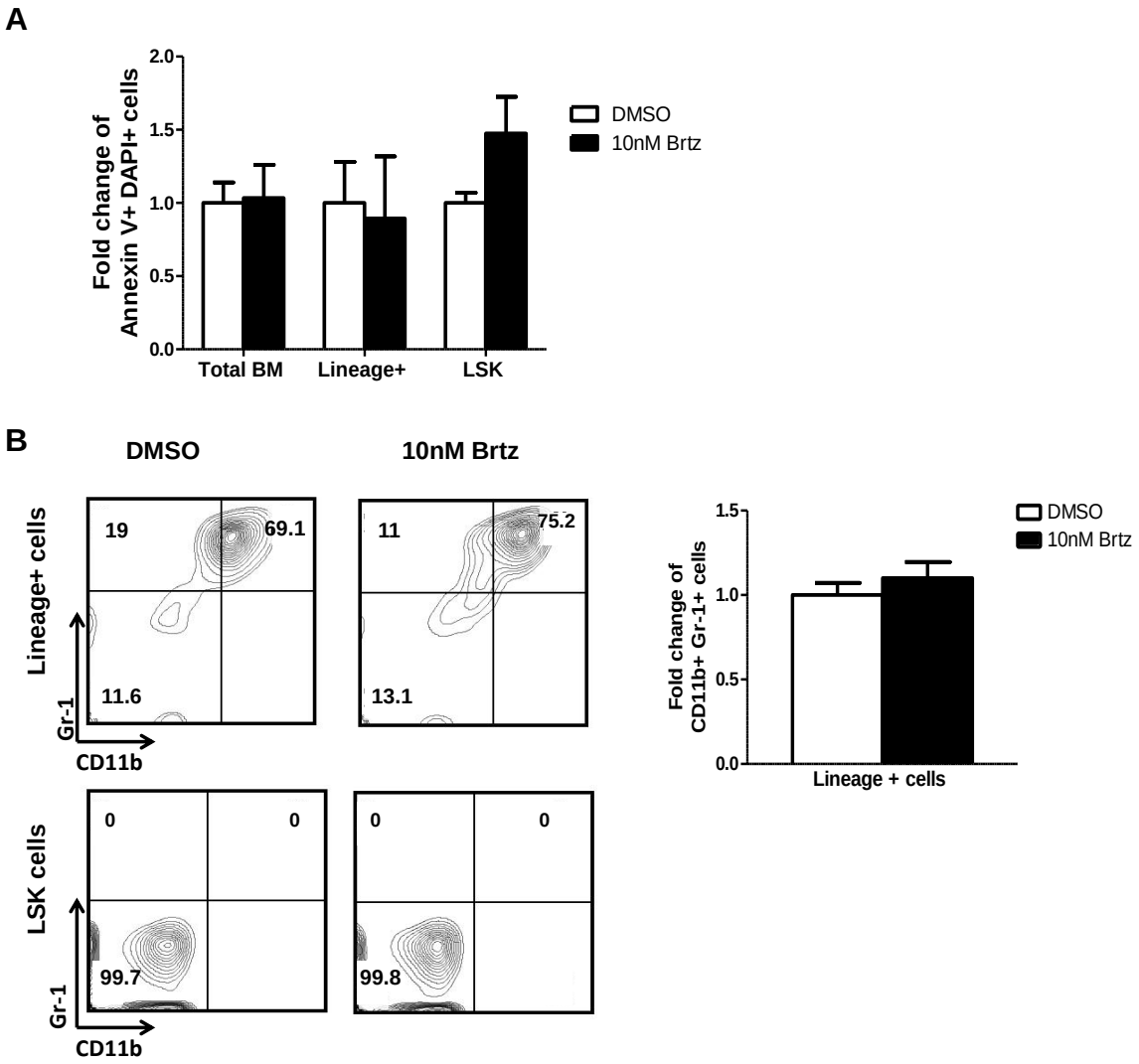

Figure 4.2 Normal murine BM cells are not responsive to Brtz *in vitro* treatment
Total BM cells, LSK and lineage positive cells from wild-type B6.SJL mice were treated with Brtz (10 nM) or DMSO only for 24 h and no significant differences were detected in cell viability or myeloid differentiation when treated cells were compared to corresponding controls. (A) Cell viability results are presented as a bar graph and results are expressed as fold change of Annexin V and DAPI positive cells ± SD of 2 technical replicates relative to vehicle-treated cells. (B) FACS analysis of CD11b-APC and Gr1-PE Cy7 is shown by representative contour plots of 2 technical replicates (left panel). For the lineage positive population, the same results are also shown as fold change of CD11b/Gr-1 double positive cells ± SD of 2 technical replicates relative to vehicle-treated cells.

4.3.3 Modulation of TRIB2 levels sensitizes AML cells to cytotoxicity induced by proteasome inhibition

The chemotherapeutic response of TRIB2-expressing AML cells was next investigated in the human setting, where the role of TRIB2 as a mediator of the Brtz-induced therapeutic response was interrogated. To address this, the human U937 cells were used, as they express detectable levels of endogenous TRIB2 and C/EBPα, and TRIB2 levels were additionally modulated by means of an expression vector. U937 cells were lentivirally transduced with Phr control (PhrCtrl) or PhrTRIB2 and treated with either vehicle or Brtz (Figure 4.3A) at 10 nM (IC50). The IC50 value of Brtz in U937 cells had been previously determined by Fiona Lohan (former PhD student in the Keeshan lab) and is in accordance with the average values reported for human AML cells (Horton et al., 2006, Fang et al., 2012). TRIB2-overexpressing U937 cells (higher transcripts levels confirmed by mRNA analysis, Figure 4.3B) showed increased DAPI positivity after treatment with Brtz (68.9% versus 45.9% for control Phr, $P \leq 0.05$; Figure 4.3C), as well as increased expression of cells arrested at sub-G1 cell cycle stage (Figure 4.3D), which reflected an augmented cytotoxic response towards proteasome inhibition upon TRIB2 modulation.

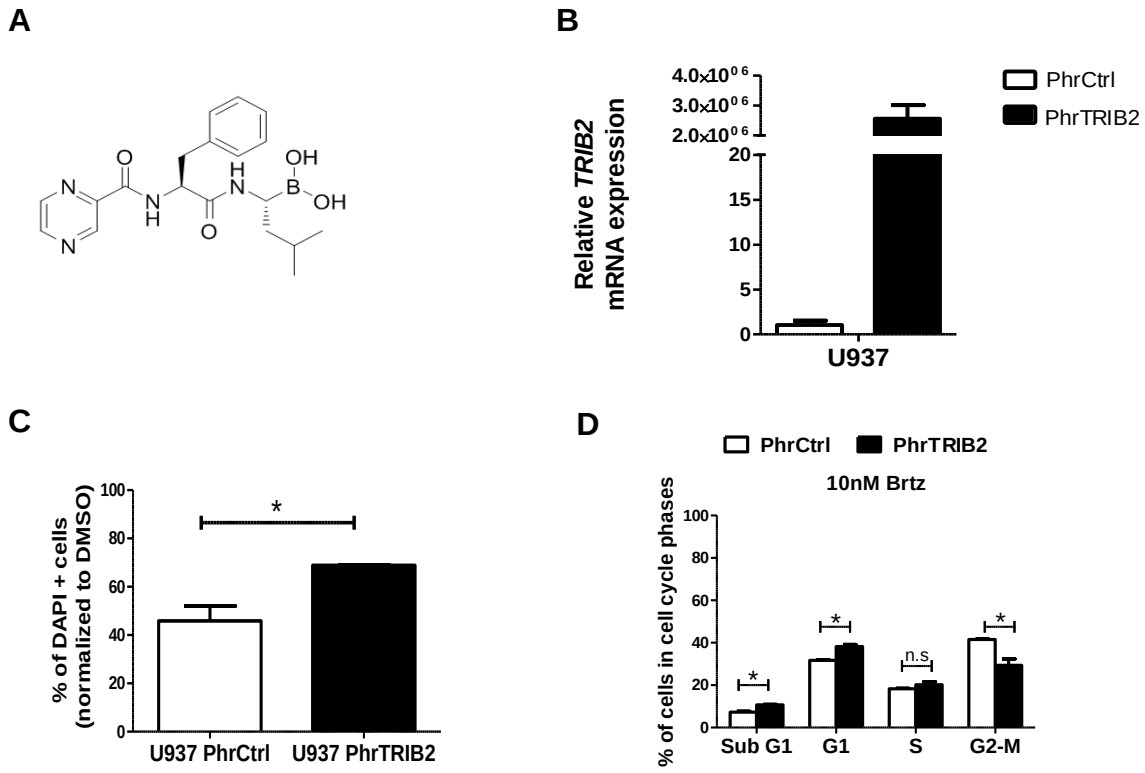

Figure 4.3 TRIB2 expression sensitizes AML cells to *in vitro* cytotoxicity induced by Brtz

(legend on next page)

Figure 4.3 TRIB2 expression sensitizes AML cells to *in vitro* cytotoxicity induced by Brtz (Figure on previous page). (A) Chemical structure of bortezomib (Brtz), $C_{19}H_{25}BN_4O_4$. (B) *TRIB2* overexpression in U937 cells transduced with PhrTRIB2 was confirmed at the mRNA level. (C) Sorted GFP+ U937 cells transduced with either PhrCtrl or PhrTRIB2 lentivirus were treated with 10 nM Brtz or DMSO only for 16 h. Cytotoxicity was assessed by DAPI staining and (D) cell cycle was assayed by PI staining. Results are presented for each condition as a percentage of vehicle treated cells and are representative of 3 independent experiments. with 2 technical replicates. n.s., not significant; *$P \leq 0.05$ by Student´s *t*-test.

To pursue this observation further, next-generation proteasome inhibitors peptido sulfonyl fluoride (SF) (Figure 4.4A) and carfilzomib (Cfz; formerly PR-171) (Figure 4.4A) were also used for *in vitro* experiments with U937 cells. Unlike Brtz, SF and Cfz cause irreversible proteasome inhibition with greater selectivity for the proteasomal CT-L activity (Brouwer et al., 2012, Demo et al., 2007). SF is an experimental proteasome inhibitor, inspired by the backbone sequences of Brtz, epoxomicin and Cbz-Leu3-aldehyde (MG132) (Brouwer et al., 2012). The epoxyketone-based inhibitor Cfz has been approved by the FDA for the treatment of relapsed/refractory multiple myeloma (Katsnelson, 2012) and showed greater efficacy and fewer side effects than Brtz (Vij et al., 2012). Both proteasome inhibitors were initially tittered in U937 cells treated with increasing concentrations of SF (10 nM-1.5 µM) and Cfz (4-500 nM). Interestingly, SF induced a similar % of DAPI+ cells to that obtained with 10 nM Brtz (included as a control) at a significant higher concentration (500 nM) (Figure 4.4B). While there are no previous IC50 values published for this drug, a higher sensitivity of U937 to SF was anticipated based on its reported greater selectivity. With regards to Cfz, it was used at 10 nM in U937 cells, even if at this concentration the effect on viability was lower than the one obtained with 10 nM Brtz (Figure 4.4B). This decision was based on published data, which reported an IC50 <10 nM in multiple cancer cell lines (Demo et al., 2007). When used for *in vitro* treatment of U937 AML cells with high TRIB2 expression (lentiviral PhrTRIB2-GFP) or endogenous levels, the next-generation proteasome inhibitors also showed selective killing of high TRIB2-expressing AML cells, as assessed by cell viability (Figure 4.4C). Finally, an altered cellular phenotype of cell-cycle arrest at Sub-G1/G1 stages confirmed that cytotoxicity induced by proteasome inhibition was higher in U937 cells overexpressing TRIB2 (Figure 4.4D). Of note, the overexpression model was used in place of downregulating TRIB2 given the relevant role of TRIB2 in supporting U937 cell growth (see Chapter 3, section 3.3.5).

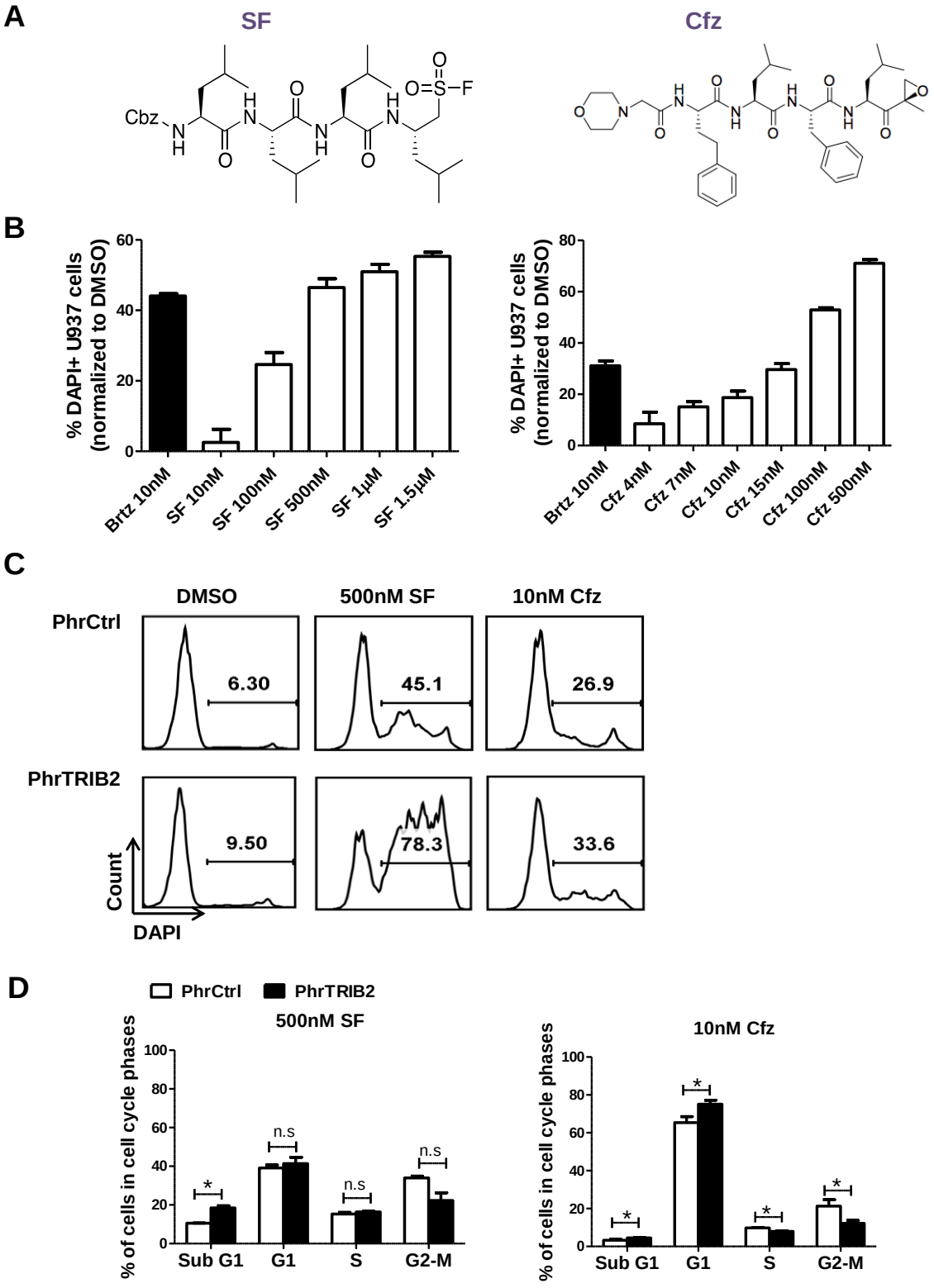

Figure 4.4 Modulation of TRIB2 levels sensitizes AML cells to cell death induced by next-generation proteasome inhibitors

(A) Chemical structure of proteasome inhibitors. Peptido sulfonyl fluoride (SF), $C_{32}H_{53}FN_4O_7S$ and carfilzomib (Cfz), $C_{40}H_{57}N_5O_7$. (B) Titration of Cfz and SF in U937 cells. (C) Sorted GFP+ U937 cells transduced with either PhrCtrl or PhrTRIB2 lentivirus were treated with 500 nM SF, 10 nM Cfz or DMSO only for 16 h. Cytotoxicity was assessed by DAPI staining. Representative FACS plots of 3 independent experiments with

2 technical replicates each are shown. (C) Cells from the previous experiment were also stained with PI for cell cycle distribution. Results are shown by representative bar graph of 2 independent experiments with 2 technical replicates. n.s., not significant; *$P \leq 0.05$ by Student´s *t*-test.

4.3.4 Brtz is selectively cytotoxic to high TRIB2 cells via the TRIB2-C/EBPα axis

Given the fact that *Trib2*'s myeloid oncogenic role results from its ability to induce degradation of C/EBPα p42 via UPS engagement (Keeshan et al., 2006, Keeshan et al., 2010), it was argued that proteasome inhibition would be an effective anti-leukaemic therapy in TRIB2-expressing AML cells. Indeed, *in vitro* cytotoxicity induced by proteasome inhibitors was found in these cells (Figure 4.3 and 4.4). In order to correlate these observations with the predicted underlying mechanism of action, the effect of Brtz on C/EBPα was next examined by western blotting. Sorted GFP+ U937 cells transduced with either PhrCtrl or PhrTRIB2 were used for protein analysis after 6 and 8 h treatment because these time points precede the measured effects on cell viability. Brtz treatment (10 nM) rescued the degradation of C/EBPα p42 detected upon overexpression of TRIB2 in U937 cells after the 6 and 8 h treatment, as evidenced by densitometry and illustrated in Figure 4.5A. To further support the hypothesis that increased sensitivity of high TRIB2 AML cells to Brtz is related to the inhibition of TRIB2-dependent proteasomal degradation of C/EBPα p42, the analysis was extended to cells differentially expressing C/EBPα. Thus, cell lines lacking expression of C/EBPα were used to assess the effect of TRIB2 overexpression upon Brtz treatment. Overexpression of TRIB2 was conducted in K562 and Kasumi-1 leukaemic cell lines. K562 cells do not express C/EBPα at protein (Scott et al., 1992) or mRNA (Radomska et al., 1998) level. Kasumi-1 cells are a t(8;21) AML-M2 cell line where C/EBPα has been shown to be undetectable at protein level and very low in mRNA analysis (Pabst et al., 2001). On this background, Brtz toxicity assessed by DAPI staining was not increased following TRIB2 overexpression (PhrTRIB2) (Figure 4.5B). Finally, it was tested whether exogenously enhanced expression of wild type C/EBPα could rescue Brtz- induced cell death in U937. Indeed, cells overexpressing MigR1-C/EBPα had decreased DAPI positivity upon *in vitro* treatment when compared to MigR1-U937 control ($P \leq 0.001$; Figure 4.5C). Together, these findings support Brtz specificity for the TRIB2-C/EBPα axis in high TRIB2 AML cells (data included in (O'Connor et al., 2016)).

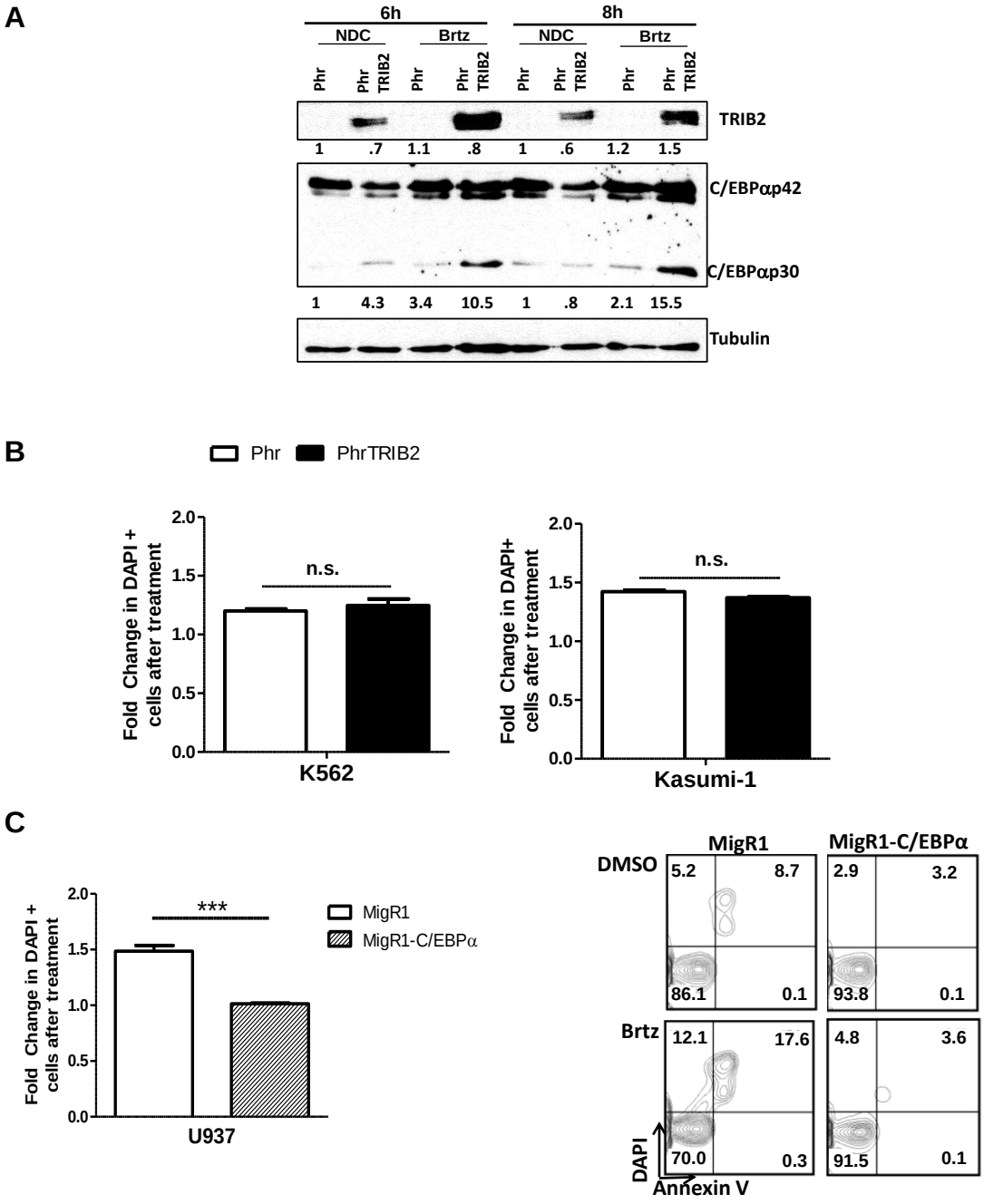

Figure 4.5 TRIB2-C/EBPα axis is a key molecular determinant of Brtz-induced cytotoxicity in high TRIB2 AML cells

(A) Sorted GFP+ U937 cells transduced with either PhrCtrl or PhrTRIB2 were treated for 6 and 8 h with 10 nM Brtz or DMSO only (NDC, no drug control) and cell lysates were analysed for C/EBPα expression by western blotting. TRIB2 overexpression was confirmed and tubulin was used as loading control. Densitometric analysis was performed for quantification of endogenous C/EBPα p42 and p30 proteins. Numbers are depicted above and below the lanes, respectively. For each time point, values represent band intensity normalized to tubulin and reported as fold change with respect to untreated control (Phr, NDC) set to 1. Representative of 2 independent experiments. (B) Sorted

GFP+ K562 and Kasumi-1 cells transduced with Phr control or Phr-TRIB2 lentivirus were treated with 10 nM Brtz or DMSO only for 16 h and analysed by flow cytometry for cell death by DAPI staining. Results are fold change of DAPI positive cells ± SD of 2/3 technical replicates relative to vehicle-treated cells and are representative of 3 independent experiments. (n.s, not significant by Student´s *t*-test). (C) Sorted GFP+ U937 cells transduced with MigR1 control or MigR1-C/EBPα retrovirus were treated +/- 10 nM Brtz for 16 h and analysed by flow cytometry for cell death by DAPI staining. Results are shown by fold change of DAPI positive cells ± SD of 2/3 technical replicates relative to vehicle-treated cells (left panel) and contour plots (right panel) and are representative of 3 independent experiments (***$P \leq 0.001$ by Student´s *t*-test).

4.3.5 High TRIB2 AML cells are chemosensitive to proteasome inhibition *in vivo*

To investigate whether chemosensitivity of high TRIB2 AML cells to Brtz could be recapitulated *in vivo* and, consequently, assess the potential clinical significance of these findings, a human AML xenograft model was established. The short latency U937-NSG model was used, as it was proven to be a fast and robust AML model, here (Chapter 3) and by others (Banerji et al., 2012). Importantly, it was previously shown that AML development in this model is tightly correlated with TRIB2 expression (Chapter 3), which makes this a suitable *in vivo* setting to investigate the TRIB2-dependent effect of Brtz. GFP+ U937 (shCtrl lentivirus) cells were, therefore, propagated in NSG recipients. Mice were treated at d5, 7 and 11 with i.p. injections of PBS or Brtz at the clinically relevant dose of 0.5 mg/kg (Liu et al., 2013). Blood samples were taken at d5 and 11 before drug administration and the mice were sacrificed at day 16 (Figure 4.6A), following the same experimental time course depicted in Chapter 3, section 3.3.6. Brtz significantly impaired the engraftment of the TRIB2 expressing U937 cells when compared to vehicle-treated animals, as detected by lower BM % of engrafting GFP+ cells, also positive for human antibody CD45 expression (Figure 4.6C). The treatment protocol was designed using previous studies as guidelines for toxicity assessment (Luo et al., 2011, Schueler et al., 2013, Ying et al., 2013). Importantly, the Brtz dose and schedule were well tolerated throughout the course of the study. There was no significant weight loss from d0 to d16 (Figure 4.6B , <10%, as defined in (Kamb, 2005),) nor any changes in the overall well-being of treated mice that would be indicative of drug-associated toxicity. No signs of gross pathological abnormalities of the major organs were noted at mice necropsy examination. These findings support Brtz pre-clinical efficacy in TRIB2-expressing AML

cells, as NSG mice more closely mimic the patient setting (data included in (O'Connor et al., 2016)).

A

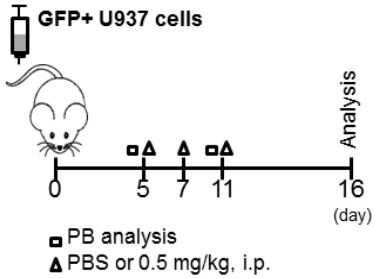

B

Groups	Body weight, g	
	d0	d16
PBS (n=3)	32.9±1.8	32.3±1.7
Brtz (n=3)	32.7±1.2	31.2±1.3

C

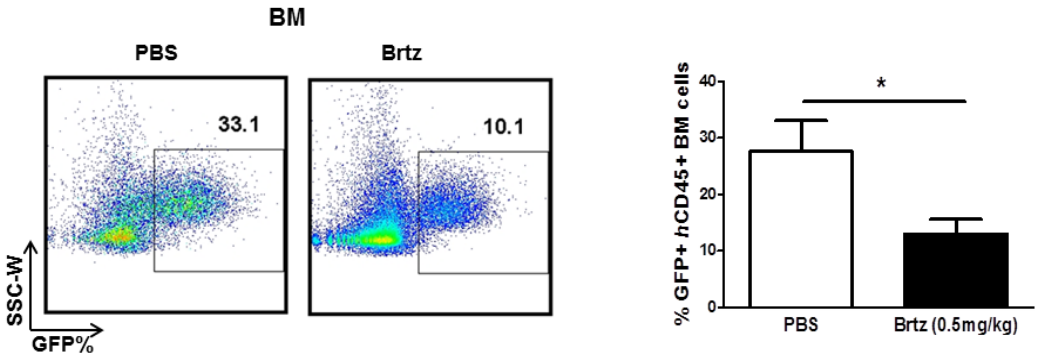

Figure 4.6 TRIB2 expression sensitizes AML cells to cytotoxicity induced by proteasome inhibition *in vivo*

(A) Schematic representation of the AML xenograft study. NSG mice (n=6) were transplanted with human GFP+ *h*CD45+ U937 cells. Each group was randomized into 2 groups for treatment with 0.5 mg/kg Brtz or PBS, i.p., on a regime schedule of 3 injections for 16 days. (B) No significant weight loss was detected throughout the 16 days of the experiment in both treated (Brtz) and untreated (PBS) cohorts. (C) GFP and *h*CD45 expression in BM were quantified by flow cytometry as a measure of disease burden in control PBS (n=3) and Brtz (n=3) treated animals and data are shown by representative FACS contour plots (left panel) and bar graph (right panel) with means ± SD. **P*≤0.05 by Student´s *t*-test.

4.3.6 AML patient samples with high *TRIB2* expression are sensitive to Brtz treatment

To extend the pre-clinical approach described above, Brtz treatment was further assessed in primary human AML samples, which were evaluated in terms of their pharmacological response to proteasome inhibition. From the cohort of AML patients stratified according to the *TRIB2* transcript levels (Chapter 3, Figure 3.8), MNCs were selected for treatment based on *TRIB2* expression status and availability of cells in the bio-bank. Cells were either cultured immediately after patient samples were collected and processed or upon thawing of the cryopreserved tubes, available from the bio-bank. While optimized cell culture conditions were used, some primary samples (AML#17 and #25) showed very poor viability after overnight incubation, hence being excluded from the analysis. When DMSO and Brtz-treated low *TRIB2* cells were compared, no statistically significant differences were found in two samples (AML#1 and #4), while in AML#10 and #11, a potential TRIB2-independent response was detected (Figure 4.7A). However, for both samples harbouring high expression of *TRIB2* (AML#15 and 24) a significant increase in apoptosis was demonstrated after 24 h incubation with Brtz (Figure 4.7B and C). Also in support of these findings, high-*TRIB2* AML#20 treated cells were previously found to have an eightfold increase in DAPI positivity when compared to the corresponding DMSO-treated cells (data not shown; experiment conducted by Fiona Lohan). These results suggest that not all AML patient samples respond to Brtz treatment and agrees with previous studies that have demonstrated a pro-apoptotic effect of Brtz on primary AML cells with heterogeneous response patterns (Stapnes et al., 2007). While cytotoxicity induced by proteasome inhibitors can be modulated by a number of molecular determinants, as exemplified by the apoptotic response found in two low *TRIB2* cells, this study importantly suggests that expression of TRIB2 sensitizes AML cells to Brtz treatment. Together with the similar effect found in U937 AML cell, these results show that TRIB2 expressing AML cells can be pharmacologically targeted with proteasome inhibition.

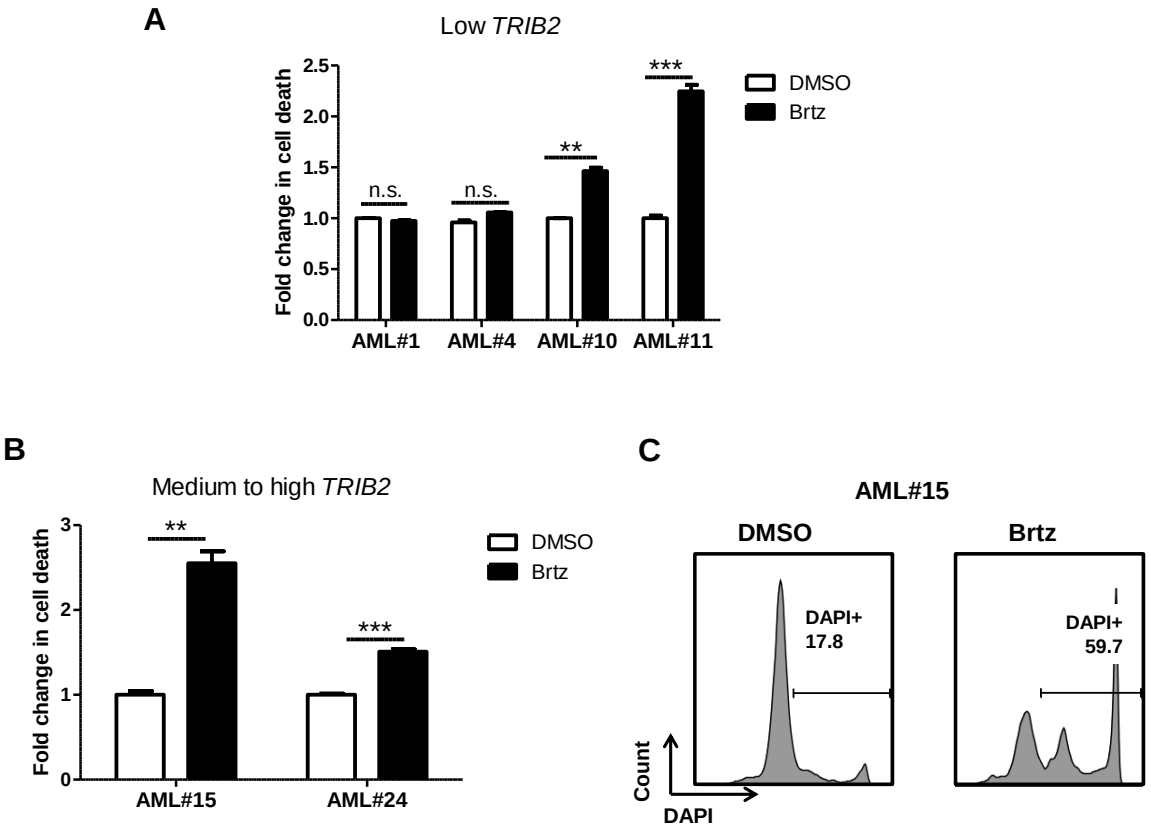

Figure 4.7 Apoptotic effect of Brtz on primary human AML cells with different *TRIB2* levels

(A) AML patient samples with low (AML#1, 4, 10 and 11) and (B) medium to high (AML#15 and 24) levels of *TRIB2* expression were treated with Bortezomib (10 nM) or DMSO *in vitro*. After 24 h, DAPI was quantified by flow cytometry as a measure of cell death. Results are expressed as fold change of DAPI positive cells ± SD of 2/3 technical replicates relative to vehicle-treated cells (n.s., not significant; $^{**}P \leq 0.01$; $^{***}P \leq 0.001$ by Student´s *t*-test). (C) Representative FACS histograms matching *in vitro* treatment of AML#15 are also shown.

4.4 Discussion

The tight correlation between Trib2-mediated proteasomal degradation of C/EBPα p42 and its ability to induce leukaemia has been thoroughly investigated and supported by a number of studies (Keeshan et al., 2006, Keeshan et al., 2010) which suggest that therapies inhibiting degradation of the full-length C/EBPα isoform may be effective in TRIB2-induced AML. The current study provides proof of concept that AML cells expressing TRIB2 oncogene can be pharmacologically targeted with proteasome inhibition due, at least in part, to inhibition of the TRIB2 proteolytic function on C/EBPα p42. To this end, a number of complementary approaches were taken to evaluate efficiency of the first-in class proteasome inhibitor Brtz in a variety of settings, including the Trib2-induced leukaemic

mice. Indeed, when murine BM cells collected from secondary recipients were treated *in vitro* with Brtz at concentrations in the low nanomolar range, a significant reduction of Trib2 expressing cells was detected, as evidenced by the decrease in GFP % used as a surrogate marker for Trib2 expression in this model. Importantly, the current study shows that the pro-apoptotic effect of Brtz in suspension cultures also affects the more immature clonogenic subset within the hierarchically organized AML cell population, as demonstrated by the inhibition of clonogenic growth upon *in vitro* treatment. The effect of Brtz treatment on AML colony formation is in agreement with previous studies (Stapnes et al., 2007, Liu et al., 2013). It should be noted that this is a very important effect, since these cells are believed to be critical for the genesis and perpetuation of leukaemic disease.

While recent research on the proteasome as a rational therapeutic target has been predominantly focused on malignant tissue, some studies have investigated the effect of Brtz on normal cells, due to its clinical relevance for BM toxicity. It has been suggested that non-malignant human CD34+ BM cells are susceptible to the apoptotic effect of Brtz, even if at slightly higher concentrations from those used for their AML counterparts (Stapnes et al., 2007). Moreover, the IC50 of Brtz with CML CD34+38- cells was not found to be significantly different from the equivalent non-CML cells (Heaney et al., 2010). In disagreement with such observations, the Brtz effect on normal murine BM cells showed pro-apoptotic selectively towards the malignant cells, as no evidence of cytotoxicity was encountered in *in vitro* assays with different subsets of normal murine bulk total BM cells, LSK cells or lineage positive cells. A consistent outcome was, in fact, illustrated by both the most primitive and most differentiated populations, at a concentration shown to have a pro-apoptotic effect on murine Trib2-AML BM cells. In line with these results, myeloid cell surface marker staining did not display any change that could suggest Brtz-induced differentiation. The discrepancy between present study and published data could be due to species-specific differences and, therefore, caution should be exercised when extrapolating obtained results to the human situation and could be further clarified by a dose-response treatment using higher concentration values. Long-term evaluation using colony-formation assay or effect on normal BM mouse engraftment would also address this subject.

Brtz was shown to be cytotoxic to a broad range of the 60 human tumour cell lines examined in the National Cancer Institute pre-clinical screen, which clearly highlights the potential of proteasome inhibitors as anticancer agents (Adams et al., 1999). However, different pathways seem to be important in different malignant cells, and the mechanisms

whereby these agents elicit cellular responses are not fully understood (Nencioni et al., 2007). Having shown an effect of Brtz on the viability of murine Trib2-AML cells, the present study moved on to establish that the response to proteasome inhibition was TRIB2-dependent. The cause-and-effect relationship between TRIB2 expression and treatment response was attained by functional studies that measured changes in Brtz-induced cytotoxicity after modulation of TRIB2 in U937cell line. This was the preferred model since both TRIB2 and C/EBPα are endogenously expressed. Response of the U937 AML cells to proteasome inhibition was previously reported by Imajoh-Ohmi *et al*, who examined the effect of another selective inhibitor of the proteasome, lactacystin, on U937´ cell proliferation. These authors found that lactacystin induces apoptotic cell death (Imajoh-Ohmi et al., 1995), without further investigating the underlying molecular mechanism. In the current study, not only was the increased *in vitro* cytotoxic response associated with higher TRIB2 expression, as similar patterns of sensitivity were successfully recapitulated with the next-generation inhibitors SF and Cfz. Unlike Brtz, these proteasome inhibitors cause irreversible proteasome inhibition and are thus expected to have enhanced efficacy, as well as increased clinical applicability.

Furthermore, the response of high TRIB2 AML cells to proteasome inhibition was deemed to be due to blockage of TRIB2 degradative function on C/EBPα p42. This was supported by western blotting analysis, which highlighted the molecular interplay between both proteins by showing a reduction in C/EBPα p42 after TRIB2 overexpression and, more importantly, rescue of the transcription factor´s full length isoform degradation after proteasome inhibition. These observations mechanistically confirmed the TRIB2-C/EBPα p42 dynamic and showed that it is indeed altered by Brtz treatment. Specificity was further addressed and supported by a panel of experiments which showed that 1) ectopic expression of C/EBPα rescued Brtz- induced death in U937 cells, while 2) TRIB2 overexpression required the presence of C/EBPα to enhance Brtz-induced cell death, since it was not found in a leukaemia background lacking C/EBPα (K562 and Kasumi-1). Consistent with these results, it has been shown that a TRIB2 mutant (VPM), unable to bind the E3 ligase COP1 responsible for TRIB2-mediated C/EBPα degradation (Keeshan et al., 2010), does not enhance Brtz-induced cell death (experiment conducted by Fiona Lohan (O'Connor et al., 2016)). Taken together, these findings uncover a novel molecular mechanism by which Brtz elicits apoptosis in leukaemia cells via modulation of the TRIB2-C/EBPα p42 axis. As previously reported, the accumulation of K48 ubiquitinated proteins is thought to mediate Brtz cytotoxicity on a cellular level by triggering ER stress, autophagy and apoptosis (Obeng et al., 2006, Fang et al., 2012). Therefore, it is likely that

the accumulation of K48 ubiquitinated- C/EBPα p42 would be implicated in the cell death response found after proteasome inhibition. Indeed, treatment with the proteasome inhibitor MG-132 was associated with an accumulation of Ub-conjugated C/EBPα, consistent with proteasome inhibition (experiment conducted by Caitriona O´Connor (O'Connor et al., 2016)). In addition, C/EBPα p42 stabilization by Brtz could promote the myeloid maturation programme triggered by this transcription factor. This was suggested by an increase in myeloid cell surface markers CD11b and Gr-1 in murine Trib2-leukaemic treated cell colonies (Figure 4.1D). Thus Brtz could be additionally implicated in the differentiation of cells, which would then senesce. In fact, an analogous role for Brtz was previously reported by Ying *et al*, who showed that Brtz synergizes with ATRA in promoting myeloid differentiation of HL60 and NB4 APL cells. These authors reported that Brtz elicits this effect by disrupting the ATRA-induced proteasomal degradation of RARα, the receptor through which ATRA paradoxically also induces myeloid differentiation (Ying et al., 2013).

The translation of laboratory experiments to the clinical arena is inherently dependent on the usefulness of mouse models, which produce a tractable preclinical system for testing new therapeutic approaches in a physiological environment. It was therefore important to detect Brtz anti-tumour activity in a U937 xenograft model, in which leukaemia burden was shown to be strongly dependent on TRIB2 expression (Chapter 3). The observation of a significant inhibition of tumour engraftment, together with minimal body weight loss, is interpreted by drug developers as indicative of an acceptable therapeutic window in humans (Kamb, 2005). Moreover, a cytotoxic response was detected in the high expressing TRIB2 AML patient samples. Together, obtained results support pre-clinical evidence that AML cells expressing high levels of endogenous TRIB2 can be successfully targeted by proteasome inhibition.

Given the central role of the proteasome in protein homeostasis and cellular physiology it is not surprising that discussions on the ultimate targets of proteasome inhibitors are ongoing. Results here present compelling evidence for a TRIB2-C/EBPα-dependent effect of Brtz in high TRIB2-expressing AML cells. However, inhibition of the proteasome also targets other proteins, E3 ligases and their substrates. This, together with the current understanding on Brtz´s overall ability to elicit cytotoxicity (see Chapter 1), suggests that other molecular determinants could be also implicated in the cellular cytotoxicity found in the current study. Such mechanisms could be related to the ones previously described (see chapter 1) or dependent on TRIB2 expression. The latter are difficult to predict, as there is

currently limited knowledge of TRIB2 degradation substrates in general, and indeed knowledge of TRIB2 as a substrate itself of the UPS in cancer.

To conclude, this study identifies TRIB2 as a novel molecular determinant of cell sensitivity to Brtz-induced apoptosis, which is achieved, at least partially, by blockage of C/EBPα proteolytic degradation. These findings are relevant in the context of a heterogeneous malignancy for which therapy driven by specific molecular subtypes of AML is thought to be a logical approach. The ATRA-APL example is a paradigm of such a strategy and other models have shown promising effects, including the case of the toxin-conjugated anti-CD33 antibody Myelotarg on core-binding factor mutated AML (Walter et al., 2012) and of FLT3 inhibitors for patients with activating FLT3 mutations (Grunwald and Levis, 2013). Moreover, TRIB2 has been implicated in non-haemopoietic human cancers so the proposed mechanism of Brtz action may extend to other malignancies where TRIB2 has an oncogenic role via UPS involvement. Therefore, this study provides the critical basis for further investigations into targeting the UPS as an emerging cancer therapy.

Chapter 5:
Potential implication of arginine methylation in TRIB2-induced AML via PRMT5 interaction

5.1 Introduction

Despite the widely accepted two-hit model of leukaemogenesis, there is growing evidence that the epigenetic landscape is important for the development of AML, as highlighted previously (Chapter 1, section 1.2.4). The term epigenetic encompasses all changes in gene expression that are not due to alterations in the underlying DNA sequence (Holliday, 1987). Examples of mechanisms that alter the transcriptional potential of a cell include modifications of DNA cytosine residues and post-translational modifications (PTMs) of histone proteins via the biochemical processes of acetylation, phosphorylation, methylation, and others (Musselman et al., 2012). Arginine methylation is an abundant PTM carried out by a family of 11 protein arginine methyltransferases (PRMTs). Based on their primary sequence and substrate specificity, PRMTs are designated as PRMT1 to 11. Except for PRMT2, 10 and 11, they have been shown to catalyse addition of one or two methyl groups to the guanidino nitrogen atoms of arginine (R) residues in both histones and non-histone substrates. Depending on whether their catalytic activity towards dimethylation is asymmetric or symmetric, PRMTs are classified as either type I or type II enzymes, respectively, even if both types catalyze the formation of monomethylated arginines as an intermediate (Pal and Sif, 2007).

PRTM5 (14q11.2) was first identified as JAK-binding protein 1 (JBP1) in a yeast two-hybrid assay (Pollack et al., 1999) and is the major type II arginine methyltransferase (Branscombe et al., 2001). The complete loss of this enzyme is not compatible with mouse viability due to the abrogation of pluripotent cells in blastocytes (Tee, 2010). PRMT5 is reported to participate in several diverse cellular processes through the methylation of a variety of cytoplasmic and nuclear substrates. Symmetrically methylated histones H3 at R8 and H4/H2A at R3 are well known epigenetic marks of PRMT5 (Pal et al., 2004, Ancelin et al., 2006) and are generally associated with gene repression (Fabbrizio et al., 2002). Moreover, PRMT5 represses γ- globin gene expression through symmetric dimethylation of H4R3, recruitment of the DNA methyltransferase DNMT3A to the γ-promoter and subsequent additional repressive epigenetic marks, indicating a potential crosstalk between repressive histone modification and DNA methylation (Zhao et al., 2009) (Figure 5.1A).

PRMT5 acts as part of a multimeric complex in concert with a variety of partner proteins that regulate its activity, as well as localization and substrate specificity. In mammalian cells, PRMT5 is tightly bound by a 50-kDa WD40 repeat-containing protein dubbed methylosome protein 50 (MEP50) and together they are assembled as an hetero-octameric

structure, as revealed by crystallography (Antonysamy et al., 2012). This interaction has been shown to be a crucial node for the regulation of PRMT5 methyltransferase activity (Friesen et al., 2002). Indeed, tyrosine phosphorylation of PRMT5 can block MEP50 binding and can attenuate PRMT5 activity, as it has been shown for the JAK2-V617F tyrosine kinase. Found in most patients with myeloproliferative neoplasms, this constitutively activated JAK2 mutant interacts with PRMT5 more avidly than does the wild-type form. JAK2-V617F phosphorylates PRMT5, greatly impairing its arginine methyltransferase activity on histones H2AR3 and H4R3 by blocking its interaction with the co-regulator MEP50 (Liu et al., 2011) (Figure 5.1B). In a second example of PRMT5-MEP50 regulation, it was found that cyclin D1/CDK4 kinase complex phosphorylates MEP50 instead and this phosphorylation at threonine 5 increases the intrinsic methyltransferase activity of PRMT5, resulting in augmented H4R3/H3R8 methylation and PRMT5-dependent transcriptional repression (Aggarwal et al., 2010).

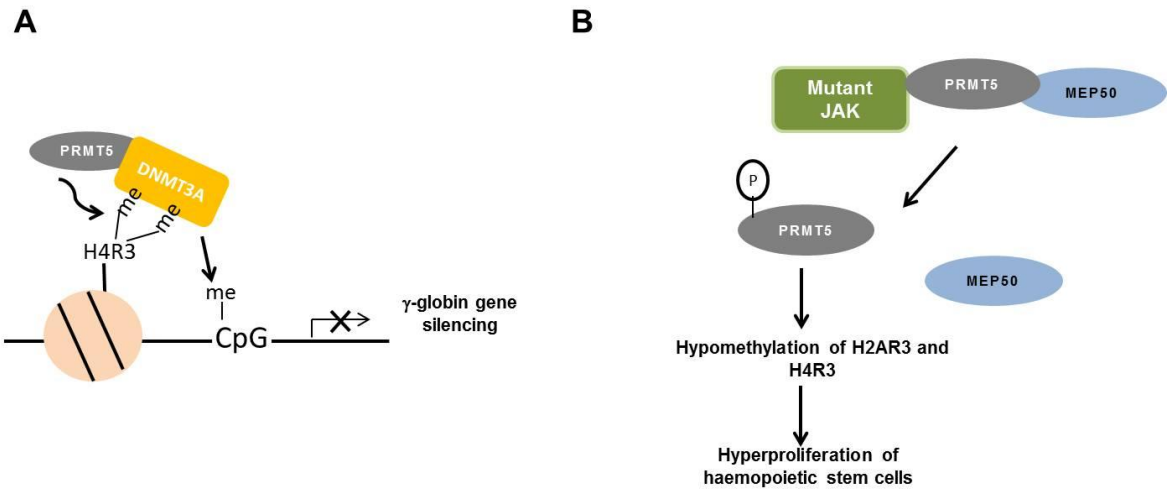

Figure 5.1 Examples of PRMT5 methyltransferase activity
(A) PRMT5 mediates symmetric dimethylation of histone H4R3 and recruits DNMT3A, coupling histone and DNA CpG methylation in γ-globin gene silencing. Figure modified from (Zhao et al., 2009). (B) Phosphorylation of PRMT5 by the oncogenic JAK kinase mutant (JAK2-V617F) results in loss of its methyltransferase activity and hyperproliferation of haemopoietic stem cells.

Although MEP50 is the primary co-regulatory factor of PRMT5 activity, other binding proteins can function as modulators or adaptors of this complex, influencing substrate specificity and the associated cellular processes. These include the human SWI/SNF and the MBD2/NuRD chromatin remodelling complexes, which enhance PRMT5-MEP50 methyltransferase activity towards histone substrates and subsequent transcriptional control on target gene expression (Pal et al., 2003, Le Guezennec et al., 2006). Another example is

the nuclear protein named cooperator of PRMT5 (COPR5) that directs PRMT5-MEP50 methyltransferase activity towards histone H4R3 rather than histone H3R8 (Lacroix et al., 2008). The same way that PRMT5 methyltransferase activity can be restricted to specific histones, association of PRMT5 with either RIOK1 (RIO-domain-containing protein kinase 1) or pICln (chloride channel, nucleotide sensitive 1A) directs its catalytic activity towards the RNA-binding protein nucleolin (Guderian et al., 2011) or the spliceosomal Sm proteins (Pesiridis et al., 2009), respectively. Together with pICln, PRMT5-MEP50 forms a 20S complex termed the methylosome that functions in RNA processing by methylating Sm proteins and affecting the small nuclear ribonucleoprotein (snRNP) biogenesis (Friesen et al., 2001, Friesen et al., 2002, Meister and Fischer, 2002, Chari et al., 2008). The RNA-binding protein Y14 also interacts with the cytoplasmic PRMT5-containing methylosome, facilitating PRMT5 activity towards Sm proteins of the snRPN core (Chuang et al., 2011).

PRMT5 has been, therefore, implicated in gene regulation processes that include histone modification, chromatin remodeling (Dacwag et al., 2007), mRNA splicing (Meister and Fischer, 2002, Chuang et al., 2011) and transcriptional elongation via methylation of SPT4/SPT5 (Kwak et al., 2003). PRMT5 also functions in DNA replication and repair (Guo et al., 2010), maintenance of the Golgi apparatus architecture (Zhou et al., 2010), ribosome biogenesis (Ren et al., 2010), cell migration (Guo and Bao, 2010) and cell reprogramming (Tee, 2010, Nagamatsu et al., 2011). The role of PRMT5 in tumorigenesis has also become evident. While recurrent PRMT5 mutations have not been detected in cancer cells, its expression is upregulated in human lymphoid cancers (Pal et al., 2007, Wang et al., 2008, Chung et al., 2013) and in many solid tumours, including lung (Wei et al., 2012), breast (Powers et al., 2011) and colorectal (Cho et al., 2012) cancer. PRMT5 is mechanistically associated with tumorigenesis through silencing of tumour suppressor genes, such as *ST7* (Pal et al., 2004) and genes encoding Rb family of proteins (Chung et al., 2013), or by mediating methylation of non-histone proteins. An example of this is the programmed cell death 4 (PDCD4) protein, which shows increased tumorigenicity when overexpressed with PRMT5 in an orthotopic model of breast cancer (Powers et al., 2011). PRMT5 also regulates a number of other non-histone proteins, namely, the transcription factors E2F1 (Cho et al., 2012), NF-kB (Wei et al., 2013) HOXA9 (Bandyopadhyay et al., 2012) and p53 (Jansson et al., 2008). Moreover, a study has demonstrated that PRMT5 knockdown results in elevated E-cadherin expression, which is implicated in epithelial-mesenchymal transition and tumour progression (Hou et al., 2008). In addition, PRMT5 overexpression promotes anchorage-independent cell growth (Pal et al., 2004), supporting the notion that PRMT5 might be an oncoprotein.

Important to this study, the epigenetic modifier PRMT5 was recently connected toTRIB2 by a mass spectrometry analysis (Prof Claire Eyers, University of Liverpool, personal communication), indicating that the epigenetic modifier could be involved in the TRIB2-induced AML.

5.2 Aims and Objectives

It is hypothesised that TRIB2 has alternate function to C/EBPα p42 degradation that provides synergy in the TRIB2-driven myeloid phenotype. Given the increasing importance of the epigenetic alterations in leukaemogenesis (Chapter 1), together with the reported interaction between TRIB2 and PRMT5, the present study sought to investigate this putative partnership to gain a better understanding of the TRIB2-induced AML.

The specific aims of this chapter were:

i To identify a phenotypic role for PRMT5 in high TRIB2 AML cells;

ii To investigate whether PRMT5 cooperates with TRIB2 by means of co-immunoprecipitation.

5.3 Results

5.3.1 *PRMT5* is elevated in AML

Overexpression of PRMT5 has been reported in various transformed cells, including those of haematological origin (Pal et al., 2007, Wang et al., 2008, Chung et al., 2013). To further address the potential regulatory role of PRMT5 in AML, its expression was examined using the Leukemia Gene Atlas (LGA) database (http://www.leukemia-gene-atlas.org, (Hebestreit et al., 2012)). This is a public platform designed to support research and analysis of genomic data published in the leukaemia field. Based on signals from two different probe sets, the expression of *PRMT5* was found to be significantly (P<0.001) increased in AML (n=542), when compared to non-leukaemia and normal BM samples (n=73) (Figure 5.2A; shown are the results obtained with probe 1564520_s_at). *In silico* analysis was performed by selecting the Haferlach *et al.* data set (Haferlach et al., 2010), as it allows stratification based on disease status and contains the largest cohort of healthy

patients available from the database. *PRMT5* mRNA expression was further examined by qPCR in the U937 cell line, as well as in primary AML cells previously screened for *TRIB2* transcript levels. This analysis found amplification of *PRMT5* in U937 cell line (average Ct value of 22.5), as well as in all examined primary cells (Figure 5.2B). *PRMT5* mRNA expression in AML patient samples was globally comparable to the levels detected in U937 cells (medium fold change, 0.86; range, 0.6-1.0). AML samples #9, 18, 26 and 28 have increasing values of *TRIB2* expression (Figure 3.8) while no correlative trend was detected for *PRMT5* (Figure 5.2B). Even though this study was limited to a small number of patients, it does not hint at a putative *PRMT5/TRIB2* cooperation at the mRNA level, like the one observed for the γ-globin gene via indirect PRMT5 activity (Zhao et al., 2009), suggesting that the alleged interaction would be better assessed at the protein level.

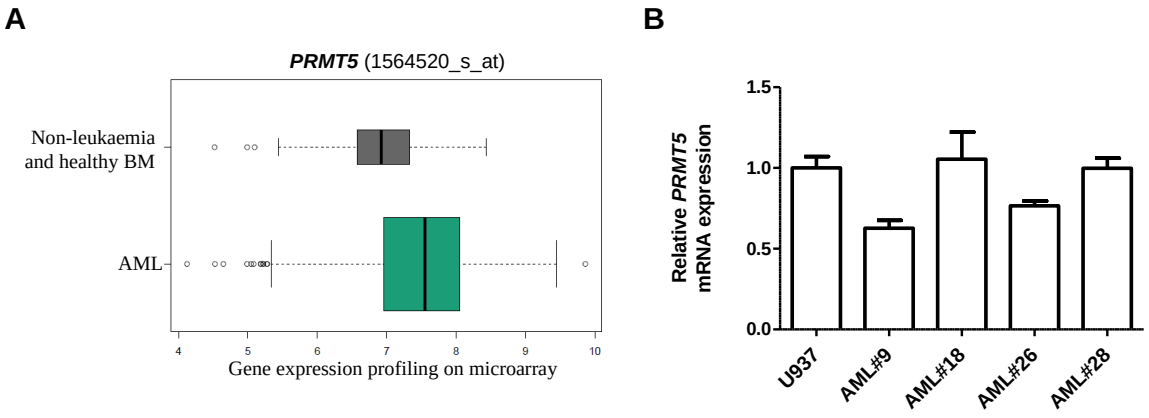

Figure 5.2 *PRMT5* is elevated in AML
(A) Expression of *PRMT5* was examined in 542 AML patients and compared with that of non-leukaemia/healthy BM (n= 73) by using the LGA platform based on the gene expression data set from Haferlach *et al*. Statistically significant increased expression was detected on the AML cohort with adjusted $P < 0.001$ determined by Welch's *t*-test. (B) qPCR analysis identified *PRMT5* expression in both U937 cells and AML patient samples. Values represent gene expression relative to U937 cells and normalize to the reference gene *ABL*.

5.3.2 PRMT5 is required for TRIB2-expressing AML cell growth and survival

The association of PRMT5 expression in human AML prompted the investigation of the potential cell-transforming activities of PRMT5. As the main aim of this chapter was to investigate the association between PRMT5 and TRIB2, the effect of PRMT5 knockdown was further examined in U937 cells, which have high levels of *TRIB2* transcripts. PRMT5

expression was downregulated using two lentiviral shRNAs (shPRMT5 #1 and #2). Expression of endogenous *PRMT5* was reduced by more than 70% as quantitated by qPCR analysis of cells surviving 2 and 5 days of puromycin selection (Figure 5.3A). Effective depletion of *PRMT5* significantly triggered growth suppression, in comparison with cells expressing a control shRNA construct (Figure 5.3B). Downregulation of *PRMT5* has previously been shown to induce cell death and/or growth arrest in HEL and K562 cells but in normal cord blood CD34+ cells it provides a proliferative signal, demonstrating the importance of cell context on PRMT5 function (Liu et al., 2011). Data presented here support a role for PRMT5 in the maintenance of U937 leukaemic cells and suggest a functional redundancy between PRMT5 and TRIB2 since both are required for U937 AML cell proliferation and survival, indicating that they may cooperate to maintain survival of leukaemic cells.

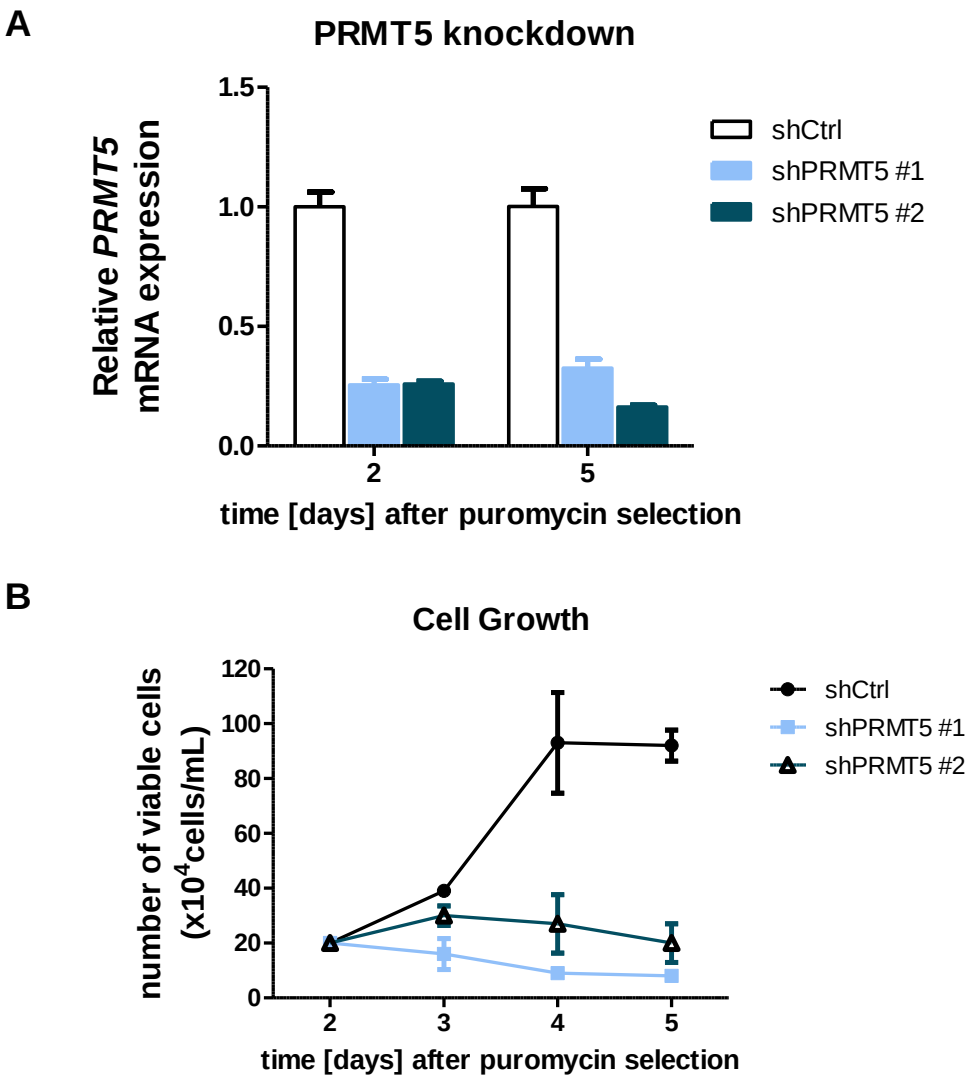

Figure 5.3 *PRMT5* knockdown induce growth inhibition in the TRIB2 expressing U937 cells

(legend on next page)

Figure 5.3 *PRMT5* knockdown induce growth inhibition in the TRIB2 expressing U937 cells (Figure on previous page). (A) *PRMT5* was knocked down following lentiviral transduction of U937 cells with two different shRNAs. Expression was assessed by qPCR after 2 and 5 days of puromycin selection (2 µg/mL) and *ABL* was used as a reference gene. (B) After 2 days of puromycin selection, cell growth of shCtrl-, shPRMT5 #1- and shPRMT5 #2 - U937 cells was assayed by trypan blue exclusion over a period of 3 days in liquid culture conditions. Data presented are representative of 2 independent experiments with 3 technical replicates each.

5.3.3 TRIB2 and PRMT5 interact in physiological conditions

To examine whether PRMT5 interacts with TRIB2, both proteins tagged with HA and Myc epitopes, respectively, were transiently co-expressed in 293T cells. Co-immunoprecipitation (Co-IP) using c-Myc antibody identified PRMT5 (~72kDa) as a TRIB2 interacting protein (Figure 5.4; Appendix B). On this note, it should be mentioned that PRMT5 is recognized by the M2-Flag antibody and has thus been purified as a 'contaminant' in many Flag-tagged protein complexes (Nishioka and Reinberg, 2003). This technical problem does not, however, compromise the present study since both PRMT5 and TRIB2 were expressed as fusions to two other affinity tags. The presence of negative controls (untransfected cells and cells transfected singly with each protein) as well as the pre-clearing step confirms this positive interaction (see Chapter 2, section 2.4). To strengthen specificity of the protein-protein interaction, the reciprocal Co-IP was also performed following the same experimental conditions (Appendix C). While PRMT5 was successfully immunoprecipitated and transfection was positively confirmed, TRIB2 was not detected in the HA-immunoprecipitate. Failure of the control experiment could be explained by the following: the α-HA antibody, used to immunoprecipitate PRMT5, can potentially interfere with the TRIB2 binding site, proving to be only suitable for recognition of the denatured form in the western blotting analysis. The use of a different HA antibody could clarify whether this is a technical issue. A different approach would be to increase transfection efficiency for PRMT5 expression. While HA-PRMT5 was successfully immunoprecipitated, the input lanes showed that this protein was consistently expressed at a lower level when compared to TRIB2. Also, when an input blot was probed with α-PRMT5 antibody, endogenous and exogenous levels were not significantly different (Appendix D). This, together with a possible uneven stoichiometry between the proteins interaction, could also explain the obtained result and be further addressed. Alternatively, a

different method could be used to validate the data, like the *in situ* proximity ligation assay that allows protein-protein interactions to be visualized and quantified *in vivo*. Nonetheless, the data here presented supports an interaction between PRMT5 and TRIB2 and, importantly, creates a framework for further investigations on the putative role of PRMT5in the molecular pathogenesis of TRIB2-driven leukaemia.

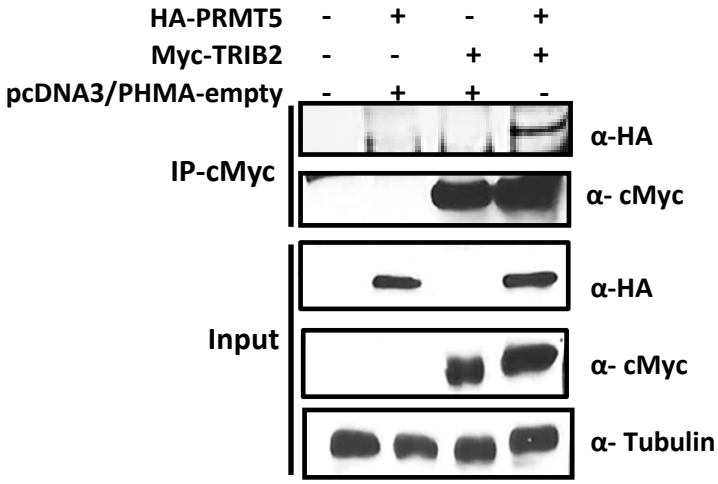

Figure 5.4 PRMT5 interacts with TRIB2 myeloid oncogene
Exogenous interaction between PRMT5 and TRIB2 was detected in 293T cells transiently transfected with vectors expressing HA-PRMT5 alone (lane 2) or with Myc-tagged TRIB2 protein (lane 4). Immunoprecipitation was performed using an anti-Myc antibody and blots were probed with antibodies specific for HA or cMyc. Complete blots of westerns are shown in Appendix B.

5.4 Discussion

While molecular interaction between TRIB2 and C/EBPα p42 has been identified as a key driver event in AML via proteolytic degradation and subsequent deregulation of the granulopoiesis-related transcription factor, interaction with other partners are yet to be fully elucidated. On this note, the widely accepted mutations from the two-hit model, which affect proliferation and haemopoietic differentiation, are no longer viewed as exclusive causes of AML development. Emerging evidence suggests that a third important mechanistic pathway involving epigenetic regulators must also occur and, indeed, a putative cooperation between TRIB2 and PRMT5 was suggested by mass spectrometry data. The relevance of this epigenetic regulator in tumorigenesis has become evident, since increased PRMT5 levels are observed in a range of cancers, including lymphoma (Pal et al., 2007). Moreover, PRMT5 has been shown to repress expression of the gene implicated

in foetal haemoglobin synthesis (γ-globin gene), which suggests a role for PRMT5 in erythropoiesis and haemopoiesis in general (Zhao et al., 2009).

Herein, analysis of a public microarray data set found *PRMT5* transcripts to be significantly higher in AML patients when compared to normal samples. Importantly, this study supports a role for PRMT5 in AML cells with high TRIB2 expression, as evidenced by the anti-proliferative effect observed upon gene knockdown in U937 cell line. It has been reported that PRMT5 preferentially promotes p53-dependent cell cycle arrest at the expense of p53-dependent apoptosis (Jansson et al., 2008), which could explain the cell death response triggered by downregulation of PRMT5. However, the *TP53* gene in U937 cells has a point mutation that converts G into A (G>A) in the splice donor site at the first base of intron 5. This intronic modification appears to inactivate the normal splicing junction and alter processing of *TP53* mRNA, which is reported to have a 46-bp deletion on exon 5 (Sugimoto et al., 1992). Even if detectable at mRNA level by qPCR (Sugimoto et al., 1992, Yeung and Lau, 1998), p53 protein synthesis is negligible or null in U937 cell line (Danova et al., 1990, Rizzo et al., 1998). Hence, in these AML cells, growth arrest detected upon PRMT5 depletion should be triggered by a p53-independent mechanism. Hypothesizing that TRIB2 mediates the effect of PRMT5 or vice versa, modulation of one should phenocopy modulation of the other, which was indeed detected. Both PRMT5 and TRIB2 were found to affect leukaemia cell growth when downregulated singly in the same model system, which suggests that PRMT5 and TRIB2 could cooperate to maintain the leukaemic cells transforming capabilities. This cooperation was suggested to be better assessed at the protein level since no association was detected between *TRIB2* and *PRMT5* mRNA levels in a subset of primary AML cells. Also in support of that, analyses retrieved from COSMIC database found *TRIB2* to be only hypermethylated in prostate and large intestine tumour tissues (Figure 3.1D).

Indeed, the present study identified a molecular partnership between PRMT5 and TRIB2, when tagged versions of both proteins were overexpressed in 293T cells and TRIB2 complexes were purified using an antibody specific for the Myc epitope. Despite the previously discussed pitfalls (section 5.3.3), this experiment strongly suggests a true physiological PRMT5/TRIB2 interaction, as it validates results previously obtained from a mass spectrometry analysis. It would be of significant importance to confirm that endogenous TRIB2 and PRMT5 proteins also interact in leukaemia cells. Although the exact mechanism(s) that orchestrate this cooperation can only be hypothesized at this stage of research, some interactions could be envisaged. TRIB2 could be post-translationally

methylated by PRMT5, as it is the case of several non-histone proteins, *e.g.*, p53 (Jansson et al., 2008) and PDCD4 (Powers et al., 2011), with functional consequences on its activity. Alternatively, and as described for the mutated form of JAK2 (Liu et al., 2011), TRIB2 could have a regulatory role on PRMT5 methyltransferase activity by altering its phosphorylation status. This would disrupt the PRMT5-MEP50 hetero-octameric structure and, ultimately, affect transcription via regulation of specific histones. Such hypothesis would seem less likely given the fact that a catalytic activity on any substrate has not yet been reported for the pseudo-kinase TRIB2. However, it has been recently shown that TRIB2 retains the ability to bind with low affinity to ATP and autophosphorylates *in vitro* (Bailey et al., 2015), hence, providing the rationale to pursue this hypothesis further. Future studies on whether TRIB2 affects the enzymatic activity of PRMT5 towards its well-known histones epigenetic marks (H2A/H4R3 and H3R8) would provide important insights on this matter. If changes in histone methylation were found, the functional consequences of this observation would then have to be determined. It is well established that post-translational modification of histones represents a fundamental regulatory mechanism that has an impact on gene expression (Strahl and Allis, 2000) and PRMT5 is generally regarded as a co-repressor. It would therefore be of interest to identify a potential subset of genes reciprocally up or downregulated by TRIB2 and PRMT5. Also, since PRMT5 functions as part of various high molecular weight protein complexes, the identification of the TRIB2/PRMT5 binding partners could provide important insights on the potential downstream targets, as they regulate PRMT5 activity, as well as localization and substrate specificity.

Therefore, the experimental finding of a partnership between PRMT5 and TRIB2 opens a new level of regulation to consider in AML and empowers further research aimed at understanding the underlying mechanism and the functional significance of this interplay. Given the multitude of roles that PRMT5 has in several biological processes, such as RNA processing, chromatin remodeling and control of gene expression, it is plausible to hypothesize that PRMT5 and TRIB2 putative cooperation affects a mechanism other than C/EBPα p42 proteolysis. Instead, this interaction would lead to a crosstalk between proteasome–dependant degradation of C/EBPα p42 and PRMT5-mediated arginine methylation, altering the gene expression profile and collaborating to bring about the TRIB2-driven myeloid phenotype.

In conclusion, the discovery of an interaction between PRMT5 and TRIB2 reveals a potential pathway of regulation in TRIB2-driven leukaemia and sets the stage for further experiments that will hopefully have important ramifications in the leukaemia field.

Chapter 6:
Conclusions

6.1 Concluding remarks

AML may best be considered an umbrella term for a heterogeneous group of myeloid leukaemias that are all characterized by proliferation of immature, clonal, myeloid precursors but differ substantially with regards to the biological cause and clinical features. Characterization of the molecular events underlying leukaemic growth furnishes distinctive insights into the nature of the disease and provides useful clues to the prognosis of individual patients. Indeed, the importance of delineating AML disease entities more sharply has gained general appreciation, and cytogenetics as well as specific gene mutations has become part of the essential and standard workup of patients with AML.

While the spectrum of the molecular abnormalities and pathways implicated in AML has been extended over the last three decades, more precise distinctions are needed. *Trib2* is known to be a potent murine oncogene capable of inducing transplantable AML with complete penetrance (Keeshan et al., 2006). Here, its tumorigenic role in the context of myeloid malignancies is characterized and strengthened in a human leukaemic setting. Data clearly show the importance of TRIB2 increased expression for the *in vitro* and *in vivo* maintenance of the oncogenic properties of AML cells. These findings, together with the detection of *TRIB2* expression in a number of AML patient samples, add significant value to the current understanding of leukaemogenesis. Since treatment of AML has evolved side by side with a refinement in the molecular characterization of this heterogeneous disease, as exemplified by the ATRA-APL case, two important questions from the clinical point of view emerged from the abovementioned findings. These questions are related to whether aberrant expression of TRIB2 has prognostic value in the context of AML and whether high TRIB2 cells can be therapeutically targeted (as discussed in the following paragraph). The xeno-engraftment study with AML patient samples harbouring different levels of *TRIB2* transcripts predicted an association with less aggressive leukaemias. These are, however, preliminary results and a more exact estimation of the prognosis can only be validated in large series of patients by multivariate analysis encompassing for example the patients´ mutational status of the main recurrent abnormalities (*i.e.*, *NPM1*, *FLT3, CEBPA* and *DNMT3A*), as well as information regarding age, WBC count or % of CD33 and CD34+ cells, which also have clinical implications (Breccia and Lo-Coco, 2011, Gerber et al., 2012).

The growth-promoting and anti-apoptotic effects of TRIB2 in AML cells, herein described, make it a rational target for antineoplastic agents. An approach to preventing TRIB2

tumorigenic role is to inhibit the proteasome, hence blocking degradation of the granulopoiesis-related C/EBPα p42 via the Ub-proteasome system. The UPS is a selective method of proteolysis that constitutes a salient example of how fundamental research can have far-reaching implications for human biology and disease. Identified after 20 years of research (Hershko, 2005), the Ub-dependent degradation system was found subsequently to be aberrantly activated in a variety of malignancies, which resulted in the development of drugs aimed at inhibiting the proteasome function. Indeed, two proteasome inhibitors (Brtz and Cfz) have entered the clinical arena for the treatment of multiple myeloma and mantle cell lymphoma. Current research and on-going clinical trials indicate that the full therapeutic potential of proteasome inhibitors is beginning to be appreciated and suggest that they will be part of our future armamentarium of drugs against a number of other diseases. In fact, there is a body of evidence supporting the use of proteasome inhibitors as a strategy for AML therapy, which may improve the currently unsatisfactory outcome of the elderly patients. In the present study, it is shown that high TRIB2-expressing AML cells are predictive for responsiveness to treatment with proteasome inhibition. These cells can be pharmacologically targeted with Brtz, as well as with next-generation proteasome inhibitors, due, at least in part, to blockage of the TRIB2 proteolytic function on C/EBPα p42. The TRIB2- C/EBPα p42 axis can, therefore, be considered a new mechanism whereby Brtz induces cytotoxicity. This is of particular importance as the apoptotic cascades induced by proteasome inhibition are not yet fully defined and understanding the molecular basis for the selectivity of the proteasome inhibitors will aid in their development as anticancer agents. In addition, the therapeutic strategy and the obtained results here presented have a potential broader applicability as they support its usefulness in other AMLs with deregulated proteasome activity. Moreover, TRIB2 has been also shown to have an oncogenic activity associated with proteasomal-degradation of its targets in other malignancies (*e.g.*, lung (Grandinetti et al., 2011) and liver (Xu et al., 2014) cancer), for which the stated therapeutic strategy could as well be considered a logical approach.

In the light of the main findings described above *i.e.* characterization of TRIB2 as an important myeloid oncogene in human AML that can be selectively targeted by proteasome inhibition, it was thereafter aimed to obtain a deeper understanding of the processes associated with TRIB2-driven leukaemia, as it is hypothesised that other molecular pathways are involved. A major mechanistic theme in AML biology is, in fact, the extensive collaboration among genetic changes, fusion oncoproteins, transcription factors and chromatin regulators to initiate and sustain an acute leukaemia phenotype

characterized by enhanced survival and impaired differentiation. Karyotype analysis of murine-Trib2 AML cells suggested that TRIB2-driven AML was associated with the CN-AML, hence excluding chromosomal alterations as the more likely cooperating events. In pursuing this question, the primary enzyme responsible for symmetric dimethylation, PRMT5, was identified as a TRIB2 binding partner, supporting previous results obtained by mass spectrometry analysis, as well as the increasingly importance given to epigenetic regulators in AML. The identification of an interaction between TRIB2 and PRMT5, which were also functionally associated by sharing an identical role in AML cell survival, reveals a potential pathway of regulation in TRIB2-driven AML that implicates the epigenetic modifier PRMT5. These findings have empowered future studies that are currently being investigated in the Keeshan lab.

In conclusion, the current study highlights the important oncogenic role of TRIB2 in human AML maintenance and, significantly in such a molecularly heterogeneous malignancy, a tailored therapeutic approach is suggested for the treatment of high TRIB2 AML by demonstration of a chemo-sensitive phenotype towards proteasome inhibitors. These data also define a new molecular mechanism of apoptosis induced by these drugs. Finally, a framework for further investigations into new TRIB2-AML partners is established by the identification of PRMT5 as a cooperating protein. Altogether, these findings have repercussions on the understanding of AML and on the portfolio of potential therapeutic targets that may improve the outcome of the disease.

Appendices

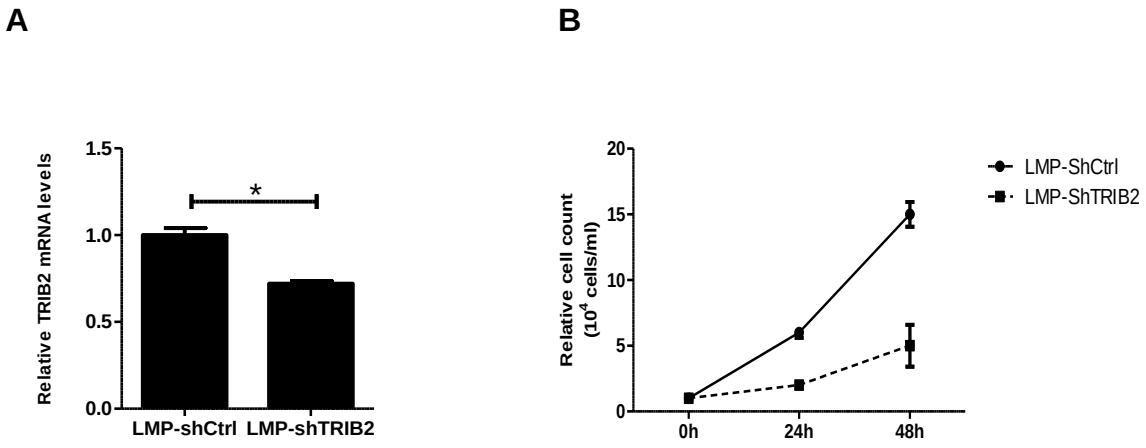

Appendix A TRIB2 expression is required for growth of U937 AML cells
(A) Real Time analysis of *TRIB2* mRNA levels in U937 cells following transduction with LMP-Ctrl or LMP-shTRIB2. (B) Cell growth analysis in U937 cells transduced with LMP-Ctrl or LMP-shTRIB2 assessed by trypan blue exclusion. Number of viable cells was normalized against % of GFP positive cells and is relative to cell count at 0h. Data presented are mean ± SD of duplicate cultures and are representative of 2 independent experiments. *$P \leq 0.05$ by Student´s *t*-test.

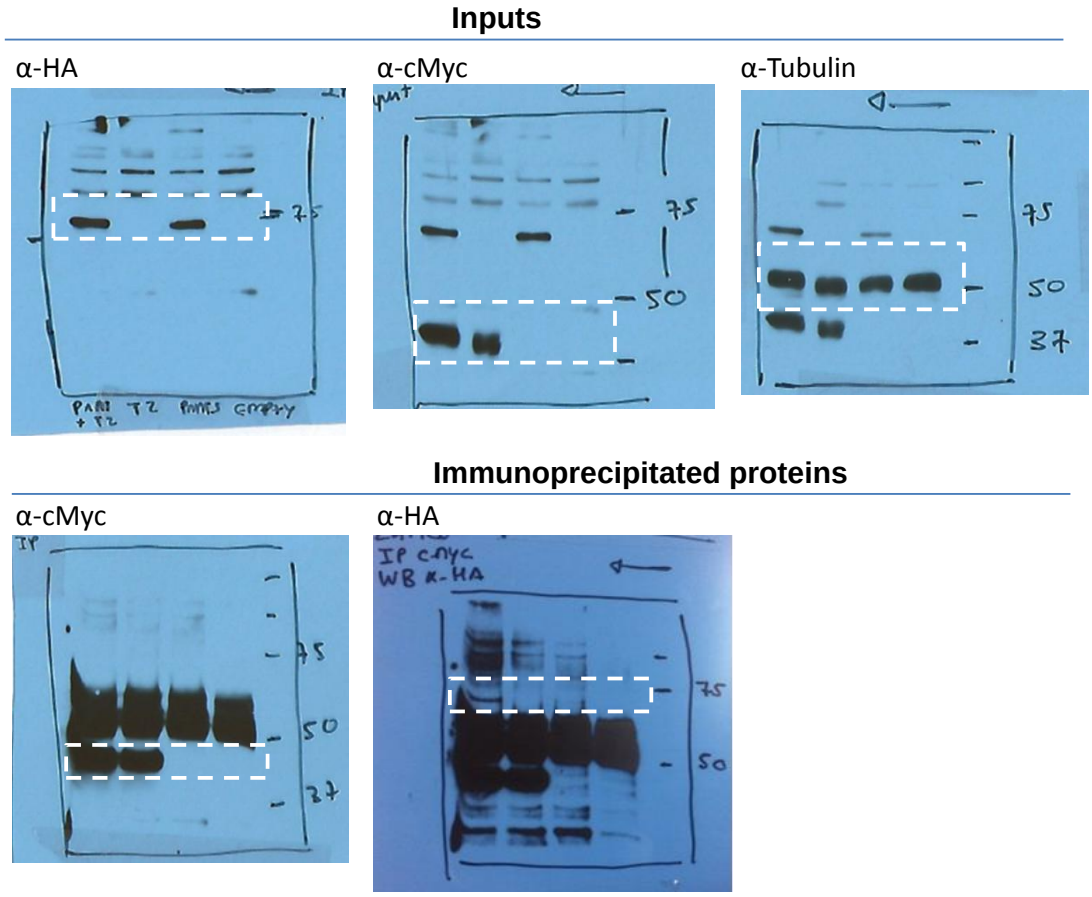

Appendix B Original western blots for Figure 5.3

Samples were analysed in an 8% polyacrylamide gel. Upper panel depicts blot with input samples probed with anti-HA, anti-cMyc and anti-Tubulin antibodies, as indicated in the Figure. Co-immunoprecipitated proteins are shown in the lower panel. Relevant sizes of the molecular ladder are written on the right side of the original films (kDa) and white boxes highlight cropped results. For assembly of Figure 5.3, blots were flipped. Samples are identified in the anti-HA film as PRMT5+T2; T2; PRMT5 and Empty. T2 symbolizes TRIB2.

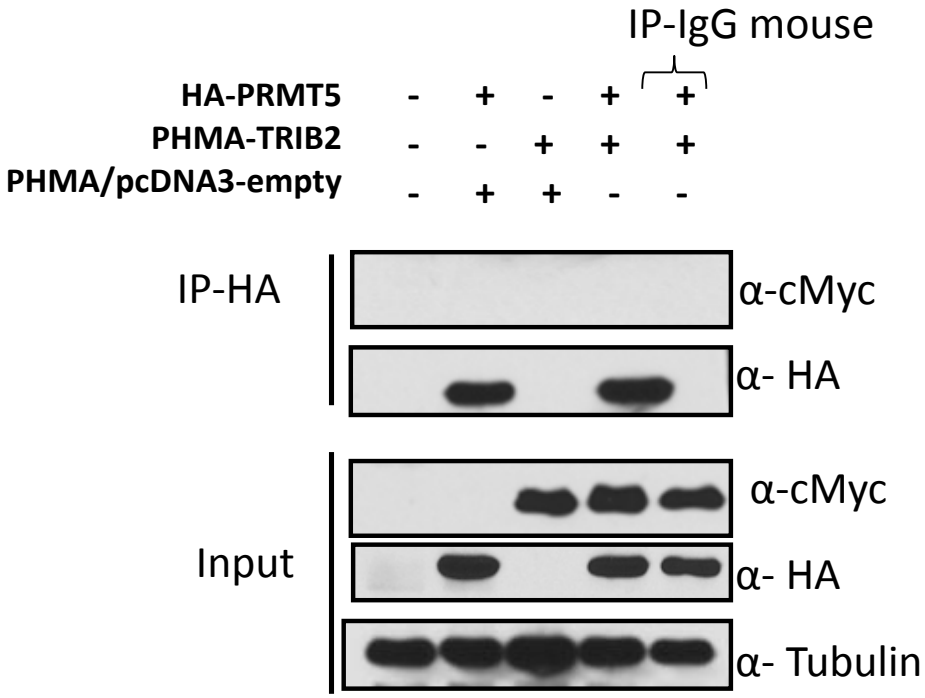

Appendix C Reciprocal Co-IP

293T cells were transiently transfected with vectors expressing HA-PRMT5 alone (lane 2) or with Myc-tagged TRIB2 protein (lane 4). Immunoprecipitation was performed using an anti-HA antibody and blots were probed with antibodies specific for HA or cMyc. Western blotting failed to detect a band at ~37kDa in sample with overexpression of both PRMT5 and TRIB2. Result is representative of 3 independent experiments.

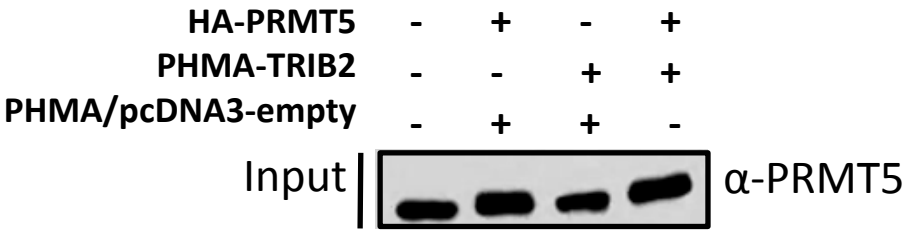

Appendix D Detection of PRMT5 in Input blot from Co-IP
Input blot was probed with α-PRMT5 antibody showing that endogenous and exogenous levels were not significantly different.

Appendix E PDF of "Regulation of Trib2 by an E2F1-C/EBPα feedback loop in AML cell proliferation"

MYELOID NEOPLASIA

Regulation of Trib2 by an E2F1-C/EBPα feedback loop in AML cell proliferation

Loveena Rishi,[1] Maura Hannon,[2] Mara Salomè,[1] Marie Hasemann,[3,4,5] Anne-Katrine Frank,[3,4,5] Joana Campos,[1] Jennifer Timoney,[2] Caitriona O'Connor,[1] Mary R. Cahill,[2] Bo Porse,[3,4,5] and Karen Keeshan[1]

[1]Paul O'Gorman Leukaemia Research Centre, Institute of Cancer Sciences, University of Glasgow, Glasgow, Scotland; [2]University College Cork, Cork, Ireland; [3]The Finsen Laboratory, Rigshospitalet, Faculty of Health Sciences, [4]Biotech Research and Innovation Center, and [5]Danish Stem Cell Centre Faculty of Health Sciences, University of Copenhagen, Copenhagen, Denmark

Key Points

- E2F1 regulates Trib2 expression and C/EBPα modulates E2F1-induced Trib2 activity at the granulocyte macrophage progenitor stage.
- Pharmacological inhibition of the cell cycle resulting in a block in E2F1 or Trib2 knockdown abrogates AML cell proliferation.

The loss of regulation of cell proliferation is a key event in leukemic transformation, and the oncogene tribbles (Trib)2 is emerging as a pivotal target of transcription factors in acute leukemias. Deregulation of the transcription factor E2F1, normally repressed by CCAAT enhancer-binding protein α (C/EBPα)-p42, occurs in acute myeloid leukemia (AML), resulting in the perturbation of cell cycle and apoptosis, emphasizing its importance in the molecular pathogenesis of AML. Here we show that E2F family members directly regulate Trib2 in leukemic cells and identify a feedback regulatory loop for E2F1, C/EBPα, and Trib2 in AML cell proliferation and survival. Further analyses revealed that E2F1-mediated Trib2 expression was repressed by C/EBPα-p42, and in normal granulocyte/macrophage progenitor cells, we detect C/EBPα bound to the Trib2 promoter. Pharmacological inhibition of the cell cycle or Trib2 knockdown resulted in a block in AML cell proliferation. Our work proposes a novel paradigm whereby E2F1 plays a key role in the regulation of Trib2 expression important for AML cell proliferation control. Importantly, we identify the contribution of dysregulated C/EBPα and E2F1 to elevated Trib2 expression and leukemic cell survival, which likely contributes to the initiation and maintenance of AML and may have significant implications for normal and malignant hematopoiesis. (*Blood*. 2014;123(15):2389-2400)

Introduction

The tribbles (Trib) family of pseudokinase genes (Trib1, Trib2, and Trib3) have recently emerged as important regulators of acute leukemia and hematopoietic development.[1] Trib proteins' diverse roles include cell proliferation, survival, motility, and metabolism.[2] There is a strong correlation between dysregulated Trib2 expression and acute myeloid and lymphoid leukemia (AML and ALL). Elevated Trib2 expression associates with a specific subset of AML characterized by dysregulated CCAAT enhancer-binding protein α (C/EBPα) and with T-cell ALL (T-ALL), both linked with NOTCH1 mutations.[3-5] Mice reconstituted with hematopoietic stem cells (HSCs) retrovirally expressing Trib2 developed AML. The proteasomal-mediated degradation and inhibition of C/EBPα was required for the leukemogenic activity of Trib2.[4-6] Although Trib2 appears to integrate a wide variety of signaling pathways, the molecular understanding of how its expression is controlled in normal and malignant hematopoiesis is limited.

We identified Trib2 as a NOTCH1-regulated transcript in T-ALL cells undergoing growth arrest. As well as NOTCH1,[3,5] PITX1[7] and TAL1[8] were also found to up-regulate Trib2 in T-ALL. Both PITX1 and TAL1 are recurrently activated transcription factors in T-ALL and importantly require the expression of Trib2 for leukemic cell growth and survival.[8] In AML cells, MEIS1 was found to bind to the Trib2 promoter, and Trib2 could confer growth-enhancing properties to NUP98-HOXD13/MEIS1-AML cells.[9] Additionally, Trib2 expression is regulated by microRNAs in leukemia cells.[10,11] It is clear therefore that Trib2 expression is controlled in a cell type–, cell context–, and cell cycle–dependent manner.

The role of Trib2 in cell cycle and cell proliferation is supported by an established role for *Drosophila* Tribbles (dTRIB) in the cell cycle. dTRIB coordinates cell division during gastrulation by promoting turnover of the cell cycle protein String/CDC25, thereby inhibiting premature mitosis.[12-14] A further study suggested that dTRIB controls mitosis through inhibition of String and positive regulation of WEE1, as coexpression of WEE1 and Tribbles showed strong synergistic interactions that resulted in severe eye and wing developmental defects.[15] Studies of mammalian Trib2 thus far indicate the genetic interactions of dTRIB and other *Drosophila* homolog proteins are conserved in the mammalian system. dTRIB promotes the degradation of Slbo, the *Drosophila* homolog of the C/EBP family of transcription factors, thereby inhibiting Slbo-dependent border cell migration

Submitted July 1, 2013; accepted February 1, 2014. Prepublished online as *Blood* First Edition paper, February 10, 2014; DOI 10.1182/blood-2013-07-511683.

The online version of this article contains a data supplement.

The publication costs of this article were defrayed in part by page charge payment. Therefore, and solely to indicate this fact, this article is hereby marked "advertisement" in accordance with 18 USC section 1734.

during oogenesis,[16] and inactivation of C/EBPα by Trib2 has been shown in the hematopoietic system to block myeloid cell differentiation.[4] Likewise, dTRIB has a positive genetic interaction with N (the *Drosophila* homolog of NOTCH),[17] and this is conserved in mammals as Trib2 was found to be a direct transcriptional target gene of NOTCH1.[5]

The transcription factor C/EBPα is a critical regulator of myeloid cell proliferation and differentiation. C/EBPα is frequently dysregulated in AML as a result of mutation, posttranscriptional modifications, posttranslational inhibition, epigenetic regulation, and proteasomal degradation. It is also an important tumor suppressor as it regulates a variety of cell cycle proteins.[18] C/EBPα mRNA encodes for 2 major protein isoforms, C/EBPα-p42 and C/EBPα-p30, produced by alternative translational start codons. We have previously shown that Trib2 degrades C/EBPα-p42 and blocks differentiation, with an increase in the C/EBPα-p30 oncogenic protein. In addition to Trib1- and Trib2-mediated dysregulation,[19] the normal protein expression ratio of p42:p30 is skewed in AML as a result of gene mutation.[20] Importantly, the p30 isoform lacks a transactivation domain in the N terminus important for antimitotic activity. This N-terminal domain is crucial for growth arrest by E2F1-mediated regulation of c-Myc expression, and C/EBPα-p42 interferes with E2F1 transactivation of the c-Myc promoter.[21-23] E2F1 is a master regulator of cell cycle progression. C/EBPα inhibition of E2F1 additionally occurs via protein-protein interaction in non–DNA-binding residues in the C-terminal region of C/EBPα present in both p30 and p42.[22] Mutation of the C-terminal residues of C/EBPα that interact with E2F1 (BRM2) leads to a transplantable disorder of the myeloid lineage with expansion of myeloid progenitors. This revealed a role of C/EBPα-mediated E2F1 repression in controlling the proliferation of myeloid progenitors.[24] Importantly, however, null mutations in *CEBPA* do not occur in AML, and C/EBPα-deficient HSCs do not lead to AML,[25,26] demonstrating that C/EBPα is required for AML to develop.

The E2F family of cell cycle regulators are generally classed as transcriptional activators (E2F1, E2F2, E2F3a, and E2F3b) or repressors (E2F4, E2F5, E2F6, E2F7, and E2F8), but this simple classification lacks in vivo validation.[27] E2F1-3–deficient hematopoietic cells have a defect in myeloid cell differentiation, with an accumulation of granulocyte/macrophage progenitor (GMP) cells and a decrease in $CD11b^+$ myeloid cells in the bone marrow. E2F1-3s are thus required for cell survival and proliferation at distinct stages during myeloid differentiation.[28] AML with *CEBPA* mutations has increased E2F3 and decreased miR-34a levels, which C/EBPα normally regulates in myeloid cells.[29] Additional studies support a molecular network involving miR-223, C/EBPα, and E2F1 as major components of the granulocyte differentiation program, which is deregulated in AML.[30]

We show here that E2F1, as well as E2F2 and E2F3, is a potent inducer of Trib2 expression and that E2F1 cooperates with C/EBPα-p30 to further activate the Trib2 promoter in preleukemic cells, resulting in elevated Trib2 expression. Conversely, in normal myeloid progenitor cells, C/EBPα-p42 is found bound to the Trib2 promoter and inhibits E2F1-mediated activation of Trib2. We demonstrate that inhibition of the E2F1-Trib2 regulatory loop results in cell cycle arrest and inhibition of leukemic cell proliferation. In addition, we show that targeted inhibition of this pathway does not affect the growth and survival of normal hematopoietic cells. Our work demonstrates that Trib2 expression is regulated by E2F1 in vivo, and C/EBPα-p30 cooperates with E2F1 to activate Trib2 expression, thus preventing C/EBPα-p42–mediated E2F1 repression, ultimately contributing to the uncontrolled proliferation and cell cycle progression seen in AML.

Methods

Trib2-dependent reporter gene assay

3T3 cells were transfected with luciferase constructs alone or in combination with other expression plasmids and luminescence readings taken (see supplemental Methods on the *Blood* Web site for details).

Electromobility shift assay

Nonradiolabeled electromobility shift assays (EMSAs) using the LightShift Chemiluminescent EMSA Kit (Thermo Scientic) were performed on nuclear extracts prepared from cells using wild-type (WT) and mutant probes. Specificity was assessed by cold competition (see supplemental Methods for details).

Chromatin immunoprecipitation

Cells were fixed and resuspended in lysis buffer. Isolated nuclei were resuspended in shearing buffer (Active Motif) and sonicated on ice. Protein/DNA complexes were immunoprecipitated with the indicated antibody, and DNA was eluted as per the manufacturer's instructions (Active Motif) and column purified (QIAquick Purification Kit; Qiagen). Eluted DNA was subjected to polymerase chain reaction (PCR) using promoter-specific primer sets (see supplemental Methods for details).

Mice

$Trib2^{-/-}$ (B6;129S5-Trib2tm1Lex) mice, backcrossed onto C57B6, were bred and housed in the University of Glasgow. Cebpa transgenic mice[31] were bred and housed in the University of Copenhagen (see supplemental Methods for details). All mouse work was performed according to national and international guidelines and approved by the local United Kingdom and Danish Animal Ethical Committees.

Dataset analysis

Gene expression values for Trib2 vs E2F1 (GSE14468 and GSE1159) were plotted, and the line of best fit was calculated using linear regression (see supplemental Methods for details).

Cell cycle and proliferation analysis

Cells were stained with carboxyfluorescein diacetate succinimidyl ester (CFSE; Molecular Probes) for 10 minutes and treated. Drug-treated cells were also fixed and stained with Propidium Iodide (PI)/RNase staining buffer (BD Pharmingen) (see supplemental Methods for details).

Annexin V/4′6 diamidino-2-phenylindole staining

Total bone marrow cells from WT or Trib2-deficient mice and green fluorescent protein–sorted U937 cells were suspended in binding buffer (containing annexin V-phycoerythrin [BD Biosciences] and 4′6 diamidino-2-phenylindole [DAPI; Sigma-Aldrich]) and were analyzed by flow cytometry.

Patient AML samples

Blood samples from newly diagnosed AML patients and normal peripheral blood samples were collected following protocol approved by the Ethics Review Board and with informed consent. Mononuclear cells were isolated using Histopaque (Sigma-Aldrich) according to the manufacturer's instructions. This study was conducted in accordance with the Declaration of Helsinki.

See supplemental Methods for all other details.

Results

To investigate how Trib2 expression is regulated, we cloned 2 promoter regions of Trib2 into the pGL3 luciferase reporter: (1)

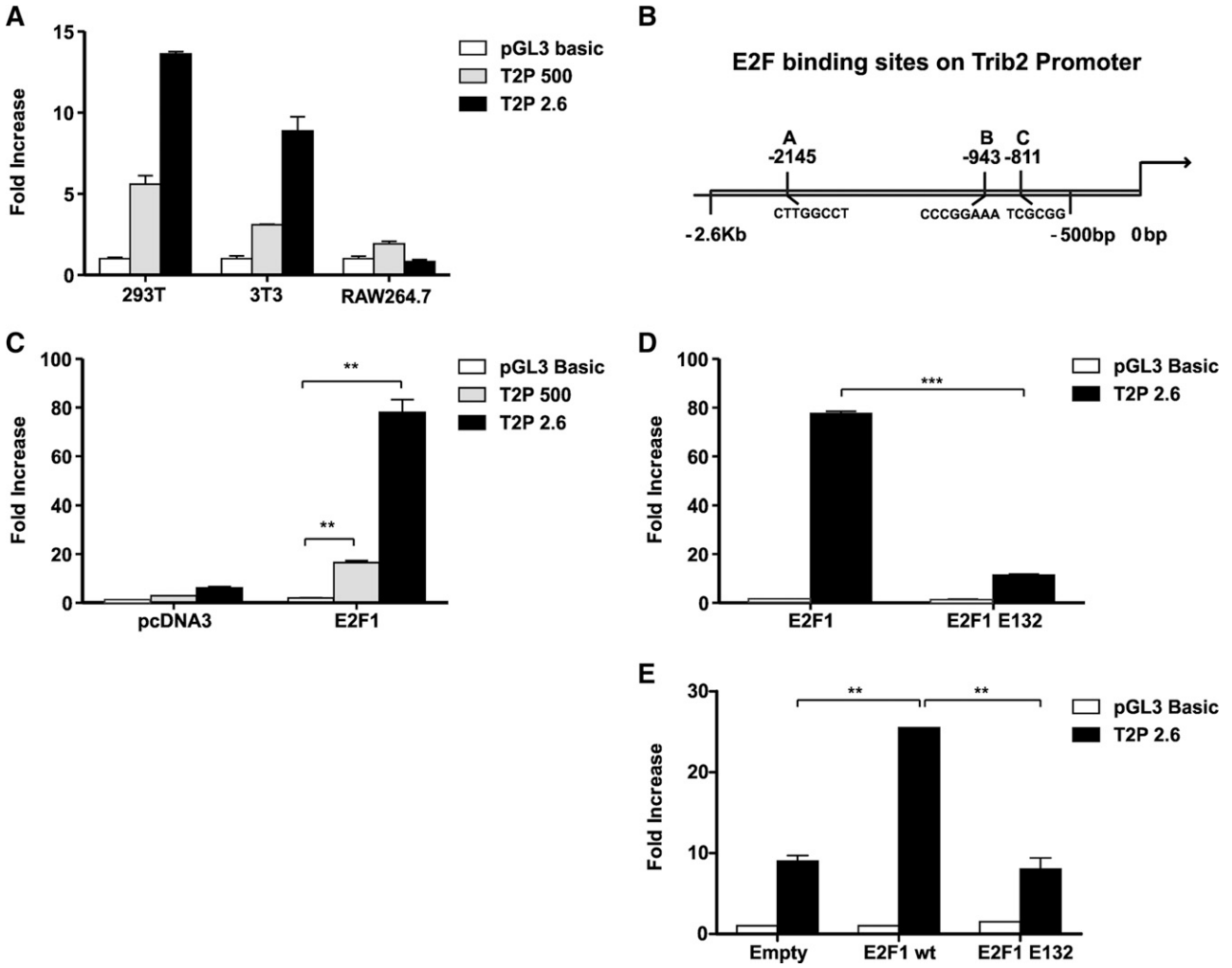

Figure 1. E2F1 binds and activates the Trib2 promoter. (A) 293T, 3T3, and RAW264.7 cells were cotransfected with empty pGL3 Basic or 500-bp Trib2 promoter or 2.6-kb Trib2 promoter constructs and luciferase activity was measured. (B) Schematic presentation of the Trib2 promoter region 2.6 kb upstream from the transcriptional start site and the location of 3 putative E2F binding sites. (C) 3T3 cells were cotransfected with E2F1 or pcDNA empty expression vector and Trib2 luciferase reporter plasmids (pGL3 control, 500-bp, or 2.6-kb promoter region) and luciferase activity was measured. (D) 3T3 cells were cotransfected with E2F1 or E2F1 E132 DNA binding deficient mutant expression vectors and Trib2 luciferase reporter constructs (pGL3 control or 2.6-kb promoter) and luciferase activity was measured. Data presented are mean ± standard deviation (SD) of duplicate cultures and representative of 3 independent experiments. $^{**}P < .005$ and $^{***}P < .001$ using an unpaired Student *t* test. (E) K562 cells were cotransfected with E2F1 or E2F1 E132 DNA binding deficient mutant expression vectors or empty control vector and Trib2 luciferase reporter constructs (pGL3 control or 2.6-kb promoter) and luciferase activity was measured. Data presented are mean ± SD and representative of 3 independent experiments. $^{**}P < .005$ using an unpaired Student *t* test.

500 bp upstream from the transcriptional start site (−500 to +1 bp) and (2) including the entire 5′ untranslated region (UTR) and upstream region (−2.6 kb to +1 bp). The promoter activity was assessed in 293T cells, 3T3 cells, and RAW264.7 cells. Increased Trib2 promoter activity was seen in 293T and 3T3 cell lines but not the RAW cell line with the 2.6-kb promoter construct compared with the 500-bp promoter (Figure 1A). We analyzed the promoter region of Trib2 using TESS bioinformatic software and found 3 putative consensus E2F binding sites within the Trib2 promoter. Two sites were located within the 1.3-kb 5′UTR (site B at −943 bp and site C at −811 bp), and 1 site was further upstream (site A at −2.1 kb; Figure 1B). We assessed the activation of the Trib2 promoter by cotransfection with E2F1 in 3T3 and K562 myeloid cells. E2F1 expression significantly increased the promoter activity of the 2.6-kb construct in both cell types (Figure 1C,E). We performed the promoter activity assay using an E2F1 DNA binding mutant (E132 mutant) and showed that, in the absence of direct DNA binding, E2F1 is unable to activate the Trib2 promoter in both 3T3 and K562 cells (Figure 1D-E). Together these data suggest that Trib2 is a target of E2F1.

To identify the role of the predicted E2F1 sites in the Trib2 promoter regions, we constructed a number of deletion and mutagenized promoter constructs in the luciferase reporter (schematic representation in Figure 2A-B, upper panels, respectively). We tested the promoter activity in the presence and absence of exogenous E2F1 expression. Activation of the 500-bp promoter region can be modestly increased by expression of E2F1 (as seen in Figures 1C and 2A), despite the lack of a consensus E2F1 binding site in that region. This indicates a potential nonconsensus E2F1 binding site or E2F1-mediated activation via protein-protein interactions. Using deletion constructs containing only site B (−963-bp construct with site C mutated) or only site C (−927-bp construct; Figure 2A, upper left) revealed that in the absence of site A and site B or C, E2F1 is able to further activate the Trib2 promoter but is unable to restore complete activation as seen in the full-length promoter construct (Figure 2A, lower). We then performed site-directed mutagenesis of sites A, B, and C in the 2.6-kb promoter construct. Luciferase activity assay revealed that mutation of site A or C alone did not abrogate or inhibit E2F1-induced promoter activity, whereas mutation of B alone or both

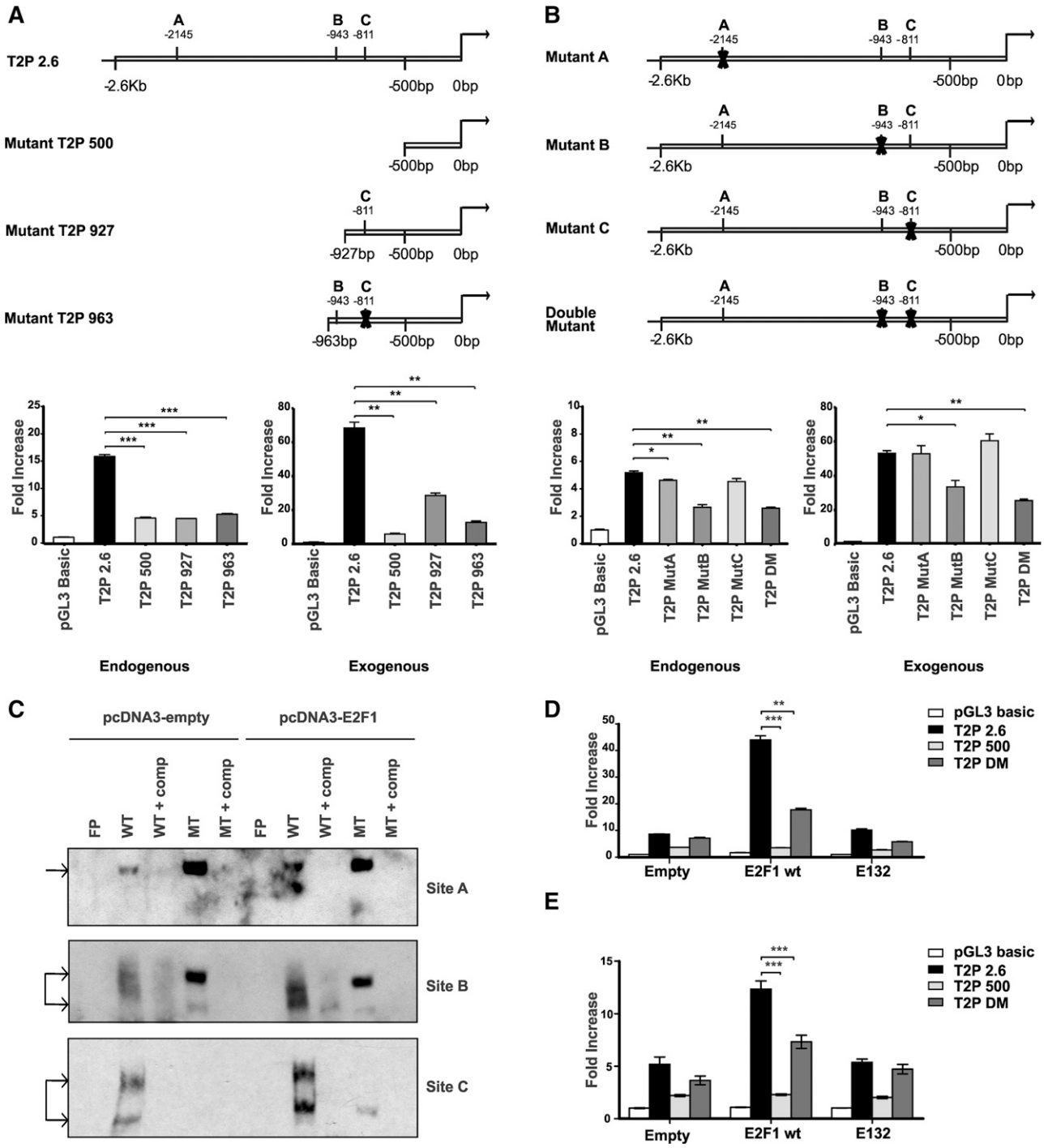

Figure 2. E2F1 binding is localized to 2 consensus binding sites on the Trib2 promoter. (A) (Upper) Schematic presentation of full-length 2.6-kb and deletion mutant Trib2 promoter constructs with the indicated E2F1 binding sites. 3T3 cells were (lower left) transfected with Trib2 luciferase reporter plasmids (pGL3 control, 2.6-kb, 500-bp, 927-bp, or 963-bp promoter region) and (lower right) cotransfected with E2F1 or pcDNA empty expression vector, and luciferase activity was measured. (B) (Upper) Schematic presentation of full-length 2.6 kb with site-directed mutations of the 3 putative E2F1 binding sites. 3T3 cells were (lower left) transfected with Trib2 luciferase reporter plasmids (pGL3 control, 2.6-kb, MutA, MutB, MutC, or double mutant DM) and (lower right) cotransfected with E2F1 or pcDNA empty expression vector, and luciferase activity was measured. Data presented are mean ± SD of duplicate cultures and representative of 3 independent experiments. $^{*}P < .05$, $^{**}P < .005$, and $^{***}P < .001$. (C) Nuclear extracts prepared from K562 cells transfected with pcDNA3 empty or E2F1 were assayed for E2F1 binding for sites A, B, and C by EMSA. Arrow indicates E2F1 binding. FP, free probe; comp, cold competition; MT, mutant type. (D) 3T3 cells were cotransfected with E2F1 WT or E2F1 E132 DNA binding deficient mutant or empty expression vector and Trib2 luciferase reporter constructs (pGL3 control, 2.6-kb, 500-bp, or DM promoter region), and luciferase activity was measured. Data presented are mean ± SD of duplicate cultures and representative of 2 independent experiments. $^{**}P < .005$ and $^{***}P < .001$ using an unpaired Student *t* test. (E) K562 cells were cotransfected with E2F1 WT or E2F1 E132 DNA binding deficient mutant or empty expression vector and Trib2 luciferase reporter constructs (pGL3 control, 2.6-kb, 500-bp, or DM promoter region), and luciferase activity was measured. Data presented are mean ± SD and representative of 2 independent experiments. $^{***}P < .001$ using an unpaired Student *t* test.

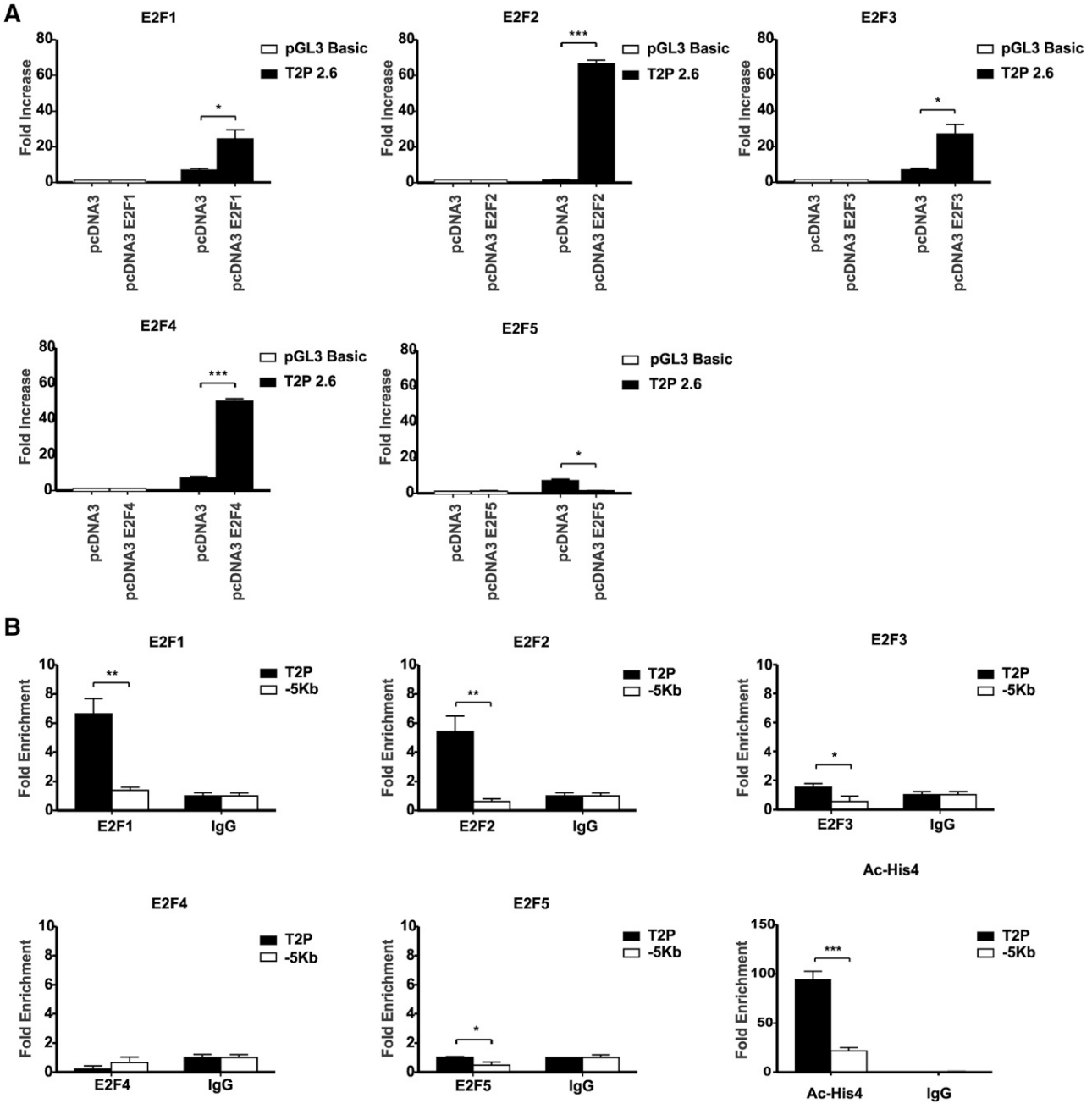

Figure 3. Other E2F family members can bind and activate Trib2 promoter. (A) 3T3 cells were cotransfected with E2F1, E2F2, E2F3, E2F4, E2F5, or pcDNA empty expression vector and Trib2 luciferase reporter plasmids (pGL3 basic control or 2.6-kb promoter region), and luciferase activity was measured. Data presented are mean ± SD of duplicate cultures and representative of 3 independent experiments. *$P < .05$ and ***$P < .001$. (B) K562 cells were chromatin immunoprecipitated using anti-E2F1, anti-E2F2, anti-E2F3, anti-E2F4, anti-E2F5, antiacetylated histone 4 (Ac-His4), or normal IgG control antibodies. PCR was performed using primers directed against the E2F binding region containing sites B and C and using primers against a −5-kb region as a negative control. Graphs represent fold enrichment of DNA compared with the IgG control and are representative of 3 independent experiments, and error bars denote ± SD of each sample. *$P < .05$, **$P < .005$, and ***$P < .001$.

sites B and C together reduced Trib2 promoter activity (Figure 2B, lower). EMSA analysis showed that, on transfection of K562 cells with E2F1, there was an increase in binding to the WT probes for the E2F1-specific sites A, B, and C and a lack of E2F1-inducible binding to 3 distinct mutant probes for sites A, B and C (Figure 2C). Mutation of B and C together significantly reduced Trib2 promoter activity in both 3T3 (Figure 2D) and K562 cells (Figure 2E) but not to as great an extent as the 500-bp promoter (lacks sites A, B, and C). Together, these data reveal that E2F1 binds at sites A, B, and C in the Trib2 promoter in fibroblasts and myeloid cells.

We next tested whether this was specific to E2F family members. Luciferase assays in 3T3 cells using the full-length 2.6-kb Trib2 promoter construct revealed that E2F1, E2F2, E2F3, and E2F4 activated the Trib2 promoter, whereas E2F5 was unable to induce Trib2 promoter activity (Figure 3A). To test the ability of these E2F family members to bind to Trib2 promoter in a myeloid leukemia cell, we performed chromatin immunoprecipitation (ChIP) analysis using antibodies for endogenous E2F1, E2F2, E2F3, E2F4, and E2F5 in K562 cells (express high levels of Trib2 protein; Figure 7E). In comparison with the IgG-negative control, there was enrichment

of E2F1, E2F2, and E2F3 on the Trib2 promoter region containing sites B and C, but not at a −5-kb Trib2 promoter region used as a negative control (Figure 3B). The Trib2 promoter region was shown to be transcriptionally active as demonstrated by the presence of acetylated histone 4. There was no significant enrichment of E2F4 or E2F5 on the Trib2 promoter. These data show that E2F1, E2F2, E2F3, and E2F4 are capable of activating the Trib2 promoter; in leukemia cells, only E2F1, 2, and 3 actually bind the Trib2 promoter. These data demonstrate that E2F proteins directly regulate Trib2 expression.

To further analyze the role of E2F1 in Trib2 regulation, we assessed E2F1-induced Trib2 mRNA expression in cells transfected with E2F1. 293T, E2F1$^{-/-}$ mouse embryonic fibroblasts (MEFs), and K562 cells were transfected with control pcDNA vector, E2F1, or intracellular activated Notch1 ([ICNX] as a positive control[5]), and Trib2 mRNA expression was measured. There was a significant increase in Trib2 mRNA following overexpression of E2F1 (Figure 4A). Indeed there was significant reduction in Trib2 mRNA expression in E2F1$^{-/-}$ MEFs compared with WT MEFs (Figure 4B). E2F1$^{-/-}$ MEFs express little to no Trib2 protein expression (Figure 4C), and on transfection with E2F1 (and ICNX as positive control), we saw an increase in Trib2 protein expression (Figure 4D, left, lane 2). Similarly, transfection of K562 cells with E2F1 leads to an increase in Trib2 protein expression (Figure 4D, right). Conversely, small interfering RNA (siRNA) directed against E2F1 in 293T, HeLa, and K562 cells resulted in decreased Trib2 mRNA expression levels compared with siRNA scramble controls (Figure 4E-G), and analysis of a previously published transcriptional profile of E2F1-3$^{-/-}$ CD11b^{+} myeloid cells[28] revealed a 4.6-fold reduction in Trib2.

We also identified putative C/EBPα binding sites in the Trib2 promoter using the TESS bioinformatics analysis tool. Indeed E2F1 binding sites B and C surround a region of the Trib2 promoter that contains a high confidence C/EBP binding site (−900 bp) (Figure 5A). C/EBPα-mediated inhibition of E2F1 is pivotal for granulopoiesis. As our previous work has shown that Trib2 degraded C/EBPα-p42 leaving increased expression of the oncogenic C/EBPα-p30 form in AML, we tested whether there was an E2F1-C/EBPα feedback loop regulating Trib2 expression. EMSA revealed that both C/EBPα-p42 and -p30 bind to this region at −900 bp using a C/EBPα binding site–specific probe (Figure 5B). Trib2 promoter assays showed a dose-dependent decrease in activity following cotransfection of increasing doses of C/EBPα-p42 compared with E2F1 alone (Figure 5C, left). Significantly, cotransfection of E2F1 and C/EBPα-p30 resulted in a dose-dependent increase in E2F1-induced Trib2 promoter activity (Figure 5C, right). These data show that the E2F1 regulation of Trib2 can be modulated by the presence of C/EBPα-p42 and C/EBPα-p30. Importantly, Trib2 mRNA expression decreased in myeloid K562 cells on C/EBPα-p42 expression, and reciprocally, Trib2 expression increased on C/EBPα-p30 expression (Figure 5D). This was not due to an increase in E2F protein expression by C/EBPα-p30 (supplemental Figure 1). This regulation was seen in K562 nuclear extracts at the DNA binding sites, as EMSA analysis showed that C/EBPα-p42 and -p30 modulated the binding of E2F1 to the Trib2 promoter at site B only (Figure 5E). The slower-migrating protein complex induced by C/EBPα-p30 contained both E2F1 and C/EBPα-p30 as seen by the disappearance of this complex in a supershift assay, indicating that these proteins are components of this complex (Figure 5F). Additionally, the E2F1-induced Trib2 promoter activity in K562 cells was modulated by C/EBPα-p42 and -p30 expression (Figure 5G). To investigate the physiological binding of C/EBPα to the Trib2 promoter in the myeloid lineage, we performed ChIP analysis for C/EBPα in normal murine GMPs at −900 bp. We detected C/EBPα bound to the Trib2 promoter in the region spanning the identified E2F1 binding sites B and C (Figure 5H) revealing that in normal GMPs, C/EBPα is recruited onto the Trib2 promoter. This is consistent with the ability of C/EBPα-p42 to inhibit E2F1 in normal myelopoiesis. Interestingly, real-time quantitative PCR analysis of normal WT GMPs compared with GMPs isolated from preleukemic mutant C/EBPα knockin mice that retain p30 expression but have lost p42 expression (Lp30, −/p30) reveals a significant increase in Trib2 expression in the mutant GMPs (Figure 5I). Therefore, in the presence of C/EBPα-p30 in the preleukemic GMP population, Trib2 mRNA expression is increased. Together, these data reveal that C/EBPα localizes to the Trib2 promoter in GMP progenitor cells, and the balance of C/EBPα-p42 and C/EBPα-p30 modulates the ability of E2F1 to activate Trib2 expression in normal and preleukemic myeloid cells.

To target the E2F1 pathway and determine the effect on Trib2 and the leukemic cell, we used known cyclin-dependent kinase inhibitors (CDKis), flavopiridol (a pan CDK inhibitor),[32] pentoxifylline (PTX, a nonspecific phosphodiesterase inhibitor), and dibutyryl cAMP (a cAMP analog).[33] We treated U937 cells (AML cells that express high levels of Trib2 protein; Figure 7E) with escalating doses of flavopiridol and PTX and assessed cell death (Figure 6A). Both flavopiridol (IC_{50} of 94 nM) and PTX (IC_{50} of 4 mM) were cytotoxic to U937, whereas up to 4 mM dibutyryl cAMP was not cytotoxic. At a lower-dose (2 mM PTX, 4 mM dibutyryl cAMP, and 62.5 nM flavopiridol) treatment at 24 hours, U937 cells underwent G1 cell cycle arrest without increased apoptosis (sub-G1 DNA content) as assessed by propidium iodide staining (Figure 6B) and had reduced proliferation as assessed by CFSE staining at 96 hours (Figure 6C). Using low drug doses that inhibit cell proliferation but have minimal cytotoxicity and apotosis, we assessed the effect on cell cycle proteins E2F1 and Trib2. Western blot analysis determined that PTX, dibutyryl cAMP, and flavopiridol led to a reduction in Cdk6, Cdk2, phospho-RB (phosphorylated-retinoblastoma), E2F1, and Trib2 with 24-hour treatment (Figure 6D). Importantly, global protein expression of RB is not decreased, and C/EBPα levels remain unchanged, if not slightly increased at the lower concentrations when cell cycle arrest occurred. These results show that the inhibition of CDKs results in cell cycle arrest and reduced proliferation, inhibition of E2F1, and a decrease in Trib2. To determine the effect in normal cells, we treated WT and Trib2 knockout (KO; Trib2$^{-/-}$) total bone marrow (BM) cells and HSCs (Lineage^{-}Sca-1^{+}c-Kit^{+}) with PTX, dibutyryl cAMP, and flavopiridol. There was very little cytotoxic effect on WT BM cells and HSCs as assessed by Annexin V/DAPI staining (Figure 6E-F), and no difference was observed in cell death in Trib2$^{-/-}$ BM and HSC cells compared with WT cells (Figure 6E-F). No cytotoxic effect was seen in colony-forming assays of untreated and treated HSCs from WT and Trib2$^{-/-}$ animals (Figure 6G). These data show that there is limited cell toxicity of targeting this pathway using these drugs in normal cells or cells that lack Trib2 expression.

To prove that inhibition of Trib2 expression plays a role in leukemic cell proliferation, we used lentiviral technology to knockdown Trib2 expression in AML cells (Figure 7A; supplemental Figure 2). Trib2 knockdown inhibited the growth of AML cells (Figure 7B), induced apopotosis and decreased cell viability (Figure 7C), and induced G1 cell cycle arrest (Figure 7D), indicating that Trib2 expression is required for the survival and proliferation of AML cells. Therefore, to assess the prevalence of high Trib2 expression in AML, we analyzed primary AML patient samples by mRNA and western blot analysis and compared the levels to normal peripheral

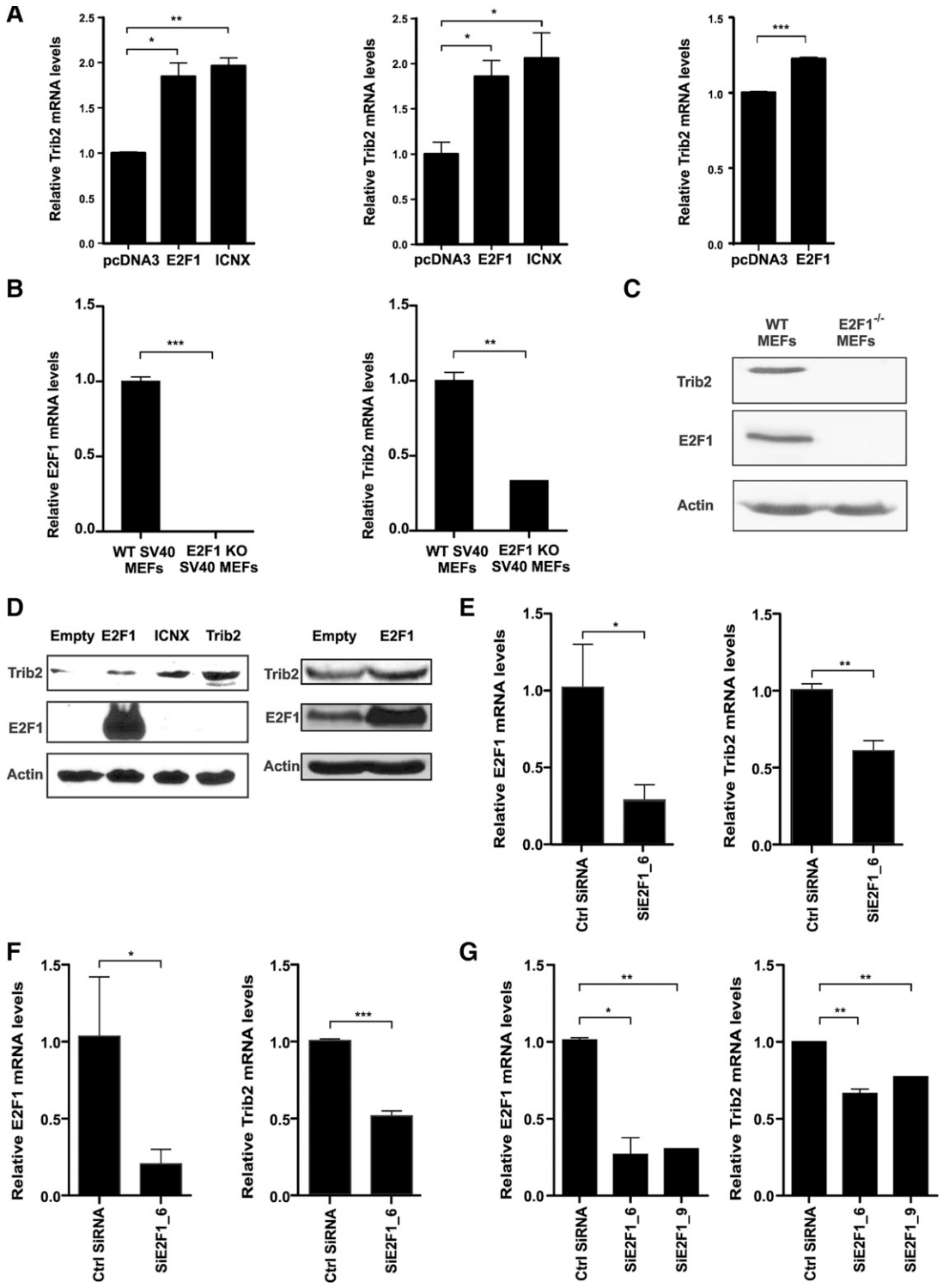

Figure 4. E2F1 regulates Trib2 mRNA and protein expression levels. (A) (Left) E2F1$^{-/-}$ (KO) MEFs, (center) 293T, or (right) K562 cells transfected with E2F1, pcDNA control, or ICNX as indicated were measured for Trib2 mRNA expression by real-time PCR analyses. Data are presented relative to control pcDNA transfected cells ± SD of duplicate cultures. *$P < .05$, **$P < .005$, and ***$P < .001$. (B) WT and E2F1$^{-/-}$ (KO) SV40 MEFs were measured for (left) E2F1 and (right) Trib2 mRNA expression by real-time PCR analyses. (C) Western blot analyses of E2F1 and Trib2 protein levels in WT and E2F1$^{-/-}$ (KO) MEFs. Actin shown as protein loading control. (D) (Left) E2F1$^{-/-}$ (KO) MEFs or (right) K562 cells were transfected with pcDNA3 empty vector, E2F1, ICNX, or Trib2 as indicated, and western blot analyses were performed for Trib2, E2F1, and actin as a loading control. (E) 293T, (F) HeLa, and (G) K562 cells were transfected with scrambled control siRNA and siE2F1 (1 or 2 different E2F1 siRNAs as indicated), and real-time PCR analysis was performed for E2F1 and Trib2. Data are presented relative to control transfected cells and representative of 2 independent experiments. Error bars denote ± SD of each sample measured in triplicate. *$P < .05$, **$P < .005$, and ***$P < .001$.

blood samples (N1-6), normal lymphoblast cell lines (CV1665 and CV1939), and myeloid leukemic cell lines (K562, U937, ML-1, Kasumi, and SB1690CB). We detected high Trib2 expression in AML patient samples compared with normal controls (Figure 7E). High E2F1 expression correlated with high Trib2 protein expression (Figure 7E). AML patient datasets were investigated for a correlative

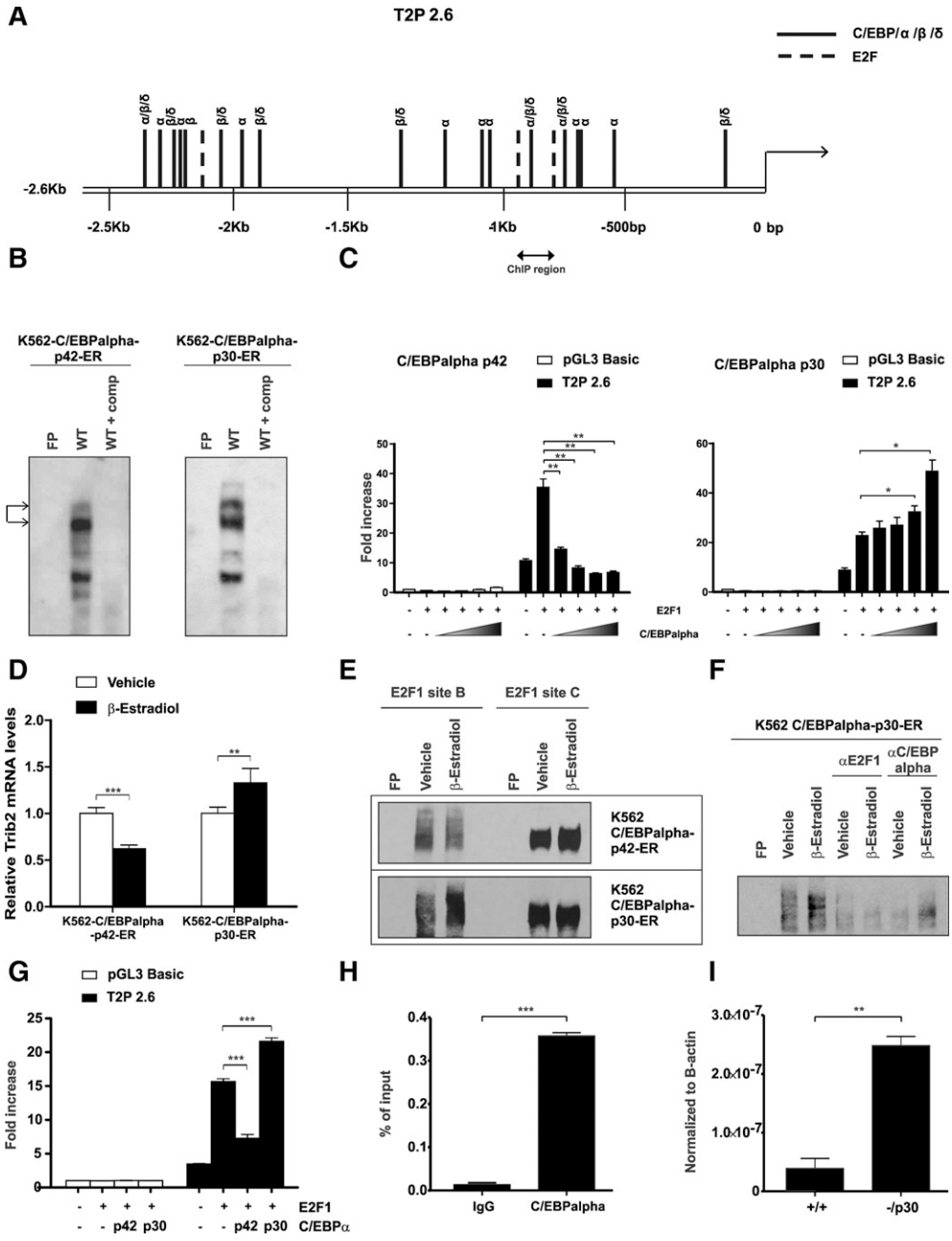

Figure 5. C/EBPα p42 and p30 oppositely modulate Trib2 expression via binding of the promoter. (A) Putative binding sites of C/EBP family of transcription factors in the Trib2 promoter. Several binding sequences are shared among members α, β, and δ of the C/EBPα family. E2F putative binding sites are also indicated (long dash line), and the region is targeted for ChIP-PCR analysis. (B) Nuclear extracts prepared from K562-C/EBPα-p42-ER or K562-C/EBPα-p30-ER cells induced with β-estradiol for 24 hours were assayed for C/EBPα binding by EMSA. Arrows indicate C/EBPα binding. FP, free probe; comp, cold competition. (C) 3T3 cells were cotransfected with empty control, E2F1 alone, or in combination with increasing amount of (left) C/EBPα-p42 or (right) C/EBPα-p30 and Trib2 luciferase reporter constructs (pGL3 control or 2.6-kb promoter), and luciferase activity was measured. Data presented are mean ± SD of duplicate cultures and representative of 2 independent experiments. $*P < .05$ and $**P < .005$. (D) K562-C/EBPα-p42-ER and K562-C/EBPα-p30-ER cells induced with β-estradiol or vehicle control for 24 hours were measured for Trib2 mRNA expression by real-time PCR analyses. Data are presented relative to vehicle control and representative of 2 independent experiments. Error bars denote ±SD of each sample measured in triplicate. $**P < .005$ and $***P < .001$. (E) Nuclear extracts prepared from (upper) K562-C/EBPα-p42-ER and (lower) K562-C/EBPα-p30-ER cells transfected with E2F1 and induced with β-estradiol or vehicle control for 24 hours were assayed for E2F1 binding for WT sites B and C by EMSA. FP, free probe. (F) Supershift EMSA assay was performed in nuclear extracts prepared from K562-C/EBPα-p30-ER cells transfected with E2F1 and induced with β-estradiol or vehicle control for 24 hours using antibody specific for E2F1 or C/EBPα. Oligonucleotide for WT site B was used as a probe. FP, free probe. (G) K562 cells were cotransfected with empty control, E2F1 alone, or E2F1 in combination with C/EBPα-p42 or C/EBPα-p30 and Trib2 luciferase reporter constructs (pGL3 control or 2.6-kb promoter region), and luciferase activity was measured. Data presented are mean ± SD and representative of 2 independent experiments. $***P < .001$ using an unpaired Student *t* test. (H) Normal murine GMP cells were chromatin immunoprecipitated using anti-C/EBPα or normal IgG control antibodies. PCR was performed using primers against the region indicated in A. Error bars denote ±SD of each sample measured in triplicate. $***P < .001$. (I) Real-time PCR analysis of Trib2 mRNA levels in WT ($^{+/+}$) GMP and −/p30 GMP cells. $**P < .005$.

relationship between elevated Trib2 expression and E2F1 expression. Using 2 previously published AML patient microarray datasets,[34,35] we found a significant positive correlation between E2F1 and the high Trib2-expressing patient samples (Figure 7F). As positive controls, we determined that there was a significant positive correlation between Trib2 and NOTCH1 and a significant negative correlation

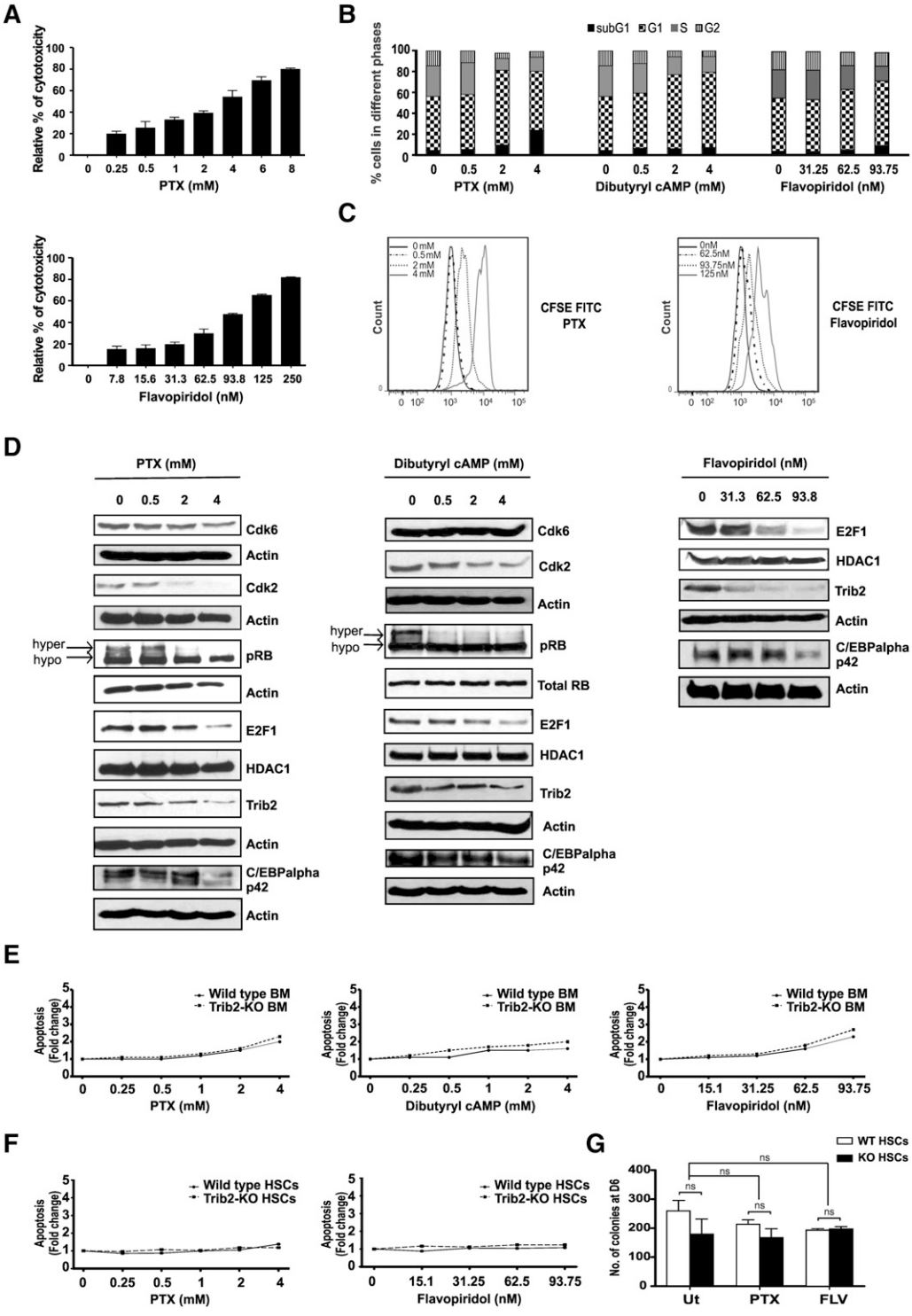

Figure 6. CDK inhibition decreases Trib2 resulting in a block in AML cell proliferation. (A) PTX and flavopiridol dose response of U937 cells assessed by 3-(4,5-dimethylthiazol-2-yl)-2,5-dimethyltetrazolium bromide; 3-[4,5-dimethylthiazol-2-yl]-2,5-diphenyltetrazolium bromide assay at 24 hours. Data are expressed as percentage over untreated control. Values are expressed as mean ± SD (N = 2, performed in triplicate). (B) Cell cycle analysis of PTX, dibutyryl cAMP, and flavopiridol dose response in U937 cells at 24 hours. (C) Cell proliferation of PTX and flavopiridol dose response of U937 cells assessed by CFSE staining 96 hours after treatment. (D) Western blot analysis of protein lysates from U937 cells treated for 24 hours with different concentrations of (left) PTX, (center) dibutyryl cAMP, and (right) flavopiridol. Shown are Cdk6, Cdk2, pRB (phosphor-RB), E2F1, Trib2, and C/EBPα-p42. Actin, total RB, and histone deacetylase 1 (HDAC1) are shown as protein loading controls. (E) WT and Trib2$^{-/-}$ (KO) total bone marrow cells were treated with different concentrations of (left) PTX, (center) dibutyryl cAMP, and (right) flavopiridol and assessed for apoptosis by AnnexinV/DAPI staining. (F) WT and Trib2$^{-/-}$ (KO) HSCs were treated with different concentrations of (left) PTX and (right) flavopiridol and assessed for apoptosis by AnnexinV/DAPI staining. (G) WT and Trib2$^{-/-}$ (KO) HSCs were treated with 2 mM PTX or 62.5 nM of flavopiridol (FLV) for 24 hours and plated in a CFC assay. Data presented are mean ± SD of duplicate cultures.

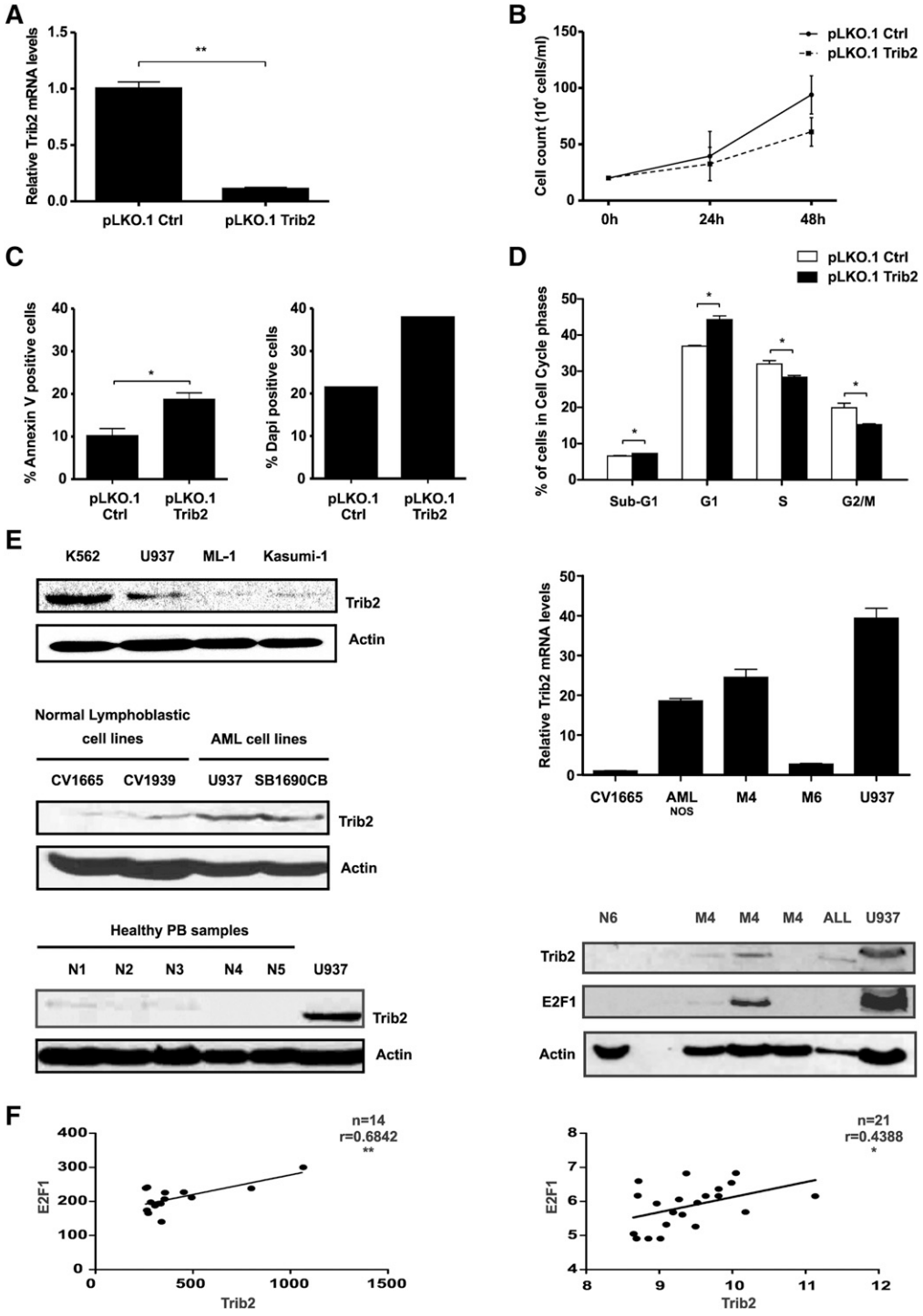

Figure 7. AML cells express high levels of Trib2 protein and correlate with E2F family members mRNA expression. (A) Real-time analysis of Trib2 mRNA levels in U937 cells following transduction with pLKO.1 control (Ctrl) or pLKO.1 Trib2. (B) Cell growth analysis in U937 cells transduced with pLKO.1 ctrl or pLKO.1 Trib2 assessed by trypan blue exclusion. (C) Cell death analysis in U937 transduced with pLKO.1 ctrl or pLKO.1 Trib2 assessed by (left) Annexin V and (right) DAPI staining. (D) Cell cycle analysis in sorted U937 cells transduced with pLKO.1 ctrl or pLKO.1 Trib2. Data presented are mean ± SD of duplicate cultures and representative of 2 independent experiments. (E) Western blot analysis of Trib2 protein expression in (top left) myeloid leukemia lines (K562, U937, ML-1, and Kasumi-1), (middle left) normal cell lines (CV1665 and CV1939), and (bottom left) normal peripheral blood (PB and N1-5). (Top right) Real-time analysis of Trib2 mRNA levels in AML patient samples. (Bottom right) Western blot analysis of Trib2 and E2F1 protein expression in normal PB (N6), AML patient samples (denoted by their subtypes), ALL patient samples, and U937 cells. Actin is shown as a protein loading control. (F) Correlation analysis of Trib2 vs E2F1 in the top 95th and 96th percentiles of patient samples from the dataset GSE1159[34](N = 14) and GSE14468[35] (N = 21). $P < .05$ and correlation coefficient (Pearson r, close to +1) show significant positive correlations.

between Trib2 and C/EBPα (data not shown). Therefore, these data strongly support the role of E2F1-regulated Trib2 expression in AML and its function in the dysregulation of myeloid cell proliferation. Our data support the finding that the perturbation of C/EBPα by Trib2 functions in a positive feedback loop to enhance E2F1-mediated Trib2 expression in AML.

Discussion

Trib2 expression may be differentially regulated depending on the cell type (myeloid or lymphoid, immature or mature), cell context (normal or malignant), and the cell cycle (quiescent or self-renewing or proliferating). Here we described the regulation of Trib2 in normal myeloid and leukemic cells via an E2F1 and C/EBPα feedback mechanism. We demonstrated a correlation between the expression levels of E2F1 and Trib2 in AML cells and showed that E2F1 is recruited to the Trib2 promoter, activating Trib2 expression. E2F1-regulated Trib2 activation was negatively and positively modulated via C/EBPα-p42 and C/EBPα-p30 expression, respectively. We demonstrated the recruitment of C/EBPα-p42 to the Trib2 promoter in normal myeloid cells and the elevation of Trib2 expression in C/EBPα-p30 expressing preleukemic myeloid cells. Our results reveal a positive feedback loop for E2F1, Trib2, and C/EBPα-p30 in AML. Our data suggest that the regulation of Trib2 expression in AML cells is pivotal for AML cell proliferation and survival.

The identification of E2F direct gene targets via consensus and nonconsensus binding sites has been globally assessed using ChIP technologies.[36] Indeed the recruitment of E2F1 to promoters does not always require DNA binding, as other transcription factors have been shown to recruit E2F1, such as nuclear factor-κB, Myc, and C/EBPα.[27] C/EBPα-p30 has been shown to recruit E2F1 to the promoter of PIN1, and increased PIN1 expression was proposed to contribute to the differentiation block in AML.[37] We showed and validated the presence of E2F1 binding sites in the Trib2 promoter. Using site-directed and deletional mutagenesis and EMSA analysis, we conclude that E2F1 binds directly to the Trib2 promoter and is modulated by C/EBPα specifically at site B at −943 bp. We demonstrate the recruitment of C/EBPα to this region in normal GMP cells. Using a ChIP assay, we were unable to distinguish between C/EBPα-p42 and C/EBPα-p30 binding to the Trib2 promoter in normal or preleukemic cells. It has been suggested that C/EBPα-p30 has independent functions of C/EBPα-p42 and that it can target and modulate a unique set of genes in addition to its role as a dominant negative of C/EBPα-p42.[38,39] Given that we have shown that C/EBPα-p30 preleukemic GMP cells have elevated Trib2 expression above that present in normal GMPs, these data support the positive feedback loop that we propose between E2F1, C/EBPα, and Trib2.

The central mechanisms identified for the negative regulation of cell proliferation by C/EBPα are repression of E2F,[22] interference with Cdk2 and Cdk4 function,[40] and p21 stabilization (a Cdk inhibitor).[41] Flavopiridol is a small molecule cyclin-dependent kinase inhibitor that induces cell cycle arrest, apoptosis, and clinical responses in AML patients. Following the inhibition of Cdks, phosphorylation of RB is inhibited, and E2F is released and drives cell cycle arrest and apoptosis. Studies have shown that flavopiridol induces apoptosis in leukemic blasts from patients with poor-risk AML or ALL[42] and represses E2F1 expression in leukemic blasts from patients with refractory AML.[43] PTX has been shown to induce cell cycle arrest and apoptosis of AML and ALL cells[44,45] and has been used in combination therapy for patients with myelodysplastic syndromes and AML.[46,47] Elevated cAMP, as a result of PTX and dibutyryl cAMP treatment, has been shown to target CDK and E2F1 in leukemic cells, leading to cell cycle arrest,[33] apoptosis,[48] and leukemic cell differentiation.[49] Notwithstanding, these drugs also target other pathways, for instance, nuclear factor-κB and antiapoptotic proteins.[44] Therefore, the inhibition of CDK has been shown to induce a number of effects in different subtypes of AML, which all prove to be detrimental to the leukemic cell (differentiation, cell cycle arrest, and apoptosis). The inhibition of CDK activity in high Trib2-expressing AML cells resulted in the arrest of cells in G1 phase of the cell cycle and a subsequent decrease in cell in S phase. Using concentrations of drug that induced minimal apoptosis and a block in proliferation, there was a decrease in E2F1 expression and a subsequent decrease in Trib2 expression, and these effects ultimately led to apoptotic cell death (sub-G1 increase) of the AML cell. The fact that we did not observe any proliferative defect following treatment in nonleukemic WT and Trib2-deficient BM cells corroborates the role of Trib2 in the control of leukemic cell proliferation.

Here we identify a positive regulatory loop controlled by E2F1 that contributes to the aberrant expression of Trib2 in AML cells. Our findings provide a novel link between oncogenic Trib2 function and AML cell proliferation. Whether E2F-mediated regulation of Trib2 occurs also in ALL remains to be investigated and of great interest.

Acknowledgments

The authors thank Prof Kevin Ryan (Beatson Institute for Cancer Research, Glasgow, Scotland) for E2F plasmids and Stefan Meyer (University of Manchester) for cell lines CV1665, CV1939, and SB1690CB. MEFs derived from E2F1-deficient or WT mouse embryos were a kind gift from Dr Lili Yamasaki (Columbia University). The authors thank the technical staff at the Paul O'Gorman Leukaemia Research Centre and at the biological services at the University of Glasgow.

The authors thank the Kay Kendall Foundation (KKL501) and the Howat Foundation for flow cytometry facility funding. K.K. was supported by funds from the Howat Foundation, Children with Cancer United Kingdom, and financial support from Science Foundation Ireland President of Ireland Young Researcher Award and Marie Curie EU-FP7-PEOPLE-IRG. This work was also supported by the Childrens Leukaemia Research Project, Irish Research Council for Science, Engineering and Technology fellowship (to M. Hannon), and Health Research Board (to J.T.). Work in the Porse laboratory was supported by the Danish Cancer Society, the Danish Research Council for Strategic Research, and through a center grant from the NovoNordisk Foundation (The Novo Nordisk Foundation Section for Stem Cell Biology in Human Disease).

Authorship

Contribution: K.K. designed the study; L.R., M.S., M. Hannon, M. Hasemann, A.-K.F., J.C., J.T., C.O., and K.K. performed the research; K.K., L.R., M.S., M. Hannon, M. Hasemann, A.F., and B.P. analyzed the data; B.P. contributed an essential mouse model and reagents; M.R.C. provided access to patient samples; L.R. and M.S. made the figures; K.K. wrote the paper; and K.K., L.R., M.S., B.P., and M. Hasemann revised and edited the paper.

Conflict-of-interest disclosure: The authors declare no competing financial interests.

Correspondence: Karen Keeshan, Paul O'Gorman Leukaemia Research Centre, Institute of Cancer Sciences, University of Glasgow, Glasgow, Scotland; e-mail: Karen.keeshan@glasgow.ac.uk.

References

1. Liang KL, Rishi L, Keeshan K. Tribbles in acute leukemia. *Blood.* 2013;121(21):4265-4270.
2. Dobens LL Jr, Bouyain S. Developmental roles of tribbles protein family members. *Dev Dyn.* 2012; 241(8):1239-1248.
3. Hannon MM, Lohan F, Erbilgin Y, et al. Elevated TRIB2 with NOTCH1 activation in paediatric/adult T-ALL. *Br J Haematol.* 2012;158(5):626-634.
4. Keeshan K, He Y, Wouters BJ, et al. Tribbles homolog 2 inactivates C/EBPalpha and causes acute myelogenous leukemia. *Cancer Cell.* 2006; 10(5):401-411.
5. Wouters BJ, Jordà MA, Keeshan K, et al. Distinct gene expression profiles of acute myeloid/ T-lymphoid leukemia with silenced CEBPA and mutations in NOTCH1. *Blood.* 2007;110(10): 3706-3714.
6. Keeshan K, Bailis W, Dedhia PH, et al. Transformation by Tribbles homolog 2 (Trib2) requires both the Trib2 kinase domain and COP1 binding. *Blood.* 2010;116(23):4948-4957.
7. Nagel S, Venturini L, Przybylski GK, et al. Activation of Paired-homeobox gene PITX1 by del(5)(q31) in T-cell acute lymphoblastic leukemia. *Leuk Lymphoma.* 2011;52(7): 1348-1359.
8. Sanda T, Lawton LN, Barrasa MI, et al. Core transcriptional regulatory circuit controlled by the TAL1 complex in human T cell acute lymphoblastic leukemia. *Cancer Cell.* 2012;22(2): 209-221.
9. Argiropoulos B, Palmqvist L, Yung E, et al. Linkage of Meis1 leukemogenic activity to multiple downstream effectors including Trib2 and Ccl3. *Exp Hematol.* 2008;36(7):845-859.
10. Vaz C, Ahmad HM, Sharma P, et al. Analysis of microRNA transcriptome by deep sequencing of small RNA libraries of peripheral blood. *BMC Genomics.* 2010;11:288.
11. Zheng YS, Zhang H, Zhang XJ, et al. MiR-100 regulates cell differentiation and survival by targeting RBSP3, a phosphatase-like tumor suppressor in acute myeloid leukemia. *Oncogene.* 2012;31(1):80-92.
12. Grosshans J, Wieschaus E. A genetic link between morphogenesis and cell division during formation of the ventral furrow in Drosophila. *Cell.* 2000;101(5):523-531.
13. Mata J, Curado S, Ephrussi A, Rørth P. Tribbles coordinates mitosis and morphogenesis in Drosophila by regulating string/CDC25 proteolysis. *Cell.* 2000;101(5):511-522.
14. Seher TC, Leptin M. Tribbles, a cell-cycle brake that coordinates proliferation and morphogenesis during Drosophila gastrulation. *Curr Biol.* 2000; 10(11):623-629.
15. Price DM, Jin Z, Rabinovitch S, Campbell SD. Ectopic expression of the Drosophila Cdk1 inhibitory kinases, Wee1 and Myt1, interferes with the second mitotic wave and disrupts pattern formation during eye development. *Genetics.* 2002;161(2):721-731.
16. Hegedus Z, Czibula A, Kiss-Toth E. Tribbles: a family of kinase-like proteins with potent signalling regulatory function. *Cell Signal.* 2007; 19(2):238-250.
17. Abdelilah-Seyfried S, Chan YM, Zeng C, et al. A gain-of-function screen for genes that affect the development of the Drosophila adult external sensory organ. *Genetics.* 2000;155(2):733-752.
18. Reckzeh K, Cammenga J. Molecular mechanisms underlying deregulation of C/EBPalpha in acute myeloid leukemia. *Int J Hematol.* 2010;91(4): 557-568.
19. Dedhia PH, Keeshan K, Uljon S, et al. Differential ability of Tribbles family members to promote degradation of C/EBPalpha and induce acute myelogenous leukemia. *Blood.* 2010;116(8): 1321-1328.
20. Pabst T, Mueller BU, Zhang P, et al. Dominant-negative mutations of CEBPA, encoding CCAAT/ enhancer binding protein-alpha (C/EBPalpha), in acute myeloid leukemia. *Nat Genet.* 2001;27(3): 263-270.
21. Lin FT, MacDougald OA, Diehl AM, Lane MD. A 30-kDa alternative translation product of the CCAAT/enhancer binding protein alpha message: transcriptional activator lacking antimitotic activity. *Proc Natl Acad Sci USA.* 1993;90(20):9606-9610.
22. Porse BT, Xu X, Lindberg B, Wewer UM, Friis-Hansen L, Nerlov C; Pedersen TA. E2F repression by C/EBPalpha is required for adipogenesis and granulopoiesis in vivo. *Cell.* 2001;107(2):247-258.
23. Johansen LM, Iwama A, Lodie TA, et al. c-Myc is a critical target for c/EBPalpha in granulopoiesis. *Mol Cell Biol.* 2001;21(11):3789-3806.
24. Porse BT, Bryder D, Theilgaard-Mönch K, et al. Loss of C/EBP alpha cell cycle control increases myeloid progenitor proliferation and transforms the neutrophil granulocyte lineage. *J Exp Med.* 2005;202(1):85-96.
25. Zhang P, Iwasaki-Arai J, Iwasaki H, et al. Enhancement of hematopoietic stem cell repopulating capacity and self-renewal in the absence of the transcription factor C/EBP alpha. *Immunity.* 2004;21(6):853-863.
26. Heath V, Suh HC, Holman M, et al. C/EBPalpha deficiency results in hyperproliferation of hematopoietic progenitor cells and disrupts macrophage development in vitro and in vivo. *Blood.* 2004;104(6):1639-1647.
27. Chen HZ, Tsai SY, Leone G. Emerging roles of E2Fs in cancer: an exit from cell cycle control. *Nat Rev Cancer.* 2009;9(11):785-797.
28. Trikha P, Sharma N, Opavsky R, et al. E2f1-3 are critical for myeloid development. *J Biol Chem.* 2011;286(6):4783-4795.
29. Pulikkan JA, Peramangalam PS, Dengler V, et al. C/EBPα regulated microRNA-34a targets E2F3 during granulopoiesis and is down-regulated in AML with CEBPA mutations. *Blood.* 2010; 116(25):5638-5649.
30. Pulikkan JA, Dengler V, Peramangalam PS, et al. Cell-cycle regulator E2F1 and microRNA-223 comprise an autoregulatory negative feedback loop in acute myeloid leukemia. *Blood.* 2010; 115(9):1768-1778.
31. Kirstetter P, Schuster MB, Bereshchenko O, et al. Modeling of C/EBPalpha mutant acute myeloid leukemia reveals a common expression signature of committed myeloid leukemia-initiating cells. *Cancer Cell.* 2008;13(4):299-310.
32. O'Hare MJ, Hou ST, Morris EJ, et al. Induction and modulation of cerebellar granule neuron death by E2F-1. *J Biol Chem.* 2000;275(33): 25358-25364.
33. Williamson EA, Burgess GS, Eder P, Litz-Jackson S, Boswell HS. Cyclic AMP negatively controls c-myc transcription and G1 cell cycle progression in p210 BCR-ABL transformed cells: inhibitory activity exerted through cyclin D1 and cdk4. *Leukemia.* 1997;11(1):73-85.
34. Valk PJ, Verhaak RG, Beijen MA, et al. Prognostically useful gene-expression profiles in acute myeloid leukemia. *N Engl J Med.* 2004; 350(16):1617-1628.
35. Wouters BJ, Löwenberg B, Erpelinck-Verschueren CA, van Putten WL, Valk PJ, Delwel R. Double CEBPA mutations, but not single CEBPA mutations, define a subgroup of acute myeloid leukemia with a distinctive gene expression profile that is uniquely associated with a favorable outcome. *Blood.* 2009;113(13): 3088-3091.
36. Rabinovich A, Jin VX, Rabinovich R, Xu X, Farnham PJ. E2F in vivo binding specificity: comparison of consensus versus nonconsensus binding sites. *Genome Res.* 2008;18(11): 1763-1777.
37. Pulikkan JA, Dengler V, Peer Zada AA, et al. Elevated PIN1 expression by C/EBPalpha-p30 blocks C/EBPalpha-induced granulocytic differentiation through c-Jun in AML. *Leukemia.* 2010;24(5):914-923.
38. Wang C, Chen X, Wang Y, Gong J, Hu G. C/EBPalphap30 plays transcriptional regulatory roles distinct from C/EBPalphap42. *Cell Res.* 2007;17(4):374-383.
39. Geletu M, Balkhi MY, Peer Zada AA, et al. Target proteins of C/EBPalphap30 in AML: C/EBPalphap30 enhances sumoylation of C/EBPalphap42 via up-regulation of Ubc9. *Blood.* 2007;110(9):3301-3309.
40. Wang H, Iakova P, Wilde M, et al. C/EBPalpha arrests cell proliferation through direct inhibition of Cdk2 and Cdk4. *Mol Cell.* 2001;8(4):817-828.
41. Timchenko NA, Harris TE, Wilde M, et al. CCAAT/ enhancer binding protein alpha regulates p21 protein and hepatocyte proliferation in newborn mice. *Mol Cell Biol.* 1997;17(12):7353-7361.
42. Karp JE, Ross DD, Yang W, et al. Timed sequential therapy of acute leukemia with flavopiridol: in vitro model for a phase I clinical trial. *Clin Cancer Res.* 2003;9(1):307-315.
43. Nelson DM, Joseph B, Hillion J, Segal J, Karp JE, Resar LM. Flavopiridol induces BCL-2 expression and represses oncogenic transcription factors in leukemic blasts from adults with refractory acute myeloid leukemia. *Leuk Lymphoma.* 2011;52(10): 1999-2006.
44. Bravo-Cuellar A, Hernández-Flores G, Lerma-Díaz JM, et al. Pentoxifylline and the proteasome inhibitor MG132 induce apoptosis in human leukemia U937 cells through a decrease in the expression of Bcl-2 and Bcl-XL and phosphorylation of p65. *J Biomed Sci.* 2013;20:13.
45. Ogawa R, Streiff MB, Bugayenko A, Kato GJ. Inhibition of PDE4 phosphodiesterase activity induces growth suppression, apoptosis, glucocorticoid sensitivity, p53, and p21(WAF1/ CIP1) proteins in human acute lymphoblastic leukemia cells. *Blood.* 2002;99(9):3390-3397.
46. Raza A, Qawi H, Lisak L, et al. Patients with myelodysplastic syndromes benefit from palliative therapy with amifostine, pentoxifylline, and ciprofloxacin with or without dexamethasone. *Blood.* 2000;95(5):1580-1587.
47. Erikci AA, Ozturk A, Karagoz B, et al. Results of combination therapy with amifostine, pentoxifylline, ciprofloxacin and dexamethasone in patients with myelodysplastic syndrome and acute myeloid leukemia. *Hematology.* 2008;13(5): 289-292.
48. Huseby S, Gausdal G, Keen TJ, et al. Cyclic AMP induces IPC leukemia cell apoptosis via CRE-and CDK-dependent Bim transcription. *Cell Death Dis.* 2011;2:e237.
49. Copsel S, Garcia C, Diez F, et al. Multidrug resistance protein 4 (MRP4/ABCC4) regulates cAMP cellular levels and controls human leukemia cell proliferation and differentiation. *J Biol Chem.* 2011;286(9):6979-6988.

Supplementary methods, figures and legends

Methods

Cell culture, transfection and siRNA knockdown

RAW 264.7 macrophage cells, NIH3T3 cells, 293T, HeLa, and wild type and E2F1-/- MEFs cells were cultured in DMEM supplemented with 10% FBS. K562 and U937 cells were cultured in RPMI with 10% FBS. K562-C/EBPalpha-p42-ER and K562-C/EBPalpha-p30-ER cell lines were cultured in RPMI (no phenol red) with 10% FBS Charcoal stripped. β-estradiol at a concentration of 5μM was used to induce translocation of the fusion proteins into the nucleus. WT and Trib2$^{-/-}$ bone marrow cells were cultured in DMEM supplemented with 15% FBS, 6ng/ml IL-3, 5ng/ml IL-6, 100ng/ml SCF. Transient transfection of expression plasmids was carried out using Turbofect (Fermentas) or Attractene (Qiagen) transfection reagent according to the manufacturer's instructions. Nucleofection of K562, K562-C/EBPalpha-p42-ER and K562-C/EBPalpha-p30-ER cell lines were carried out using the Amaxa kit for nucleofection and the Nucleofector™ II device (Amaxa) according to manufacturer's instruction. For siRNA transfection, cells were incubated with control siNEG (Scrambled siRNA, AllStar, Qiagen 1027281) or siRNA directed against E2F1 (Validated E2F1 Flexitube siRNA Qiagen, SI02664410, Hs_E2F1_6 FlexiTube siRNA) (Qiagen), Hs_E2F1_9 FlexiTube siRNA) (Qiagen).

Trib2-dependent reporter gene assay

3T3 cells were transfected with luciferase constructs alone (firefly luciferase constructs in pGL3-Basic and the internal control Renilla luciferase plasmid pRL-TK) or in combination with other expression plasmids using Turbofect transfection reagent (Fermentas). 24 hours post-transfection Trib2 firefly luminescence readings were normalised for renilla values and reported relative to a calibrator sample. The two-tailed unpaired t-test was used to assess the significance of data.

Chromatin Immunoprecipitation

For K562 cell line, cells were fixed in 1% formaldehyde for 10min with agitation. Fixation was ceased by adding 1ml of 1.25M glycine and incubating for 5 min with agitation. Cells were pelleted and resuspended in 1ml of lysis buffer (Active Motif) for 30 mins and dounce homogenised to isolate nuclei. Nuclei were pelleted and resuspended in 350μl shearing buffer (Active Motif) and sonicated on ice (K562 cells, 5 pulses, 50% duty cycle and 30% output). Sheared chromatin samples were

centrifuge at 15,000 rpm for 10 min at 4º C. Protein/DNA complexes were immunoprecipitated with indicated antibody, DNA was eluted as per manufacturer's instructions (Active Motif) and column purified (QIAquick Purification Kit, Qiagen). Eluted DNA was subjected to PCR using promoter-specific primer sets (flanking putative E2F1-binding sites in the Trib2 promoter: Forward 5'-GGGGAGACGGGGTGATTGCA-3', Reverse 5'-CGGGCTGGGCGCAGGTA-3', negative control -5kb Trib2 Promoter: Forward 5'-GAGGCTCCGTGGAAAACTCACTTG-3', Reverse 5'-TTCCCAACTCTCAAGCGC TCTGC-3'). The two-tailed unpaired t-test was used to assess the significance of data.

For GMP cells, 500.000 were FACS sorted, fixed and quenched as above for 2 min. Cells were resuspended in lysis buffer (100mM NaCl, 66mM tris-HCl, 5mM EDTA, 0.3% SDS, 1.5% triton X-100) and incubated for 20 min at RT with vortexing every 5 min. Cell lysates were sonicated (30 cycles, 15 s burst, 30 s break) using a bioruptor (Diagenode), and centrifuged for 10 min. Protein/DNA complexes were immunoprecipitated with antibodies for IgG (sc-2027, Santa Cruz) or C/EBPalpha(14-AA, Santa Cruz) and the complexes were treated with RNase A for 30 min at 37°C followed by addition of SDS (0.5%) and proteinase K (0.5 mg/ml) and an additional incubation for 16 hours at 37°C. Finally, chromatin complexes were de-cross-linked by incubation at 65°C for 6 h, phenol-chloroform extracted and precipitated using NaOAc and EtOH supplemented with glycogen. Eluted DNA was subjected to qPCR using primers targeting the C/EBPalpha site in the Trib2 promoter: Forward 5'-AGCTGAGTAGGGAGTGCGCGGAGTA-3' and Reverse 5'-TCATCGGAGGAGGATCTGGGACGT-3'.

Electromobility shift assay (EMSA)

For making nuclear extracts, cells were allowed to swell in buffer A (10 mM HEPES pH 7.9, 10 mM KCl, 0.1 mM EDTA pH 8.0, 0.1 mM EGTA pH 7.0 and protease inhibitors) for 45 min on ice followed by addition of NP-40, sedimenting the nuclei by centrifugation for 1 mint at 10,000 rpm and incubating the nuclear pellet in buffer B (20 mM HEPES pH 7.9, 400 mM NaCl, 1 mM EDTA pH 8.0, 1 mM EGTA pH 7.0 and protease inhibitors) for 30 min on ice and collecting nuclear extract by centrifugation for 5 min at 10,000 rpm at 4°C. EMSAs were performed using LightShift Chemiluminescent EMSA Kit (Thermo Scientific). Briefly, 10 μg of

nuclear extract were incubated with 3'-biotin labeled oligonucleotide in a binding reaction mixture containing 10mM Tris (pH 7.5), 50 mM KCl, 1 mM DTT, 2.5% glycerol, 5 mM $MgCl_2$, 2 ug BSA, 1 ug poly (dI-dC) for 20 min at 37°C. The DNA-protein complexes were resolved on 4.5% nondenaturing polyacrylamide gel in 0.5X Tris borate EDTA at 100 V at 4°C, transferred onto nylon membrane, UV crosslinked followed by the streptavidin detection of biotinylated oligonucleotides. For the cold competition, nuclear extracts in the presence of binding buffer were incubated with 100 fold excess of unlabelled oligonucleotide for 15 min at 37°C. After incubation, labeled oligo was added and proceeded for regular binding reaction.

For supershift assay, nuclear extracts were preincubated with 2μg antibody specific for E2F1 (sc-193X, Santa Cruz) or C/EBPalpha (sc-61X, Santa Cruz) for 30 min at room temperature and thereafter were proceeded for binding with oligonucleotide as described above. The oligonucleotides used for the EMSAs were as follows: E2F1(site A, wild type) 5' – ATGTGTTCTTGGCCTAAATACT -3', E2F1 (siteB, wild type) 5'-CAGGACCCCCGGAAAGCTCCTG- 3', E2F1 (site C, wild type) 5'-GGCTTTGTCGCGGTACCTGT -3', C/EBPalpha (between site E2F1 site B and C, wild type) 5'- TCACCGCCCGCACTTCTTGCTTCATCGGAG -3'. The underlined indicates the putative binding site within murine Trib2 promoter. For mutant, the sequences of putative binding sites were considerably changed as follows and underlined: E2F1 (site A, mutant type) 5'- ATGTGTTTAAAAGGCAAATACT -3', E2F1 (site B, mutant type) 5'-CAGGACCTGGAATTGGCTCCTG-3', E2F1 (site C, mutant type) 5'- GGCTTTGCGCTACTACCTGT -3', C/EBPalpha (between site E2F1 site B and C, mutant type) 5'-TCACCGTGGATTCTTTAAATAATGTCGGAG -3'.

Immunoblotting

Whole cell lysates were prepared using modified radioimmune precipitation assay buffer (50mM Tris, pH 8.0, containing 0.5% NP-40, 0.25% sodium deoxycholate, 150mM NaCl, 1mM EDTA, with protease and phosphatase inhibitors). Cytoplasmic lysates were prepared in ice cold lysis buffer (10 mM HEPES pH 7.9, 10 mM KCl, 0.1 mM EDTA pH 8.0, 0.1 mM EGTA pH 7.0, 1 mM DTT, with protease and phosphatase inhibitors). Nuclear lysates were prepared using ice-cold nuclear extraction buffer (20 mM HEPES pH 7.9, 400 mM NaCl, 1 mM EDTA pH 8.0, 1 mM EGTA pH 7.0, 1 mM DTT, with protease and phosphatase inhibitors). Samples were

resolved on SDS-PAGE gels, transferred to nitrocellulose membrane and analysed by immunoblotting with antibodies against Trib2 (sc-100878, Santa Cruz), E2F1 (sc-193, Santa Cruz), C/EBPalpha (sc-61, Santa Cruz), Actin (A5441, Sigma Aldrich), Cdk6 (sc-177-G, Santa Cruz), Cdk2 (2546, cell signaling), phospho-RB (sc-16670-R, Santa Cruz), RB (9309, cell signaling), HDAC1 (sc-7872, Santa Cruz). Patient protein samples were prepared by direct lysis of the mononuclear cells in 2X SDS sample buffer.

Quantitative Real-Time RT-PCR (qPCR)

RNA was extracted from cells using the RNeasy Mini Kit (Qiagen) and reverse transcribed with SuperScriptIII reverse transcriptase (Invitrogen). qPCR was performed using KAPA SYBR® FAST Universal 2X qPCR Master Mix (Anachem) on a MJ Research Opticon 2 (3200 model). 18S and B-actin was used as internal controls, and relative mRNA expression levels were calculated using the 2 -ΔΔCT method. Primers for human Trib2: Forward 5'- AGCCAGACTGTTCTACCAGA -3', Reverse 5'- GGCGTCTTCCAGGCTTTCCA -3', murine Trib2: Forward 5'- AGCCCGACTGTTCTACCAGA -3', Reverse 5'- AGCGTCTTCCAAACTCTCCA -3'. mRNA expression levels between samples were compared by two-tailed student t-test.

shTrib2 lentiviral and retroviral transduction and qPCR

U937 cells were transduced either with lentiviral constructs (pLKO.1-puro-CMV-TurboGFP or pLKO.1-puro-CMV-TurboGFP-shTrib2, Sigma-Aldrich) or retroviral constructs (LMP control or LMP-shTrib2, (sequence TCCTAATCTCTTCAATCAATAAA) and sorted for GFP expression. Trib2 knockdown was analyzed at mRNA levels by qPCR. Total RNA was extracted using RNeasy Mini Kit (QIAGEN) and reverse transcribed with the High Capacity cDNA Reverse Transcription Kit (Applied Biosystems). qPCR was performed using Fast SYBR® Green Master Mix (Applied Biosystems) on a 7900HT Fast Real-Time PCR System (Applied Biosystems). ABL was used as internal control, and relative mRNA levels were calculated using the 2 -ΔΔCT method. Primers for human Trib2 (forward, 5'- AGCCCGACTGTTCTACCAGA-3'; reverse, 5'- GGCGTCTTCCAGGCTTTCCA-3') and ABL (forward, 5'- TGGAGATAACACTCTAAGCATAACTAAAGGT-3'; reverse, 5'- GATGTAGTTGCTTGGGACCCA-3').

Mice

Trib2$^{-/-}$ (B6;129S5-Trib2tm1Lex) mice were purchased from Lexicon pharmaceuticals, and backcrossed onto C57B6 to F6. The Trib2$^{-/-}$ mice were bred and housed in the University of Glasgow. Cebpa transgenic mice [35] were bred and housed in the University of Copenhagen. Young adult (10-12 weeks old) *Cebpa$^{fl/p30}$;Mx1Cre (n=2) , Cebpa$^{+/+}$;Mx1Cre (n=3)* mice were injected every other day for a total of 3 times with 0.3 mg polyinosinic-polycytidylic acid (pIpC) (Amersham Biosciences). Mice were sacrificed and bone marrow (BM) cells were isolated 3 weeks after first injection. All mice used were female. All mouse work was performed according to national and international guidelines and approved by the local UK and Danish Animal Ethical Committees.

Preparation of GMP cell isolation

The total isolated BM cells were c-Kit enriched using CD117 microbeads and MACS LS separations columns (Miltenyi Biotec) prior to staining with CD41-FITC, CD135-PE, Gr-1-PECy5, B220-PECy5, CD3-PECy5, Ter199-PerCp5.5, CD16/CD32-Alexa Flour 700, c-Kit APC-Alexa 750, CD127-Biotin, Sca1-PB (All eBioscience), Mac1-PECy5 (BD Biosciences), CD105-PECy7 and CD150-APC (BioLegend), Streptavidin-QD655, and 7-AAD (Invitrogen) as viability marker. GMPs (defined as previously described [36]) were sorted on a FACSAria Cytometer (BD Biosciences, San Jose, CA, USA) using FACSDiva software.

Bioinformatic dataset analysis

Gene-expression values for Trib2 versus E2F1 were plotted and the line of best fit calculated using linear regression. Patient samples that showed Trib2 expression in the top 96% percentile of the Valk and Wouters dataset (GSE14468 and GSE1159) were used. Standard P value (significance below 0.05) and Pearson's R values were calculated. A positive and negative R value indicates a positive and negative correlation respectively, and the closer the r-value is to 1 (or -1 in the case of a negative correlation) the stronger the correlation.

Cytotoxic assay

Cells (10^4/100 μl) were seeded in 96-well plates and treated with different concentrations of pentoxifylline (0–8 mM) or flavopiridol (0-250 nM) for 24 h. At the end of the treatment, 10 μl of MTT (3 mg/ml in PBS) was added to each well and cells were further incubated for 3 h. Formazan crystals formed were dissolved in

100 µl of solubilizing solution (10% sodium dodecyl sulphate- 0.01N HCl). The absorbance of solubilized formazan was read at 570 nm using ELISA reader (Molecular devices).

CFSE proliferation assay

U937 cells were harvested, washed in PBS-2%FBS and stained with 1µM carboxyfluorescein diacetate succinimidyl ester (CFSE) (Molecular Probes) for 10 min at 37^0C. The staining was quenched with ice cold PBS containing 20% FBS. Residual CFSE was removed by washing with PBS-2%FBS. CFSE-labeled cells were then seeded in 24-well plate, treated with different concentrations of Pentoxifylline, Dibutyryl cAMP or flavopiridol and grown for 96 hours in cell culture medium. The CFSE fluorescence intensity was measured by flow cytometry using a BD FACS Canto^{TM} II.

Cell cycle analysis

Cells treated with different concentrations of PTX, Dibutyryl cAMP, flavopiridol or transduced with pLKO.1-puro-CMV-TurboGFP or pLKO.1-puro-CMV-TurboGFP-shTrib2 were harvested, washed in ice-cold PBS, fixed in 70% ethanol. Cells were stained with PI/ RNase staining buffer (BD Pharmingen) for 15 min at room temperature and analyzed at BD FACS Canto^{TM} II. The populations of cells in various phases of cell cycle were quantified using the FlowJo program.

Annexin V/DAPI staining

Total bone marrow cells, HSCs (Lin^- c-kit^+ $Sca1^+$) isolated from wild type or Trib2-deficient mice and GFP sorted U937 cells were suspended in binding buffer (containing annexin V-PE (BD Biosciences) and DAPI (Sigma). Thereafter, the samples were incubated in the dark for 15 min at room temperature and then analyzed at BD FACS Canto^{TM} II.

CFC (Colony forming cell) assay

Total bone marrow cells, HSCs (Lin^- c-kit^+ $Sca1^+$) were sorted from total wild type or Trib2 –deficient mice bone marrow and treated with 2mM PTX or 62.5nM of flavopiridol for 24 h. Cells were then seeded in duplicate in methylcellulose media (Methocult M3434; Stem Cell Technologies). Colonies with >50 cells were scored and assessed at D6.

Statistical Analysis

All statistics were performed using GRAPHPAD PRISM5.

Supplementary Figures and Legends

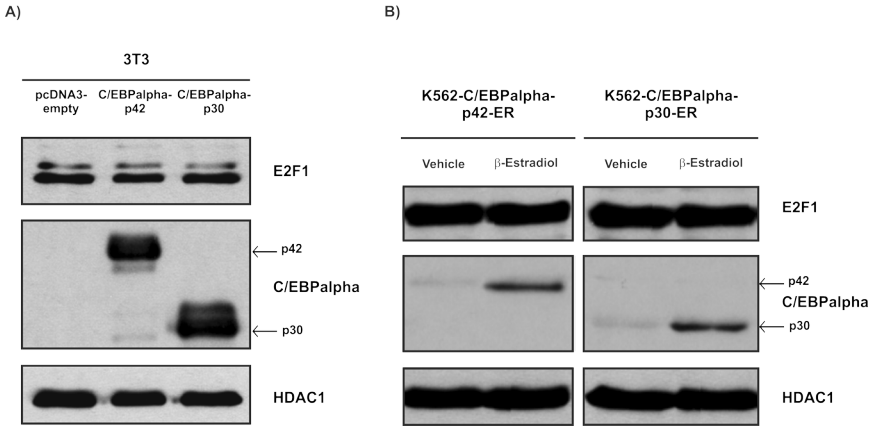

Figure S1. Western blot analysis for E2F1 and C/EBPalpha in nuclear extracts prepared from (A) 3T3 cells transfected with pcDNA empty, C/EBPalpha-p42 or C/EBPalpha-p30 and (B) K562-C/EBPalpha-p42-ER or K562-C/EBPalpha-p30-ER cells induced with β-estradiol or vehicle control for 24 hours. HDAC1 is shown as protein loading control.

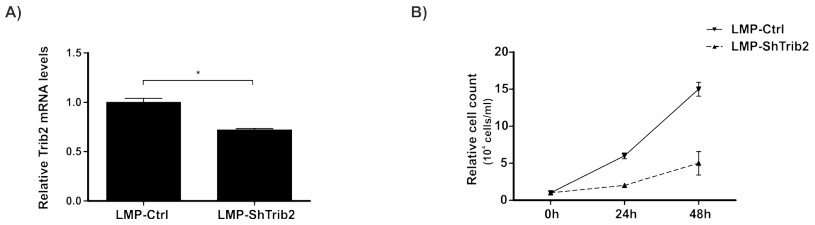

Figure S2. A) Real Time analysis of Trib2 mRNA levels in U937 cells following transduction with LMP-control (Ctrl) or LMP-shTrib2. B) Cell growth analysis in U937 cells transduced with LMP-Ctrl or LMP-shTrib2 assessed by trypan blue exclusion and normalized to GFP values.

Appendix F PDF of "TRIB2 and the ubiquitin proteasome system in cancer"

TRIB2 and the ubiquitin proteasome system in cancer

Mara Salomè*, Joana Campos* and Karen Keeshan*[1]
*Paul O'Gorman Leukaemia Research Centre, Institute of Cancer Sciences, University of Glasgow, Glasgow, G12 0ZD, Scotland

Abstract

Tribbles family of pseudokinase proteins are known to mediate the degradation of target proteins in *Drosophila* and mammalian systems. The main protein proteolysis pathway in eukaryotic cells is the ubiquitin proteasome system (UPS). The tribbles homolog 2 (TRIB2) mammalian family member has been well characterized for its role in murine and human leukaemia, lung and liver cancer. One of the most characterized substrates for TRIB2-mediated degradation is the myeloid transcription factor CCAAT enhancer binding protein α (C/EBPα). However, across a number of cancers, the molecular interactions that take place between TRIB2 and factors involved in the UPS are varied and have differential downstream effects. This review summarizes our current knowledge of these interactions and how this information is important for our understanding of TRIB2 in cancer.

TRIB2 gene dysregulation in cancer

Tribbles homolog 2 (TRIB2) is a pseudokinase that functions as a molecular adaptor mediating degradation and changes to signalling cascades [1]. *TRIB2* is also shown to be a potent oncogene in a variety of malignancies, including myeloid [2] and lymphoid [3] leukaemia, melanoma [4], lung cancer [5], and liver cancer [6]. The oncogenic activity of *TRIB2* is linked to its dysregulated expression, rather than its dysregulation via mutation in the majority of cancers. We analysed *TRIB2* gene in the catalogue of somatic mutations in cancer (COSMIC) database (http://cancer.sanger.ac.uk, [7]), the most comprehensive source of curated analysed somatic mutations in human cancer to date. This analysis has allowed us determine whether *TRIB2* is altered at the genomic level across a panel of tumour samples identified by the tissue of origin. From a total number of 23,983 unique tumour samples, 86 were found with missense (51%), synonymous (46%), nonsense (2%) and inframe deletion (1%) mutations in *TRIB2* (Figure 1A). Interestingly, although the overall point mutation rate is low, tumours with documented roles for TRIB2 oncogene such as malignant melanoma and lung cancer do have detectable TRIB2 point mutations. In tissues matching acute myeloid leukaemia (AML), which has a very strong association with TRIB2 oncogenic activity, no mutations were retrieved from COSMIC curated data provided by scientific literature and resequencing results from the Cancer Genome Project at the Wellcome Trust Sanger Institute (1/1942 haematopoietic and lymphoid tissue samples identified with a TRIB2 mutation corresponded to a multiple myeloma patient sample). Indeed no mutations have been found in ~75 AML samples analysed by exome sequencing with good coverage across all exons (Ross Levine, personal communication). Interrogation of other genomic alterations affecting TRIB2 in the COSMIC database identified subsets of tumour tissues with *TRIB2* overexpressed (Figure 1B). Overall the frequency rate for these alterations is higher and includes lung, skin, liver and haematopoietic and lymphoid tissues samples. Of note, 4/9 samples overexpressing *TRIB2* in the haematopoietic and lymphoid tissues matched AML samples. Given that there is strong evidence for *TRIB2* oncogenic function in these tumours, these analyses suggest that elevated *TRIB2* expression has potential implications in other tumour tissue contexts yet to be explored e.g. endometrium (endometrioid carcinoma), central nervous system (astrocytoma grade V), prostate and large intestine samples (both matching adenocarcinoma). Other *TRIB2* gene alterations include copy number variation (CNV), which albeit rare, are found across different tumours tissues and mainly associated with increased copy number (all except for breast, thyroid and kidney which showed CNV loss) (Figure 1C). Hypermethylation, associated with chromatin silencing, was found exclusively in prostate and large intestine tumour tissues (Figure 1D). Together these analyses suggest that *TRIB2* oncogenic activity is related to its elevated gene expression rather than associated with different genomic alterations or mutations.

It is important to understand how *TRIB2* gene expression is regulated given its elevated expression in cancer. *TRIB2* gene expression has been shown to be regulated by a number of genes in normal and malignant haematopoietic cells, including NOTCH1 [8], MEIS1 [9], E2F1 and C/EBPα [10], GATA2 and FOG1 [11], PITX1 [12] and TAL1/E

Key words: cancer, leukaemia, TRIB2, ubiquitin proteasome.
Abbreviations: AML, acute myeloid leukaemia; ATF4, activating transcription factor 4; CNV, copy number variation; COP1, constitutive photomorphogenesis 1; COSMIC, catalogue of somatic mutations in cancer; DUBs, deubiquitinases; PI, proteasome inhibitors; SCF, SKP1–CUL1 (Cullin)–F-box; SMURF1, Smad ubiquitination regulatory factor 1; TRIB2, tribbles homolog 2; UPS, ubiquitin proteasome system; YAP, Yes-associated protein.
[1]To whom correspondence should be addressed (email Karen.keeshan@glasgow.ac.uk).

Figure 1 | Genomic alterations in *TRIB2* gene

(**A**) Histogram presentation of point mutations in *TRIB2* gene in tumour samples using the COSMIC database (top). Pie chart referring to the frequency of missense (51%), synonymous (46%), nonsense (2%) and deletion inframe (1%) point mutations in the identified tumour samples (bottom). (**B**) Histogram presentation of gain of *TRIB2* gene expression in the tumour samples indicated. Among them 4/9 haematopoietic and lymphoid tissues samples match AML as part of the acute myeloid leukaemia study (COSU377) from The Cancer Genome Atlas [TCGA] in which over expression is defined after a *z*-score > 2. (**C**) Histogram displaying tumour tissues where CNV of the *TRIB2* gene was identified, with the respective frequency in tumour samples. (**D**) Histogram presenting tumour tissues where hypermethylation of the *TRIB2* gene locus was identified and respective frequency. Data were retrieved by v72 of COSMIC database (http://www.sanger.ac.uk) and only tissues displaying *TRIB2* alterations are shown. NS*, not specified with histology matching malignant melanoma; NS, not specified.

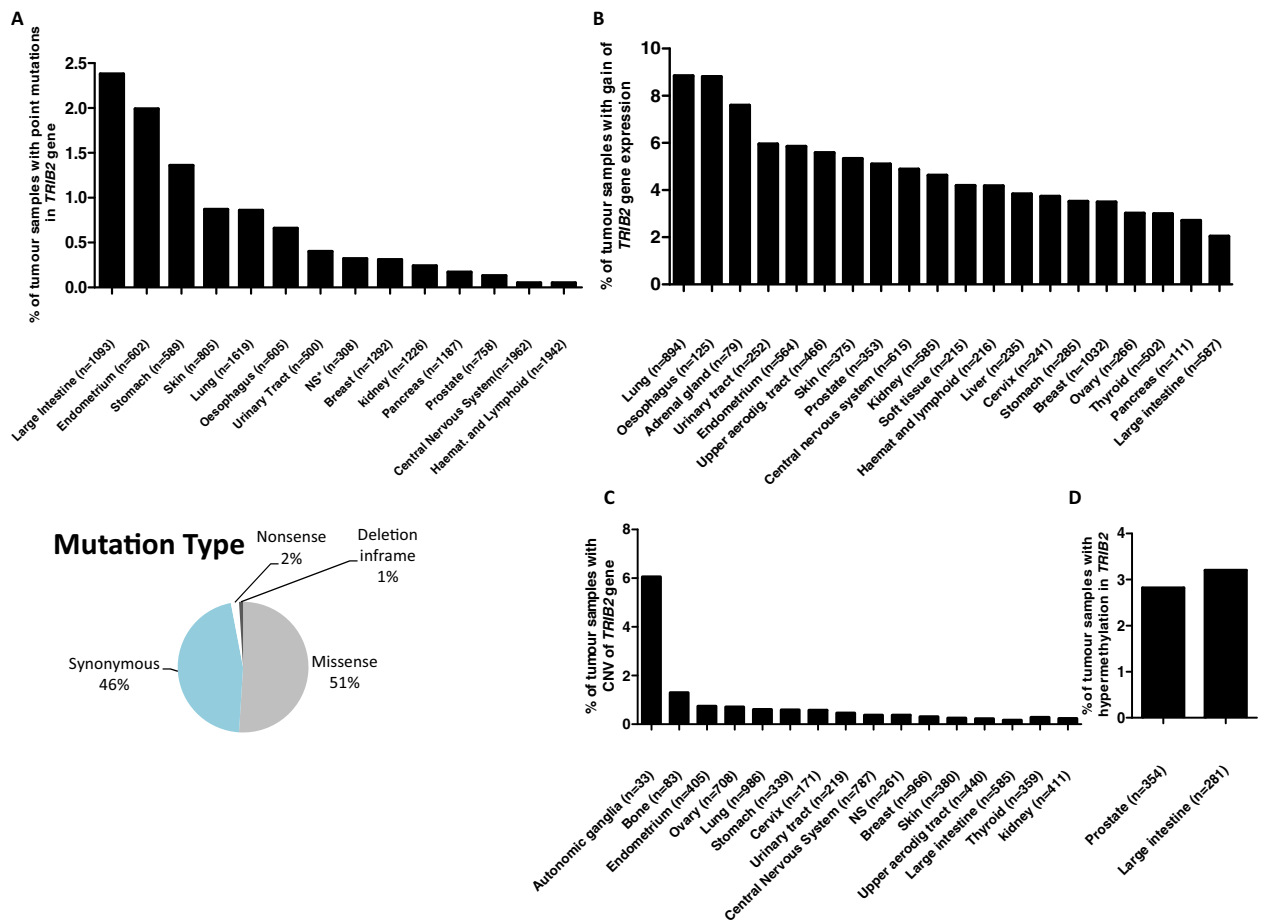

protein complex [3]. A number of microRNAs also regulate the expression levels of *TRIB2*, including but not limited to miR-511, miR-1297 [13], miR-99 [14,15], miR-155 [16], and let-7 [17]. An example of how *TRIB2* expression is regulated in AML has been shown where E2F1 cooperates with the C/EBPα p30 oncogenic isoform to activate the *TRIB2* promoter in AML cells. Indeed, wild type C/EBPα p42 is bound to the TRIB2 promoter in normal granulocyte macrophage progenitor (GMP) cells. This study detailed the feedback loop between TRIB2, C/EBPα p42 and p30, and E2F1 that contributes to AML cell growth and survival [10]. The central mechanism of TRIB2-induced AML identified in this study is based on specific TRIB2-C/EBPα interactions, with C/EBPα being a key substrate of TRIB2 induced proteasomal degradation. The proteasomal mediated degradation of TRIB substrates and interaction with proteins of the ubiquitin proteasome system (UPS) are central to TRIB function in a number of cancers and will be discussed further.

TRIB2: the ruler of E3 ubiquitin ligase activities

The degradation of damaged or no longer necessary proteins is mainly regulated by the UPS. The targets of this pathway are marked by the addition of a ubiquitin tag. Ubiquitin is a short peptide covalently bound to a lysine (Lys) residue

on the target. This complex protein modification requires the activity of at least three enzymes: an E1 ubiquitin activating enzyme, an E2 ubiquitin conjugating enzyme and an E3 ubiquitin ligase. The E3 ligase family comprise over 1000 enzymes with different substrate specificities. Moreover homologous ubiquitin like proteins (UBL) and deubiquitinases (DUBs), which hydrolyse ubiquitin moieties, represent additional layers of regulation for the proteolysis of specific targets [18]. In addition to the 26S proteasome complex, an immunoproteasome complex is present in cells of haematopoietic origin and potentially relates to the higher sensitivity of proteasome inhibition in leukaemic cells [19].

The first connections between TRIB and protein degradation functions were identified in drosophila, where drosophila tribbles was shown to promote degradation of its targets; string (homologous of the mammalian CDC25 phosphatase, positive regulator of cell cycle progression) and slow border cells (Slbo) (promoter of cell migration and homologous of the human C/EBPα) [20]. The members of the C/EBP family of transcription factors are involved in regulation of differentiation in many tissues and control proliferation through interaction with cell cycle proteins. In the haematopoietic system C/EBPα acts as a tumour suppressor that promotes cell cycle arrest and induces granulocytic differentiation through inhibition of E2F activity [21,22]. Both mammalian TRIB1 and TRIB2 have been shown to retain the degradative functions towards the C/EBPα protein and promote C/EBPα p42 degradation and this function underlies their oncogenic potential in leukaemia [2,23,24]. Moreover, TRIB2-dependent C/EBPα p42 degradation is mediated by the proteasome and constitutive photomorphogenesis 1 (COP1). COP1 is an E3 ubiquitin ligase recruited by TRIB2 for the interaction with C/EBPα, suggesting TRIB2 functions as a scaffold protein to colocalize the enzyme with its target [25]. The COP1 binding site in the C-terminus is conserved among the TRIB family of proteins and indeed COP1 is the E3 ligase responsible for TRIB1-mediated degradation of C/EBPα [23] and TRIB3-mediated degradation of acetyl-coenzyme A carboxylase (ACC) in fasting condition [26]. TRIB2 also regulates C/EBPα protein levels in liver cells, and mediates C/EBPα degradation in lung cancer models [5,6]. In the latter case, the E3 ligase TRIM21 was identified to function in TRIB2-mediated C/EBPα degradation. With regard to specific TRIB2 substrates, another member of the C/EBP family, C/EBPβ, has been shown to be degraded by TRIB2 in adipogenesis. In this study, TRIB2 functions as a negative regulator of adipogenesis associated with Akt inhibition [27]. Another example of TRIB-dependent degradation of target proteins in cancer is represented by activating transcription factor 4 (ATF4) which occurs during hypoxia in human tumour cells overexpressing TRIB3 [28]. Interestingly, the murine ortholog of TRIB3 Neuronal cell death-inducible putative kinase (NIPK) has also been associated with down-regulation of ATF4 transcriptional activity, but in absence of proteolytic degradation [29]. The protein interaction of ATF4 with TRIB2 or TRIB1 as not been reported.

Cell context, especially with regard to protein–protein interactions is highly relevant in deciphering the function of many signalling molecules, including TRIB proteins. TRIB2 has been implicated as a positive or negative mediator of proteasomal degradation. For example, TRIB2 interacts with the substrate binding subunit of the ubiquitin complex SKP1–CUL1 (Cullin)–F-box (SCF) βTrCP in liver cancer cells [6]. This complex is responsible for Yes-associated protein (YAP) degradation, but TRIB2 binding on βTrCP subunit leads to YAP stabilization and transactivation of YAP target genes. The C-terminal domain of TRIB2 was shown to be responsible for the interaction with βTrCP in these liver cancer cells. Noteworthy in the same study, TRIB2 also targets C/EBPα for degradation, but this was not via βTrCP E3 ligase. As described above, COP1 or TRIM21 are known to mediate TRIB2 dependent C/EBPα degradation in AML and lung cancer, whereas the E3 ligase has not been clarified in liver cells. TRIB2 and the E3 ligase Smad ubiquitination regulatory factor 1 (SMURF1) also interact in liver cancer cells. SMURF1 is the enzyme responsible for TRIB2 ubiquitination and proteasomal dependent degradation and SMURF1 inhibition triggers TRIB2-dependent carcinogenesis in the liver [30]. Nonetheless, TRIB2 is also a partner of SMURF1 in the inhibition of the Wnt signalling effector β-catenin and TCF4. Indeed, deletion of the SMURF1 binding sites on the TRIB2 protein abolished its ability to down-regulate β-catenin and transcription factor 4 (TCF4) [31]. COP1 or βTrCP were also described as additional modulators in this same pathway [32]. Together these data reveal the complexity of TRIB2 and UPS interactions in liver cancer cells, and highlight the importance of cell context in TRIB family protein function.

UPS aberration in leukaemia

Dysregulation of E3 ligase enzymatic activity has been reported in different malignancies. Transforming mutant variants of the E3 ubiquitin ligase Casitas B-lineage lymphoma proto-oncogene (cClb) have been found in human myeloid malignancies and all these mutations were associated with loss of E3 ubiquitin ligase activity in addition to a malignant gain of function [33]. Mutations in the E3 ligase FBW7 have been associated with oncogenic signalling mechanisms in different cancers including NOTCH1 activation in T-ALL [34]. Moreover, the recent profiling of the somatic mutation landscape of epigenetic regulators in paediatric cancer identified the deubiquitinase USP7 as one of the most frequent mutations in T-ALL [35]. This DUB is associated with chromatin remodelling and it is referred as an ‘eraser’ among epigenetic modifiers. Its physiological function is to stabilize the histone H2B (as well as other targets), removing ubiquitin subunits from the substrates. In 8% of T-ALL cases sequence variation translates to loss of function of the protein and the consequent epigenetic alteration is associated with the leukaemic disease [35]. This case supports the important role of ubiquitination signalling beyond terminal protein degradation in leukaemic transformation. The proteolytic

pathways of UPS and autophagy in AML cell lines are directly involved in the response to chemotherapeutic drugs cytarabine and doxorubicin. Studies show that the response to chemotherapy is highly dependent on the basal level of activation of the UPS in leukaemic cells [36]. It is possible to measure the proteasome expression and activities in the plasma of AML, ALL and MDS patient samples and higher levels of UPS protein and activities are detectable in patients plasma samples [37]. Importantly, the levels of proteasome activities can be used to risk stratify for the prognosis of different blood tumours. Since it is likely that the activities detected in the AML patients' plasma is reflecting the activities in the leukaemic cells, screening of the proteasome activities in the plasma samples from patients could be advantageous not only as a biomarker, but also to identify the most suitable therapeutic combination taking advantage of the new drugs available in clinical trials targeting the UPS system.

Targeting UPS in blood tumours

Proteasome inhibitors

Leukaemic cells express high levels of proteasomes [38] and this is probably one of the reasons why therapeutic proteasome inhibition has shown better results in blood cancers than in solid tumours [39]. Multiple toxicity mechanisms of proteasome inhibition have been validated in preclinical studies. These comprise NFkB inhibition through stabilization of its regulator IkBα; cell cycle arrest due to deregulation of cyclins and other cell cycle regulator proteins; induction of a proapoptotic state through stabilization of p53 and Bax and down-regulation of Bcl-2; ROS production; transmembrane mitochondrial potential gradient dissipation; aggresome formation; endoplasmic reticulum (ER) and unfolded protein response (UPR) [40].

Eight classes of proteasome inhibitors (PI) have been recognized across natural compounds and synthetic molecules (peptide aldehydes, peptide vinyl sulfones, syrbactins, peptide boronates, peptide $\alpha'\beta'$-epoxyketones, peptide ketoaldehydes, β-lactones, and oxatiazol-2-ones). Only representative members of some classes have reached the stage of clinical trials investigations in cancer. Many have failed due to lack of specificity and or toxicity in preclinical studies. The main PIs of interest in the treatment of haematological malignancies include three peptide boronates, two peptide epoxyketones and one marine natural product, β-lactone. The boronate compound Bortezomib (BTZ) is a reversible inhibitor of the proteasome and the immunoproteasome and the first PI ever entered in clinical trials [41]. BTZ is currently approved for use as single agent or in combination therapies in multiple myeloma or mantle cell lymphoma patients. Moreover a number of clinical trials have been assessing its efficacy in aggressive disease like acute leukaemias (CALGB (Alliance) Study 10502, COG AAML 1031) [42]. To overcome toxicity and resistance challenges with BTZ, a great effort has been spent in the design and characterization of next generation inhibitors. Among them Carfilzomib has been approved by the FDA for the treatment of relapsed/refractory multiple myeloma [43], and Oprozomib, Ixazomib, Marizomib and Delanzomib have already reached clinical trials investigation. The activity of immunoproteasome specific inhibitors is also currently being assessed in preclinical investigation in models of immunological disorders [41].

Other UPS targets

The recent interest in targeting the UPS system has brought attention to the identification of druggable targets upstream of the proteasome, which by their nature are predicted to lead to more specific inhibition and fewer side effects. In this category there are E1 activating enzyme inhibitors, E2 conjugating enzyme inhibitors, E3 ubiquitin ligases inhibitors and DUB enzyme inhibitors [44]. Indeed the inhibition of the UBL modifier Nedd8 is currently in clinical trials for AML and MDS [45]. More than one E3 ligases have been chosen as potential targets in the drug discovery process for treatment of haematological malignancies and many small molecules have been studied. Examples among the most targeted E3 ligases are MDM2, involved in p53 regulation [46], and SCF multi-subunit E3 ligases [47].

Concluding remarks and future perspective

Given that C/EBPα stability is tightly regulated at molecular level and that TRIB2 mediated dysregulation of this pathway is linked to AML, liver and lung carcinogenesis, targeting the related network of E3 ligases could open new exciting therapeutic windows, resulting in a more specific and possibly more effective treatment of these malignancies. There is an urgent need for alternative therapeutic strategies in the treatment of blood diseases. Increasing interest has been raised around the modulation of proteolytic pathways such as autophagy and UPS, which often play critical roles in cancer cells. TRIB2, as a signalling pathway modulator and binding partner of different E3 ubiquitin ligase enzymes has gained attention over the past decade as a major regulator in solid tumours and different leukaemia subtypes. TRIB2 has been proposed as a valid biomarker for diagnosis and progression of melanoma, correlating higher TRIB2 expression levels with advanced stages of the disease [48]. Given the strong preclinical data regarding TRIB2 in AML, the screening of TRIB2 protein expression in leukaemia patients would be extremely useful to complement the current information available on TRIB2 carcinogenesis and mutational profile.

Acknowledgements

We wish to thank the members of the Keeshan lab for thoughtful discussion and proofreading. We thank the Biochemical society for travel bursaries to attend the independent meeting Tribbles Pseudokinases on the Crossroads of Metabolism, Cancer, Immunity and Development, in Budapest. We also thank the Organising Committee for covering the registration fees.

Funding

KK and JC were supported by the Howat Foundation and Children with Cancer UK. MS was supported by Friends of Paul O'Gorman Leukaemia Research Centre.

References

1 Lohan, F. and Keeshan, K. (2013) The functionally diverse roles of tribbles. Biochem. Soc. Trans. **41**, 1096–1100 CrossRef PubMed
2 Keeshan, K., He, Y., Wouters, B.J., Shestova, O., Xu, L., Sai, H., Rodriguez, C.G., Maillard, I., Tobias, J.W., Valk, P. et al. (2006) Tribbles homolog 2 inactivates C/EBPalpha and causes acute myelogenous leukemia. Cancer Cell **10**, 401–411 CrossRef PubMed
3 Sanda, T., Lawton, L.N., Barrasa, M.I., Fan, Z.P., Kohlhammer, H., Gutierrez, A., Ma, W., Tatarek, J., Ahn, Y., Kelliher, M.A. et al. (2012) Core transcriptional regulatory circuit controlled by the TAL1 complex in human T cell acute lymphoblastic leukemia. Cancer Cell **22**, 209–221 CrossRef PubMed
4 Zanella, F., Renner, O., Garcia, B., Callejas, S., Dopazo, A., Peregrina, S., Carnero, A. and Link, W. (2010) Human TRIB2 is a repressor of FOXO that contributes to the malignant phenotype of melanoma cells. Oncogene **29**, 2973–2982 CrossRef PubMed
5 Grandinetti, K.B., Stevens, T.A., Ha, S., Salamone, R.J., Walker, J.R., Zhang, J., Agarwalla, S., Tenen, D.G., Peters, E.C. and Reddy, V.A. (2011) Overexpression of TRIB2 in human lung cancers contributes to tumorigenesis through downregulation of C/EBPα. Oncogene **30**, 3328–3335 CrossRef PubMed
6 Wang, J., Park, J.S., Wei, Y., Rajurkar, M., Cotton, J.L., Fan, Q., Lewis, B.C., Ji, H. and Mao, J. (2013) TRIB2 acts downstream of Wnt/TCF in liver cancer cells to regulate YAP and C/EBPα function. Mol. Cell **51**, 1–15 CrossRef PubMed
7 Forbes, S.A., Beare, D., Gunasekaran, P., Leung, K., Bindal, N., Boutselakis, H., Ding, M., Bamford, S., Cole, C., Ward, S. et al. (2015) COSMIC: exploring the world's knowledge of somatic mutations in human cancer. Nucleic Acids Res. **43**, D805–D811 CrossRef PubMed
8 Wouters, B.J., Jordà, M.A., Keeshan, K., Louwers, I., Erpelinck-Verschueren, C.A.J., Tielemans, D., Langerak, A.W., He, Y., Yashiro-Ohtani, Y., Zhang, P. et al. (2007) Distinct gene expression profiles of acute myeloid/T-lymphoid leukemia with silenced CEBPA and mutations in NOTCH1. Blood **110**, 3706–3714 CrossRef PubMed
9 Argiropoulos, B., Palmqvist, L., Yung, E., Kuchenbauer, F., Heuser, M., Sly, L.M., Wan, A., Krystal, G. and Humphries, R.K. (2008) Linkage of Meis1 leukemogenic activity to multiple downstream effectors including Trib2 and Ccl3. Exp. Hematol. **36**, 845–859 CrossRef PubMed
10 Rishi, L., Hannon, M., Salome, M., Hasemann, M., Frank, A.K., Campos, J., Timoney, J., O'Connor, C., Cahill, M.R., Porse, B. et al. (2014) Regulation of Trib2 by an E2F1-C/EBPalpha feedback loop in AML cell proliferation. Blood **123**, 2389–2400 CrossRef PubMed
11 Mancini, E., Sanjuan-Pla, A., Luciani, L., Moore, S., Grover, A., Zay, A., Rasmussen, K.D., Luc, S., Bilbao, D., Carroll, D.O.A. et al. (2012) FOG-1 and GATA-1 act sequentially to specify definitive megakaryocytic and erythroid progenitors. EMBO J. **31**, 351–365 CrossRef PubMed
12 Nagel, S., Venturini, L., Przybylski, G.K., Grabarczyk, P., Schneider, B., Meyer, C., Kaufmann, M., Schmidt, C.A., Scherr, M., Drexler, H.G. et al. (2011) Activation of paired-homeobox gene PITX1 by del(5)(q31) in T-cell acute lymphoblastic leukemia. Leuk. Lymph. **52**, 1348–1359 CrossRef
13 Zhang, C., Chi, Y.L., Wang, P.Y., Wang, Y.Q., Zhang, Y.X., Deng, J., Lv, C.J. and Xie, S.Y. (2012) miR-511 and miR-1297 inhibit human lung adenocarcinoma cell proliferation by targeting oncogene TRIB2. PLoS ONE **7**, e46090–e46090 CrossRef PubMed
14 Zhang, L., Li, X., Ke, Z., Huang, L., Liang, Y., Wu, J., Zhang, X., Chen, Y., Zhang, H. and Luo, X. (2013) MiR-99a may serve as a potential oncogene in pediatric myeloid leukemia. Cancer Cell. Int. **13**, 110 CrossRef PubMed
15 Xin, J.-X., Yue, Z., Zhang, S., Jiang, Z.-H., Wang, P.Y., Li, Y.-J., Pang, M. and Xie, S.Y. (2013) miR-99 inhibits cervical carcinoma cell proliferation by targeting TRIB2. Oncol. Lett. **6**, 1025–1030 PubMed
16 Palma, C.A., Al Sheikha, D., Lim, T.K., Bryant, A., Vu, T.T., Jayaswal, V. and Ma, D.D. (2014) MicroRNA-155 as an inducer of apoptosis and cell differentiation in Acute Myeloid Leukaemia. Mol. Cancer **13**, 79 CrossRef PubMed
17 Wang, P.Y., Sun, Y.X., Zhang, S., Pang, M., Zhang, H.-H., Gao, S.-Y., Zhang, C., Lv, C.J. and Xie, S.Y. (2013) Let-7c inhibits A549 cell proliferation through oncogenic TRIB2 related factors. FEBS Lett. **587**, 2675–2681 CrossRef PubMed
18 Komander, D. (2009) The emerging complexity of protein ubiquitination. Biochem. Soc. Trans. **37**, 937–953 CrossRef PubMed
19 Niewerth, D., Franke, N.E., Jansen, G., Assaraf, Y.G., van Meerloo, J., Kirk, C.J., Degenhardt, J., Anderl, J., Schimmer, A.D., Zweegman, S. et al. (2013) Higher ratio immune versus constitutive proteasome level as novel indicator of sensitivity of pediatric acute leukemia cells to proteasome inhibitors. Haematologica **98**, 1896–1904 CrossRef PubMed
20 Dobens, Jr, L.L. and Bouyain, S. (2012) Developmental roles of tribbles protein family members. Dev. Dyn. **241**, 1239–1248 CrossRef PubMed
21 Keeshan, K., Santilli, G., Corradini, F., Perrotti, D. and Calabretta, B. (2003) Transcription activation function of C/EBPalpha is required for induction of granulocytic differentiation. Blood **102**, 1267–1275 CrossRef PubMed
22 Porse, B.T. (2005) Loss of C/EBPα cell cycle control increases myeloid progenitor proliferation and transforms the neutrophil granulocyte lineage. J. Exp. Med. **202**, 85–96 CrossRef PubMed
23 Dedhia, P.H., Keeshan, K., Uljon, S., Xu, L., Vega, M.E., Shestova, O., Zaks-Zilberman, M., Romany, C., Blacklow, S.C. and Pear, W.S. (2010) Differential ability of tribbles family members to promote degradation of C/EBP and induce acute myelogenous leukemia. Blood **116**, 1321–1328 CrossRef PubMed
24 Yokoyama, T., Kanno, Y., Yamazaki, Y., Takahara, T., Miyata, S. and Nakamura, T. (2010) Trib1 links the MEK1/ERK pathway in myeloid leukemogenesis. Blood **116**, 2768–2775 CrossRef PubMed
25 Keeshan, K., Bailis, W., Dedhia, P.H., Vega, M.E., Shestova, O., Xu, L., Toscano, K., Uljon, S.N., Blacklow, S. C. and Pear, W.S. (2010) Transformation by tribbles homolog 2 (Trib2) requires both the Trib2 kinase domain and COP1 binding. Blood **116**, 4948–4957 CrossRef PubMed
26 Qi, L., Heredia, J.E., Altarejos, J.Y., Screaton, R., Goebel, N., Niessen, S., Macleod, I.X., Liew, C.W., Kulkarni, R.N., Bain, J. et al. (2006) TRB3 links the E3 ubiquitin ligase COP1 to lipid metabolism. Science **312**, 1763–1766 CrossRef PubMed
27 Naiki, T., Saijou, E., Miyaoka, Y., Sekine, K. and Miyajima, A. (2007) TRB2, a mouse tribbles ortholog, suppresses adipocyte differentiation by inhibiting AKT and C/EBPbeta. J. Biol. Chem. **282**, 24075–24082 CrossRef PubMed
28 Bowers, A.J., Scully, S. and Boylan, J.F. (2003) SKIP3, a novel *Drosophila* tribbles ortholog, is overexpressed in human tumors and is regulated by hypoxia. Oncogene **22**, 2823–2835 CrossRef PubMed
29 Örd, D. and Örd, T. (2003) Mouse NIPK interacts with ATF4 and affects its transcriptional activity. Exp. Cell Res. **286**, 308–320 CrossRef PubMed
30 Wang, J., Zhang, Y., Weng, W., Qiao, Y., Ma, L., Xiao, W., Yu, Y., Pan, Q. and Sun, F. (2013) Impaired phosphorylation and ubiquitination by P70 S6 kinase (P70S6K) and Smad ubiquitination regulatory factor 1 (Smurf1) promotes tribbles homolog 2 (TRIB2) stability and carcinogenic property in liver cancer. J. Biol. Chem. **288**, 33667–33681 CrossRef PubMed
31 Xu, S., Tong, M., Huang, J., Zhang, Y., Qiao, Y., Weng, W., Liu, W., Wang, J. and Sun, F. (2014) TRIB2 inhibits Wnt/beta-Catenin/TCF4 signaling through its associated ubiquitin E3 ligases, beta-TrCP, COP1 and Smurf1, in liver cancer cells. FEBS Lett **588**, 4334–4341 CrossRef PubMed
32 Qiao, Y., Zhang, Y. and Wang, J. (2013) Ubiquitin E3 ligase SCF(β-TRCP) regulates TRIB2 stability in liver cancer cells. Biochem. Biophys. Res. Commun. **441**, 555–559 CrossRef PubMed
33 Kales, S.C., Ryan, P.E., Nau, M. M. and Lipkowitz, S. (2010) Cbl and human myeloid neoplasms: the Cbl oncogene comes of age. Cancer Res. **70**, 4789–4794 CrossRef PubMed
34 Thompson, B.J., Buonamici, S., Sulis, M.L., Palomero, T., Vilimas, T., Basso, G., Ferrando, A. and Aifantis, I. (2007) The SCFFBW7 ubiquitin ligase complex as a tumor suppressor in T cell leukemia. J. Exp. Med. **204**, 1825–1835 CrossRef PubMed
35 Huether, R., Dong, L., Chen, X., Wu, G., Parker, M., Wei, L., Ma, J., Edmonson, M.N., Hedlund, E.K., Rusch, M.C. et al. (2014) The landscape of somatic mutations in epigenetic regulators across 1,000 paediatric cancer genomes. Nat. Commun. **5**, 3630 CrossRef PubMed
36 Fernandes, A., Azevedo, M.M., Pereira, O., Sampaio-Marques, B., Paiva, A., Correia-Neves, M., Castro, I. and Ludovico, P. (2014) Proteolytic systems and AMP-activated protein kinase are critical targets of acute myeloid leukemia therapeutic approaches. Oncotarget 1–13, in press PubMed

37 Ma, W., Kantarjian, H., Zhang, X., Wang, X., Estrov, Z., O'Brien, S. and Albitar, M. (2011) Ubiquitin-proteasome system profiling in acute leukemias and its clinical relevance. Leuk. Res. **35**, 526–533 CrossRef PubMed
38 Kumatori, A., Tanaka, K., Inamura, N., Sone, S., Ogura, T., Matsumoto, T., Tachikawa, T., Shin, S. and Ichihara, A. (1990) Abnormally high expression of proteasomes in human leukemic cells. Proc. Natl. Acad. Sci. U.S.A. **87**, 7071–7075 CrossRef PubMed
39 Orlowski, R.Z. and Kuhn, D.J. (2008) Proteasome inhibitors in cancer therapy: lessons from the first decade. Clin. Cancer Res. **14**, 1649–1657 CrossRef PubMed
40 Nencioni, A., Grünebach, F., Patrone, F., Ballestrero, A. and Brossart, P. (2007) Proteasome inhibitors: antitumor effects and beyond. Leukemia **21**, 30–36 CrossRef PubMed
41 Niewerth, D., Jansen, G., Assaraf, Y.G., Zweegman, S., Kaspers, G.J. L. and Cloos, J. (2015) Molecular basis of resistance to proteasome inhibitors in hematological malignancies. Drug Resist. Updat. **18**, 18–35 CrossRef PubMed
42 Attar, E.C., Johnson, J.L., Amrein, P.C., Lozanski, G., Wadleigh, M., DeAngelo, D.J., Kolitz, J.E., Powell, B.L., Voorhees, P., Wang, E.S. et al. (2013) Bortezomib added to daunorubicin and cytarabine during induction therapy and to intermediate-dose cytarabine for consolidation in patients with previously untreated acute myeloid leukemia age 60 to 75 years: CALGB (Alliance) Study 10502. J. Clin. Oncol. **31**, 923–929 CrossRef PubMed
43 Katsnelson, A. (2012) Next-generation proteasome inhibitor approved in multiple myeloma. Nat. Biotechnol. **30**, 1011–1012 CrossRef PubMed
44 Crawford, L.J. and Irvine, A.E. (2013) Targeting the ubiquitin proteasome system in haematological malignancies. Blood Rev. **27**, 297–304 CrossRef PubMed
45 Swords, R.T., Erba, H.P., DeAngelo, D.J., Bixby, D.L., Altman, J.K., Maris, M., Hua, Z., Blakemore, S.J., Faessel, H., Sedarati, F. et al. (2015) Pevonedistat (MLN4924), a First-in-Class NEDD8-activating enzyme inhibitor, in patients with acute myeloid leukaemia and myelodysplastic syndromes: a phase 1 study. Br. J. Haematol. **169**, 534–543 CrossRef PubMed
46 Zhao, Y., Aguilar, A., Bernard, D. and Wang, S. (2015) Small-molecule inhibitors of the MDM2-p53 protein–protein interaction (MDM2 inhibitors) in clinical trials for cancer treatment. J. Med. Chem. **58**, 1038–1052 CrossRef PubMed
47 Chan, C.H., Morrow, J.K., Li, C.F., Gao, Y., Jin, G., Moten, A., Stagg, L.J., Ladbury, J.E., Cai, Z., Xu, D. et al. (2013) Pharmacological inactivation of Skp2 SCF ubiquitin ligase restricts cancer stem cell traits and cancer progression. Cell **154**, 556–568 CrossRef PubMed
48 Hill, R., Kalathur, R.K.R., Colaco, L., Brandao, R., Ugurel, S., Futschik, M. and Link, W. (2015) TRIB2 as a biomarker for diagnosis and progression of melanoma. Carcinogenesis **36**, 469–477 CrossRef PubMed

Received 6 May 2015
doi:10.1042/BST20150103

Appendix G PDF of "The presence of C/EBPα and its degradation are both required for TRIB2-mediated leukaemia"

Oncogene (2016), 1–10

www.nature.com/onc

ORIGINAL ARTICLE

The presence of C/EBPα and its degradation are both required for TRIB2-mediated leukaemia

C O'Connor[1], F Lohan[1], J Campos[1], E Ohlsson[2,3,4], M Salomè[1], C Forde[5], R Artschwager[6], RM Liskamp[6], MR Cahill[7], PA Kiely[8], B Porse[2,3,4] and K Keeshan[1]

C/EBPα (p42 and p30 isoforms) is commonly dysregulated in cancer via the action of oncogenes, and specifically in acute myeloid leukaemia (AML) by mutation. Elevated TRIB2 leads to the degradation of C/EBPα p42, leaving p30 intact in AML. Whether this relationship is a cooperative event in AML transformation is not known and the molecular mechanism involved remains elusive. Using mouse genetics, our data reveal that in the complete absence of C/EBPα, TRIB2 was unable to induce AML. Only in the presence of C/EBPα p42 and p30, were TRIB2 and p30 able to cooperate to decrease the latency of disease. We demonstrate that the molecular mechanism involved in the degradation of C/EBPα p42 requires site-specific direct interaction between TRIB2 and C/EBPα p42 for the K48-specific ubiquitin-dependent proteasomal degradation of C/EBPα p42. This interaction and ubiquitination is dependent on a critical C terminal lysine residue on C/EBPα. We show effective targeting of this pathway pharmacologically using proteasome inhibitors in TRIB2-positive AML cells. Together, our data show that excess p30 cooperated with TRIB2 only in the presence of p42 to accelerate AML, and the direct interaction and degradation of C/EBPα p42 is required for TRIB2-mediated AML.

Oncogene advance online publication, 21 March 2016; doi:10.1038/onc.2016.66

INTRODUCTION

The C/EBPα (CCAAT/enhancer binding protein α) transcription factor is commonly mutated in acute myeloid leukaemia (AML) and dysregulated in a number of cancers (that is, liver, prostate, lung, squamous cell carcinoma). Mutations in CEBPA occur exclusively in haematological diseases and result in perturbed C/EBPα protein expression and function. C/EBPα promoter methylation perturbs C/EBPα expression in AML,[1] chronic myeloid leukaemia[2] and head and neck squamous cell carcinoma.[3] In AML, oncogene-mediated dysregulation of C/EBPα mRNA expression and/or protein activity occurs in cytogenetically abnormal subtypes of AML, including AMLs with t(8;21)[AML1-ETO], inv(16)[CBFb-MYH11], t(15;17)[PML-RARA] and t(3;21)(AML-1-MDS-1-Evi-1 fusion protein) translocations, and in cytogenetically normal AMLs with FLT3-ITD mutation, or with elevated TRIB2 expression.[4] C/EBPα protein is also dysregulated by a number of posttranslational modifications including phosphorylation, sumoylation and ubiquitination.[5]

CEBPA is an intronless gene with N terminal transcriptional activation domains and a C terminal basic region leucine zipper (LZ) domain. CEBPA mutations, which occur across the entire coding region, are present in 5% and 10% of childhood and adult AML, respectively.[6] Somatic and inherited mutations in CEBPA co-occur, are often biallelic and are found with higher frequency in cytogenetically normal AML.[7,8] CEBPA is a favourable prognosis factor in AML, specifically for cases that present with double mutations in CEBPA, typically an N terminal and a C terminal basic region LZ gene mutation. C/EBPα protein exists as two isoforms, a full length C/EBPα p42 isoform classified as a tumour suppressor and an N terminally truncated p30 isoform classified as an oncogene. N terminal mutations typically are frame-shift mutations that lead to a premature stop in translation of p42, while retaining p30 expression. In contrast, C terminal mutations typically are in-frame insertions/deletions in the LZ domain that disrupt DNA binding or dimerization. C/EBPα functions by forming stable homodimers and heterodimers with itself and other C/EBP family members, which act to stabilize their protein expression.[9]

TRIB2 is a potent oncogene capable of inducing fully penetrant AML in murine models, and can cooperate with other AML oncogenes to disrupt signalling pathways and transcription factors in AML disease.[10–13] TRIB2 expression was shown to be elevated in a cohort of AML patients with a mixed myeloid/lymphoid phenotype and a dysregulated CEBPA gene expression signature. In fact, TRIB2 leads to the degradation of C/EBPα p42 via E3 ligase COP1 binding whilst sparing p30 from degradation, resulting in disturbed granulopoiesis. This modulation of C/EBPα was found to be critical for the induction of AML *in vivo*.[10,13] E2F1 cooperates with C/EBPα p30 to activate the Trib2 promoter in preleukaemic cells resulting in elevated TRIB2 expression. This was shown to be an important mechanism regulating TRIB2 expression and survival of AML cells.[12]

In normal cells, C/EBPα is a key transcription factor in the transition from the pre-granulocyte macrophage to the granulocyte-macrophage progenitor stage of differentiation, and in the transcriptional and epigenetic control of haematopoietic stem cell (HSC) self-renewal.[14–16] In granulocyte-macrophage progenitor cells, C/EBPα p42 is found bound to the Trib2 promoter

[1]Paul O'Gorman Leukaemia Research Centre, Institute of Cancer Sciences, University of Glasgow, Glasgow, UK; [2]The Finsen Laboratory, Rigshospitalet, Faculty of Health Sciences, University of Copenhagen, Copenhagen, Denmark; [3]Biotech Research and Innovation Center (BRIC), University of Copenhagen, Copenhagen, Denmark; [4]Danish Stem Cell Centre (DanStem) Faculty of Health Sciences, University of Copenhagen, Copenhagen, Denmark; [5]University College Cork, Cork, Ireland; [6]School of Chemistry, University of Glasgow, Glasgow, UK; [7]Department of Haematology, Cork University Hospital, Cork, Ireland and [8]Department of Life Sciences, Materials and Surface Science Institute and Stokes Institute, University of Limerick, Limerick, Ireland. Correspondence: Dr K Keeshan, Paul O'Gorman Leukaemia Research Centre, Institute of Cancer Sciences, University of Glasgow, 21 Shelley Road, Glasgow G12 0XB, UK.
E-mail: Karen.keeshan@glasgow.ac.uk
Received 1 April 2015; revised 6 October 2015; accepted 8 January 2016

and inhibits E2F1-mediated activation of Trib2. At the HSC stage, C/EBPα acts to prime HSCs for differentiation along the myeloid lineage via DNA binding to regulatory regions of genes induced during differentiation.[16] Although conditional *Cebpa* knockout mice do not develop disease, the loss of *Cebpa* in adult HSCs leads to an increased number of functional and proliferative HSCs[15,17] and loss of HSC pool maintenance in serial transplantations.[16] *Cebpa* expression is required for AML disease initiation by the oncogene MLL-ENL but not for disease maintenance.[18] In contrast, *Cebpa* is required for the maintenance of Hoxa9/Meis1 AML disease.[19] Loss of *Cebpa* did not abrogate BCR/ABL-induced leukaemia but it did alter the resultant disease phenotype.[20] Thus, it appears that a certain threshold of C/EBPα expression is important for the development of myeloid leukaemic disease. This is supported by the observation that leukaemia-derived CEBPA mutations are virtually never null mutations.[21,22] The combination of N and C terminal mutations have distinct features that result in leukaemia development.[23,24] Murine knockin studies investigating p30 oncogenicity in the absence of C/EBPα p42 showed that p30 induced fully penetrant transplantable AML.[25] p30 is sufficient for haematopoietic commitment to the myeloid lineage, it enables transition from the common myeloid progenitor to the granulocyte-macrophage progenitor stage. However, it does not retain the ability to control proliferation and myeloid progenitors have greatly increased self-renewal capacities.[25]

Although TRIB2 disrupts the ratio of C/EBPα p42:p30 and functions to degrade C/EBPα, it is unclear whether the loss of C/EBPα p42 or the expression of C/EBPα p30 is critical for TRIB2-mediated AML disease. Here, we show using mouse genetics that the presence of C/EBPα is paradoxically required for TRIB2-induced AML, and only in the presence of C/EBPα p42, is there a cooperative effect seen with TRIB2 and C/EBPα p30. We dissect the molecular details of the degradative relationship between TRIB2 and C/EBPα p42, and show that the direct interaction between TRIB2 and C/EBPα p42 is required for TRIB2-mediated ubiquitin-dependent proteasomal degradation of C/EBPα p42. We identify lysine 313 of C/EBPα as a site of TRIB2-mediated ubiquitination. We show that we can target TRIB2 AML cells with proteasome inhibition. Together, these data show that C/EBPα presence is required for the initiation of TRIB2-induced AML and subsequent C/EBPα p42/p30 disruption is critical for TRIB2 AML disease.

RESULTS

C/EBPα p42 accelerates AML in the presence of TRIB2 and excess p30

To establish whether C/EBPα is essential for TRIB2-induced AML, we performed a bone marrow (BM) transplant using a previously described conditional *Cebpa*$^{fl/fl}$*; Mx1Cre* mouse model and used polyinosinic-polycytidylic acid (pIpC) to facilitate ablation of *Cebpa* #x003B1; in the haematopoietic compartment. Two weeks post deletion, c-Kit$^+$ haematopoietic stem and progenitor cells from the BM of pIpC-treated control *Cebpa*$^{fl/fl}$ and *Cebpa*$^{\Delta/\Delta}$ animals were transduced with either empty MigR1 or MigR1-TRIB2 retrovirus. Transduced cells were transplanted into irradiated recipients, and monitored for disease progression. As expected, all mice reconstituted with *Cebpa*$^{fl/fl}$ cells expressing TRIB2 developed lethal AML with a median latency of 33 weeks, accompanied by accumulation of GFP$^+$ cells (mean fraction of *Cebpa*$^{fl/fl}$ GFP-expressing cells 93% +/− 5.2%) in the BM and splenomegaly (data not shown). In striking contrast, TRIB2-transduced *Cebpa*$^{\Delta/\Delta}$ haematopoietic stem and progenitor cells did not give rise to AML (Figure 1a and Supplementary Figure 1B). Notably, 14 months after transplantation, CD45.2$^+$GFP$^+$ cells were detected suggesting that the TRIB2-expressing *Cebpa*$^{\Delta/\Delta}$ cells are able to properly home to the BM but do not give rise to leukaemia. Therefore, although TRIB2 functions to degrade C/EBPα p42 leading to AML,[10] the complete absence of C/EBPα abrogates TRIB2 oncogenicity. Thus, it appears that a certain threshold of C/EBPα (p42 or p30) expression is necessary for the initiation of TRIB2 AML.

Having established the necessity of C/EBPα expression for TRIB2 AML, we next sought to elucidate whether p42 degradation or p30 accumulation is the key driver of this pathway, and whether p30 can cooperate with TRIB2 to accelerate disease onset. To investigate this, we designed a transplant model which utilized donor cells from an established *Cebpa* conditional knockout model that only expressed p30 isoform (referred to here as *Cebpa*$^{\Delta/p30}$), or were heterozygous for this allele still expressing p42 on one allele (referred to as *Cebpa*$^{fl/p30}$ cells) (see methods and Figure 1b). CD45.2$^+$ donor cells from pIpC-treated 8–14-week-old *Cebpa*$^{fl/+}$*, Cebpa*$^{fl/p30}$ *and Cebpa*$^{fl/p30}$*; Mx1Cre* mice were harvested 2 weeks post deletion, transduced with MigR1 or MigR1-TRIB2 retrovirus and transplanted into CD45.1$^+$ recipients. CD45.2 and GFP expression were monitored at 7 weeks post transplant in peripheral blood (Supplementary Figures 1C and D) and every 2 weeks thereafter, showing recipient reconstitution with donor cells. The cohort of mice transplanted with TRIB2-transduced *Cebpa*$^{fl/+}$ cells developed AML disease as previously published[10] with a median latency of 49 weeks. However, mice transplanted with TRIB2-transduced *Cebpa*$^{fl/p30}$ cells developed a much more aggressive AML with an accelerated latency of 29 weeks (Figure 1c) as evidenced by accumulation of GFP$^+$ cells in the BM, elevated white blood cell counts and splenomegaly (Supplementary Figures 1E-J). Mice transplanted with MigR1 transduced *Cebpa*$^{\Delta/p30}$ cells developed AML with a median latency of 40 weeks, as expected and previously published for *Cebpa*$^{L/L}$ mice[25]('L' refers to p30), and no significant acceleration of the disease was seen in mice transplanted with TRIB2 transduced *Cebpa*$^{\Delta/p30}$ cells (median latency of 35 weeks) (Figure 1d). Comparing TRIB2 AML in *Cebpa*$^{fl/p30}$ and *Cebpa*$^{\Delta/p30}$ cohorts, p42 accelerated AML in the presence of TRIB2 and excess p30 (Figure 1e). Control cohorts of mice transplanted with *Cebpa*$^{fl/p30}$ and *Cebpa*$^{fl/+}$ cells transduced with MigR1 as expected did not develop any disease. Flow cytometry analysis showed that mice in both of these groups had normal haematopoietic compartments (Supplementary Figures 1E-I). Flow cytometry analysis revealed that the leukaemic profile of GFP$^+$ *Cebpa*$^{fl/+}$-TRIB2, *Cebpa*$^{fl/p30}$-TRIB2, *Cebpa*$^{\Delta/p30}$-TRIB2 and *Cebpa*$^{\Delta/p30}$-MigR1 AML cells was predominantly c-Kit$^+$ (Figure 1f). Protein analysis of the leukaemic BM cells between the GFP$^+$ *Cebpa*$^{fl/+}$-TRIB2, *Cebpa*$^{fl/p30}$-TRIB2, *Cebpa*$^{\Delta/p30}$-TRIB2 and *Cebpa*$^{\Delta/p30}$-MigR1 AML cells groups verified expected p42 and p30 expression levels in mice (leukaemic ratio p42:p30 in *Cebpa*$^{fl/+}$-TRIB2 cohort, p42 and increased p30 in *Cebpa*$^{fl/p30}$-TRIB2 and *Cebpa*$^{fl/p30}$-MigR1 cohort, comparable p30 in the absence of p42 in *Cebpa*$^{\Delta/p30}$-MigR1 and *Cebpa*$^{\Delta/p30}$-TRIB2 cohorts (Figure 1g)). Taken together, these data show that despite TRIB2 functioning to degrade p42, C/EBPα is essential for the initiation of TRIB2-mediated AML and only in the presence of C/EBPα p42 is there a cooperative effect seen with p30.

Identification of specific amino acids involved in the TRIB2 and C/EBPα interaction

Having shown the requirement for C/EBPα p42 in the initiation of TRIB2-induced AML, we next focused on the interaction between C/EBPα and TRIB2. We first determined using subcellular fractionation and confocal microscopy that the co-localization of TRIB2-C/EBPα was nuclear (Supplementary Figures 2A and B). Using GST pull-down experiments, we show that the C terminal LZ domain of C/EBPα is required for the interaction with TRIB2 as a GZ mutant expressing an unrelated LZ could no longer bind TRIB2. However, TRIB2 can still bind a C/EBPα LZ mutant (L12V) that can no longer dimerize, indicating TRIB2 binding to C/EBPα is

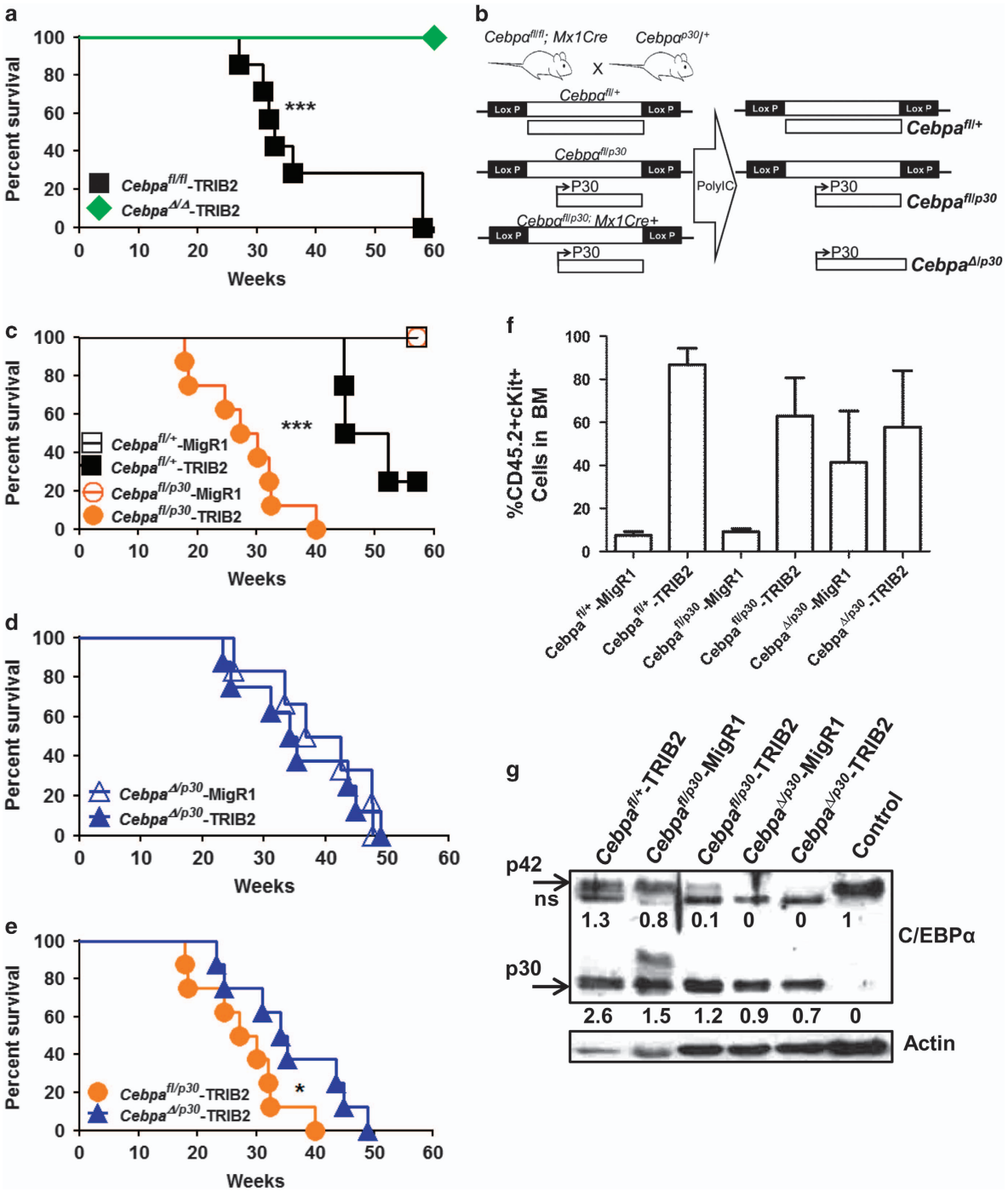

Figure 1. C/EBPα p42 accelerates AML in the presence of TRIB2 and excess p30. (**a**) Kaplan–Meier survival curve of mice reconstituted with either *Cebpa*$^{fl/fl}$ or *Cebpa*$^{\Delta/\Delta}$ BM cells transduced with TRIB2-expressing retrovirus. The median survival of mice reconstituted with *Cebpa*$^{fl/fl}$-TRIB2 cells was 33 weeks ($n = 12$), none of the mice reconstituted with *Cebpa*$^{\Delta/\Delta}$-TRIB2 cells developed leukaemia within 60 weeks ($n = 10$). ***$P < 0.0001$ by Log-rank test. (**b**) Schematic representation of *Cebpa* alleles. (**c**) Kaplan–Meier survival curve of mice reconstituted with either *Cebpa*$^{fl/+}$ or *Cebpa*$^{fl/p30}$ BM cells transduced with MigR1- or TRIB2-expressing retrovirus. None of the mice reconstituted with *Cebpa*$^{fl/+}$-MigR1 ($n = 9$) or *Cebpa*$^{fl/p30}$-MigR1 ($n = 6$) developed leukaemia within 60 weeks. The median survival of mice reconstituted with *Cebpa*$^{fl/+}$-TRIB2 cells was 49 weeks ($n = 4$), while the median survival of mice reconstituted with *Cebpa*$^{fl/p30}$-TRIB2 was 29 weeks ($n = 8$). ***$P < 0.0001$ by Log-rank test. (**d**) Kaplan–Meier survival curve of mice reconstituted with *Cebpa*$^{\Delta/p30}$ BM cells transduced with MigR1- or TRIB2-expressing retrovirus. The median survival of mice reconstituted with *Cebpa*$^{\Delta/p30}$-MigR1 cells was 40 weeks ($n = 6$), while the median survival of mice reconstituted with *Cebpa*$^{\Delta/p30}$-TRIB2 cells was 35 weeks ($n = 8$). $P = 0.8111$ by Log-Rank test. (**e**) Kaplan–Meier survival curve comparing mice reconstituted with *Cebpa*$^{fl/p30}$-TRIB2 or *Cebpa*$^{\Delta/p30}$-TRIB2 BM cells. *$P \leqslant 0.05$ by Log-rank test. (**f**) Average percentage of c-Kit expression in CD45.2+ BM of each group +/− s.d. (**g**) Protein analysis of C/EBPαp42 and p30 expression in BM of mice. n.s. = non-specific band.

independent of amino acids involved in C/EBPα dimerization (Supplementary Figures 2C, D and E). To more precisely identify specific regions of interaction with TRIB2, we SPOT-synthesized a peptide array containing a series of 18-amino acid overlapping peptides identical to the C terminus LZ domain of C/EBPα. GST-TRIB2 bound to eight peptides within the C terminus LZ of C/EBPα (Figure 2a). To identify the specific amino acids required for the interaction, we used a Specific Alanine Scanning Substitution Array, where consecutive amino acids of the parent peptides were substituted to an alanine. This identified residues R333, R339 and R343 of C/EBPα as potential mediators of interaction with TRIB2 (Figure 2b). Using site-directed mutagenesis, we show that mutation of R339A abolished the interaction with GST-TRIB2 in a pull-down assay (Figure 2c). This was confirmed by co-immunoprecipitation in mammalian cells (Supplementary Figure 2F) indicating that R339 of C/EBPα is required for interaction with TRIB2.

Reciprocally, we used TRIB2 peptide arrays that covered the entire TRIB2 protein to identify specific amino acids in TRIB2 responsible for the interaction with C/EBPα. Recombinant C/EBPα protein bound to peptides that spanned from amino acids 25–318 indicating extensive interaction of C/EBPα with TRIB2 (Figure 3a). Specific Alanine Scanning Substitution Array of amino acids in peptide 2 (DHVFRAVLHSHGEELVCK) identified R77, which is homologous to R107 in TRIB1 that exists as a gain-of-function TRIB1 mutation in AML.[26] Specific Alanine Scanning Substitution Array of amino acids in peptide 4 (PEILNTSGSYSGKAADVW) identified a putative GSK3 phosphorylation site (which has the consensus GSK3 phosphorylation site motif S/TXXXS/T). Specific Alanine Scanning Substitution Array of peptide 5 (HPWFSTDFSVSNSGFGAK) identified K322 (Figure 3b). Three mutants R77A, S227A/S229A/S231A/K233A (4-AA) and K322A were generated (Figure 3c). Co-immunoprecipitation showed that mutation of the sequence S227A/S229A/S231A/K233A (4-AA) abolished the interaction with C/EBPα completely, and K322A and R77A although reduced could still bind C/EBPα (Figure 3d and Supplementary Figure 2G).

Ubiquitin-mediated mechanism of TRIB2-induced p42 degradation

We next assessed the ability of TRIB2 to induce ubiquitin-specific degradation of C/EBPα. A ubiquitination assay was performed in 293 T cells transfected with C/EBPα, TRIB2 and Ubiquitin (Ub). Increased C/EBPα ubiquitination was observed in TRIB2-expressing cells compared with controls and this was exclusively K48-mediated ubiquitination (proteasome degradation K48-specific polychains as opposed to non-degradative ubiquitination mediated by K63 polychains) as detected by K48- and K63-specific antibodies (Figure 4a). This was confirmed using ubiquitin mutants, which do not express the K48 ubiquitin polychain (UB/K48R-HA) and the K63 ubiquitin polychain (UB/K63R-HA) in a ubiquitination assay (Figure 4b, compare lanes 7, 8 and 9). We show using the R339A C/EBPα-binding mutant that the direct binding between TRIB2 and C/EBPα was required for TRIB2-mediated ubiquitination of C/EBPα compared with the control mutant R343A that retains the TRIB2 interaction (Figure 4c). Reciprocally, using the TRIB2-binding mutant S227A/S229A/S231A/K233A (4-AA) revealed a loss in C/EBPα ubiquitination as compared with the mutants R77A and K322A that retain higher C/EBPα-binding affinity or WT TRIB2 (Figure 4d). Together these data show that the direct binding interaction between TRIB2 and C/EBPα was required for TRIB2-mediated ubiquitination of C/EBPα.

To investigate the site on C/EBPα susceptible to TRIB2-mediated ubiquitination, Ubpred online software analysis of C/EBPα was performed, and it identified a number of lysine residues as

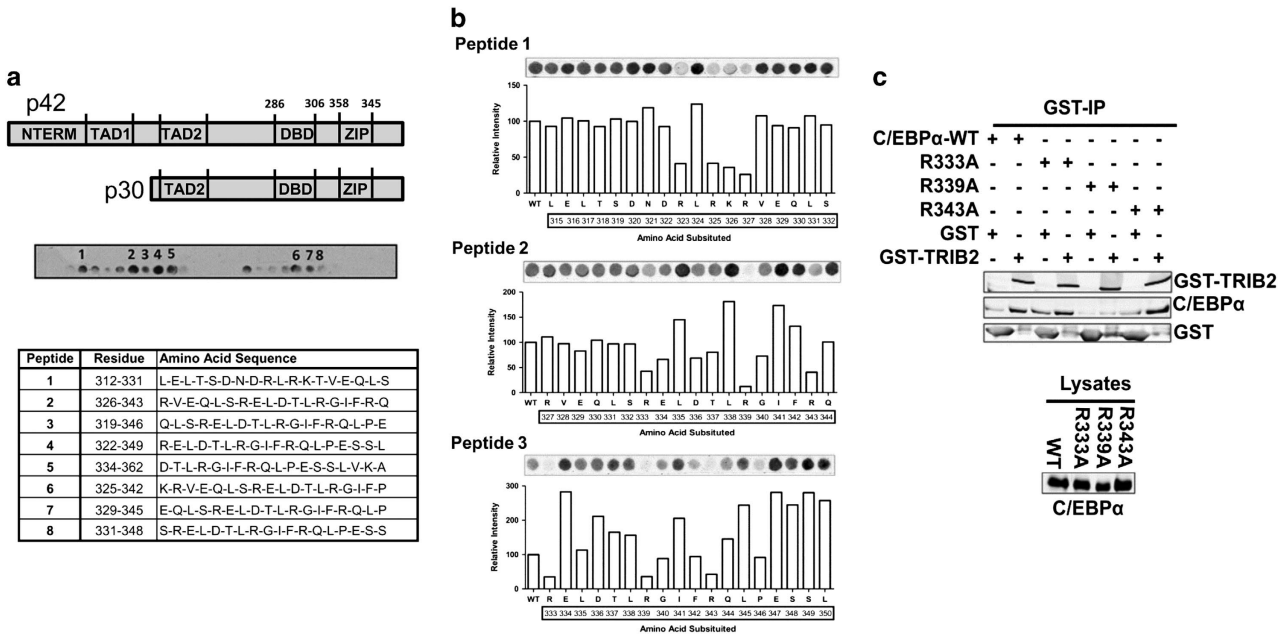

Peptide	Residue	Amino Acid Sequence
1	312-331	L-E-L-T-S-D-N-D-R-L-R-K-T-V-E-Q-L-S
2	326-343	R-V-E-Q-L-S-R-E-L-D-T-L-R-G-I-F-R-Q
3	319-346	Q-L-S-R-E-L-D-T-L-R-G-I-F-R-Q-L-P-E
4	322-349	R-E-L-D-T-L-R-G-I-F-R-Q-L-P-E-S-S-L
5	334-362	D-T-L-R-G-I-F-R-Q-L-P-E-S-S-L-V-K-A
6	325-342	K-R-V-E-Q-L-S-R-E-L-D-T-L-R-G-I-F-P
7	329-345	E-Q-L-S-R-E-L-D-T-L-R-G-I-F-R-Q-L-P
8	331-348	S-R-E-L-D-T-L-R-G-I-F-R-Q-L-P-E-S-S

Figure 2. Identification of R339 as crucial C/EBPα amino acid in TRIB2 binding. (**a**) Peptide arrays encompassing C terminus of C/EBPα were generated as described in Materials and methods. Eight binding peptides unique to C/EBPα were identified. The table displays the amino acid identity of these peptides. This array is representative of two independent SPOT-synthesized arrays. Dark spots are indicative of peptide binding. (**b**) Specific Alanine Scanning Substitution Arrays on a region spanning the C terminus of C/EBPα were probed with GST-TRIB2. The binding of GST-TRIB2 to each alanine-substituted peptide was quantified by densitometry and presented as a percentage of the control unmutated WT sequence, with an underlay identifying the amino acid, which was substituted with an alanine. More than 50% reduction in binding intensity indicative of involvement in the interaction. (**c**) Western blot analysis of 293 T cell lysates expressing WT C/EBPα and C/EBPα mutants (left panel). GST pull-down, performed in the presence of MG-132, using GST-TRIB2 followed by western blot analysis for GST (top and bottom panels) and C/EBPα (middle panel).

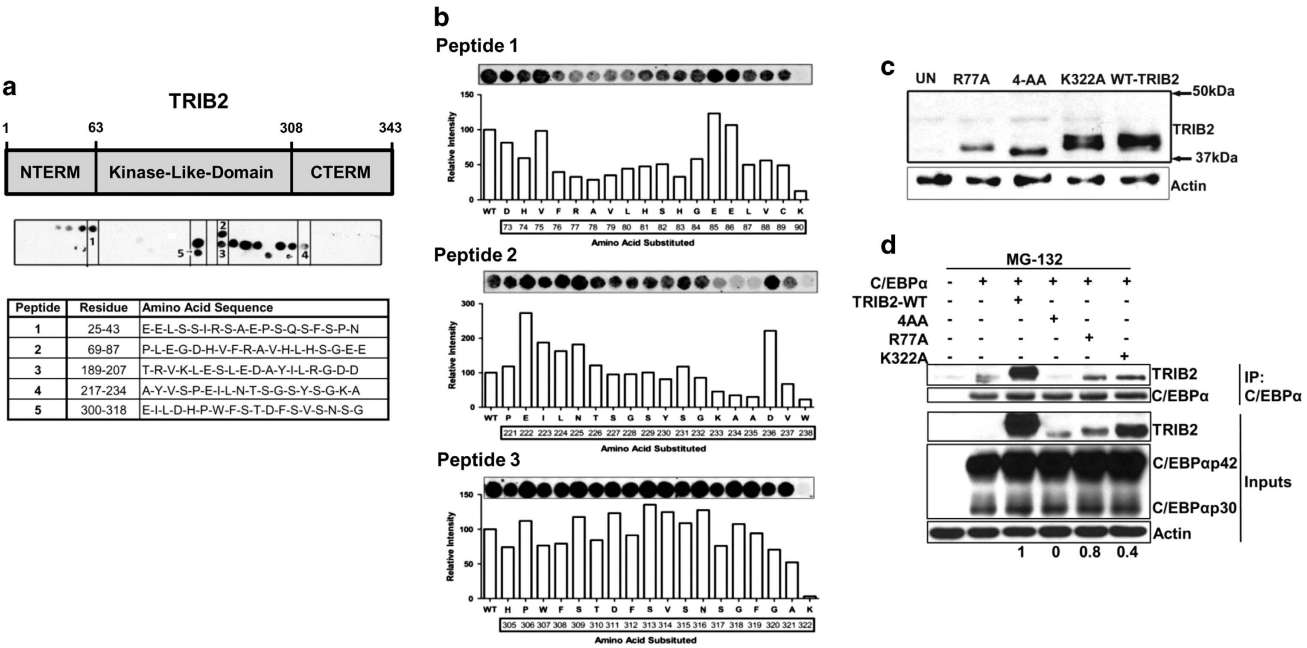

Figure 3. Identification of the C/EBPα-binding site on TRIB2. (**a**) Peptide arrays encompassing TRIB2 were generated as described in Materials and methods. Five binding peptides spanning amino acids 25–318 of C/EBPα protein were identified. The table displays the amino acid identity of these. This array is representative of two independent SPOT-synthesized arrays. Dark spots are indicative of peptide binding. (**b**) Specific Alanine Scanning Substitution Arrays on regions spanning TRIB2 were probed with C/EBPα protein. The binding of C/EBPα protein to each alanine-substituted peptide was quantified by densitometry and presented as relative intensity of the control unmutated WT sequence, with an underlay identifying the amino acid which was substituted with an alanine. More than 50% reduction in binding intensity indicative of involvement in the interaction. (**c**) 293 T lysates expressing WT TRIB2 and mutants R77A, 4-AA (S227A/S229A/S231A/K233A) immunoblotted with anti-TRIB2 and actin serving as a loading control. (**d**) TRIB2-binding mutants 4-AA (S227A/S229A/S231A/K233A), R77A and K322A and WT C/EBPα were expressed in 293 T cells and C/EBPα was immunoprecipitated and lysates were immunoblotted for TRIB2 and C/EBPα (top panels). Western blot of total input lysates shows levels of protein expression (bottom panels). Densitometric analysis was performed and the ratio of IP:Input, normalized to actin are presented (underneath bottom panels).

potential ubiquitination sites with low to high confidence scores. K313 was predicted with medium confidence as a potential ubiquitination site (Figures 5a and b) which has been identified as a recurrent C/EBPα mutation (K313dup) that results in an extra lysine adjacent to K313. This duplication occurs in 10% of C/EBPα-mutated AMLs and identified to have a shorter protein half-life than wild-type C/EBPα as determined by cycloheximide assay.[27] Mutation of K313 to K313R resulted in the loss of TRIB2-induced C/EBPα ubiquitination as compared with WT C/EBPα (Figure 5c). As a control, we show that this mutation retains functional C/EBPα transcriptional activity as both WT and mutant C/EBPα stimulated the G-CSFR luciferase reporter construct, a known C/EBPα target gene (Figure 5d). These data show that K313 serves as the site of ubiquitin conjugation on C/EBPα in the presence of TRIB2 and mutation of K313 abrogates TRIB2-mediated ubiquitin-dependent proteasomal degradation of C/EBPα. This site is also present in p30 yet we do not observe TRIB2-mediated p30 ubiquitination (Figure 5e), suggesting that perhaps the N terminus of C/EBPα p42 functions in the degradative complex.

Proteasome inhibition selectively targets AML with high TRIB2 expression

Our data suggest that inhibition of the proteasome would effectively inhibit the function of TRIB2 by abrogating C/EBPα protein degradation and would be an effective pharmacological targeting strategy in TRIB2-positive AMLs. To test this, U937 cells (express detectable levels of endogenous TRIB2 and C/EBPα) transduced with retroviral MigR1-GFP control and MigR1-TRIB2-GFP were treated with 10 nM bortezomib (a reversible inhibitor of the proteasome chymotryptic activity resulting in the accumulation of K48 ubiquitin-linked proteins). An increase in cytotoxicity in the TRIB2-overexpressing cells compared with MigR1 control transduced cells was observed and cells expressing TRIB2-VPM that cannot degrade C/EBPα behaved similarly to control cells (Figure 6a, panels 1 and 2). Overexpression of MigR1-C/EBPα was able to rescue bortezomib-induced cell death in U937 cells (Figure 6a, panels 3). In C/EBPα-negative leukaemia cells, K562 and Kasumi 1 bortezomib toxicity was not increased following TRIB2 overexpression supporting the specificity of bortezomib on the TRIB2-C/EBPα axis (Figure 6a, panels 4 and 5). Second generation irreversible proteasome inhibitors[28,29] also showed selective killing of high TRIB2 (lentiviral Phr-GFP)-expressing AML cells as assessed by cell viability (Figure 6b). Bortezomib treatment rescued the degradation of C/EBPα p42 seen with TRIB2 overexpression in U937 cells (Figure 6c). In fact, p30 expression remains upon TRIB2 overexpression, confirming our ubiquitination data in Figure 5. We next established a human AML orthotopic xenograft model in which U937 cells were propagated in NSG xenografts and mice were either treated with bortezomib *in vivo* (Figure 6d and described in methods), or TRIB2 was knocked down using shRNA lentivirus (Figure 6e[12]). *In vivo* bortezomib treatment significantly impaired the engraftment of U937 cells as determined by lower % of engrafting GFP^+ cells positive for human antibody CD45 expression (Figure 6f). In addition, engraftment of U937 cells expressing shTRIB2 lentivirus in NSG xenografts showed that in comparison with control (shctrl), knockdown of TRIB2 impaired the progression of U937 orthotopic xenografts (Figure 6g). Together our data show that TRIB2-expressing AML cells can be pharmacologically targeted with

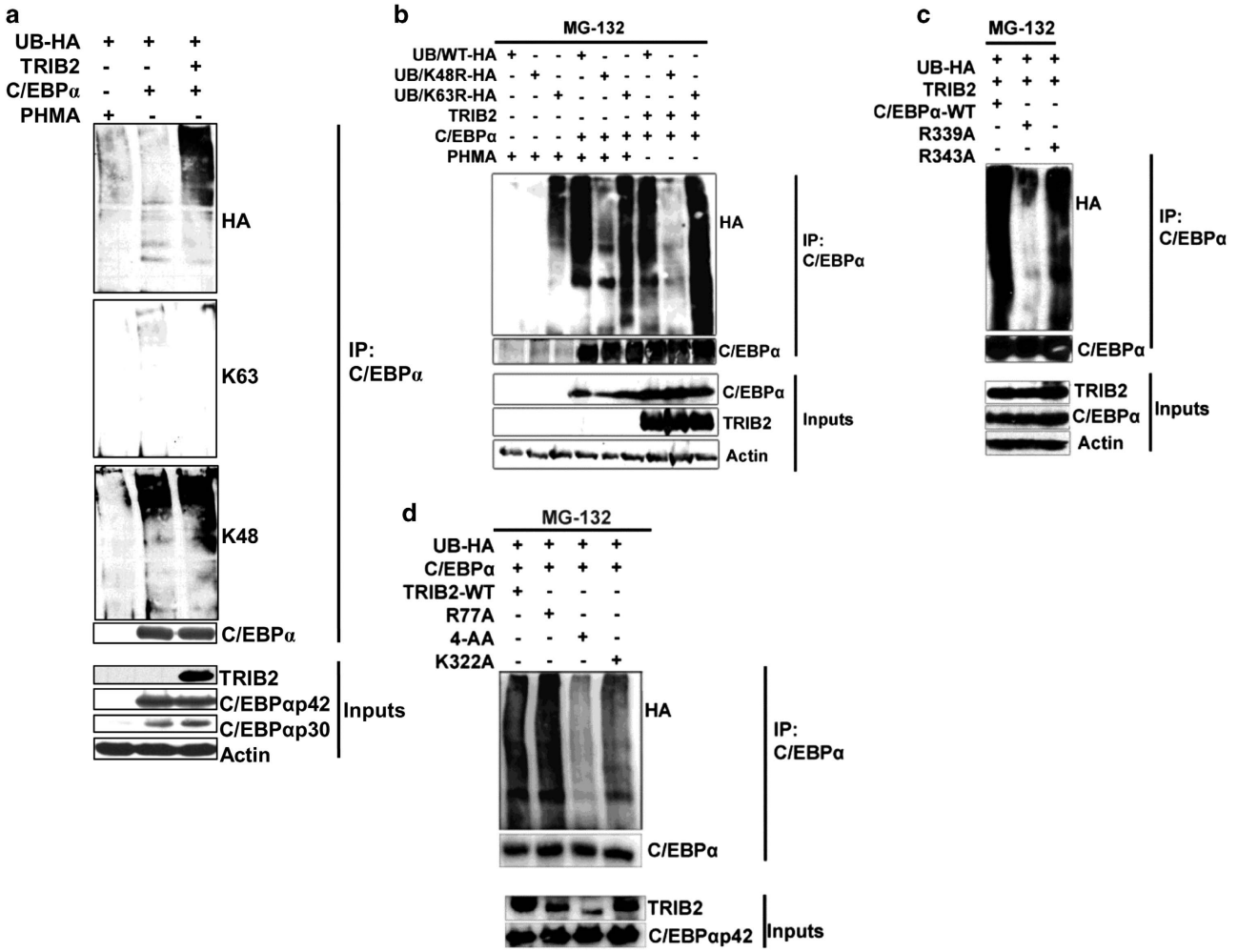

Figure 4. TRIB2 induces binding-dependent K48-specific ubiquitin-dependent proteasomal degradation of C/EBPα. (**a**) 293 T cells were transfected with ubiquitin-HA, TRIB2, C/EBPα and PHMA empty vector control. Ubiquitination assay was performed. Immunoblotting for HA detects ubiquitination (top IP panel), K63 species of polyubiquitination (second IP panel), K48 species of polyubiquination (third IP panel) and C/EBPα detects IP protein (bottom IP panel). Immunoblotting for TRIB2 and C/EBPα detects input levels and actin serves as a loading control (input panels). (**b**) Ubiquitination assay as outlined in (**a**) including ubiquitin mutants that do not express the K48 (K48R) ubiquitin polychain and the K63 (K63R) ubiquitin polychain. (**c**) Ubiquitination assay as outlined in (**a**) including C/EBPα mutants; R339A and R343A. (**d**) Ubiquitination assay as outlined in (**a**) including TRIB2 binding mutants R77A, 4-AA (S227A/S229A/S231/K233A) and K322A. Indicated experiments (**b–d**) were treated with 10 μM MG-132 for 5 h before ubiquitination assay was performed.

proteasome inhibition due, in part, to inhibition of the TRIB2 proteolytic function on C/EBPα.

DISCUSSION

Although C/EBPα dysfunction is a common occurrence in different cancers, details on the mechanisms involved in bringing about the loss of C/EBPα protein expression in *Cebpa* wild-type and mutated AML are yet to be fully elucidated. In this study, we identify the molecular mechanism involved in the dysregulation of C/EBPα expression via TRIB2 in AML. We and others[10,13,30] have previously demonstrated that TRIB2 overexpression induces AML and that it degrades C/EBPα p42. Here, we provide novel insights on this process and show that the presence of C/EBPα p42 is required not only to initiate TRIB2 AML, but also for TRIB2 to cooperate with C/EBPα (p42 loss and increased p30) in driving AML disease. Our data support the emerging notion that C/EBPα functions in the initial transformation, as supported by the data showing that C/EBPα regulated a transcriptional programme essential for initiation yet dispensable for the maintenance of MLL-ENL disease.[18] Our data clearly show loss of C/EBPα p42 via TRIB2-induced ubiquitin-mediated degradation and excess p30 expression cooperates to accelerate AML.

Using BM transduction and transplantation approaches, we show that C/EBPα p42 isoform expression from one *Cebpa* allele is necessary and sufficient for TRIB2 to cooperate with p30 isoform in AML. The addition of TRIB2 does not further accelerate AML induced by excess p30 itself, but does accelerate AML when p42 is present. This suggests that p30 is necessary for TRIB2-mediated AML induction. The possibility remains that TRIB2 may convert p42 to p30 to form additional p30 protein but we do not have any evidence for this here. Under normal physiological conditions, the protein levels of C/EBPα p42 are greater than p30 protein levels, and when this balance changes toward more p30 levels, it is considered 'leukaemic', as observed in leukaemic cell lines and AML patients.[22] We showed that K313 in the C terminus of C/EBPα p42 was critical for TRIB2-mediated ubiquitination and proteasomal degradation. This lysine residue is a common mutation in AML patients (~10% of all C/EBPα mutations) which results in the duplication of the single lysine to KK leading to

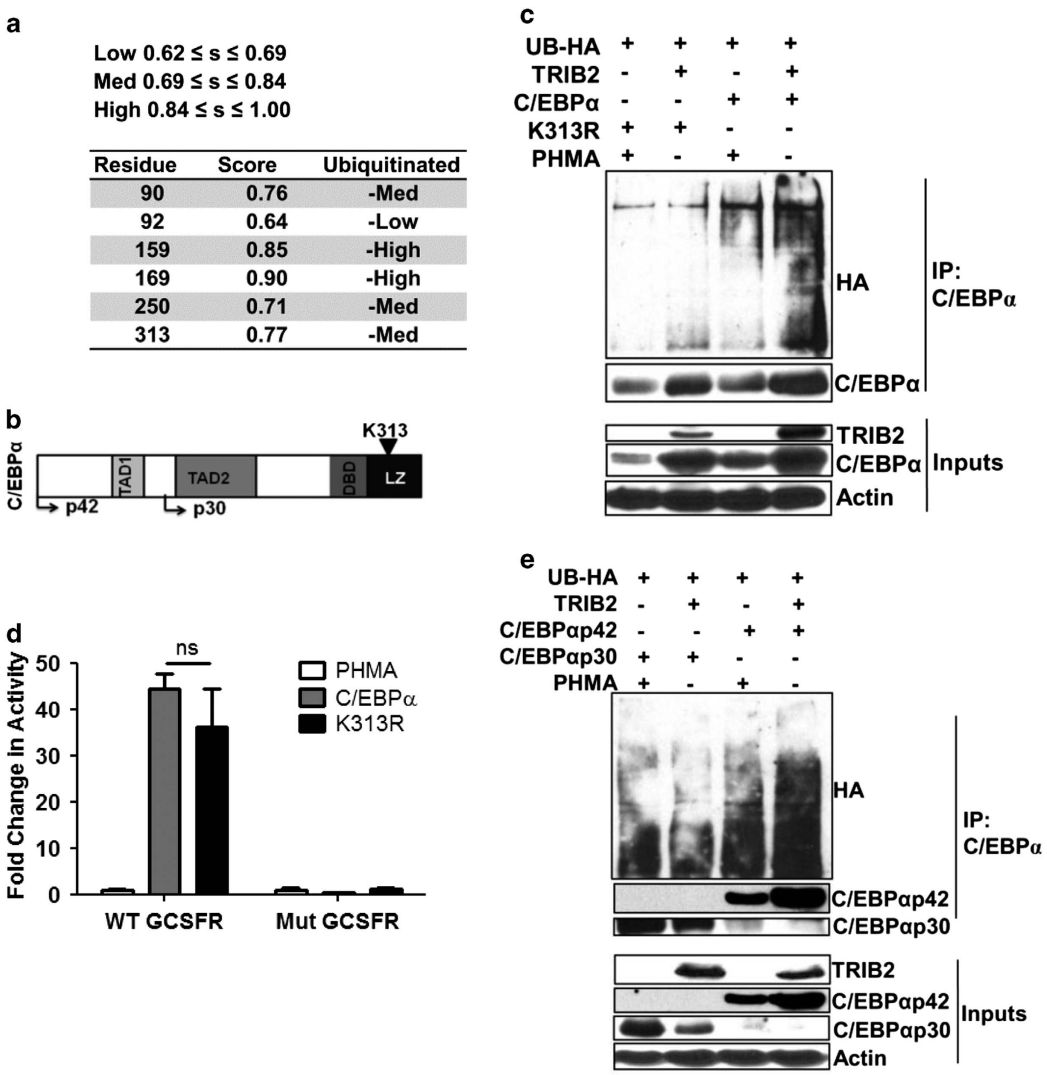

Figure 5. TRIB2 ubiquitinates C/EBPα on K313. (**a**) Ubpred analysis of C/EBPα Ensembl gene ID (ENSRNOG00000010918) showing the probability of each lysine acting as ubiquitination sites. (**b**) Schematic diagram displaying the localization of K313 in C/EBPα. (**c**) Ubiquitination assay performed with C/EBPα-K313R and TRIB2 in 293 T cells. (**d**) 293 T cells were co-transfected with the G-CSFR promoter firefly luciferase constructs containing either the C/EBPα WT (WT G-CSFR) or mutant binding sites (Mut GCSFR), and either an empty PHMA vector or vector containing C/EBPα or K313R, along with a pRL-TK Renilla luciferase internal control plasmid. Luciferase activity was measured 24 h post transfection. Bar chart represents reporter luciferase activity for each sample normalized for renilla values, and graphed relative to the control sample. Results analysed using two-tailed unpaired *t* test and representative of three independent experiments. (**e**) Ubiquitination assay performed with C/EBPα p30 and TRIB2 in 293 T cells.

reduced protein stability.[27] Using mouse genetics, it was shown that this duplication of K313 to K313KK (K313dup) resulted in an increased proliferation of long-term HSCs leading to an expansion of premaligant HSCs not seen with the N terminal mutations.[23] Our data show that the absence of this lysine by mutation to an arginine (K313R) abrogates the susceptibility of C/EBPα to degradation whilst retaining its DNA-binding and transcriptional activation function. This suggests that TRIB2 degrades C/EBPα p42 via ubiquitination of K313 and duplication of this residue as occurs in AML patients samples would lead to an increase in C/EBPα p42 degradation in the presence of TRIB2. Patients with K313dup had TCR rearrangements and CD7 expression,[27] lymphoid features associated with unfavourable outcome and which we have previously linked with TRIB2 and C/EBPα perturbation.[31] Previous investigation of the combination of a C terminal mutation (K313 duplication) with C/EBPα p30 expression revealed cooperation and provides a possible explanation for the high prevalence of one N terminal mutation and one C terminal mutation in ~90% of biallelic C/EBPα-mutant AMLs.[23] We propose that the K313dup mutation in patients contributes to leukaemic transformation by increasing the susceptibility of C/EBPα to ubiquitination resulting in increased degradation of C/EBPα p42. A thorough investigation of TRIB2 function in K313 mutant patient cells would further validate this.

C/EBPα p42 R339 and K313 amino acids are both present in p30 yet TRIB2 does not degrade p30. One explanation may be that the protein complexes containing TRIB2 and C/EBPα p42 or TRIB2 and p30 are different. Our previous work showed that TRIB2 binds with COP1 E3 ligase and this interaction is necessary for C/EBPα p42 degradation.[13] Although our peptide mapping clearly shows specific sites in both TRIB2 and C/EBPα responsible for the direct interaction, in the absence of crystal structure information, we cannot predict further based on our data the reason why p30 is not targeted by TRIB2 for degradation. Our

data do not discount a role for p30 in TRIB2-mediated AML; p30 presence may, for example, activate a unique set of genes, inhibit other C/EBPs or bind to a unique set of proteins distinct from C/EBPα p42 as previously reported.[32,33] Indeed, U937 cells express endogenous C/EBPα but are less sensitive to bortezomib-induced killing compared with TRIB2-overexpressing cells. This suggests that TRIB2 must be affecting something in addition to C/EBPα p42 degradation to provide synergy in AML. Our data

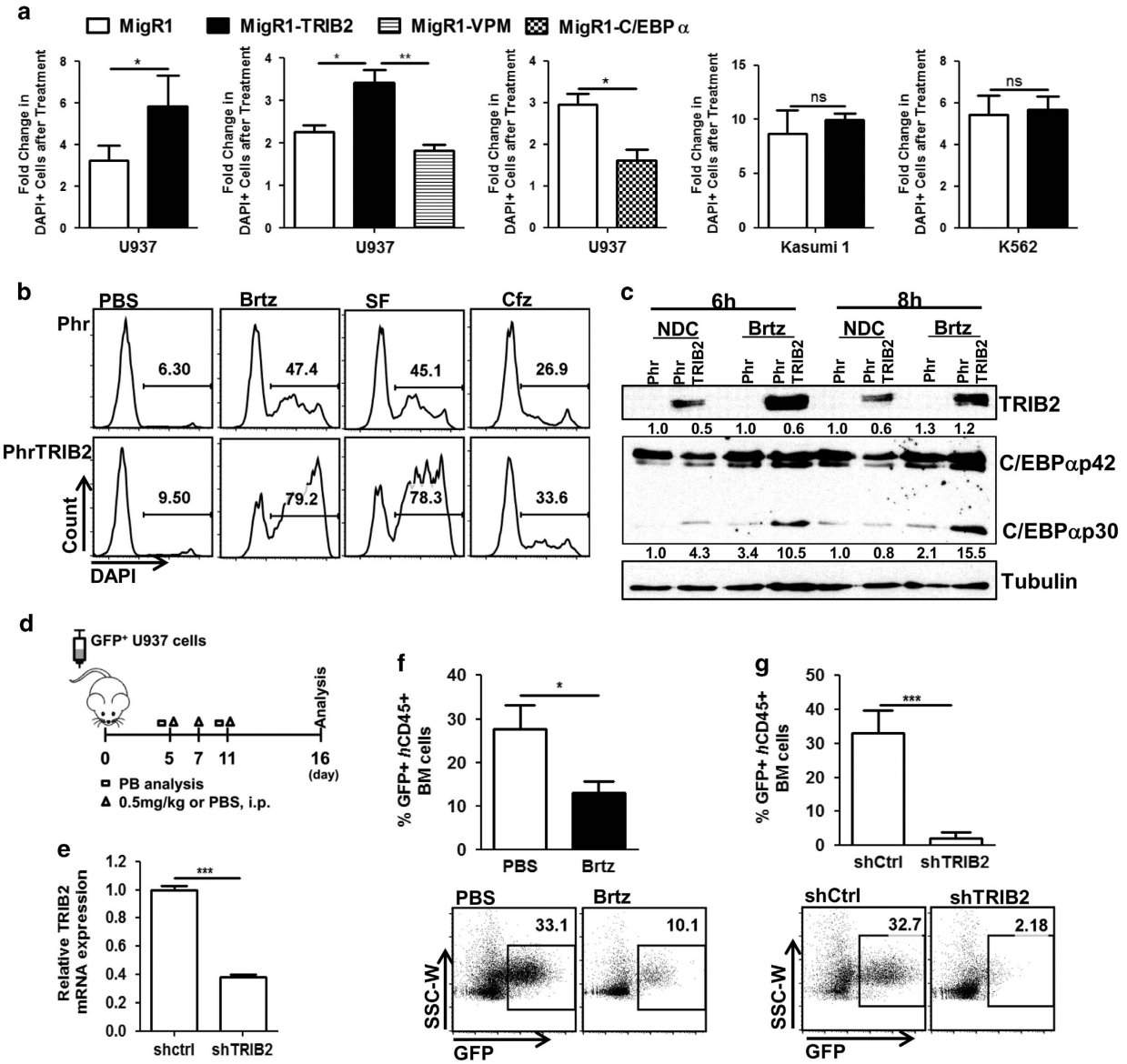

Figure 6. Modulation of TRIB2 levels sensitizes AML cells to cell death induced by proteasome inhibition. (**a**) Sorted GFP$^+$ cells transduced with MigR1 control, MigR1-TRIB2, MigR1-VPM or MigR1-C/EBPα retrovirus were treated +/− 10 nM bortezomib for 16–24 h and analysed by flow cytometry for cell death by 4',6-diamidino-2-phenylindole (DAPI). Graph of fold change in cell death as determined by DAPI-positive cells. Data displayed are average of three technical replicates, and are representative of two independent experiments. (n.s. denotes not significant, $^*P < 0.05$, $^{**}P < 0.005$ by Student's unpaired *t* test). (**b**) Sorted GFP$^+$ U937 cells transduced with either Phr or Phr-TRIB2 were treated with 10 nM bortezomib, 500 nM sulfonyl fluoride (SF), 10 nM carfilzomib (Cfz) or dimethyl sulfoxide (DMSO) only for 16 h. Cytotoxicity was assessed by DAPI staining. Representative fluorescence-activated cell sorting (FACS) plots of three independent experiments with two technical replicates each are shown. (**c**) Sorted GFP$^+$ U937 cells transduced with either Phr or Phr-TRIB2 were treated for 6 and 8 h with 10 nM bortezomib or DMSO only (NDC, no drug control) and cell lysates were analysed for C/EBPα expression by western blotting. TRIB2 overexpression was confirmed and tubulin was used as the loading control. Representative of two independent experiments. (**d**) Schematic representation of the AML xenograft study. NOD-SCID IL2Rγ^{null} mice (NSG) were transplanted with GFP$^+$*hCD45*$^+$ U937 cells ($n = 6$). Each group was randomized into two groups for treatment with 0.5 mg/kg bortezomib or phosphate-buffered saline (PBS), intraperitoneally, on a regime schedule of three injections for 16 days. (**e**) TRIB2 gene knockdown was confirmed at the mRNA level in shTRIB2-U937 cells selected with 2 μg/ml puromycin for 48 h. Values represent gene expression relative to shctrl-U937 cells and normalized to the reference gene ABL ($^{***}P < 0.001$ by Student's *t* test). (**f**) GFP and hCD45 expression in BM were quantified by flow cytometry as a measure of disease burden in control PBS ($n = 3$)- and bortezomib ($n = 3$)-treated animals and data are shown by representative FACS contour plots (lower panel) and bar graphs (upper panel) with means ± s.d. ($^*P < 0.05$ by Student's *t* test). (**g**) GFP and hCD45 expression in BM were quantified by flow cytometry as a measure of disease burden in shctrl ($n = 5$) and shTRIB2-U937 ($n = 8$) mice and data are shown by representative FACS contour plots (lower panel) and bar graphs (upper panel) with means ± s.d. ($^{***}P < 0.001$ by Student's *t* test).

support further investigations into the proteomic profiling of AML, with a focus on the involvement of C/EBPα ubiquitination and the need for an in-depth understanding of the C/EBPα ubiquitin regulatory pathway in normal versus leukaemic (CEBPA WT and mutant) settings.

Whilst TRIB2 itself is an oncogene capable of driving AML, the molecular interaction identified here between TRIB2 and C/EBPα leading to dysregulated C/EBPα may have implications in other models of AML and indeed other cancers. It is clear that the loss of C/EBPα function is a common occurrence in a number of different cancer types. What is not clear at this point is the extent of the involvement of TRIB2 function across different haematological malignancies and other cancers. To date, cooperation between TRIB proteins and other oncogenes in AML has been demonstrated, most often with Hoxa9 and Meis1, suggesting that TRIB2 protein function downstream of commonly occurring oncogenic events may impact on C/EBPα.[34,35] TRIB2 is found elevated in lung cancer and associated with the E3 ligase TRIM21.[30] In liver cancer cells, TRIB2 associated with other E3 ligases including β-TrCP, COP1 and Smurf1.[36] Thus, there is a strong link between TRIB2 and the ubiquitin-proteasome system in cancer.

As shown here, high TRIB2-expressing cells are sensitive to bortezomib-induced cellular toxicity. However, inhibition of the proteasome also targets other proteins, E3 ligases and their substrates. We currently have limited knowledge of TRIB2 degradation substrates in general, and indeed knowledge of TRIB2 as a substrate itself of the ubiquitin-proteasome system in cancer. This study highlights the important molecular interplay between TRIB2 and C/EBPα in driving AML, and provides a framework for further investigations into targeting the ubiquitin-proteasome system as an emerging cancer therapy.

MATERIALS AND METHODS

Murine BM transduction and transplantation

Cebpa$^{fl/fl}$*; Mx1cre* were crossed to *Cebpa*$^{+/p30}$ (^{25}p30 referred to as 'L' allele previously) to yield *Cebpa*$^{fl/+}$*; Mx1Cre, Cebpa*$^{fl/p30}$*; Mx1cre, Cebpa*$^{fl/+}$ and *Cebpa*$^{fl/p30}$. Genotyping and evaluation of *Cebpa* excision methods provided in Supplementary Information. Eight- to 14-week-old *Cebpa*$^{fl/fl}$*, Cebpa*$^{fl/fl}$*; Mx1Cre, Cebpa*$^{fl/+}$*, Cebpa*$^{fl/p30}$ *and Cebpa*$^{fl/p30}$*; Mx1Cre* mice were plpC-treated (three injections every second day with 300 ug plpC) to excise the *Cebpa* allele. Resultant genotypes are *Cebpa*$^{fl/fl}$ (expressing solely p42 alleles which can give rise to p30), *Cebpa*$^{\Delta/\Delta}$ (null for p42 and p30), *Cebpa*$^{fl/+}$ (expressing solely p42 alleles which can give rise to p30), *Cebpa*$^{fl/p30}$ (expressing one p42 and one solely p30 allele) and *Cebpa*$^{fl/p30}$*; Mx1Cre* (referred to as *Cebpa*$^{\Delta/p30}$, solely expressing one p30 allele) (Figure 1b). Two weeks post deletion, CD45.2$^+$ BM cells were collected and either c-Kit-purified by magnetic-activated cell sorting (Figure 1a), or total BM (Figures 1c and d) was transduced with 40% titre-matched retrovirus in the presence of IL3, IL6 and SCF. Freshly transduced unsorted cells (1×10^6 Figure 1a, 3×10^6 Figure 1c) were injected by tail vein into lethally irradiated CD45.1$^+$ recipients generating *Cebpa*$^{fl/fl}$-TRIB2 ($n=12$), *Cebpa*$^{\Delta/\Delta}$-TRIB2 ($n=10$), *Cebpa*$^{fl/+}$-MigR1 ($n=9$), *Cebpa*$^{fl/+}$-TRIB2 ($n=4$), *Cebpa*$^{fl/p30}$-MigR1 ($n=6$), *Cebpa*$^{fl/p30}$-TRIB2 ($n=8$), *Cebpa*$^{\Delta/p30}$-MigR1 ($n=6$), *Cebpa*$^{\Delta/p30}$-TRIB2 ($n=8$). Mice were monitored for 14 months and killed when they developed physical signs of disease (behavioural changes, laboured breathing, hunched posture) or high white blood cell counts. For NOD-SCID IL2Rγnull (NSG) mice Xenograft transplantation, 1×10^6 U937 cells transduced with shTRIB2-GFP ($n=5$) or shCtrl-GFP ($N=8$) were transplanted into non-irradiated NSG mice via tail vein injection. To assess bortezomib *in vivo* efficacy, GFP ctrl transduced U937 cells were injected, and 5 days post injection, mice were randomized and treated with either bortezomib (0.5 mg/kg, $n=3$) or phosphate-buffered saline (intraperitoneal administration, $n=3$) at days 5, 7 and 11 post transplant, which was well tolerated. Mice were killed on day 16. Animals were maintained at the University of Copenhagen and the University of Glasgow, housed in accordance with their respective institutional guidelines. All work was carried out under the approval of the Danish Ethical Committee and the Home Office of the United Kingdom.

Flow cytometry

Cell suspensions were stained on ice in fluorescence-activated cell sorting buffer (phosphate-buffered saline pH 7.0, 10 mM Hepes, 0.02% sodium azide, 0.2% bovine serum albumin). Analytical flow cytometry was performed on a FACS Canto (Becton Dickinson), sorting was performed on a FACS Aria II (Becton Dickinson, Oxford, UK) and data were analysed using FlowJo software (Treestar, Version 10, Ashland, OR, USA). Dead cells were excluded using 4′,6-diamidino-2-phenylindole and doublets excluded based on FSC-H and FSC-A. For apoptosis assays, Annexin V-PE (BD Biosciences 556422) or Annexin V-APC (BD Biosciences 550475, Oxford, UK) was used.

Details of vectors, antibodies, cell culture/transfections and real-time PCR provided in Supplementary Information.

Ubiquitination assay, co-immunoprecipitation and western blotting

293 T cells transfected with described vectors were treated with 10 μM MG-132 5 h prior to lysis where indicated. For ubiquitination assay, cells were lysed in 1% SDS, sonicated and supernatants precleared with Protein G Sepharose 4 fast flow beads (GE Healthcare, Amersham, UK), then incubated with C/EBPα antibody overnight. For co-immunoprecipitation, cells were lysed in Tris buffer (50 mM Tris pH 7.4, 150 mM NaCl, 1 mM EDTA, 0.5% NP-40, 5% glycerol, with protease and phosphatase inhibitors) and precleared lysates were incubated with C/EBPα antibody overnight. Whole cell proteins were isolated by RIPA lysis buffer (50 mM Tris, pH 8.0, containing 0.5% NP-40, 0.25% sodium deoxycholate, 150 mM NaCl, 1 mM EDTA, 20 mM N-Ethylmaleimide with protease and phosphatase inhibitors) or by direct lysis (2 × SDS sample buffer). Details of antibodies provided in Supplementary Information. For GST-IP, 3 mg of indicated cell lysate was added to 50 μl of GSH slurry with pull-down performed using 25 ug of GST or GST-TRIB2 (details of GST protein production are provided in Supplementary Information). Densitometric analysis of bands was carried out with ImageJ Software. $n\geqslant3$ for all co-immunoprecipitation and ubiquitination assays.

Spot synthesis of peptides and overlay analysis

Peptide arrays were performed as previously described[37,38] ($n=2$) and details are provided in Supplementary Information. Briefly, peptide arrays encompassing the C terminus of C/EBPα and the entire TRIB2 protein were generated and incubated with GST-TRIB2 or purified C-teminal C/EBPα (Genway, San Diego, CA, USA). Arrays were incubated with secondary antibodies and bound protein detected using ECL or the Odyssey Infrared Imaging System (LI-COR Biosciences, Cambridge, UK).

Statistical analysis

Statisitcal analysis and graphing was performed on GraphPad Prism (version 5.03). When comparing two groups, an unpaired, two-tailed Student's *t* test was used. The Log-rank test was used to compare groups on a survival curves. Statistical significance was attained when the *P* value $\leqslant0.05$ and was indicated in the related figure legends and graphs.

CONFLICT OF INTEREST

The authors declare no conflict of interest.

ACKNOWLEDGEMENTS

We thank all the technical staff at the Paul O'Gorman Leukaemia Research Centre. We thank the Cancer Research UK Glasgow Centre (C596/A18076) and the Biological Service Unit facilities at the Cancer Research UK Beatson Institute (C596/A17196) and the Biological Services at the University of Glasgow. We thank Ruaidhrí Carmody for reagents and critical review of the work. We thank the Kay Kendall foundation (KKL501) and the Howat foundation for Flow cytometry facility funding. Work in the Keeshan lab was supported by the Howat Foundation and Children with Cancer UK. CO'C was supported by Childrens Leukaemia Research Project grant. PK was supported by Science Foundation Ireland Infrastructure award and the Mid-Western Cancer Foundation. Work in the Porse lab was supported by a centre grant from the NovoNordisk Foundation (The Novo Nordisk Foundation Section for Stem Cell Biology in Human Disease).

AUTHOR CONTRIBUTIONS

KK designed the study. FL, CO'C, CF, EO, MS and JC performed the research. BP provided transgenic mouse models. BP, PK, RL, RA and MC provided essential reagents and expertise. KK, FL, CO'C, MS, EO and JC analysed the data. CO'C and FL made the figures. KK wrote the paper. All authors edited the paper.

REFERENCES

1 Fasan A, Alpermann T, Haferlach C, Grossmann V, Roller A, Kohlmann A *et al.* Frequency and prognostic impact of CEBPA proximal, distal and core promoter methylation in normal karyotype AML: a study on 623 cases. *PLoS One* 2013; **8**: e54365.
2 Annamaneni S, Kagita S, Gorre M, Digumarti RR, Satti V, Battini MR. Methylation status of CEBPAgene promoter in chronic myeloid leukemia. *Hematology* 2014; **19**: 42–44.
3 Bennett KL, Hackanson B, Smith LT, Morrison CD, Lang JC, Schuller DE *et al.* Tumor suppressor activity of CCAAT/enhancer binding protein is epigenetically down-regulated in head and neck squamous cell carcinoma. *Cancer Res* 2007; **67**: 4657–4664.
4 Paz-Priel I, Friedman A. C/EBPalpha dysregulation in AML and ALL. *Crit Rev Oncog* 2011; **16**: 93–102.
5 Friedman AD. C/EBPα in normal and malignant myelopoiesis. *Int J Hematol* 2015; **101**: 330–341.
6 Taskesen E, Bullinger L, Corbacioglu A, Sanders MA, Erpelinck CAJ, Wouters BJ *et al.* Prognostic impact, concurrent genetic mutations, and gene expression features of AML with CEBPA mutations in a cohort of 1182 cytogenetically normal AML patients: further evidence for CEBPA double mutant AML as a distinctive disease entity. *Blood* 2011; **117**: 2469–2475.
7 Pabst T, Eyholzer M, Haefliger S, Schardt J, Mueller BU. Somatic CEBPA mutations are a frequent second event in families with germline CEBPA mutations and familial acute myeloid leukemia. *J Clin Oncol* 2008; **26**: 5088–5093.
8 Fasan A, Haferlach C, Alpermann T, Jeromin S, Grossmann V, Eder C *et al.* The role of different genetic subtypes of CEBPA mutated AML. *Leukemia* 2014; **28**: 794–803.
9 Hattori T, Ohoka N, Inoue Y, Hayashi H, Onozaki K. C/EBP family transcription factors are degraded by the proteasome but stabilized by forming dimer. *Oncogene* 2003; **22**: 1273–1280.
10 Keeshan K, He Y, Wouters BJ, Shestova O, Xu L, Sai H *et al.* Tribbles homolog 2 inactivates C/EBPalpha and causes acute myelogenous leukemia. *Cancer Cell* 2006; **10**: 401–411.
11 Keeshan K, Shestova O, Ussin L, Pear WS. Tribbles homolog 2 (Trib2) and HoxA9 cooperate to accelerate acute myelogenous leukemia. *Blood Cells Mol Dis* 2008; **40**: 119–121.
12 Rishi L, Hannon M, Salomè M, Hasemann M, Frank A-K, Campos J *et al.* Regulation of Trib2 by an E2F1-C/EBPalpha feedback loop in AML cell proliferation. *Blood* 2014; **123**: 2389–2400.
13 Keeshan K, Bailis W, Dedhia PH, Vega ME, Shestova O, Xu L *et al.* Transformation by Tribbles homolog 2 (Trib2) requires both the Trib2 kinase domain and COP1 binding. *Blood* 2010; **116**: 4948–4957.
14 Mancini E, Sanjuan-Pla A, Luciani L, Moore S, Grover A, Zay A *et al.* FOG-1 and GATA-1 act sequentially to specify definitive megakaryocytic and erythroid progenitors. *EMBO J* 2011; **8**;:1–15.
15 Ye M, Zhang H, Amabile G, Yang H, Staber PB, Zhang P *et al.* C/EBPa controls acquisition and maintenance of adult haematopoietic stem cell quiescence. *Nat Cell Biol* 2013; **15**: 385–394.
16 Hasemann MS, Lauridsen FKB, Waage J, Jakobsen JS, Frank A-K, Schuster MB *et al.* C/EBPα is required for long-term self-renewal and lineage priming of hematopoietic stem cells and for the maintenance of epigenetic configurations in multipotent progenitors. *PLoS Genet* 2014; **10**: e1004079–e1004079.
17 Zhang P, Iwasaki-Arai J, Iwasaki H, Fenyus ML, Dayaram T, Owens BM *et al.* Enhancement of hematopoietic stem cell repopulating capacity and self-renewal in the absence of the transcription factor C/EBP alpha. *Immunity* 2004; **21**: 853–863.
18 Ohlsson E, Hasemann MS, Willer A, Lauridsen FK, Rapin N, Jendholm J *et al.* Initiation of MLL-rearranged AML is dependent on C/EBPα. *J Exp Med* 2013; **211**: 5–13.
19 Collins C, Wang J, Miao H, Bronstein J, Nawer H, Xu T *et al.* C/EBP is an essential collaborator in Hoxa9/Meis1-mediated leukemogenesis. *Proc Natl Acad Sci USA* 2014; **111**: 9899–9904.
20 Wagner K, Zhang P, Rosenbauer F, Drescher B, Kobayashi S, Radomska HS *et al.* Absence of the transcription factor CCAAT enhancer binding protein alpha results in loss of myeloid identity in bcr/abl-induced malignancy. *Proc Natl Acad Sci USA* 2006; **103**: 6338–6343.
21 Pabst T, Mueller BU, Zhang P, Radomska HS, Narravula S, Schnittger S *et al.* Dominant-negative mutations of CEBPA, encoding CCAAT/enhancer binding protein-alpha (C/EBPalpha), in acute myeloid leukemia. *Nat Genet* 2001; **27**: 263–270.
22 Leroy H, Roumier C, Huyghe P, Biggio V, Fenaux P, Preudhomme C. CEBPA point mutations in hematological malignancies. *Leukemia* 2005; **19**: 329–334.
23 Bereshchenko O, Mancini E, Moore S, Bilbao D, Månsson R, Luc S *et al.* Hematopoietic stem cell expansion precedes the generation of committed myeloid leukemia-initiating cells in C/EBPα mutant AML. *Cancer Cell* 2009; **16**: 390–400.
24 Quintana-Bustamante O, Lan-Lan Smith S, Griessinger E, Reyal Y, Vargaftig J, Lister TA *et al.* Overexpression of wild-type or mutants forms of CEBPA alter normal human hematopoiesis. *Leukemia* 2012; **26**: 1537–1546.
25 Kirstetter PP, Schuster MB, Bereshchenko OO, Moore SS, Dvinge HH, Kurz EE *et al.* Modeling of C/EBPalpha mutant acute myeloid leukemia reveals a common expression signature of committed myeloid leukemia-initiating cells. *Cancer Cell* 2008; **13**: 299–310.
26 Yokoyama T, Toki T, Aoki Y, Kanezaki R, Park M-J, Kanno Y *et al.* Identification of TRIB1 R107L gain-of-function mutation in human acute megakaryocytic leukemia. *Blood* 2012; **119**: 2608–2611.
27 Carnicer MJ, Lasa A, Buschbeck M, Serrano E, Carricondo M, Brunet S *et al.* K313dup is a recurrent CEBPA mutation in de novo acute myeloid leukemia (AML). *Ann Hematol* 2008; **87**: 819–827.
28 Brouwer AJ, Jonker A, Werkhoven P, Kuo E, Li N, Gallastegui N *et al.* Peptido sulfonyl fluorides as new powerful proteasome inhibitors. *J Med Chem* 2012; **55**: 10995–11003.
29 Claudia Andreu-Vieyra JRB, Berenson JR. Carfilzomib in multiple myeloma. *Expert Opin Biol Ther* 2014; **14**: 1685–1699.
30 Grandinetti KB, Stevens TA, Ha S, Salamone RJ, Walker JR, Zhang J *et al.* Overexpression of TRIB2 in human lung cancers contributes to tumorigenesis through downregulation of C/EBPalpha. *Oncogene* 2011; **14**: 1–8.
31 Wouters BJ, Jorda MA, Keeshan K, Louwers I, Erpelinck-Verschueren CA, Tielemans D *et al.* Distinct gene expression profiles of acute myeloid/T-lymphoid leukemia with silenced CEBPA and mutations in NOTCH1. *Blood* 2007; **110**: 3706–3714.
32 Geletu M, Balkhi MY, Peer Zada AA, Christopeit M, Pulikkan JA, Trivedi AK *et al.* Target proteins of C/EBP p30 in AML: C/EBP p30 enhances sumoylation of C/EBP p42 via up-regulation of Ubc9. *Blood* 2007; **110**: 3301–3309.
33 Pulikkan JA, Dengler V, Zada AAP, Kawasaki A, Geletu M, Pasalic Z *et al.* Elevated PIN1 expression by C/EBPalpha-p30 blocks C/EBPalpha-induced granulocytic differentiation through c-Jun in AML. *Leukemia* 2010; **24**: 914–923.
34 Trivedi AK, Bararia D, Christopeit M, PeerZada AA, Singh SM, Kieser A *et al.* Proteomic identification of C/EBP-DBD multiprotein complex: JNK1 activates stem cell regulator C/EBPα by inhibiting its ubiquitination. *Oncogene* 2006; **26**: 1789–1801.
35 Jin G, Yamazaki Y, Takuwa M, Takahara T, Kaneko K, Kuwata T *et al.* Trib1 and Evi1 cooperate with Hoxa and Meis1 in myeloid leukemogenesis. *Blood* 2007; **109**: 3998–4005.
36 Xu S, Tong M, Huang J, Zhang Y, Qiao Y, Weng W *et al.* TRIB2 inhibits Wnt/beta-Catenin/TCF4 signaling through its associated ubiquitin E3 ligases, beta-TrCP, COP1 and Smurf1, in liver cancer cells. *FEBS Lett* 2014; **588**: 4334–4341.
37 Frank R. The SPOT-synthesis technique. Synthetic peptide arrays on membrane supports--principles and applications. *J Immunol Methods* 2002; **267**: 13–26.
38 Colleran A, Collins PE, O'Carroll C, Ahmed A, Mao X, McManus B *et al.* Deubiquitination of NF-kappaB by ubiquitin-specific protease-7 promotes transcription. *Proc Natl Acad Sci USA* 2013; **110**: 618–623.

Supplementary Information accompanies this paper on the Oncogene website (http://www.nature.com/onc)

List of references

ABBAS, S., LUGTHART, S., KAVELAARS, F. G., SCHELEN, A., KOENDERS, J. E., ZEILEMAKER, A., VAN PUTTEN, W. J., RIJNEVELD, A. W., LOWENBERG, B. & VALK, P. J. 2010. Acquired mutations in the genes encoding IDH1 and IDH2 both are recurrent aberrations in acute myeloid leukemia: prevalence and prognostic value. *Blood,* 116**,** 2122-6.

ADAMS, J. 2004. The proteasome: a suitable antineoplastic target. *Nat Rev Cancer,* 4**,** 349-360.

ADAMS, J., PALOMBELLA, V. J., SAUSVILLE, E. A., JOHNSON, J., DESTREE, A., LAZARUS, D. D., MAAS, J., PIEN, C. S., PRAKASH, S. & ELLIOTT, P. J. 1999. Proteasome inhibitors: a novel class of potent and effective antitumor agents. *Cancer Res,* 59**,** 2615-22.

ADOLFSSON, J., MANSSON, R., BUZA-VIDAS, N., HULTQUIST, A., LIUBA, K., JENSEN, C. T., BRYDER, D., YANG, L., BORGE, O. J., THOREN, L. A., ANDERSON, K., SITNICKA, E., SASAKI, Y., SIGVARDSSON, M. & JACOBSEN, S. E. 2005. Identification of Flt3+ lympho-myeloid stem cells lacking erythro-megakaryocytic potential a revised road map for adult blood lineage commitment. *Cell,* 121**,** 295-306.

AGGARWAL, P., VAITES, L. P., KIM, J. K., MELLERT, H., GURUNG, B., NAKAGAWA, H., HERLYN, M., HUA, X., RUSTGI, A. K., MCMAHON, S. B. & DIEHL, J. A. 2010. Nuclear cyclin D1/CDK4 kinase regulates CUL4 expression and triggers neoplastic growth via activation of the PRMT5 methyltransferase. *Cancer Cell,* 18**,** 329-40.

AILLES, L. E., GERHARD, B., KAWAGOE, H. & HOGGE, D. E. 1999. Growth characteristics of acute myelogenous leukemia progenitors that initiate malignant hematopoiesis in nonobese diabetic/severe combined immunodeficient mice. *Blood,* 94**,** 1761-72.

AKASHI, K., TRAVER, D., MIYAMOTO, T. & WEISSMAN, I. L. 2000. A clonogenic common myeloid progenitor that gives rise to all myeloid lineages. *Nature,* 404**,** 193-197.

AKIYAMA, K., KAGAWA, S., TAMURA, T., SHIMBARA, N., TAKASHINA, M., KRISTENSEN, P., HENDIL, K. B., TANAKA, K. & ICHIHARA, A. 1994. Replacement of proteasome subunits X and Y by LMP7 and LMP2 induced by interferon-gamma for acquirement of the functional diversity responsible for antigen processing. *FEBS Lett,* 343**,** 85-8.

ALMOND, J. B. & COHEN, G. M. 2002. The proteasome: a novel target for cancer chemotherapy. *Leukemia,* 16**,** 433-43.

AMERICAN CANCER SOCIETY, A. C. S. 2015. Cancer Facts & Figures 2015. *Atlanta: American Cancer Society*.

ANCELIN, K., LANGE, U. C., HAJKOVA, P., SCHNEIDER, R., BANNISTER, A. J., KOUZARIDES, T. & SURANI, M. A. 2006. Blimp1 associates with Prmt5 and directs histone arginine methylation in mouse germ cells. *Nat Cell Biol,* 8**,** 623-30.

ANTONYSAMY, S., BONDAY, Z., CAMPBELL, R. M., DOYLE, B., DRUZINA, Z., GHEYI, T., HAN, B., JUNGHEIM, L. N., QIAN, Y., RAUCH, C., RUSSELL, M., SAUDER, J. M., WASSERMAN, S. R., WEICHERT, K., WILLARD, F. S., ZHANG, A. & EMTAGE, S. 2012. Crystal structure of the human PRMT5:MEP50 complex. *Proceedings of the National Academy of Sciences of the United States of America,* 109**,** 17960-17965.

ARBER, D. A., ORAZI, A., HASSERJIAN, R., THIELE, J., BOROWITZ, M. J., LE BEAU, M. M., BLOOMFIELD, C. D., CAZZOLA, M. & VARDIMAN, J. W.

2016. The 2016 revision to the World Health Organization classification of myeloid neoplasms and acute leukemia. *Blood,* 127**,** 2391-405.

ARGIROPOULOS, B., PALMQVIST, L., YUNG, E., KUCHENBAUER, F., HEUSER, M., SLY, L. M., WAN, A., KRYSTAL, G. & HUMPHRIES, R. K. 2008. Linkage of Meis1 leukemogenic activity to multiple downstream effectors including Trib2 and Ccl3. *Exp Hematol,* 36**,** 845-59.

ARLT, A., BAUER, I., SCHAFMAYER, C., TEPEL, J., MUERKOSTER, S. S., BROSCH, M., RODER, C., KALTHOFF, H., HAMPE, J., MOYER, M. P., FOLSCH, U. R. & SCHAFER, H. 2009. Increased proteasome subunit protein expression and proteasome activity in colon cancer relate to an enhanced activation of nuclear factor E2-related factor 2 (Nrf2). *Oncogene,* 28**,** 3983-96.

ATTAR, E. C., JOHNSON, J. L., AMREIN, P. C., LOZANSKI, G., WADLEIGH, M., DEANGELO, D. J., KOLITZ, J. E., POWELL, B. L., VOORHEES, P., WANG, E. S., BLUM, W., STONE, R. M., MARCUCCI, G., BLOOMFIELD, C. D., MOSER, B. & LARSON, R. A. 2013. Bortezomib added to daunorubicin and cytarabine during induction therapy and to intermediate-dose cytarabine for consolidation in patients with previously untreated acute myeloid leukemia age 60 to 75 years: CALGB (Alliance) study 10502. *J Clin Oncol,* 31**,** 923-9.

AVIEL, S., WINBERG, G., MASSUCCI, M. & CIECHANOVER, A. 2000. Degradation of the epstein-barr virus latent membrane protein 1 (LMP1) by the ubiquitin-proteasome pathway. Targeting via ubiquitination of the N-terminal residue. *J Biol Chem,* 275**,** 23491-9.

BAILEY, F. P., BYRNE, D. P., ORUGANTY, K., EYERS, C. E., NOVOTNY, C. J., SHOKAT, K. M., KANNAN, N. & EYERS, P. A. 2015. The Tribbles 2 (TRB2) pseudokinase binds to ATP and autophosphorylates in a metal-independent manner. *Biochem J,* 467**,** 47-62.

BALDUS, C. D., MROZEK, K., MARCUCCI, G. & BLOOMFIELD, C. D. 2007. Clinical outcome of de novo acute myeloid leukaemia patients with normal cytogenetics is affected by molecular genetic alterations: a concise review. *Br J Haematol,* 137**,** 387-400.

BALDUS, C. D., TANNER, S. M., RUPPERT, A. S., WHITMAN, S. P., ARCHER, K. J., MARCUCCI, G., CALIGIURI, M. A., CARROLL, A. J., VARDIMAN, J. W., POWELL, B. L., ALLEN, S. L., MOORE, J. O., LARSON, R. A., KOLITZ, J. E., DE LA CHAPELLE, A. & BLOOMFIELD, C. D. 2003. BAALC expression predicts clinical outcome of de novo acute myeloid leukemia patients with normal cytogenetics: a Cancer and Leukemia Group B Study. *Blood,* 102**,** 1613-8.

BANDYOPADHYAY, S., HARRIS, D. P., ADAMS, G. N., LAUSE, G. E., MCHUGH, A., TILLMAAND, E. G., MONEY, A., WILLARD, B., FOX, P. L. & DICORLETO, P. E. 2012. HOXA9 methylation by PRMT5 is essential for endothelial cell expression of leukocyte adhesion molecules. *Mol Cell Biol,* 32**,** 1202-13.

BANERJI, V., FRUMM, S. M., ROSS, K. N., LI, L. S., SCHINZEL, A. C., HAHN, C. K., KAKOZA, R. M., CHOW, K. T., ROSS, L., ALEXE, G., TOLLIDAY, N., INGUILIZIAN, H., GALINSKY, I., STONE, R. M., DEANGELO, D. J., ROTI, G., ASTER, J. C., HAHN, W. C., KUNG, A. L. & STEGMAIER, K. 2012. The intersection of genetic and chemical genomic screens identifies GSK-3α as a target in human acute myeloid leukemia. *The Journal of Clinical Investigation,* 122**,** 935-947.

BARTH, B., KEASEY, N., WANG, X., SHANMUGAVELANDY, S., RAMPAL, R., HRICIK, T., CABOT, M., KESTER, M., WANG, H., L, S., M, T., LEVINE, R., LOUGHRAN JR., T. & CLAXTON, D. 2014. Engraftment of Human Primary Acute Myeloid Leukemia Defined by Integrated Genetic Profiling in

NOD/SCID/IL2rγnull Mice for Preclinical Ceramide-Based Therapeutic Evaluation. *Journal of Leukemia,* 2**,** 1-4.

BAUM, C. M., WEISSMAN, I. L., TSUKAMOTO, A. S., BUCKLE, A. M. & PEAULT, B. 1992. Isolation of a candidate human hematopoietic stem-cell population. *Proceedings of the National Academy of Sciences of the United States of America,* 89**,** 2804-2808.

BAZZARO, M., LEE, M. K., ZOSO, A., STIRLING, W. L., SANTILLAN, A., SHIH IE, M. & RODEN, R. B. 2006. Ubiquitin-proteasome system stress sensitizes ovarian cancer to proteasome inhibitor-induced apoptosis. *Cancer Res,* 66**,** 3754-63.

BEILLARD, E., PALLISGAARD, N., VAN DER VELDEN, V. H., BI, W., DEE, R., VAN DER SCHOOT, E., DELABESSE, E., MACINTYRE, E., GOTTARDI, E., SAGLIO, G., WATZINGER, F., LION, T., VAN DONGEN, J. J., HOKLAND, P. & GABERT, J. 2003. Evaluation of candidate control genes for diagnosis and residual disease detection in leukemic patients using 'real-time' quantitative reverse-transcriptase polymerase chain reaction (RQ-PCR) - a Europe against cancer program. *Leukemia,* 17**,** 2474-86.

BENAROUDJ, N., TARCSA, E., CASCIO, P. & GOLDBERG, A. L. 2001. The unfolding of substrates and ubiquitin-independent protein degradation by proteasomes. *Biochimie,* 83**,** 311-8.

BENNETT, J. M., CATOVSKY, D., DANIEL, M. T., FLANDRIN, G., GALTON, D. A., GRALNICK, H. R. & SULTAN, C. 1976. Proposals for the classification of the acute leukaemias. French-American-British (FAB) co-operative group. *Br J Haematol,* 33**,** 451-8.

BENNETT, J. M., CATOVSKY, D., DANIEL, M. T., FLANDRIN, G., GALTON, D. A., GRALNICK, H. R. & SULTAN, C. 1985. Proposed revised criteria for the classification of acute myeloid leukemia. A report of the French-American-British Cooperative Group. *Ann Intern Med,* 103**,** 620-5.

BENNETT, M. K. & KIRK, C. J. 2008. Development of proteasome inhibitors in oncology and autoimmune diseases. *Curr Opin Drug Discov Devel,* 11**,** 616-25.

BEUTLER, E. 2001. The treatment of acute leukemia: past, present, and future. *Leukemia,* 15**,** 658-661.

BLUM, W., MROZEK, K., RUPPERT, A. S., CARROLL, A. J., RAO, K. W., PETTENATI, M. J., ANASTASI, J., LARSON, R. A. & BLOOMFIELD, C. D. 2004. Adult de novo acute myeloid leukemia with t(6;11)(q27;q23): results from Cancer and Leukemia Group B Study 8461 and review of the literature. *Cancer,* 101**,** 1420-7.

BLUM, W., SCHWIND, S., TARIGHAT, S. S., GEYER, S., EISFELD, A. K., WHITMAN, S., WALKER, A., KLISOVIC, R., BYRD, J. C., SANTHANAM, R., WANG, H., CURFMAN, J. P., DEVINE, S. M., JACOB, S., GARR, C., KEFAUVER, C., PERROTTI, D., CHAN, K. K., BLOOMFIELD, C. D., CALIGIURI, M. A., GREVER, M. R., GARZON, R. & MARCUCCI, G. 2012. Clinical and pharmacodynamic activity of bortezomib and decitabine in acute myeloid leukemia. *Blood,* 119**,** 6025-31.

BRADFORD, G. B., WILLIAMS, B., ROSSI, R. & BERTONCELLO, I. 1997. Quiescence, cycling, and turnover in the primitive hematopoietic stem cell compartment. *Exp Hematol,* 25**,** 445-53.

BRANSCOMBE, T. L., FRANKEL, A., LEE, J. H., COOK, J. R., YANG, Z., PESTKA, S. & CLARKE, S. 2001. PRMT5 (Janus kinase-binding protein 1) catalyzes the formation of symmetric dimethylarginine residues in proteins. *J Biol Chem,* 276**,** 32971-6.

BRECCIA, M. & LO-COCO, F. 2011. Gemtuzumab ozogamicin for the treatment of acute promyelocytic leukemia: mechanisms of action and resistance, safety and efficacy. *Expert Opin Biol Ther,* 11**,** 225-34.

BREITSCHOPF, K., BENGAL, E., ZIV, T., ADMON, A. & CIECHANOVER, A. 1998. A novel site for ubiquitination: the N-terminal residue, and not internal lysines of MyoD, is essential for conjugation and degradation of the protein. *Embo j,* 17**,** 5964-73.

BROCA, C., VARIN, E., ARMANET, M., TOURREL-CUZIN, C., BOSCO, D., DALLE, S. & WOJTUSCISZYN, A. 2014. Proteasome dysfunction mediates high glucose-induced apoptosis in rodent beta cells and human islets. *PLoS One,* 9**,** e92066.

BROUWER, A. J., JONKER, A., WERKHOVEN, P., KUO, E., LI, N., GALLASTEGUI, N., KEMMINK, J., FLOREA, B. I., GROLL, M., OVERKLEEFT, H. S. & LISKAMP, R. M. J. 2012. Peptido Sulfonyl Fluorides as New Powerful Proteasome Inhibitors. *Journal of Medicinal Chemistry,* 55**,** 10995-11003.

BURNETT, A. K. 2013. The Challenge of AML in Older Patients. *Mediterr J Hematol Infect Dis,* 5**,** e2013038.

BUZZEO, R., ENKEMANN, S., NIMMANAPALLI, R., ALSINA, M., LICHTENHELD, M. G., DALTON, W. S. & BEAUPRE, D. M. 2005. Characterization of a R115777-resistant human multiple myeloma cell line with cross-resistance to PS-341. *Clin Cancer Res,* 11**,** 6057-64.

CALKHOVEN, C. F., MÜLLER, C. & LEUTZ, A. 2000. Translational control of C/EBPα and C/EBPβ isoform expression. *Genes & Development,* 14**,** 1920-1932.

CAO, Z., UMEK, R. M. & MCKNIGHT, S. L. 1991. Regulated expression of three C/EBP isoforms during adipose conversion of 3T3-L1 cells. *Genes Dev,* 5**,** 1538-52.

CHARI, A., GOLAS, M. M., KLINGENHÄGER, M., NEUENKIRCHEN, N., SANDER, B., ENGLBRECHT, C., SICKMANN, A., STARK, H. & FISCHER, U. 2008. An Assembly Chaperone Collaborates with the SMN Complex to Generate Spliceosomal SnRNPs. *Cell,* 135**,** 497-509.

CHATURVEDI, A., ARAUJO CRUZ, M. M., JYOTSANA, N., SHARMA, A., YUN, H., GORLICH, K., WICHMANN, M., SCHWARZER, A., PRELLER, M., THOL, F., MEYER, J., HAEMMERLE, R., STRUYS, E. A., JANSEN, E. E., MODLICH, U., LI, Z., SLY, L. M., GEFFERS, R., LINDNER, R., MANSTEIN, D. J., LEHMANN, U., KRAUTER, J., GANSER, A. & HEUSER, M. 2013. Mutant IDH1 promotes leukemogenesis in vivo and can be specifically targeted in human AML. *Blood,* 122**,** 2877-87.

CHEN, D., FREZZA, M., SCHMITT, S., KANWAR, J. & DOU, Q. P. 2011. Bortezomib as the First Proteasome Inhibitor Anticancer Drug: Current Status and Future Perspectives. *Current Cancer Drug Targets,* 11**,** 239-253.

CHESHIER, S. H., MORRISON, S. J., LIAO, X. & WEISSMAN, I. L. 1999. In vivo proliferation and cell cycle kinetics of long-term self-renewing hematopoietic stem cells. *Proc Natl Acad Sci U S A,* 96**,** 3120-5.

CHO, E. C., ZHENG, S., MUNRO, S., LIU, G., CARR, S. M., MOEHLENBRINK, J., LU, Y. C., STIMSON, L., KHAN, O., KONIETZNY, R., MCGOURAN, J., COUTTS, A. S., KESSLER, B., KERR, D. J. & THANGUE, N. B. 2012. Arginine methylation controls growth regulation by E2F-1. *Embo j,* 31**,** 1785-97.

CHOU, W. C., LEI, W. C., KO, B. S., HOU, H. A., CHEN, C. Y., TANG, J. L., YAO, M., TSAY, W., WU, S. J., HUANG, S. Y., HSU, S. C., CHEN, Y. C., CHANG, Y. C., KUO, K. T., LEE, F. Y., LIU, M. C., LIU, C. W., TSENG, M. H., HUANG, C. F. & TIEN, H. F. 2011. The prognostic impact and stability of Isocitrate dehydrogenase 2 mutation in adult patients with acute myeloid leukemia. *Leukemia,* 25**,** 246-53.

CHUANG, T.-W., PENG, P.-J. & TARN, W.-Y. 2011. The Exon Junction Complex Component Y14 Modulates the Activity of the Methylosome in Biogenesis of Spliceosomal Small Nuclear Ribonucleoproteins. *Journal of Biological Chemistry,* 286**,** 8722-8728.

CHUNG, J., KARKHANIS, V., TAE, S., YAN, F., SMITH, P., AYERS, L. W., AGOSTINELLI, C., PILERI, S., DENIS, G. V., BAIOCCHI, R. A. & SIF, S. 2013. Protein arginine methyltransferase 5 (PRMT5) inhibition induces lymphoma cell death through reactivation of the retinoblastoma tumor suppressor pathway and polycomb repressor complex 2 (PRC2) silencing. *J Biol Chem,* 288**,** 35534-47.

CIECHANOVER, A. 1994. The ubiquitin-proteasome proteolytic pathway. *Cell,* 79**,** 13-21.

CIECHANOVER, A. 1998. The ubiquitin-proteasome pathway: on protein death and cell life. *Embo j,* 17**,** 7151-60.

COLADO, E., ALVAREZ-FERNANDEZ, S., MAISO, P., MARTIN-SANCHEZ, J., VIDRIALES, M. B., GARAYOA, M., OCIO, E. M., MONTERO, J. C., PANDIELLA, A. & SAN MIGUEL, J. F. 2008. The effect of the proteasome inhibitor bortezomib on acute myeloid leukemia cells and drug resistance associated with the CD34+ immature phenotype. *Haematologica,* 93**,** 57-66.

COOK, G. J. & PARDEE, T. S. 2013. Animal Models of Leukemia: Any closer to the real thing? *Cancer metastasis reviews,* 32**,** 63-76.

CORTES, J., THOMAS, D., KOLLER, C., GILES, F., ESTEY, E., FADERL, S., GARCIA-MANERO, G., MCCONKEY, D., RUIZ, S. L., GUERCIOLINI, R., WRIGHT, J. & KANTARJIAN, H. 2004. Phase I study of bortezomib in refractory or relapsed acute leukemias. *Clin Cancer Res,* 10**,** 3371-6.

COZZIO, A., PASSEGUE, E., AYTON, P. M., KARSUNKY, H., CLEARY, M. L. & WEISSMAN, I. L. 2003. Similar MLL-associated leukemias arising from self-renewing stem cells and short-lived myeloid progenitors. *Genes Dev,* 17**,** 3029-35.

CRAWFORD, L. J. & IRVINE, A. E. 2013. Targeting the ubiquitin proteasome system in haematological malignancies. *Blood Rev,* 27**,** 297-304.

DACWAG, C. S., OHKAWA, Y., PAL, S., SIF, S. & IMBALZANO, A. N. 2007. The Protein Arginine Methyltransferase Prmt5 Is Required for Myogenesis because It Facilitates ATP-Dependent Chromatin Remodeling. *Molecular and Cellular Biology,* 27**,** 384-394.

DANG, L., WHITE, D. W., GROSS, S., BENNETT, B. D., BITTINGER, M. A., DRIGGERS, E. M., FANTIN, V. R., JANG, H. G., JIN, S., KEENAN, M. C., MARKS, K. M., PRINS, R. M., WARD, P. S., YEN, K. E., LIAU, L. M., RABINOWITZ, J. D., CANTLEY, L. C., THOMPSON, C. B., VANDER HEIDEN, M. G. & SU, S. M. 2009. Cancer-associated IDH1 mutations produce 2-hydroxyglutarate. *Nature,* 462**,** 739-744.

DANOVA, M., GIORDANO, M., MAZZINI, G. & RICCARDI, A. 1990. Expression of p53 protein during the cell cycle measured by flow cytometry in human leukemia. *Leuk Res,* 14**,** 417-22.

DE GUZMAN, C. G., WARREN, A. J., ZHANG, Z., GARTLAND, L., ERICKSON, P., DRABKIN, H., HIEBERT, S. W. & KLUG, C. A. 2002. Hematopoietic stem cell expansion and distinct myeloid developmental abnormalities in a murine model of the AML1-ETO translocation. *Mol Cell Biol,* 22**,** 5506-17.

DEDHIA, P. H., KEESHAN, K., ULJON, S., XU, L., VEGA, M. E., SHESTOVA, O., ZAKS-ZILBERMAN, M., ROMANY, C., BLACKLOW, S. C. & PEAR, W. S. 2010. Differential ability of Tribbles family members to promote degradation of C/EBPalpha and induce acute myelogenous leukemia. *Blood,* 116**,** 1321-8.

DEMO, S. D., KIRK, C. J., AUJAY, M. A., BUCHHOLZ, T. J., DAJEE, M., HO, M. N., JIANG, J., LAIDIG, G. J., LEWIS, E. R., PARLATI, F., SHENK, K. D., SMYTH, M. S., SUN, C. M., VALLONE, M. K., WOO, T. M., MOLINEAUX, C. J. & BENNETT, M. K. 2007. Antitumor activity of PR-171, a novel irreversible inhibitor of the proteasome. *Cancer Res,* 67**,** 6383-91.

DESCOMBES, P. & SCHIBLER, U. 1991. A liver-enriched transcriptional activator protein, LAP, and a transcriptional inhibitory protein, LIP, are translated from the same mRNA. *Cell,* 67**,** 569-79.

DOHNER, H., ESTEY, E. H., AMADORI, S., APPELBAUM, F. R., BUCHNER, T., BURNETT, A. K., DOMBRET, H., FENAUX, P., GRIMWADE, D., LARSON, R. A., LO-COCO, F., NAOE, T., NIEDERWIESER, D., OSSENKOPPELE, G. J., SANZ, M. A., SIERRA, J., TALLMAN, M. S., LOWENBERG, B. & BLOOMFIELD, C. D. 2010. Diagnosis and management of acute myeloid leukemia in adults: recommendations from an international expert panel, on behalf of the European LeukemiaNet. *Blood,* 115**,** 453-74.

DOHNER, K. & DOHNER, H. 2008. Molecular characterization of acute myeloid leukemia. *Haematologica,* 93**,** 976-82.

DOHNER, K., SCHLENK, R. F., HABDANK, M., SCHOLL, C., RUCKER, F. G., CORBACIOGLU, A., BULLINGER, L., FROHLING, S. & DOHNER, H. 2005. Mutant nucleophosmin (NPM1) predicts favorable prognosis in younger adults with acute myeloid leukemia and normal cytogenetics: interaction with other gene mutations. *Blood,* 106**,** 3740-6.

DOLCET, X., LLOBET, D., ENCINAS, M., PALLARES, J., CABERO, A., SCHOENENBERGER, J. A., COMELLA, J. X. & MATIAS-GUIU, X. 2006. Proteasome inhibitors induce death but activate NF-kappaB on endometrial carcinoma cell lines and primary culture explants. *J Biol Chem,* 281**,** 22118-30.

DORANTES-ACOSTA, E. & PELAYO, R. 2012. Lineage switching in acute leukemias: a consequence of stem cell plasticity? *Bone Marrow Res,* 2012**,** 406796.

DOULATOV, S., NOTTA, F., LAURENTI, E. & DICK, J. E. 2012. Hematopoiesis: a human perspective. *Cell Stem Cell,* 10**,** 120-36.

DUFOUR, A., SCHNEIDER, F., METZELER, K. H., HOSTER, E., SCHNEIDER, S., ZELLMEIER, E., BENTHAUS, T., SAUERLAND, M. C., BERDEL, W. E., BUCHNER, T., WORMANN, B., BRAESS, J., HIDDEMANN, W., BOHLANDER, S. K. & SPIEKERMANN, K. 2010. Acute myeloid leukemia with biallelic CEBPA gene mutations and normal karyotype represents a distinct genetic entity associated with a favorable clinical outcome. *J Clin Oncol,* 28**,** 570-7.

ESTEY, E. 2010. High cytogenetic or molecular genetic risk acute myeloid leukemia. *Hematology Am Soc Hematol Educ Program,* 2010**,** 474-80.

ESTEY, E. & DOHNER, H. 2006. Acute myeloid leukaemia. *Lancet,* 368**,** 1894-907.

ESTEY, E. H. 2012. Acute myeloid leukemia: 2012 update on diagnosis, risk stratification, and management. *Am J Hematol,* 87**,** 89-99.

FABBRIZIO, E., EL MESSAOUDI, S., POLANOWSKA, J., PAUL, C., COOK, J. R., LEE, J. H., NEGRE, V., ROUSSET, M., PESTKA, S., LE CAM, A. & SARDET, C. 2002. Negative regulation of transcription by the type II arginine methyltransferase PRMT5. *EMBO Rep,* 3**,** 641-5.

FALINI, B., MECUCCI, C., TIACCI, E., ALCALAY, M., ROSATI, R., PASQUALUCCI, L., LA STARZA, R., DIVERIO, D., COLOMBO, E., SANTUCCI, A., BIGERNA, B., PACINI, R., PUCCIARINI, A., LISO, A., VIGNETTI, M., FAZI, P., MEANI, N., PETTIROSSI, V., SAGLIO, G., MANDELLI, F., LO-COCO, F., PELICCI, P. G. & MARTELLI, M. F. 2005. Cytoplasmic nucleophosmin in acute myelogenous leukemia with a normal karyotype. *N Engl J Med,* 352**,** 254-66.

FANG, J., RHYASEN, G., BOLANOS, L., RASCH, C., VARNEY, M., WUNDERLICH, M., GOYAMA, S., JANSEN, G., CLOOS, J., RIGOLINO, C., CORTELEZZI, A., MULLOY, J. C., OLIVA, E. N., CUZZOLA, M. & STARCZYNOWSKI, D. T. 2012. Cytotoxic effects of bortezomib in myelodysplastic syndrome/acute myeloid leukemia depend on autophagy-mediated lysosomal degradation of TRAF6 and repression of PSMA1. *Blood,* 120**,** 858-67.

FANG, Y., ZHOU, X., LIN, M., YING, M., LUO, P., ZHU, D., LOU, J., YANG, B. & HE, Q. 2011. Inhibition of all-trans-retinoic acid-induced proteasome activation potentiates the differentiating effect of retinoid in acute myeloid leukemia cells. *Mol Carcinog,* 50**,** 24-35.

FASAN, A., HAFERLACH, C., ALPERMANN, T., JEROMIN, S., GROSSMANN, V., EDER, C., WEISSMANN, S., DICKER, F., KOHLMANN, A., SCHINDELA, S., KERN, W., HAFERLACH, T. & SCHNITTGER, S. 2014. The role of different genetic subtypes of CEBPA mutated AML. *Leukemia,* 28**,** 794-803.

FERRARA, F. & SCHIFFER, C. A. 2013. Acute myeloid leukaemia in adults. *The Lancet,* 381**,** 484-495.

FERREIRA, H. J., HEYN, H., VIZOSO, M., MOUTINHO, C., VIDAL, E., GOMEZ, A., MARTINEZ-CARDUS, A., SIMO-RIUDALBAS, L., MORAN, S., JOST, E. & ESTELLER, M. 2015. DNMT3A mutations mediate the epigenetic reactivation of the leukemogenic factor MEIS1 in acute myeloid leukemia. *Oncogene*.

FIGUEROA, M. E., ABDEL-WAHAB, O., LU, C., WARD, P. S., PATEL, J., SHIH, A., LI, Y., BHAGWAT, N., VASANTHAKUMAR, A., FERNANDEZ, H. F., TALLMAN, M. S., SUN, Z., WOLNIAK, K., PEETERS, J. K., LIU, W., CHOE, S. E., FANTIN, V. R., PAIETTA, E., LOWENBERG, B., LICHT, J. D., GODLEY, L. A., DELWEL, R., VALK, P. J., THOMPSON, C. B., LEVINE, R. L. & MELNICK, A. 2010. Leukemic IDH1 and IDH2 mutations result in a hypermethylation phenotype, disrupt TET2 function, and impair hematopoietic differentiation. *Cancer Cell,* 18**,** 553-67.

FINCO, T. S. & BALDWIN, A. S. 1995. Mechanistic aspects of NF-kappa B regulation: The emerging role of phosphorylation and proteolysis. *Immunity,* 3**,** 263-272.

FLANDRIN, G. 2002. Classification of acute myeloid leukemias. *Atlas Genet Cytogenet Oncol Haematol. ,* 6**,** 215-219.

FORBES, S. A., BEARE, D., GUNASEKARAN, P., LEUNG, K., BINDAL, N., BOUTSELAKIS, H., DING, M., BAMFORD, S., COLE, C., WARD, S., KOK, C. Y., JIA, M., DE, T., TEAGUE, J. W., STRATTON, M. R., MCDERMOTT, U. & CAMPBELL, P. J. 2015. COSMIC: exploring the world's knowledge of somatic mutations in human cancer. *Nucleic Acids Res,* 43**,** D805-11.

FORD, C. E., HAMERTON, J. L., BARNES, D. W. H. & LOUTIT, J. F. 1956. Cytological Identification of Radiation-Chimaeras. *Nature,* 177**,** 452-454.

FOULKES, D. M., BYRNE, D. P., BAILEY, F. P. & EYERS, P. A. 2015. Tribbles pseudokinases: novel targets for chemical biology and drug discovery? *Biochem Soc Trans,* 43**,** 1095-103.

FREIREICH, E. J., WIERNIK, P. H. & STEENSMA, D. P. 2014. The Leukemias: A Half-Century of Discovery. *Journal of Clinical Oncology,* 32**,** 3463-3469.

FRIESEN, W. J., PAUSHKIN, S., WYCE, A., MASSENET, S., PESIRIDIS, G. S., VAN DUYNE, G., RAPPSILBER, J., MANN, M. & DREYFUSS, G. 2001. The Methylosome, a 20S Complex Containing JBP1 and pICln, Produces Dimethylarginine-Modified Sm Proteins. *Molecular and Cellular Biology,* 21**,** 8289-8300.

FRIESEN, W. J., WYCE, A., PAUSHKIN, S., ABEL, L., RAPPSILBER, J., MANN, M. & DREYFUSS, G. 2002. A novel WD repeat protein component of the methylosome binds Sm proteins. *J Biol Chem,* 277**,** 8243-7.

GEEST, C. R., BUITENHUIS, M., LAARHOVEN, A. G., BIERINGS, M. B., BRUIN, M. C., VELLENGA, E. & COFFER, P. J. 2009. p38 MAP kinase inhibits neutrophil development through phosphorylation of C/EBPalpha on serine 21. *Stem Cells,* 27**,** 2271-82.

GERBER, J. M., SMITH, B. D., NGWANG, B., ZHANG, H., VALA, M. S., MORSBERGER, L., GALKIN, S., COLLECTOR, M. I., PERKINS, B., LEVIS, M. J., GRIFFIN, C. A., SHARKIS, S. J., BOROWITZ, M. J., KARP, J. E. &

JONES, R. J. 2012. A clinically relevant population of leukemic CD34(+)CD38(-) cells in acute myeloid leukemia. *Blood,* 119**,** 3571-7.

GILLILAND, D. G. & TALLMAN, M. S. 2002. Focus on acute leukemias. *Cancer Cell,* 1**,** 417-20.

GLICKMAN, M. H. & CIECHANOVER, A. 2002. The ubiquitin-proteasome proteolytic pathway: destruction for the sake of construction. *Physiol Rev,* 82**,** 373-428.

GRANDINETTI, K. B., STEVENS, T. A., HA, S., SALAMONE, R. J., WALKER, J. R., ZHANG, J., AGARWALLA, S., TENEN, D. G., PETERS, E. C. & REDDY, V. A. 2011. Overexpression of TRIB2 in human lung cancers contributes to tumorigenesis through downregulation of C/EBPalpha. *Oncogene,* 30**,** 3328-35.

GREENBLATT, S. M. & NIMER, S. D. 2014. Chromatin modifiers and the promise of epigenetic therapy in acute leukemia. *Leukemia,* 28**,** 1396-1406.

GRIMWADE, D., WALKER, H., HARRISON, G., OLIVER, F., CHATTERS, S., HARRISON, C. J., WHEATLEY, K., BURNETT, A. K. & GOLDSTONE, A. H. 2001. The predictive value of hierarchical cytogenetic classification in older adults with acute myeloid leukemia (AML): analysis of 1065 patients entered into the United Kingdom Medical Research Council AML11 trial. *Blood,* 98**,** 1312-20.

GRIMWADE, D., WALKER, H., OLIVER, F., WHEATLEY, K., HARRISON, C., HARRISON, G., REES, J., HANN, I., STEVENS, R., BURNETT, A. & GOLDSTONE, A. 1998. The importance of diagnostic cytogenetics on outcome in AML: analysis of 1,612 patients entered into the MRC AML 10 trial. The Medical Research Council Adult and Children's Leukaemia Working Parties. *Blood,* 92**,** 2322-33.

GROLL, M., BAJOREK, M., KOHLER, A., MORODER, L., RUBIN, D. M., HUBER, R., GLICKMAN, M. H. & FINLEY, D. 2000. A gated channel into the proteasome core particle. *Nat Struct Biol,* 7**,** 1062-7.

GROLL, M., DITZEL, L., LOWE, J., STOCK, D., BOCHTLER, M., BARTUNIK, H. D. & HUBER, R. 1997. Structure of 20S proteasome from yeast at 2.4 A resolution. *Nature,* 386**,** 463-71.

GROSSHANS, J. & WIESCHAUS, E. 2000. A genetic link between morphogenesis and cell division during formation of the ventral furrow in Drosophila. *Cell,* 101**,** 523-31.

GRUNWALD, M. R. & LEVIS, M. J. 2013. FLT3 inhibitors for acute myeloid leukemia: a review of their efficacy and mechanisms of resistance. *Int J Hematol,* 97**,** 683-94.

GUDERIAN, G., PETER, C., WIESNER, J., SICKMANN, A., SCHULZE-OSTHOFF, K., FISCHER, U. & GRIMMLER, M. 2011. RioK1, a New Interactor of Protein Arginine Methyltransferase 5 (PRMT5), Competes with pICln for Binding and Modulates PRMT5 Complex Composition and Substrate Specificity. *The Journal of Biological Chemistry,* 286**,** 1976-1986.

GUO, S. & BAO, S. 2010. srGAP2 Arginine Methylation Regulates Cell Migration and Cell Spreading through Promoting Dimerization. *Journal of Biological Chemistry,* 285**,** 35133-35141.

GUO, Z., ZHENG, L., XU, H., DAI, H., ZHOU, M., PASCUA, M. R., CHEN, Q. M. & SHEN, B. 2010. Methylation of FEN1 suppresses nearby phosphorylation and facilitates PCNA binding. *Nat Chem Biol,* 6**,** 766-73.

GUPTA, K., GULEN, F., SUN, L., AGUILERA, R., CHAKRABARTI, A., KISELAR, J., AGARWAL, M. K. & WALD, D. N. 2012. GSK3 is a regulator of RAR-mediated differentiation. *Leukemia,* 26**,** 1277-85.

HAFERLACH, T., KOHLMANN, A., WIECZOREK, L., BASSO, G., KRONNIE, G. T., BENE, M. C., DE VOS, J., HERNANDEZ, J. M., HOFMANN, W. K., MILLS, K. I., GILKES, A., CHIARETTI, S., SHURTLEFF, S. A., KIPPS, T. J., RASSENTI, L. Z., YEOH, A. E., PAPENHAUSEN, P. R., LIU, W. M., WILLIAMS, P. M. & FOA, R. 2010. Clinical utility of microarray-based gene expression profiling in the

diagnosis and subclassification of leukemia: report from the International Microarray Innovations in Leukemia Study Group. *J Clin Oncol,* 28**,** 2529-37.
HAGLUND, K. & DIKIC, I. 2005. Ubiquitylation and cell signaling. *Embo j,* 24**,** 3353-9.
HEANEY, N. B., PELLICANO, F., ZHANG, B., CRAWFORD, L., CHU, S., KAZMI, S. M., ALLAN, E. K., JORGENSEN, H. G., IRVINE, A. E., BHATIA, R. & HOLYOAKE, T. L. 2010. Bortezomib induces apoptosis in primitive chronic myeloid leukemia cells including LTC-IC and NOD/SCID repopulating cells. *Blood,* 115**,** 2241-50.
HEBESTREIT, K., GROTTRUP, S., EMDEN, D., VEERKAMP, J., RUCKERT, C., KLEIN, H. U., MULLER-TIDOW, C. & DUGAS, M. 2012. Leukemia gene atlas-a public platform for integrative exploration of genome-wide molecular data. *PLoS One,* 7**,** e39148.
HEGEDUS, Z., CZIBULA, A. & KISS-TOTH, E. 2006. Tribbles: novel regulators of cell function; evolutionary aspects. *Cell Mol Life Sci,* 63**,** 1632-41.
HEGEDUS, Z., CZIBULA, A. & KISS-TOTH, E. 2007. Tribbles: A family of kinase-like proteins with potent signalling regulatory function. *Cellular Signalling,* 19**,** 238-250.
HENDRICKS-TAYLOR, L. R. & DARLINGTON, G. J. 1995. Inhibition of cell proliferation by C/EBP alpha occurs in many cell types, does not require the presence of p53 or Rb, and is not affected by large T-antigen. *Nucleic Acids Research,* 23**,** 4726-4733.
HERSHKO, A. 2005. The ubiquitin system for protein degradation and some of its roles in the control of the cell division cycle. *Cell Death Differ,* 12**,** 1191-7.
HERSHKO, A. & CIECHANOVER, A. 1998. The ubiquitin system. *Annu Rev Biochem,* 67**,** 425-79.
HEUSER, M., WINGEN, L. U., STEINEMANN, D., CARIO, G., VON NEUHOFF, N., TAUSCHER, M., BULLINGER, L., KRAUTER, J., HEIL, G., DOHNER, H., SCHLEGELBERGER, B. & GANSER, A. 2005. Gene-expression profiles and their association with drug resistance in adult acute myeloid leukemia. *Haematologica,* 90**,** 1484-92.
HICKE, L. 2001. Protein regulation by monoubiquitin. *Nat Rev Mol Cell Biol,* 2**,** 195-201.
HIDESHIMA, T., IKEDA, H., CHAUHAN, D., OKAWA, Y., RAJE, N., PODAR, K., MITSIADES, C., MUNSHI, N. C., RICHARDSON, P. G., CARRASCO, R. D. & ANDERSON, K. C. 2009. Bortezomib induces canonical nuclear factor-kappaB activation in multiple myeloma cells. *Blood,* 114**,** 1046-52.
HIDESHIMA, T., RICHARDSON, P., CHAUHAN, D., PALOMBELLA, V. J., ELLIOTT, P. J., ADAMS, J. & ANDERSON, K. C. 2001. The proteasome inhibitor PS-341 inhibits growth, induces apoptosis, and overcomes drug resistance in human multiple myeloma cells. *Cancer Res,* 61**,** 3071-6.
HILL, R., KALATHUR, R. K., COLACO, L., BRANDAO, R., UGUREL, S., FUTSCHIK, M. & LINK, W. 2015. TRIB2 as a biomarker for diagnosis and progression of melanoma. *Carcinogenesis,* 36**,** 469-77.
HOCHSTRASSER, M. 1995. Ubiquitin, proteasomes, and the regulation of intracellular protein degradation. *Curr Opin Cell Biol,* 7**,** 215-23.
HOLLIDAY, R. 1987. The inheritance of epigenetic defects. *Science,* 238**,** 163-70.
HORTON, T. M., GANNAVARAPU, A., BLANEY, S. M., D'ARGENIO, D. Z., PLON, S. E. & BERG, S. L. 2006. Bortezomib interactions with chemotherapy agents in acute leukemia in vitro. *Cancer Chemother Pharmacol,* 58**,** 13-23.
HORTON, T. M., PATI, D., PLON, S. E., THOMPSON, P. A., BOMGAARS, L. R., ADAMSON, P. C., INGLE, A. M., WRIGHT, J., BROCKMAN, A. H., PATON, M. & BLANEY, S. M. 2007. A phase 1 study of the proteasome inhibitor bortezomib in pediatric patients with refractory leukemia: a Children's Oncology Group study. *Clin Cancer Res,* 13**,** 1516-22.

HOU, Z., PENG, H., AYYANATHAN, K., YAN, K.-P., LANGER, E. M., LONGMORE, G. D. & RAUSCHER, F. J. 2008. The LIM Protein AJUBA Recruits Protein Arginine Methyltransferase 5 To Mediate SNAIL-Dependent Transcriptional Repression. *Molecular and Cellular Biology,* 28**,** 3198-3207.

HOWARD, D. S., LIESVELD, J., PHILLIPS, G. L., 2ND, HAYSLIP, J., WEISS, H., JORDAN, C. T. & GUZMAN, M. L. 2013. A phase I study using bortezomib with weekly idarubicin for treatment of elderly patients with acute myeloid leukemia. *Leuk Res,* 37**,** 1502-8.

HUNTLY, B. J. & GILLILAND, D. G. 2005. Leukaemia stem cells and the evolution of cancer-stem-cell research. *Nat Rev Cancer,* 5**,** 311-21.

IKEDA, F. & DIKIC, I. 2008. Atypical ubiquitin chains: new molecular signals. 'Protein Modifications: Beyond the Usual Suspects' review series. *EMBO Rep,* 9**,** 536-42.

IM, A. P., SEHGAL, A. R., CARROLL, M. P., SMITH, B. D., TEFFERI, A., JOHNSON, D. E. & BOYIADZIS, M. 2014. DNMT3A and IDH mutations in acute myeloid leukemia and other myeloid malignancies: associations with prognosis and potential treatment strategies. *Leukemia,* 28**,** 1774-83.

IMAJOH-OHMI, S., KAWAGUCHI, T., SUGIYAMA, S., TANAKA, K., OMURA, S. & KIKUCHI, H. 1995. Lactacystin, a specific inhibitor of the proteasome, induces apoptosis in human monoblast U937 cells. *Biochem Biophys Res Commun,* 217**,** 1070-7.

IWASAKI, H., MIZUNO, S.-I., WELLS, R. A., CANTOR, A. B., WATANABE, S. & AKASHI, K. 2003. GATA-1 Converts Lymphoid and Myelomonocytic Progenitors into the Megakaryocyte/Erythrocyte Lineages. *Immunity,* 19**,** 451-462.

JACOBSON, L. O., SIMMONS, E. L., MARKS, E. K. & ELDREDGE, J. H. 1951. Recovery from radiation injury. *Science,* 113**,** 510-11.

JANSSON, M., DURANT, S. T., CHO, E. C., SHEAHAN, S., EDELMANN, M., KESSLER, B. & LA THANGUE, N. B. 2008. Arginine methylation regulates the p53 response. *Nat Cell Biol,* 10**,** 1431-9.

JARIEL-ENCONTRE, I., BOSSIS, G. & PIECHACZYK, M. 2008. Ubiquitin-independent degradation of proteins by the proteasome. *Biochim Biophys Acta,* 1786**,** 153-77.

JIN, G., YAMAZAKI, Y., TAKUWA, M., TAKAHARA, T., KANEKO, K., KUWATA, T., MIYATA, S. & NAKAMURA, T. 2007. Trib1 and Evi1 cooperate with Hoxa and Meis1 in myeloid leukemogenesis. *Blood,* 109**,** 3998-4005.

JING, Y. & WAXMAN, S. 2007. The design of selective and non-selective combination therapy for acute promyelocytic leukemia. *Curr Top Microbiol Immunol,* 313**,** 245-69.

JOHANSSON, P., EISELE, L., KLEIN-HITPASS, L., SELLMANN, L., DUHRSEN, U., DURIG, J. & NUCKEL, H. 2010. Percentage of smudge cells determined on routine blood smears is a novel prognostic factor in chronic lymphocytic leukemia. *Leuk Res,* 34**,** 892-8.

KALEJTA, R. F. & SHENK, T. 2003. Proteasome-dependent, ubiquitin-independent degradation of the Rb family of tumor suppressors by the human cytomegalovirus pp71 protein. *Proc Natl Acad Sci U S A,* 100**,** 3263-8.

KAMB, A. 2005. What's wrong with our cancer models? *Nat Rev Drug Discov,* 4**,** 161-5.

KANDOTH, C., MCLELLAN, M. D., VANDIN, F., YE, K., NIU, B., LU, C., XIE, M., ZHANG, Q., MCMICHAEL, J. F., WYCZALKOWSKI, M. A., LEISERSON, M. D. M., MILLER, C. A., WELCH, J. S., WALTER, M. J., WENDL, M. C., LEY, T. J., WILSON, R. K., RAPHAEL, B. J. & DING, L. 2013. Mutational landscape and significance across 12 major cancer types. *Nature,* 502**,** 333-339.

KANE, R. C., BROSS, P. F., FARRELL, A. T. & PAZDUR, R. 2003. Velcade: U.S. FDA approval for the treatment of multiple myeloma progressing on prior therapy. *Oncologist,* 8**,** 508-13.

KANE, R. C., DAGHER, R., FARRELL, A., KO, C. W., SRIDHARA, R., JUSTICE, R. & PAZDUR, R. 2007. Bortezomib for the treatment of mantle cell lymphoma. *Clin Cancer Res,* 13**,** 5291-4.

KATSNELSON, A. 2012. Next-generation proteasome inhibitor approved in multiple myeloma. *Nat Biotech,* 30**,** 1011-1012.

KEESHAN, K., BAILIS, W., DEDHIA, P. H., VEGA, M. E., SHESTOVA, O., XU, L., TOSCANO, K., ULJON, S. N., BLACKLOW, S. C. & PEAR, W. S. 2010. Transformation by Tribbles homolog 2 (Trib2) requires both the Trib2 kinase domain and COP1 binding. *Blood,* 116**,** 4948-57.

KEESHAN, K., HE, Y., WOUTERS, B. J., SHESTOVA, O., XU, L., SAI, H., RODRIGUEZ, C. G., MAILLARD, I., TOBIAS, J. W., VALK, P., CARROLL, M., ASTER, J. C., DELWEL, R. & PEAR, W. S. 2006. Tribbles homolog 2 inactivates C/EBPalpha and causes acute myelogenous leukemia. *Cancer Cell,* 10**,** 401-11.

KEESHAN, K., SHESTOVA, O., USSIN, L. & PEAR, W. S. 2008. Tribbles homolog 2 (Trib2) and HoxA9 cooperate to accelerate acute myelogenous leukemia. *Blood Cells Mol Dis,* 40**,** 119-21.

KELLER, J. N., HANNI, K. B. & MARKESBERY, W. R. 2000a. Impaired proteasome function in Alzheimer's disease. *J Neurochem,* 75**,** 436-9.

KELLER, J. N., HUANG, F. F., ZHU, H., YU, J., HO, Y. S. & KINDY, T. S. 2000b. Oxidative stress-associated impairment of proteasome activity during ischemia-reperfusion injury. *J Cereb Blood Flow Metab,* 20**,** 1467-73.

KELLY, L. M. & GILLILAND, D. G. 2002. Genetics of myeloid leukemias. *Annu Rev Genomics Hum Genet,* 3**,** 179-98.

KIRSTETTER, P., SCHUSTER, M. B., BERESHCHENKO, O., MOORE, S., DVINGE, H., KURZ, E., THEILGAARD-MÖNCH, K., MÅNSSON, R., PEDERSEN, T. Å., PABST, T., SCHROCK, E., PORSE, B. T., JACOBSEN, S. E. W., BERTONE, P., TENEN, D. G. & NERLOV, C. 2008. Modeling of C/EBPα Mutant Acute Myeloid Leukemia Reveals a Common Expression Signature of Committed Myeloid Leukemia-Initiating Cells. *Cancer Cell,* 13**,** 299-310.

KISS-TOTH, E., WYLLIE, D. H., HOLLAND, K., MARSDEN, L., JOZSA, V., OXLEY, K. M., POLGAR, T., QWARNSTROM, E. E. & DOWER, S. K. 2006. Functional mapping and identification of novel regulators for the Toll/Interleukin-1 signalling network by transcription expression cloning. *Cell Signal,* 18**,** 202-14.

KONDO, M., WEISSMAN, I. L. & AKASHI, K. 1997. Identification of clonogenic common lymphoid progenitors in mouse bone marrow. *Cell,* 91**,** 661-72.

KONG, X., ALVAREZ-CASTELAO, B., LIN, Z., CASTANO, J. G. & CARO, J. 2007. Constitutive/hypoxic degradation of HIF-alpha proteins by the proteasome is independent of von Hippel Lindau protein ubiquitylation and the transactivation activity of the protein. *J Biol Chem,* 282**,** 15498-505.

KUMATORI, A., TANAKA, K., INAMURA, N., SONE, S., OGURA, T., MATSUMOTO, T., TACHIKAWA, T., SHIN, S. & ICHIHARA, A. 1990. Abnormally high expression of proteasomes in human leukemic cells. *Proc Natl Acad Sci U S A,* 87**,** 7071-5.

KUTER, D. J., BAIN, B., MUFTI, G., BAGG, A. & HASSERJIAN, R. P. 2007. Bone marrow fibrosis: pathophysiology and clinical significance of increased bone marrow stromal fibres. *Br J Haematol,* 139**,** 351-62.

KWAK, Y. T., GUO, J., PRAJAPATI, S., PARK, K. J., SURABHI, R. M., MILLER, B., GEHRIG, P. & GAYNOR, R. B. 2003. Methylation of SPT5 regulates its interaction with RNA polymerase II and transcriptional elongation properties. *Mol Cell,* 11**,** 1055-66.

LACROIX, M., MESSAOUDI, S. E., RODIER, G., LE CAM, A., SARDET, C. & FABBRIZIO, E. 2008. The histone-binding protein COPR5 is required for nuclear

functions of the protein arginine methyltransferase PRMT5. *EMBO reports,* 9**,** 452-458.

LAIOSA, C. V., STADTFELD, M., XIE, H., DE ANDRES-AGUAYO, L. & GRAF, T. 2006. Reprogramming of Committed T Cell Progenitors to Macrophages and Dendritic Cells by C/EBPα and PU.1 Transcription Factors. *Immunity,* 25**,** 731-744.

LE GUEZENNEC, X., VERMEULEN, M., BRINKMAN, A. B., HOEIJMAKERS, W. A. M., COHEN, A., LASONDER, E. & STUNNENBERG, H. G. 2006. MBD2/NuRD and MBD3/NuRD, Two Distinct Complexes with Different Biochemical and Functional Properties. *Molecular and Cellular Biology,* 26**,** 843-851.

LEE, A. H., IWAKOSHI, N. N., ANDERSON, K. C. & GLIMCHER, L. H. 2003. Proteasome inhibitors disrupt the unfolded protein response in myeloma cells. *Proc Natl Acad Sci U S A,* 100**,** 9946-51.

LIANG, K. L., RISHI, L. & KEESHAN, K. 2013. Tribbles in acute leukemia. *Blood,* 121**,** 4265-70.

LIM, H. S., ARCHER, C. T. & KODADEK, T. 2007. Identification of a peptoid inhibitor of the proteasome 19S regulatory particle. *J Am Chem Soc,* 129**,** 7750-1.

LIN, F. T., MACDOUGALD, O. A., DIEHL, A. M. & LANE, M. D. 1993. A 30-kDa alternative translation product of the CCAAT/enhancer binding protein alpha message: transcriptional activator lacking antimitotic activity. *Proceedings of the National Academy of Sciences of the United States of America,* 90**,** 9606-9610.

LING, Y. H., LIEBES, L., NG, B., BUCKLEY, M., ELLIOTT, P. J., ADAMS, J., JIANG, J. D., MUGGIA, F. M. & PEREZ-SOLER, R. 2002. PS-341, a novel proteasome inhibitor, induces Bcl-2 phosphorylation and cleavage in association with G2-M phase arrest and apoptosis. *Mol Cancer Ther,* 1**,** 841-9.

LIU, C. Y., SHIAU, C. W., KUO, H. Y., HUANG, H. P., CHEN, M. H., TZENG, C. H. & CHEN, K. F. 2013. Cancerous inhibitor of protein phosphatase 2A determines bortezomib-induced apoptosis in leukemia cells. *Haematologica,* 98**,** 729-38.

LIU, F., ZHAO, X., PERNA, F., WANG, L., KOPPIKAR, P., ABDEL-WAHAB, O., HARR, M. W., LEVINE, R. L., XU, H., TEFFERI, A., DEBLASIO, A., HATLEN, M., MENENDEZ, S. & NIMER, S. D. 2011. JAK2V617F-mediated phosphorylation of PRMT5 downregulates its methyltransferase activity and promotes myeloproliferation. *Cancer Cell,* 19**,** 283-94.

LOHAN, F. & KEESHAN, K. 2013. The functionally diverse roles of tribbles. *Biochem Soc Trans,* 41**,** 1096-100.

LÖWENBERG, B. 2001. Prognostic factors in acute myeloid leukaemia. *Best Practice & Research Clinical Haematology,* 14**,** 65-75.

LOWENBERG, B., DOWNING, J. R. & BURNETT, A. 1999. Acute myeloid leukemia. *N Engl J Med,* 341**,** 1051-62.

LUO, P., LIN, M., LI, L., YANG, B. & HE, Q. 2011. The proteasome inhibitor bortezomib enhances ATRA-induced differentiation of neuroblastoma cells via the JNK mitogen-activated protein kinase pathway. *PLoS One,* 6**,** e27298.

MA, W., KANTARJIAN, H., BEKELE, B., DONAHUE, A. C., ZHANG, X., ZHANG, Z. J., O'BRIEN, S., ESTEY, E., ESTROV, Z., CORTES, J., KEATING, M., GILES, F. & ALBITAR, M. 2009. Proteasome Enzymatic Activities in Plasma as Risk Stratification of Patients with Acute Myeloid Leukemia and Advanced Myelodysplastic Syndrome. *Clinical cancer research : an official journal of the American Association for Cancer Research,* 15**,** 3820-3826.

MANCINI, E., SANJUAN-PLA, A., LUCIANI, L., MOORE, S., GROVER, A., ZAY, A., RASMUSSEN, K. D., LUC, S., BILBAO, D., O'CARROLL, D., JACOBSEN, S. E. & NERLOV, C. 2012. FOG-1 and GATA-1 act sequentially to specify definitive megakaryocytic and erythroid progenitors. *Embo j,* 31**,** 351-65.

MANSSON, R., HULTQUIST, A., LUC, S., YANG, L., ANDERSON, K., KHARAZI, S., AL-HASHMI, S., LIUBA, K., THOREN, L., ADOLFSSON, J., BUZA-VIDAS,

N., QIAN, H., SONEJI, S., ENVER, T., SIGVARDSSON, M. & JACOBSEN, S. E. 2007. Molecular evidence for hierarchical transcriptional lineage priming in fetal and adult stem cells and multipotent progenitors. *Immunity,* 26**,** 407-19.

MANZ, M. G., TRAVER, D., MIYAMOTO, T., WEISSMAN, I. L. & AKASHI, K. 2001. Dendritic cell potentials of early lymphoid and myeloid progenitors. *Blood,* 97**,** 3333-41.

MARCUCCI, G., BALDUS, C. D., RUPPERT, A. S., RADMACHER, M. D., MROZEK, K., WHITMAN, S. P., KOLITZ, J. E., EDWARDS, C. G., VARDIMAN, J. W., POWELL, B. L., BAER, M. R., MOORE, J. O., PERROTTI, D., CALIGIURI, M. A., CARROLL, A. J., LARSON, R. A., DE LA CHAPELLE, A. & BLOOMFIELD, C. D. 2005. Overexpression of the ETS-related gene, ERG, predicts a worse outcome in acute myeloid leukemia with normal karyotype: a Cancer and Leukemia Group B study. *J Clin Oncol,* 23**,** 9234-42.

MARDIS, E. R., DING, L., DOOLING, D. J., LARSON, D. E., MCLELLAN, M. D., CHEN, K., KOBOLDT, D. C., FULTON, R. S., DELEHAUNTY, K. D., MCGRATH, S. D., FULTON, L. A., LOCKE, D. P., MAGRINI, V. J., ABBOTT, R. M., VICKERY, T. L., REED, J. S., ROBINSON, J. S., WYLIE, T., SMITH, S. M., CARMICHAEL, L., ELDRED, J. M., HARRIS, C. C., WALKER, J., PECK, J. B., DU, F., DUKES, A. F., SANDERSON, G. E., BRUMMETT, A. M., CLARK, E., MCMICHAEL, J. F., MEYER, R. J., SCHINDLER, J. K., POHL, C. S., WALLIS, J. W., SHI, X., LIN, L., SCHMIDT, H., TANG, Y., HAIPEK, C., WIECHERT, M. E., IVY, J. V., KALICKI, J., ELLIOTT, G., RIES, R. E., PAYTON, J. E., WESTERVELT, P., TOMASSON, M. H., WATSON, M. A., BATY, J., HEATH, S., SHANNON, W. D., NAGARAJAN, R., LINK, D. C., WALTER, M. J., GRAUBERT, T. A., DIPERSIO, J. F., WILSON, R. K. & LEY, T. J. 2009. Recurring mutations found by sequencing an acute myeloid leukemia genome. *N Engl J Med,* 361**,** 1058-66.

MARTINEAU, M., BERGER, R., LILLINGTON, D. M., MOORMAN, A. V. & SECKER-WALKER, L. M. 1998. The t(6;11)(q27;q23) translocation in acute leukemia: a laboratory and clinical study of 30 cases. EU Concerted Action 11q23 Workshop participants. *Leukemia,* 12**,** 788-91.

MATA, J., CURADO, S., EPHRUSSI, A. & RORTH, P. 2000. Tribbles coordinates mitosis and morphogenesis in Drosophila by regulating string/CDC25 proteolysis. *Cell,* 101**,** 511-22.

MEISTER, G. & FISCHER, U. 2002. Assisted RNP assembly: SMN and PRMT5 complexes cooperate in the formation of spliceosomal UsnRNPs. *The EMBO Journal,* 21**,** 5853-5863.

MELNICK, A. & LICHT, J. D. 1999. Deconstructing a disease: RARalpha, its fusion partners, and their roles in the pathogenesis of acute promyelocytic leukemia. *Blood,* 93**,** 3167-215.

MITSIADES, N., MITSIADES, C. S., POULAKI, V., CHAUHAN, D., FANOURAKIS, G., GU, X., BAILEY, C., JOSEPH, M., LIBERMANN, T. A., TREON, S. P., MUNSHI, N. C., RICHARDSON, P. G., HIDESHIMA, T. & ANDERSON, K. C. 2002. Molecular sequelae of proteasome inhibition in human multiple myeloma cells. *Proc Natl Acad Sci U S A,* 99**,** 14374-9.

MIYAMOTO, T., IWASAKI, H., REIZIS, B., YE, M., GRAF, T., WEISSMAN, I. L. & AKASHI, K. 2002. Myeloid or lymphoid promiscuity as a critical step in hematopoietic lineage commitment. *Dev Cell,* 3**,** 137-47.

MORRISON, S. J., WANDYCZ, A. M., HEMMATI, H. D., WRIGHT, D. E. & WEISSMAN, I. L. 1997. Identification of a lineage of multipotent hematopoietic progenitors. *Development,* 124**,** 1929-39.

MORRISON, S. J. & WEISSMAN, I. L. 1994. The long-term repopulating subset of hematopoietic stem cells is deterministic and isolatable by phenotype. *Immunity,* 1**,** 661-73.

MOTEGI, A., MURAKAWA, Y. & TAKEDA, S. 2009. The vital link between the ubiquitin-proteasome pathway and DNA repair: impact on cancer therapy. *Cancer Lett,* 283**,** 1-9.

MROZEK, K., HEINONEN, K. & BLOOMFIELD, C. D. 2001. Clinical importance of cytogenetics in acute myeloid leukaemia. *Best Pract Res Clin Haematol,* 14**,** 19-47.

MURAKAMI, Y., MATSUFUJI, S., KAMEJI, T., HAYASHI, S., IGARASHI, K., TAMURA, T., TANAKA, K. & ICHIHARA, A. 1992. Ornithine decarboxylase is degraded by the 26S proteasome without ubiquitination. *Nature,* 360**,** 597-9.

MURPHY, J. M., NAKATANI, Y., JAMIESON, S. A., DAI, W., LUCET, I. S. & MACE, P. D. 2015. Molecular Mechanism of CCAAT-Enhancer Binding Protein Recruitment by the TRIB1 Pseudokinase. *Structure,* 23**,** 2111-21.

MUSSELMAN, C. A., LALONDE, M. E., COTE, J. & KUTATELADZE, T. G. 2012. Perceiving the epigenetic landscape through histone readers. *Nat Struct Mol Biol,* 19**,** 1218-27.

NAGAMATSU, G., KOSAKA, T., KAWASUMI, M., KINOSHITA, T., TAKUBO, K., AKIYAMA, H., SUDO, T., KOBAYASHI, T., OYA, M. & SUDA, T. 2011. A Germ Cell-specific Gene, Prmt5, Works in Somatic Cell Reprogramming. *The Journal of Biological Chemistry,* 286**,** 10641-10648.

NAGEL, S., VENTURINI, L., PRZYBYLSKI, G. K., GRABARCZYK, P., SCHNEIDER, B., MEYER, C., KAUFMANN, M., SCHMIDT, C. A., SCHERR, M., DREXLER, H. G. & MACLEOD, R. A. F. 2011. Activation of Paired-homeobox gene PITX1 by del(5)(q31) in T-cell acute lymphoblastic leukemia. *Leukemia & Lymphoma,* 52**,** 1348-1359.

NAKAO, M., YOKOTA, S., IWAI, T., KANEKO, H., HORIIKE, S., KASHIMA, K., SONODA, Y., FUJIMOTO, T. & MISAWA, S. 1996. Internal tandem duplication of the flt3 gene found in acute myeloid leukemia. *Leukemia,* 10**,** 1911-8.

NAVON, A. & GOLDBERG, A. L. 2001. Proteins are unfolded on the surface of the ATPase ring before transport into the proteasome. *Mol Cell,* 8**,** 1339-49.

NENCIONI, A., GRUNEBACH, F., PATRONE, F., BALLESTRERO, A. & BROSSART, P. 2007. Proteasome inhibitors: antitumor effects and beyond. *Leukemia,* 21**,** 30-6.

NERLOV, C. 2004. C/EBP[alpha] mutations in acute myeloid leukaemias. *Nat Rev Cancer,* 4**,** 394-400.

NISHIOKA, K. & REINBERG, D. 2003. Methods and tips for the purification of human histone methyltransferases. *Methods,* 31**,** 49-58.

NOTTA, F., DOULATOV, S. & DICK, J. E. 2010. Engraftment of human hematopoietic stem cells is more efficient in female NOD/SCID/IL-2Rgc-null recipients. *Blood,* 115**,** 3704-7.

NOTTA, F., ZANDI, S., TAKAYAMA, N., DOBSON, S., GAN, O. I., WILSON, G., KAUFMANN, K. B., MCLEOD, J., LAURENTI, E., DUNANT, C. F., MCPHERSON, J. D., STEIN, L. D., DROR, Y. & DICK, J. E. 2015. Distinct routes of lineage development reshape the human blood hierarchy across ontogeny. *Science*.

NUTT, S. L., HEAVEY, B., ROLINK, A. G. & BUSSLINGER, M. 1999. Commitment to the B-lymphoid lineage depends on the transcription factor Pax5. *Nature,* 401**,** 556-62.

O'CONNOR, C., LOHAN, F., CAMPOS, J., OHLSSON, E., SALOME, M., FORDE, C., ARTSCHWAGER, R., LISKAMP, R. M., CAHILL, M. R., KIELY, P. A., PORSE, B. & KEESHAN, K. 2016. The presence of C/EBPα and its degradation are both required for TRIB2-mediated leukaemia. *Oncogene*.

O'CONNOR, L., STRASSER, A., O'REILLY, L. A., HAUSMANN, G., ADAMS, J. M., CORY, S. & HUANG, D. C. 1998. Bim: a novel member of the Bcl-2 family that promotes apoptosis. *Embo j,* 17**,** 384-95.

O´BRIEN, E., PRIDEAUX, S. & CHEVASSUT, T. 2014. The Epigenetic Landscape of Acute Myeloid Leukemia. *Advances in Hematology,* 2014**,** 103175.

OBENG, E. A., CARLSON, L. M., GUTMAN, D. M., HARRINGTON, W. J., JR., LEE, K. P. & BOISE, L. H. 2006. Proteasome inhibitors induce a terminal unfolded protein response in multiple myeloma cells. *Blood,* 107**,** 4907-16.

OLIVIER, M., HOLLSTEIN, M. & HAINAUT, P. 2010. TP53 Mutations in Human Cancers: Origins, Consequences, and Clinical Use. *Cold Spring Harbor Perspectives in Biology,* 2**,** a001008.

ORKIN, S. H. 2000. Diversification of haematopoietic stem cells to specific lineages. *Nat Rev Genet,* 1**,** 57-64.

ORKIN, S. H. & ZON, L. I. 2008. Hematopoiesis: An Evolving Paradigm for Stem Cell Biology. *Cell,* 132**,** 631-644.

ORLOWSKI, R. Z., ESWARA, J. R., LAFOND-WALKER, A., GREVER, M. R., ORLOWSKI, M. & DANG, C. V. 1998. Tumor growth inhibition induced in a murine model of human Burkitt's lymphoma by a proteasome inhibitor. *Cancer Res,* 58**,** 4342-8.

ORLOWSKI, R. Z. & KUHN, D. J. 2008. Proteasome inhibitors in cancer therapy: lessons from the first decade. *Clin Cancer Res,* 14**,** 1649-57.

OSAWA, M., HANADA, K., HAMADA, H. & NAKAUCHI, H. 1996. Long-term lymphohematopoietic reconstitution by a single CD34-low/negative hematopoietic stem cell. *Science,* 273**,** 242-5.

OSSIPOW, V., DESCOMBES, P. & SCHIBLER, U. 1993. CCAAT/enhancer-binding protein mRNA is translated into multiple proteins with different transcription activation potentials. *Proceedings of the National Academy of Sciences of the United States of America,* 90**,** 8219-8223.

PABST, C., KROSL, J., FARES, I., BOUCHER, G., RUEL, R., MARINIER, A., LEMIEUX, S., HEBERT, J. & SAUVAGEAU, G. 2014. Identification of small molecules that support human leukemia stem cell activity ex vivo. *Nat Methods,* 11**,** 436-42.

PABST, T., EYHOLZER, M., FOS, J. & MUELLER, B. U. 2009. Heterogeneity within AML with CEBPA mutations; only CEBPA double mutations, but not single CEBPA mutations are associated with favourable prognosis. *Br J Cancer,* 100**,** 1343-6.

PABST, T., MUELLER, B. U., HARAKAWA, N., SCHOCH, C., HAFERLACH, T., BEHRE, G., HIDDEMANN, W., ZHANG, D. E. & TENEN, D. G. 2001. AML1-ETO downregulates the granulocytic differentiation factor C/EBPalpha in t(8;21) myeloid leukemia. *Nat Med,* 7**,** 444-51.

PAGANO, M., TAM, S. W., THEODORAS, A. M., BEER-ROMERO, P., DEL SAL, G., CHAU, V., YEW, P. R., DRAETTA, G. F. & ROLFE, M. 1995. Role of the ubiquitin-proteasome pathway in regulating abundance of the cyclin-dependent kinase inhibitor p27. *Science,* 269**,** 682-5.

PAL, S., BAIOCCHI, R. A., BYRD, J. C., GREVER, M. R., JACOB, S. T. & SIF, S. 2007. Low levels of miR-92b/96 induce PRMT5 translation and H3R8/H4R3 methylation in mantle cell lymphoma. *Embo j,* 26**,** 3558-69.

PAL, S. & SIF, S. 2007. Interplay between chromatin remodelers and protein arginine methyltransferases. *J Cell Physiol,* 213**,** 306-15.

PAL, S., VISHWANATH, S. N., ERDJUMENT-BROMAGE, H., TEMPST, P. & SIF, S. 2004. Human SWI/SNF-associated PRMT5 methylates histone H3 arginine 8 and negatively regulates expression of ST7 and NM23 tumor suppressor genes. *Mol Cell Biol,* 24**,** 9630-45.

PAL, S., YUN, R., DATTA, A., LACOMIS, L., ERDJUMENT-BROMAGE, H., KUMAR, J., TEMPST, P. & SIF, S. 2003. mSin3A/Histone Deacetylase 2- and PRMT5-Containing Brg1 Complex Is Involved in Transcriptional Repression of the Myc Target Gene cad. *Molecular and Cellular Biology,* 23**,** 7475-7487.

PALMA, C. A., AL SHEIKHA, D., LIM, T. K., BRYANT, A., VU, T. T., JAYASWAL, V. & MA, D. D. 2014. MicroRNA-155 as an inducer of apoptosis and cell differentiation in Acute Myeloid Leukaemia. *Mol Cancer,* 13**,** 79.

PALOMBELLA, V. J., CONNER, E. M., FUSELER, J. W., DESTREE, A., DAVIS, J. M., LAROUX, F. S., WOLF, R. E., HUANG, J., BRAND, S., ELLIOTT, P. J., LAZARUS, D., MCCORMACK, T., PARENT, L., STEIN, R., ADAMS, J. & GRISHAM, M. B. 1998. Role of the proteasome and NF-kappaB in streptococcal cell wall-induced polyarthritis. *Proc Natl Acad Sci U S A,* 95**,** 15671-6.

PARLATI, F., LEE, S. J., AUJAY, M., SUZUKI, E., LEVITSKY, K., LORENS, J. B., MICKLEM, D. R., RUURS, P., SYLVAIN, C., LU, Y., SHENK, K. D. & BENNETT, M. K. 2009. Carfilzomib can induce tumor cell death through selective inhibition of the chymotrypsin-like activity of the proteasome. *Blood,* 114**,** 3439-47.

PEREZ-GALAN, P., ROUE, G., VILLAMOR, N., MONTSERRAT, E., CAMPO, E. & COLOMER, D. 2006. The proteasome inhibitor bortezomib induces apoptosis in mantle-cell lymphoma through generation of ROS and Noxa activation independent of p53 status. *Blood,* 107**,** 257-64.

PESIRIDIS, G. S., DIAMOND, E. & VAN DUYNE, G. D. 2009. Role of pICLn in Methylation of Sm Proteins by PRMT5. *Journal of Biological Chemistry,* 284**,** 21347-21359.

PETITJEAN, A., ACHATZ, M. I., BORRESEN-DALE, A. L., HAINAUT, P. & OLIVIER, M. 2007. TP53 mutations in human cancers: functional selection and impact on cancer prognosis and outcomes. *Oncogene,* 26**,** 2157-65.

PICKART, C. M. & EDDINS, M. J. 2004. Ubiquitin: structures, functions, mechanisms. *Biochim Biophys Acta,* 1695**,** 55-72.

PILLER, G. 2001. Leukaemia - a brief historical review from ancient times to 1950. *Br J Haematol,* 112**,** 282-92.

PODAR, K., SHRINGARPURE, R., TAI, Y. T., SIMONCINI, M., SATTLER, M., ISHITSUKA, K., RICHARDSON, P. G., HIDESHIMA, T., CHAUHAN, D. & ANDERSON, K. C. 2004. Caveolin-1 is required for vascular endothelial growth factor-triggered multiple myeloma cell migration and is targeted by bortezomib. *Cancer Res,* 64**,** 7500-6.

POLLACK, B. P., KOTENKO, S. V., HE, W., IZOTOVA, L. S., BARNOSKI, B. L. & PESTKA, S. 1999. The human homologue of the yeast proteins Skb1 and Hsl7p interacts with Jak kinases and contains protein methyltransferase activity. *J Biol Chem,* 274**,** 31531-42.

POWERS, M. A., FAY, M. M., FACTOR, R. E., WELM, A. L. & ULLMAN, K. S. 2011. Protein arginine methyltransferase 5 accelerates tumor growth by arginine methylation of the tumor suppressor programmed cell death 4. *Cancer Res,* 71**,** 5579-87.

QI, L., HEREDIA, J. E., ALTAREJOS, J. Y., SCREATON, R., GOEBEL, N., NIESSEN, S., MACLEOD, I. X., LIEW, C. W., KULKARNI, R. N., BAIN, J., NEWGARD, C., NELSON, M., EVANS, R. M., YATES, J. & MONTMINY, M. 2006. TRB3 links the E3 ubiquitin ligase COP1 to lipid metabolism. *Science,* 312**,** 1763-6.

QIAO, Y., ZHANG, Y. & WANG, J. 2013. Ubiquitin E3 ligase SCFβ-TRCP regulates TRIB2 stability in liver cancer cells. *Biochemical and Biophysical Research Communications,* 441**,** 555-559.

RADOMSKA, H. S., HUETTNER, C. S., ZHANG, P., CHENG, T., SCADDEN, D. T. & TENEN, D. G. 1998. CCAAT/enhancer binding protein alpha is a regulatory

switch sufficient for induction of granulocytic development from bipotential myeloid progenitors. *Mol Cell Biol,* 18**,** 4301-14.

RAIBORG, C., SLAGSVOLD, T. & STENMARK, H. 2006. A new side to ubiquitin. *Trends Biochem Sci,* 31**,** 541-4.

RALPH, P., HARRIS, P. E., PUNJABI, C. J., WELTE, K., LITCOFSKY, P. B., HO, M. K., RUBIN, B. Y., MOORE, M. A. & SPRINGER, T. A. 1983. Lymphokine inducing "terminal differentiation" of the human monoblast leukemia line U937: a role for gamma interferon. *Blood,* 62**,** 1169-75.

REINSTEIN, E., SCHEFFNER, M., OREN, M., CIECHANOVER, A. & SCHWARTZ, A. 2000. Degradation of the E7 human papillomavirus oncoprotein by the ubiquitin-proteasome system: targeting via ubiquitination of the N-terminal residue. *Oncogene,* 19**,** 5944-50.

REN, J., WANG, Y., LIANG, Y., ZHANG, Y., BAO, S. & XU, Z. 2010. Methylation of Ribosomal Protein S10 by Protein-arginine Methyltransferase 5 Regulates Ribosome Biogenesis. *Journal of Biological Chemistry,* 285**,** 12695-12705.

RENNEVILLE, A., BOISSEL, N., NIBOUREL, O., BERTHON, C., HELEVAUT, N., GARDIN, C., CAYUELA, J. M., HAYETTE, S., REMAN, O., CONTENTIN, N., BORDESSOULE, D., PAUTAS, C., BOTTON, S., REVEL, T., TERRE, C., FENAUX, P., THOMAS, X., CASTAIGNE, S., DOMBRET, H. & PREUDHOMME, C. 2012. Prognostic significance of DNA methyltransferase 3A mutations in cytogenetically normal acute myeloid leukemia: a study by the Acute Leukemia French Association. *Leukemia,* 26**,** 1247-54.

RENNEVILLE, A., ROUMIER, C., BIGGIO, V., NIBOUREL, O., BOISSEL, N., FENAUX, P. & PREUDHOMME, C. 2008. Cooperating gene mutations in acute myeloid leukemia: a review of the literature. *Leukemia,* 22**,** 915-31.

RISHI, L., HANNON, M., SALOME, M., HASEMANN, M., FRANK, A. K., CAMPOS, J., TIMONEY, J., O'CONNOR, C., CAHILL, M. R., PORSE, B. & KEESHAN, K. 2014. Regulation of Trib2 by an E2F1-C/EBPalpha feedback loop in AML cell proliferation. *Blood,* 123**,** 2389-400.

RIZZO, M. G., ZEPPARONI, A., CRISTOFANELLI, B., SCARDIGLI, R., CRESCENZI, M., BLANDINO, G., GIULIACCI, S., FERRARI, S., SODDU, S. & SACCHI, A. 1998. Wt-p53 action in human leukaemia cell lines corresponding to different stages of differentiation. *Br J Cancer,* 77**,** 1429-38.

ROCCARO, A. M., HIDESHIMA, T., RAJE, N., KUMAR, S., ISHITSUKA, K., YASUI, H., SHIRAISHI, N., RIBATTI, D., NICO, B., VACCA, A., DAMMACCO, F., RICHARDSON, P. G. & ANDERSON, K. C. 2006. Bortezomib mediates antiangiogenesis in multiple myeloma via direct and indirect effects on endothelial cells. *Cancer Res,* 66**,** 184-91.

ROCK, K. L., GRAMM, C., ROTHSTEIN, L., CLARK, K., STEIN, R., DICK, L., HWANG, D. & GOLDBERG, A. L. 1994. Inhibitors of the proteasome block the degradation of most cell proteins and the generation of peptides presented on MHC class I molecules. *Cell,* 78**,** 761-71.

ROMBOUTS, W. J., BLOKLAND, I., LOWENBERG, B. & PLOEMACHER, R. E. 2000. Biological characteristics and prognosis of adult acute myeloid leukemia with internal tandem duplications in the Flt3 gene. *Leukemia,* 14**,** 675-83.

RORTH, P., SZABO, K. & TEXIDO, G. 2000. The level of C/EBP protein is critical for cell migration during Drosophila oogenesis and is tightly controlled by regulated degradation. *Mol Cell,* 6**,** 23-30.

ROSENWALD, I. B., RHOADS, D. B., CALLANAN, L. D., ISSELBACHER, K. J. & SCHMIDT, E. V. 1993. Increased expression of eukaryotic translation initiation factors eIF-4E and eIF-2 alpha in response to growth induction by c-myc. *Proceedings of the National Academy of Sciences of the United States of America,* 90**,** 6175-6178.

ROSS, S. E., RADOMSKA, H. S., WU, B., ZHANG, P., WINNAY, J. N., BAJNOK, L., WRIGHT, W. S., SCHAUFELE, F., TENEN, D. G. & MACDOUGALD, O. A. 2004. Phosphorylation of C/EBPalpha inhibits granulopoiesis. *Mol Cell Biol,* 24**,** 675-86.

SALOME, M., CAMPOS, J. & KEESHAN, K. 2015. TRIB2 and the ubiquitin proteasome system in cancer. *Biochem Soc Trans,* 43**,** 1089-94.

SALVESTRINI, V., ZINI, R., ROSSI, L., GULINELLI, S., MANFREDINI, R., BIANCHI, E., PIACIBELLO, W., CAIONE, L., MIGLIARDI, G., RICCIARDI, M. R., TAFURI, A., ROMANO, M., SALATI, S., DI VIRGILIO, F., FERRARI, S., BACCARANI, M., FERRARI, D. & LEMOLI, R. M. 2012. Purinergic signaling inhibits human acute myeloblastic leukemia cell proliferation, migration, and engraftment in immunodeficient mice. *Blood,* 119**,** 217-26.

SANCHEZ, P. V., PERRY, R. L., SARRY, J. E., PERL, A. E., MURPHY, K., SWIDER, C. R., BAGG, A., CHOI, J. K., BIEGEL, J. A., DANET-DESNOYERS, G. & CARROLL, M. 2009. A robust xenotransplantation model for acute myeloid leukemia. *Leukemia,* 23**,** 2109-17.

SANDA, T., LAWTON, L. N., BARRASA, M. I., FAN, Z. P., KOHLHAMMER, H., GUTIERREZ, A., MA, W., TATAREK, J., AHN, Y., KELLIHER, M. A., JAMIESON, C. H., STAUDT, L. M., YOUNG, R. A. & LOOK, A. T. 2012. Core transcriptional regulatory circuit controlled by the TAL1 complex in human T cell acute lymphoblastic leukemia. *Cancer Cell,* 22**,** 209-21.

SARRY, J.-E., MURPHY, K., PERRY, R., SANCHEZ, P. V., SECRETO, A., KEEFER, C., SWIDER, C. R., STRZELECKI, A.-C., CAVELIER, C., XE, CHER, C., MANSAT-DE MAS, V., XE, RONIQUE, DELABESSE, E., DANET-DESNOYERS, G. & CARROLL, M. 2011. Human acute myelogenous leukemia stem cells are rare and heterogeneous when assayed in NOD/SCID/IL2Rγc-deficient mice. *The Journal of Clinical Investigation,* 121**,** 384-395.

SCHMITTGEN, T. D. & LIVAK, K. J. 2008. Analyzing real-time PCR data by the comparative C(T) method. *Nat Protoc,* 3**,** 1101-8.

SCHNITTGER, S., SCHOCH, C., KERN, W., MECUCCI, C., TSCHULIK, C., MARTELLI, M. F., HAFERLACH, T., HIDDEMANN, W. & FALINI, B. 2005. Nucleophosmin gene mutations are predictors of favorable prognosis in acute myelogenous leukemia with a normal karyotype. *Blood,* 106**,** 3733-9.

SCHUELER, J., WIDER, D., KLINGNER, K., SIEGERS, G. M., MAY, A. M., WASCH, R., FIEBIG, H. H. & ENGELHARDT, M. 2013. Intratibial injection of human multiple myeloma cells in NOD/SCID IL-2Rgamma(null) mice mimics human myeloma and serves as a valuable tool for the development of anticancer strategies. *PLoS One,* 8**,** e79939.

SCOTT, L. M., CIVIN, C. I., RORTH, P. & FRIEDMAN, A. D. 1992. A novel temporal expression pattern of three C/EBP family members in differentiating myelomonocytic cells. *Blood,* 80**,** 1725-35.

SEHER, T. C. & LEPTIN, M. 2000. Tribbles, a cell-cycle brake that coordinates proliferation and morphogenesis during Drosophila gastrulation. *Current Biology,* 10**,** 623-629.

SHEAFF, R. J., SINGER, J. D., SWANGER, J., SMITHERMAN, M., ROBERTS, J. M. & CLURMAN, B. E. 2000. Proteasomal turnover of p21Cip1 does not require p21Cip1 ubiquitination. *Mol Cell,* 5**,** 403-10.

SHIVAROV, V., GUEORGUIEVA, R., STOIMENOV, A. & TIU, R. 2013. DNMT3A mutation is a poor prognosis biomarker in AML: Results of a meta-analysis of 4500 AML patients. *Leukemia Research,* 37**,** 1445-1450.

SHULTZ, L. D., LYONS, B. L., BURZENSKI, L. M., GOTT, B., CHEN, X., CHALEFF, S., KOTB, M., GILLIES, S. D., KING, M., MANGADA, J., GREINER, D. L. & HANDGRETINGER, R. 2005. Human lymphoid and myeloid cell development in

NOD/LtSz-scid IL2R gamma null mice engrafted with mobilized human hemopoietic stem cells. *J Immunol,* 174**,** 6477-89.

SIJTS, E. J. & KLOETZEL, P. M. 2011. The role of the proteasome in the generation of MHC class I ligands and immune responses. *Cell Mol Life Sci,* 68**,** 1491-502.

SMITH, M., BARNETT, M., BASSAN, R., GATTA, G., TONDINI, C. & KERN, W. 2004. Adult acute myeloid leukaemia. *Crit Rev Oncol Hematol,* 50**,** 197-222.

SOLE, F., LUNO, E., SANZO, C., ESPINET, B., SANZ, G. F., CERVERA, J., CALASANZ, M. J., CIGUDOSA, J. C., MILLA, F., RIBERA, J. M., BUREO, E., MARQUEZ, M. L., ARRANZ, E. & FLORENSA, L. 2005. Identification of novel cytogenetic markers with prognostic significance in a series of 968 patients with primary myelodysplastic syndromes. *Haematologica,* 90**,** 1168-78.

SPANGRUDE, G. J., HEIMFELD, S. & WEISSMAN, I. L. 1988. Purification and characterization of mouse hematopoietic stem cells. *Science,* 241**,** 58-62.

SPECK, N. A. & GILLILAND, D. G. 2002. Core-binding factors in haematopoiesis and leukaemia. *Nat Rev Cancer,* 2**,** 502-513.

STAPNES, C., DOSKELAND, A. P., HATFIELD, K., ERSVAER, E., RYNINGEN, A., LORENS, J. B., GJERTSEN, B. T. & BRUSERUD, O. 2007. The proteasome inhibitors bortezomib and PR-171 have antiproliferative and proapoptotic effects on primary human acute myeloid leukaemia cells. *Br J Haematol,* 136**,** 814-28.

STOHWASSER, R., STANDERA, S., PETERS, I., KLOETZEL, P. M. & GROETTRUP, M. 1997. Molecular cloning of the mouse proteasome subunits MC14 and MECL-1: reciprocally regulated tissue expression of interferon-gamma-modulated proteasome subunits. *Eur J Immunol,* 27**,** 1182-7.

STRAHL, B. D. & ALLIS, C. D. 2000. The language of covalent histone modifications. *Nature,* 403**,** 41-45.

SUGIMOTO, K., TOYOSHIMA, H., SAKAI, R., MIYAGAWA, K., HAGIWARA, K., ISHIKAWA, F., TAKAKU, F., YAZAKI, Y. & HIRAI, H. 1992. Frequent mutations in the p53 gene in human myeloid leukemia cell lines. *Blood,* 79**,** 2378-83.

SUNDSTRÖM, C. & NILSSON, K. 1976. Establishment and characterization of a human histiocytic lymphoma cell line (U-937). *International Journal of Cancer,* 17**,** 565-577.

TALLMAN, M. S., GILLILAND, D. G. & ROWE, J. M. 2005. Drug therapy for acute myeloid leukemia. *Blood,* 106**,** 1154-63.

TALLMANN, M. S. 2004. Curative therapeutic approaches to APL. *Ann Hematol,* 83 Suppl 1**,** S81-2.

TANNER, S. M., AUSTIN, J. L., LEONE, G., RUSH, L. J., PLASS, C., HEINONEN, K., MROZEK, K., SILL, H., KNUUTILA, S., KOLITZ, J. E., ARCHER, K. J., CALIGIURI, M. A., BLOOMFIELD, C. D. & DE LA CHAPELLE, A. 2001. BAALC, the human member of a novel mammalian neuroectoderm gene lineage, is implicated in hematopoiesis and acute leukemia. *Proc Natl Acad Sci U S A,* 98**,** 13901-6.

TASKESEN, E., BULLINGER, L., CORBACIOGLU, A., SANDERS, M. A., ERPELINCK, C. A., WOUTERS, B. J., VAN DER POEL-VAN DE LUYTGAARDE, S. C., DAMM, F., KRAUTER, J., GANSER, A., SCHLENK, R. F., LOWENBERG, B., DELWEL, R., DOHNER, H., VALK, P. J. & DOHNER, K. 2011. Prognostic impact, concurrent genetic mutations, and gene expression features of AML with CEBPA mutations in a cohort of 1182 cytogenetically normal AML patients: further evidence for CEBPA double mutant AML as a distinctive disease entity. *Blood,* 117**,** 2469-75.

TEE, W. W. 2010. Prmt5 is essential for early mouse development and acts in the cytoplasm to maintain ES cell pluripotency. *Genes Dev.,* 24**,** 2772-2777.

TENEN, D. G., HROMAS, R., LICHT, J. D. & ZHANG, D. E. 1997. Transcription factors, normal myeloid development, and leukemia. *Blood,* 90**,** 489-519.

THIEDE, C. 2012. Impact of mutational analysis in acute myeloid leukemia. *Haematology Education: the education programme for the annual congress of the European Haematology Association,* 6**,** 33-40.

THIEDE, C., KOCH, S., CREUTZIG, E., STEUDEL, C., ILLMER, T., SCHAICH, M. & EHNINGER, G. 2006. Prevalence and prognostic impact of NPM1 mutations in 1485 adult patients with acute myeloid leukemia (AML). *Blood,* 107**,** 4011-20.

THIEDE, C., STEUDEL, C., MOHR, B., SCHAICH, M., SCHAKEL, U., PLATZBECKER, U., WERMKE, M., BORNHAUSER, M., RITTER, M., NEUBAUER, A., EHNINGER, G. & ILLMER, T. 2002. Analysis of FLT3-activating mutations in 979 patients with acute myelogenous leukemia: association with FAB subtypes and identification of subgroups with poor prognosis. *Blood,* 99**,** 4326-35.

THROWER, J. S., HOFFMAN, L., RECHSTEINER, M. & PICKART, C. M. 2000. Recognition of the polyubiquitin proteolytic signal. *Embo j,* 19**,** 94-102.

TILL, J. E. & MCCULLOCH, E. A. 1961. A Direct Measurement of the Radiation Sensitivity of Normal Mouse Bone Marrow Cells. *Radiation Research,* 14**,** 213-222.

TIMCHENKO, N. A., WILDE, M., NAKANISHI, M., SMITH, J. R. & DARLINGTON, G. J. 1996. CCAAT/enhancer-binding protein alpha (C/EBP alpha) inhibits cell proliferation through the p21 (WAF-1/CIP-1/SDI-1) protein. *Genes Dev,* 10**,** 804-15.

TOYOSHIMA, H. & HUNTER, T. 1994. p27, a novel inhibitor of G1 cyclin-Cdk protein kinase activity, is related to p21. *Cell,* 78**,** 67-74.

ULJON, S., XU, X., DURZYNSKA, I., STEIN, S., ADELMANT, G., MARTO, J. A., PEAR, W. S. & BLACKLOW, S. C. 2016. Structural Basis for Substrate Selectivity of the E3 Ligase COP1. *Structure,* 24**,** 687-96.

VALK, P. J., VERHAAK, R. G., BEIJEN, M. A., ERPELINCK, C. A., BARJESTEH VAN WAALWIJK VAN DOORN-KHOSROVANI, S., BOER, J. M., BEVERLOO, H. B., MOORHOUSE, M. J., VAN DER SPEK, P. J., LOWENBERG, B. & DELWEL, R. 2004. Prognostically useful gene-expression profiles in acute myeloid leukemia. *N Engl J Med,* 350**,** 1617-28.

VARDIMAN, J. W., THIELE, J., ARBER, D. A., BRUNNING, R. D., BOROWITZ, M. J., PORWIT, A., HARRIS, N. L., LE BEAU, M. M., HELLSTROM-LINDBERG, E., TEFFERI, A. & BLOOMFIELD, C. D. 2009. The 2008 revision of the World Health Organization (WHO) classification of myeloid neoplasms and acute leukemia: rationale and important changes. *Blood,* 114**,** 937-51.

VASSILEV, L. T., VU, B. T., GRAVES, B., CARVAJAL, D., PODLASKI, F., FILIPOVIC, Z., KONG, N., KAMMLOTT, U., LUKACS, C., KLEIN, C., FOTOUHI, N. & LIU, E. A. 2004. In vivo activation of the p53 pathway by small-molecule antagonists of MDM2. *Science,* 303**,** 844-8.

VELDERS, G. A., VAN OS, R., HAGOORT, H., VERZAAL, P., GUIOT, H. F., LINDLEY, I. J., WILLEMZE, R., OPDENAKKER, G. & FIBBE, W. E. 2004. Reduced stem cell mobilization in mice receiving antibiotic modulation of the intestinal flora: involvement of endotoxins as cofactors in mobilization. *Blood,* 103**,** 340-6.

VIJ, R., WANG, M., KAUFMAN, J. L., LONIAL, S., JAKUBOWIAK, A. J., STEWART, A. K., KUKRETI, V., JAGANNATH, S., MCDONAGH, K. T., ALSINA, M., BAHLIS, N. J., REU, F. J., GABRAIL, N. Y., BELCH, A., MATOUS, J. V., LEE, P., ROSEN, P., SEBAG, M., VESOLE, D. H., KUNKEL, L. A., WEAR, S. M., WONG, A. F., ORLOWSKI, R. Z. & SIEGEL, D. S. 2012. An open-label, single-

arm, phase 2 (PX-171-004) study of single-agent carfilzomib in bortezomib-naive patients with relapsed and/or refractory multiple myeloma. *Blood,* 119**,** 5661-70.

VON BONIN, M., WERMKE, M., COSGUN, K. N., THIEDE, C., BORNHAUSER, M., WAGEMAKER, G. & WASKOW, C. 2013. In vivo expansion of co-transplanted T cells impacts on tumor re-initiating activity of human acute myeloid leukemia in NSG mice. *PLoS One,* 8**,** e60680.

WALKER, A. & MARCUCCI, G. 2012. Molecular prognostic factors in cytogenetically normal acute myeloid leukemia. *Expert Rev Hematol,* 5**,** 547-58.

WALTER, R. B., APPELBAUM, F. R., ESTEY, E. H. & BERNSTEIN, I. D. 2012. Acute myeloid leukemia stem cells and CD33-targeted immunotherapy. *Blood,* 119**,** 6198-208.

WANG, J., PARK, J. S., WEI, Y., RAJURKAR, M., COTTON, J. L., FAN, Q., LEWIS, B. C., JI, H. & MAO, J. 2013a. TRIB2 acts downstream of Wnt/TCF in liver cancer cells to regulate YAP and C/EBPalpha function. *Mol Cell,* 51**,** 211-25.

WANG, J., ZHANG, Y., WENG, W., QIAO, Y., MA, L., XIAO, W., YU, Y., PAN, Q. & SUN, F. 2013b. Impaired phosphorylation and ubiquitination by p70 S6 kinase (p70S6K) and Smad ubiquitination regulatory factor 1 (Smurf1) promote tribbles homolog 2 (TRIB2) stability and carcinogenic property in liver cancer. *J Biol Chem,* 288**,** 33667-81.

WANG, L., PAL, S. & SIF, S. 2008. Protein arginine methyltransferase 5 suppresses the transcription of the RB family of tumor suppressors in leukemia and lymphoma cells. *Mol Cell Biol,* 28**,** 6262-77.

WANG, N. D., FINEGOLD, M. J., BRADLEY, A., OU, C. N., ABDELSAYED, S. V., WILDE, M. D., TAYLOR, L. R., WILSON, D. R. & DARLINGTON, G. J. 1995. Impaired energy homeostasis in C/EBP alpha knockout mice. *Science,* 269**,** 1108-12.

WANG, P. Y., SUN, Y. X., ZHANG, S., PANG, M., ZHANG, H. H., GAO, S. Y., ZHANG, C., LV, C. J. & XIE, S. Y. 2013c. Let-7c inhibits A549 cell proliferation through oncogenic TRIB2 related factors. *FEBS Lett,* 587**,** 2675-81.

WATKINS, P. J., CONDREAY, J. P., HUBER, B. E., JACOBS, S. J. & ADAMS, D. J. 1996. Impaired proliferation and tumorigenicity induced by CCAAT/enhancer-binding protein. *Cancer Res,* 56**,** 1063-7.

WEI, H., WANG, B., MIYAGI, M., SHE, Y., GOPALAN, B., HUANG, D. B., GHOSH, G., STARK, G. R. & LU, T. 2013. PRMT5 dimethylates R30 of the p65 subunit to activate NF-kappaB. *Proc Natl Acad Sci U S A,* 110**,** 13516-21.

WEI, T. Y., JUAN, C. C., HISA, J. Y., SU, L. J., LEE, Y. C., CHOU, H. Y., CHEN, J. M., WU, Y. C., CHIU, S. C., HSU, C. P., LIU, K. L. & YU, C. T. 2012. Protein arginine methyltransferase 5 is a potential oncoprotein that upregulates G1 cyclins/cyclin-dependent kinases and the phosphoinositide 3-kinase/AKT signaling cascade. *Cancer Sci,* 103**,** 1640-50.

WEIMANN, M., GROSSMANN, A., WOODSMITH, J., OZKAN, Z., BIRTH, P., MEIERHOFER, D., BENLASFER, N., VALOVKA, T., TIMMERMANN, B., WANKER, E. E., SAUER, S. & STELZL, U. 2013. A Y2H-seq approach defines the human protein methyltransferase interactome. *Nat Meth,* 10**,** 339-342.

WEISSMAN, I. L. 2000. Translating stem and progenitor cell biology to the clinic: barriers and opportunities. *Science,* 287**,** 1442-6.

WHITMAN, S. P., RUPPERT, A. S., RADMACHER, M. D., MROZEK, K., PASCHKA, P., LANGER, C., BALDUS, C. D., WEN, J., RACKE, F., POWELL, B. L., KOLITZ, J. E., LARSON, R. A., CALIGIURI, M. A., MARCUCCI, G. & BLOOMFIELD, C. D. 2008. FLT3 D835/I836 mutations are associated with poor disease-free survival and a distinct gene-expression signature among younger adults with de novo cytogenetically normal acute myeloid leukemia lacking FLT3 internal tandem duplications. *Blood,* 111**,** 1552-9.

WILKIN, F., SAVONET, V., RADULESCU, A., PETERMANS, J., DUMONT, J. E. & MAENHAUT, C. 1996. Identification and characterization of novel genes modulated in the thyroid of dogs treated with methimazole and propylthiouracil. *J Biol Chem,* 271**,** 28451-7.

WILKIN, F., SUAREZ-HUERTA, N., ROBAYE, B., PEETERMANS, J., LIBERT, F., DUMONT, J. E. & MAENHAUT, C. 1997. Characterization of a phosphoprotein whose mRNA is regulated by the mitogenic pathways in dog thyroid cells. *Eur J Biochem,* 248**,** 660-8.

WOUTERS, B. J., JORDÀ, M. A., KEESHAN, K., LOUWERS, I., ERPELINCK-VERSCHUEREN, C. A. J., TIELEMANS, D., LANGERAK, A. W., HE, Y., YASHIRO-OHTANI, Y., ZHANG, P., HETHERINGTON, C. J., VERHAAK, R. G. W., VALK, P. J. M., LÖWENBERG, B., TENEN, D. G., PEAR, W. S. & DELWEL, R. 2007. Distinct gene expression profiles of acute myeloid/T-lymphoid leukemia with silenced CEBPA and mutations in NOTCH1. *Blood,* 110**,** 3706-3714.

WOUTERS, B. J., LOWENBERG, B., ERPELINCK-VERSCHUEREN, C. A., VAN PUTTEN, W. L., VALK, P. J. & DELWEL, R. 2009. Double CEBPA mutations, but not single CEBPA mutations, define a subgroup of acute myeloid leukemia with a distinctive gene expression profile that is uniquely associated with a favorable outcome. *Blood,* 113**,** 3088-91.

XIE, H. & ORKIN, S. H. 2007. Immunology: Changed destiny. *Nature,* 449**,** 410-411.

XIE, H., YE, M., FENG, R. & GRAF, T. 2004. Stepwise reprogramming of B cells into macrophages. *Cell,* 117**,** 663-76.

XU, S., TONG, M., HUANG, J., ZHANG, Y., QIAO, Y., WENG, W., LIU, W., WANG, J. & SUN, F. 2014. TRIB2 inhibits Wnt/beta-Catenin/TCF4 signaling through its associated ubiquitin E3 ligases, beta-TrCP, COP1 and Smurf1, in liver cancer cells. *FEBS Lett,* 588**,** 4334-41.

YEUNG, M. C. & LAU, A. S. 1998. Tumor suppressor p53 as a component of the tumor necrosis factor-induced, protein kinase PKR-mediated apoptotic pathway in human promonocytic U937 cells. *J Biol Chem,* 273**,** 25198-202.

YING, M., ZHOU, X., ZHONG, L., LIN, N., JING, H., LUO, P., YANG, X., SONG, H., YANG, B. & HE, Q. 2013. Bortezomib sensitizes human acute myeloid leukemia cells to all-trans-retinoic acid-induced differentiation by modifying the RARalpha/STAT1 axis. *Mol Cancer Ther,* 12**,** 195-206.

YOKOYAMA, T., KANNO, Y., YAMAZAKI, Y., TAKAHARA, T., MIYATA, S. & NAKAMURA, T. 2010. Trib1 links the MEK1/ERK pathway in myeloid leukemogenesis. *Blood,* 116**,** 2768-75.

YOKOYAMA, T. & NAKAMURA, T. 2011. Tribbles in disease: Signaling pathways important for cellular function and neoplastic transformation. *Cancer Sci,* 102**,** 1115-22.

YOSHIDA, A., KATO, J. Y., NAKAMAE, I. & YONEDA-KATO, N. 2013. COP1 targets C/EBPalpha for degradation and induces acute myeloid leukemia via Trib1. *Blood,* 122**,** 1750-60.

YU, J. C., DING, S. L., CHANG, C. H., KUO, S. H., CHEN, S. T., HSU, G. C., HSU, H. M., HOU, M. F., JUNG, L. Y., CHENG, C. W., WU, P. E. & SHEN, C. Y. 2009. Genetic susceptibility to the development and progression of breast cancer associated with polymorphism of cell cycle and ubiquitin ligase genes. *Carcinogenesis,* 30**,** 1562-70.

ZANELLA, F., RENNER, O., GARCIA, B., CALLEJAS, S., DOPAZO, A., PEREGRINA, S., CARNERO, A. & LINK, W. 2010. Human TRIB2 is a repressor of FOXO that contributes to the malignant phenotype of melanoma cells. *Oncogene,* 29**,** 2973-82.

ZHANG, C., CHI, Y. L., WANG, P. Y., WANG, Y. Q., ZHANG, Y. X., DENG, J., LV, C. J. & XIE, S. Y. 2012. miR-511 and miR-1297 inhibit human lung adenocarcinoma cell proliferation by targeting oncogene TRIB2. *PLoS One,* 7**,** e46090.

ZHANG, D. E., ZHANG, P., WANG, N. D., HETHERINGTON, C. J., DARLINGTON, G. J. & TENEN, D. G. 1997. Absence of granulocyte colony-stimulating factor signaling and neutrophil development in CCAAT enhancer binding protein alpha-deficient mice. *Proc Natl Acad Sci U S A,* 94**,** 569-74.

ZHANG, H. G., WANG, J., YANG, X., HSU, H. C. & MOUNTZ, J. D. 2004a. Regulation of apoptosis proteins in cancer cells by ubiquitin. *Oncogene,* 23**,** 2009-15.

ZHANG, L., LI, X., KE, Z., HUANG, L., LIANG, Y., WU, J., ZHANG, X., CHEN, Y., ZHANG, H. & LUO, X. 2013. MiR-99a may serve as a potential oncogene in pediatric myeloid leukemia. *Cancer Cell International,* 13**,** 1-11.

ZHANG, L., YANG, W., HUBBARD, A. E. & SMITH, M. T. 2005. Nonrandom aneuploidy of chromosomes 1, 5, 6, 7, 8, 9, 11, 12, and 21 induced by the benzene metabolites hydroquinone and benzenetriol. *Environ Mol Mutagen,* 45**,** 388-96.

ZHANG, P., IWASAKI-ARAI, J., IWASAKI, H., FENYUS, M. L., DAYARAM, T., OWENS, B. M., SHIGEMATSU, H., LEVANTINI, E., HUETTNER, C. S., LEKSTROM-HIMES, J. A., AKASHI, K. & TENEN, D. G. 2004b. Enhancement of hematopoietic stem cell repopulating capacity and self-renewal in the absence of the transcription factor C/EBP alpha. *Immunity,* 21**,** 853-63.

ZHAO, Q., RANK, G., TAN, Y. T., LI, H., MORITZ, R. L., SIMPSON, R. J., CERRUTI, L., CURTIS, D. J., PATEL, D. J., ALLIS, C. D., CUNNINGHAM, J. M. & JANE, S. M. 2009. PRMT5-mediated methylation of histone H4R3 recruits DNMT3A, coupling histone and DNA methylation in gene silencing. *Nat Struct Mol Biol,* 16**,** 304-311.

ZHOU, Z., SUN, X., ZOU, Z., SUN, L., ZHANG, T., GUO, S., WEN, Y., LIU, L., WANG, Y., QIN, J., LI, L., GONG, W. & BAO, S. 2010. PRMT5 regulates Golgi apparatus structure through methylation of the golgin GM130. *Cell Res,* 20**,** 1023-1033.